NASA CR-134636

CONCEPTUAL DESIGN STUDIES OF LIFT/CRUISE FANS FOR MILITARY TRANSPORTS

by

GENERAL ELECTRIC COMPANY

prepared for

NATIONAL AERONAUTICS AND SPACE ADMINISTRATION

NASA-Lewis Research Center

Contract NAS3-17850

1. Report No.	2. Government Accession No.	3. Recipient's Catalog No.
CR-134636		

4. Title and Subtitle	5. Report Date
Conceptual Design Studies of Lift/Cruise Fans for Military Transports	May 3, 1974
	6. Performing Organization Code
7. Author(s)	8. Performing Organization Report No. R74AEG283
	10. Work Unit No.
9. Performing Organization Name and Address General Electric Company Aircraft Engine Group Cincinnati, Ohio 45215	11. Contract or Grant No. NAS3-17850
	13. Type of Report and Period Covered Contractor Report
12. Sponsoring Agency Name and Address National Aeronautics and Space Administration Washington DC 20546	14. Sponsoring Agency Code

15. Supplementary Notes

Project Manager, Arthur J. Glassman, Fluid Systems Components Div., NASA Lewis Research Center, Cleveland, Ohio

16. Abstract

This is the final technical report presenting the results of a study program for conceptual design studies of remote lift and lift/cruise fan systems to meet the requirements of military V/STOL aircraft. Parametric performance and design data are presented for fans covering a range of pressure ratios, including both single and two stage fan concepts. The gas generator selected for these fan systems was the J101-GE-100 engine. Noise generation and transient response were determined for selected fan systems.

17. Key Words (Suggested by Author(s))	18. Distribution Statement
Lift Fans Noise V/STOL Propulsion	Unclassified

19. Security Classif. (of this report)	20. Security Classif. (of this page)	21. No. of Pages	22. Price*
Unclassified - Unlimited	Unclassified	264	

* For sale by the National Technical Information Service, Springfield, Virginia 22151

TABLE OF CONTENTS

LIST OF TABLES

LIST OF FIGURES

Figure No.		Page

Figure No.		Page

INTENTIONALLY BLANK

SUMMARY

This report is the final report documenting the results of a parametric performance and conceptual design study of lift fans for application in military V/STOL transport aircraft. The study was performed under Contract NAS3-17850 and covered a period from June, 1973 to March, 1974. The turbotip lift fan studies covered both the single stage and two stage fan concepts. The gas flow for operation of the tip turbine was derived from a gas generator, based on the J101 engine. The J101 is an advanced technology, afterburning, two-spool engine designed for lightweight fighter application. The non-after-burning engine configuration was selected as the gas generator for these studies.

The parametric performance studies covered a range of fan pressure ratios between 1.2 and 1.5 for the single stage fan system and 1.3 to 1.7 for the two-stage concept. Two fan design criteria were also considered, "designed for cruise" or "designed for VTO." The designed for cruise fan system is powered by the full flow of the gas generator operating at its military power level. Consequently, this design concept does not provide the capability of increased fan thrust as desired for aircraft VTOL control. Conversely, the design for VTO system is intentionally oversized to provide thrust margin for control. A fan thrust increase of approximately 20 percent was assumed in the design criteria. The actual thrust margin must be determined through the integrated propulsion-aircraft system studies.

The fan system covering the complete range of pressure ratios were then used as a basis for estimating cruise and VTO performance data. The cruise performance data covers a range of select flight speeds at altitudes between sea level and 40,000 feet (12,200 meters). The VTO performance was determined for hot day, 90° F (306° K), operating with application of short time VTO engine ratings. Typical VTO short time ratings were defined for 2 minute operation, equivalent to trimmed VTO flight, and three second operation, as anticipated for a maximum input of the propulsion derived aircraft attitude control during VTO flight.

Two basic fan systems, one single stage and one two stage, were selected for conceptual mechanical design studies to define a reference fan configuration and weight. A fan pressure ratio of 1.40 was selected for the single stage fan system and a 1.55 was selected for the two stage system. Both conceptual study fans were established by the "design for cruise" application. The following table summarizes the significant fan design parameters and weights of these two fan systems.

	Single Stage	Two Stage
Pressure Ratio	1.4	1.55
Tip Diameter, in. (m)	64.96 (1.65)	52.47 (1.33)
Tip Speed ft/sec (m/sec)	1125 (343)	1018 (310)
Radius Ratio	0.47	0.42
Ideal Total Thrust lb (kN)	22,000 (9.79)	19,200 (854)
Weight lb (kg)	1000 (454)	720 (336)

Although fan noise generation was not a design consideration, noise levels were estimated for selected single and two stage fan configurations. The noise levels were determined for operation of the propulsion in the hover (VTO) mode on a hot day. The engine power setting was set at the two-minute rating with the fan receiving 2/3 of the engine flow for systems designed for cruise and full flow for the designed for VTO configurations. The following table summarizes the estimated perceived noise levels at the 500 foot sideline for the six configurations considered, operating as a lift fan and also operating as a cruise fan with the fan axis oriented horizontally and the thrust axis vertical.

Pressure Ratio	Stages	Designed for	PNL (dB) Lift	PNL (dB) Cruise
1.4	1	Cruise	111.0	112.5
1.4	1	VTO	113.0	114.8
1.4	2	Cruise	113.8	113.6
1.4	2	VTO	115.1	116.6
1.55	2	Cruise	114.2	113.6
1.55	2	VTO	117.5	117.7

INTRODUCTION

The General Electric Company, in a joint effort with NASA, has been engaged in a continuing program to define advancements in component and system technology which will lead to advanced lift fan systems applicable to V/STOL aircraft systems. Specific objectives of these programs include improvements in areas of performance, weight, size, time response, and reliability and maintainability of the turbotip lift fan systems.

The turbotip lift fan concept of V/STOL propulsion was initially demonstrated as a viable propulsion system during flight tests of the XV-5A aircraft. This aircraft has been actively engaged in various flight test programs beginning with the first flight in 1964 and terminating with tests at NASA, Ames Research Center, in 1972. Other NASA-sponsored programs have included the LF336, the LF446, the LF460 and advanced commercial lift fan systems. The LF336 lift fan program, initiated in early 1967, included design and development of two turbotip lift fan test vehicles. The lift fan was designed to develop a fan pressure ratio of 1.30 with a fan tip diameter of 36 inches (0.91 meters). These two non-flightweight fans were involved in numerous static and wind tunnel test programs. Later programs were initiated to modify the fan to include acoustic features such as rotor-stator spacing, variable stator vane numbers, stator lean and exhaust noise suppression. This acoustic technology demonstrator program continued through August of 1972. The fan configuration was then modified into a statorless, rotor only, configuration with tests occurring in 1973 and 1974 for both serrated and unserrated leading edge rotor blading.

The design studies of advanced fan concepts were initiated with studies of the LF446 fan system. This lift fan, a 1.35 pressure ratio, was designed for future application, with an advanced gas generator, in the XV-5 aircraft flight research program. In late 1969, the program was redirected by NASA toward a large research aircraft that would provide technology applicable to the design of future V/STOL commercial transports. With this redirection, the LF446, a 46-inch (1.17 meter) diameter fan, was increased in size to a 60-inch (1.52 meter) diameter. The configuration was identified as the LF460 turbotip lift fan system and was driven by the exhaust gases of the YJ97 engine system. Preliminary and detailed design studies of the LF460 lift fan were completed in May, 1971. The results of this detailed design study, Reference 1, has provided the basis for the existing family of proposed advanced single stage lift fan systems.

In mid-1973, NASA initiated study programs for the evaluation of lift fan powered V/STOL aircraft systems applicable to a proposed carrier on-board delivery (COD) mission. Aircraft and propulsion studies were initiated through the joint efforts of the NASA Ames and Lewis Research Centers. This report describes the results of these military lift fan propulsion studies performed in conjunction with the aircraft system studies.

The study program was directed towards a parametric study of single stage lift fans intended for military transport systems. The lift fan technology level was established based on the already completed LF446 and LF460 lift fan studies. The gas generator selected to power these lift fans was derived from the J101 engine. The J101 engine represents the advanced engine technology consistent with the lift fan system that is required for an application in 1980-1985 time period. The design studies were also extended to include the two stage lift fan concept. The two stage fan incorporates two fan compressor stages and a single-tip-turbine-stage attached to the second fan stage. This new lift fan design concept was considered during the studies for direct comparison with the single stage fan system. Thus, by using consistent technology levels and the same gas generator, a valid evaluation of the relative merits of two systems is possible. The preliminary design studies for the single stage and two stage fan systems covered a range of fan pressure ratios and fan design criteria consistent with the requirements of the aircraft studies. The results of these parametric performance and conceptual design studies are documented in this final report covering the contract period between June, 1973 and March, 1974.

SYSTEM DESCRIPTION

The lift fan system of propulsion for VTOL aircraft consists of gas generators and turbotip lift fans with associated interconnect ducting and valves. The dependency of the aircraft on the propulsion system for attitude control establishes the ducting and valve arrangements and the exhaust systems for the lift fans. In addition, the lift fans may be employed as propulsion for VTOL only or for both VTOL and cruise operation. For this reason, two basic combinations of lift fans and gas generators were considered in this study. The two concepts considered are defined as "designed for cruise" or "designed for VTOL."

The systems designed for cruise incorporate a single gas generator and lift fan as an integral cruise propulsion unit. This requires that the lift fan is a long life cruise design which receives all the flow from a single gas generator and operates with full or 360 degrees of tip turbine admission arc. The fan design point is thus dictated by the cruise mode of operation with sea level static established as the design conditons. During VTOL operation, multiple engine and fan systems are interconnected to provide for engine-out operation and power transfer for aircraft attitude control. Additional isolated lift fans are then required to absorb the excess gas horsepower associated with the engine short time ratings and the flow transfer. Figure 1 presents a typical schematic for lift fans designed for cruise operation. The system is a three fan, two gas generator arrangement. In the cruise or CTOL mode, two fans each receive the full gas generator flow with the third fan inoperative. During VTOL operation, all fans operate with 240 degrees scroll arc and receive flow from the two gas generators. Operation at this reduced flow level then provides the added fan thrust capability or fan oversizing to cover the increased power due to short time ratings and flow transfer. The flow transfer system used during these studies is the Energy Transfer for Control (ETC) system as employed in the LF460 design, Reference 1. A detailed description of the control concept and results of full-scale testing performed by McDonnell Aircraft Company, McDonnell Douglas Corporation under NASA contract, is given in Reference 2.

The second general type of fan arrangement considered is systems designed for VTO. The system utilizes equal numbers of fans and gas generators, as shown schematically in Figure 2. The fan maximum thrust or design point is established by the VTOL mode of operation with maximum flow transfer associated with the ETC system. During normal VTOL operation and also during cruise each lift fan receives full engine flow. The lift fan systems are then oversized during cruise operation, as compared to the previously discussed system which is sized for cruise with the fans oversized for VTOL operation.

The basic propulsion components are the lift fans and the gas generators. All interconnecting ducting and valving are aircraft design oriented and are considered as aircraft components. This applies equally for the fan inlet and exhaust systems. Therefore, during the studies, certain basic assumptions are required regarding the performance of the ducting, inlet and exhaust components. A typical minimum length interconnecting ducting system was assumed, with a total pressure loss between the engine discharge and fan inlet of 3 percent. The losses assumed for the engine and fan inlet and the fan exhaust systems will be presented during the discussion of fan and gas generator performance.

GAS GENERATOR

The scope of this study was limited to turbotip lift fans designed for operation with a selected advanced gas generator. The initial task of this study was to select the gas generator based on an advanced engine system with an introduction into operation capability in the 1980 to 1985 time period. This restriction limited the selection to already developed engine systems, or engine systems which are presently undergoing development testing. Table I lists the candidate General Electric engines which fall into this category. Significant engine performance parameters are given in the tabulation and show the advanced technology of the J97 and J101 engine systems. These two engines exceed all others in horsepower per pound of flow (HP/W) with minimum levels of duct flow function parameter ($\sqrt{T}/P$). These trends of the two parameters are indicative of smaller gas generator and ducting sizes, a desirable feature for lift fan systems. Based on these comparisons, the J101 engine was selected as the gas generator for this study. An additional incentive for selection of this engine is its larger size which was estimated to closely match the requirements of military transports in the 40 to 60,000 pound gross weight category.

Engine Description

The J101 gas generator used in these studies was derived from the J101-GE-100 Augmented Mixed-Flow Engine, Reference 3. As a gas generator, the engine is modified by removal of the augmentation section and its associated controls and accessories. This modification produces a low bypass (0.2 nominal) turbojet gas generator with a dual-spool compressor which develops an overall pressure ratio of 24 to 1. The engine incorporates a three-stage low-pressure compressor and a seven-stage high-pressure compressor, each driven by a single stage turbine. Variable stator geometry is employed in each of the compressors. The combustor is a carbureting, through-flow annular type. A photograph of an early YJ101-GE-100 engine on test is shown in Figure 3.

Installation

The J101 gas generator employs a conventional three-point engine mounting system. The two forward main trunnion mounts and aft stabilizing mount are shown in the installation drawing in Figure 4. Engine inlet duct attachment is provided at the forward edge of the engine front frame.

The engine discharge terminates in the annular flowpaths of the main core engine and the bypass flows. The engine configuration includes the inner flowpath tail cone since this component is an integral part of the engine rear frame and bearing sump. A flange is provided on the engine outer diameter for attachement of the aircraft furnished ducting system. At the inlet to the ducting, the main and bypass duct flows are separated. A flow mixer must be provided in the initial section of the ducting to achieve an intermixed pressure and temperature for inlet to the fan tip turbine system.

VTO Ratings

The ratings normally established for an engine system are based on the requirements for conventional aircraft flight. In order to more efficiently utilize the short-time capability of the engine performance potential, a special set of VTOL ratings is desirable. These ratings are required for hot, 90° F, (306° K) day operation since VTOL aircraft performance criteria is usually based on that level of ambient temperature.

The ratings were defined for the J101 gas generator for the special case of VTOL operation with a turbotip lift fan system. For this study, the use of combustor inlet water injection was considered as a method of increasing the performance potential. The three rating points considered are:

- VTO (Nominal)

  This rating applies to the nominal trimmed aircraft operation during VTO maneuver which is estimated not to exceed 2 minutes per flight.

- VTO (Maximum Control)

  This rating applies to the conditions associated with maximum flow transfer. The duration of this maximum flow transfer condition is estimated not to exceed a three-second utilization. The nominal and maximum control power settings are achieved with no change of engine throttle setting.

- VTO (Emergency)

  This emergency rating is a once-per-engine life rating which can be used to save the aircraft in the event of a propulsion failure. With the engine operating at this condition, there is no further capability for aircraft attitude control through power transfer.

The rating points for the J101 engine were determined for specific limiting relationships of rotational speeds and high pressure turbine inlet temperature. Fan compressor stall margin becomes a factor during power transfer operation. Combustor inlet water injection was considered as a method for reducing the turbine inlet temperature to provide increased performance through further increases in engine fuel flow and the added mass of the injected water. The short time ratings which were established for this design study are given in Table II. The three rating points are identified for either with or without water injection. For comparison, the conventional intermediate power setting is shown for both the standard and hot day conditions and show the gains achieved in engine discharge gas horsepower. The maximum control rating with water injection yields a power increase of 43 percent above the normal hot day intermediate power setting. Higher maximum control power levels can be achieved because the data shown in Table II does not account for the flow increase due to power transfer between pairs of engines.

Comparable engine rating points for the installed system are given in Table IV with installation assumptions used to derive this performance given in Table III.

Performance

Engine performance was obtained using estimated component performance and the engine computer deck established for a minimum level J101-GE-100 engine. The computational procedures were modified to reflect the removal of the afterburner section. The engine discharge pressure (P_{51}) and temperature (T_{51}) are based on an ideal mixing of the primary and bypass streams. The estimated performance for the installed J101 gas generator is given in Table V and presented graphically in Figures 5 through 11. These engine data, and all following fan performance, will be presented in a corrected parametric notation based on ambient pressure and temperatures.

Engine Scaling

All performance data to be provided in this report is representative of turbotip lift fan systems operating with full flow of a unity size J101 gas generator. Engine and fan size scaling data were provided to meet the requirements of the concurrent aircraft system studies. The appropriate engine scaling factors are given in Figure 12, for a range of engine flow sizes. The base weight for the J101 gas generator configuration is 1480 pounds (671 kg).

SINGLE STAGE FAN SYSTEMS

The single stage remote lift fans are derivatives of the LF460/J97 lift fans system described in Reference 1. The LF460 fan was a 60 inch (1.52 m) diameter fan powered by the exhaust gases of the YJ97-GE-100 turbojet engine. The fan design included features such as a shallow bellmouth inlet, rotor-stator spacing, and other acoustic features as required to provide a low noise fan design for use in a proposed NASA V/STOL research aircraft. The design analysis of the LF460 lift fan was carried into the detail design phase, with the intent of completing the design and manufacture of test fan hardware. The program was terminated during the detail design phase when the interest diminished for development of the NASA V/STOL research transport.

Using this in depth design as a base, the single stage fan design was modified to include those features which differ from the base design but are required for a lift/cruise fan applicable in a military transport aircraft. The major design changes were:

- Front frame design changed to a cylindrical case in place of the inlet bellmouth inherent with the lift fan design.
- Removal of rotor-stator spacing and exhaust noise suppression features.
- Incorporation of a three-strut front frame and single bubble scroll arrangement. These design concepts were studied previously and are described in References 4 and 5.
- Use of lubricated bearings and sumps as required for long time cruise type of operation.

The single stage lift fan system used as a base for these studies is shown in Figure 13. This reference design has a 65 inch (1.65 m) tip diameter and developes a fan pressure ratio of 1.4 at the cruise design point.

Parametric Performance

The single stage fan performance studies covered a range for fan design pressure ratios between 1.2 and 1.5. Fan design points were established for two conditions:

- Designed for Cruise - The fan design point is established by uninstalled engine and fan operation at intermediate power on a sea level static standard day. The fan receives full engine airflow.
- Designed for VTO - The fan design point is established by an uninstalled engine at the 3 second VTOL power setting. The fan is designed for sea level static conditions on the hot, 90° F, (308° K) day. The design is established by the maximum control condition where the fan receives full engine flow plus an additional 10 percent flow from the interconnected engine.

The uninstalled J101 gas conditions used for the fan sizing are listed in Table VI. The assumptions employed in the design procedure were as follows:

- The corrected tip speed for all designs is 1125 ft/sec.
- The fans are designed for confluent flow of the fan and tip turbine exhaust flows.
- The fan stream and turbine exit Mach numbers at the mixing station are 0.55.
- The hub radius ratio is established by a hub loading parameter of 2.14 and an assumed pressure rise distribution across the fan annulus. The radius ratio established by this criteria is shown in Figure 14.
- The fan inlet corrected specific flow at the design point is 40 lbs/sec-ft^2.
- The fan turbine nozzle throat contour is designed for optimum performance at a turbine pressure ratio of 2.50.

Application of these design criteria to both the VTO and cruise systems produced the family of single stage fans as given in Tables VII and VIII. The most interesting design parameters, such as flow, size and thrust, are presented in Figures 15 through 17. The thrust levels shown are ideal uninstalled levels, which are predicted for a confluent flow, no loss, nozzle system.

The eight fan designs were used as the basis for estimating VTOL, transition and cruise performance. This performance was estimated for typical engine and installation corrections as listed in Table IX. The VTO performance was estimated for sea level static hot day operation at the short-time ratings of the J101 gas generator. The performance for the single stage fan, designed for VTO, is given in Table X. At this design condition, the fans are operating with 360 degrees of scroll arc. At all operating points, except the 3 second VTO rating, the fan receives full engine flow. At the 3 second VTO point, the flow has been increased to reflect the power transfer levels. Comparable VTO performance for the cruise designed is given in Table XI. For these designs, the fan is operating with 240 degrees of turbine admission arc and thus receives 2/3 of the normal engine airflow.

Cruise performance was determined for the combination of one J101 gas generator delivering flow to one lift fan system. These performance data are listed in Tables XII through XIX for the four fan pressure ratios and the two design cases. Representative performance, in parametric notation, is shown in Figures 18 through 23 for the fan systems with a 1.4 design pressure ratio. The curves in these figures are a fairing of the performance data covering the Mach number and altitude ranges given in the tabulated data.

Transition performance of lift fan systems covers the range of forward speeds between VTO and full aircraft wing supported flight. The transitional performance for the family of lift fan systems designed for VTO may be obtained from the conventional cruise performance. The cruise performance must be corrected to break down the fan net thrust into the individual gross thrust and ram drag components as required for the transitional performance studies where the fan thrust axis is not aligned with the direction of flight. The procedure for calculating the gross thrust and ram drag components is as follows. The net thrust is defined as:

$$F_N = C_V F_G - (W_{22}/g)V_o \quad (W_2/g)V_o$$

Where F_N = fan system net thrust

W_{22} = fan inlet airflow

W_2 = engine inlet airflow

C_V = nozzle velocity coefficient = 0.98

The engine inlet airflow for each flight condition may be obtained from the data in Table V with appropriate corrections for ambient temperature and pressure altitude. Using the net thrust and airflow data for the particular VTO fan design, then

$$F_G = [F_N + (W_{22}/g)V_o + (W_2/g)V_o]/0.98$$

$$F_{DR} = (W_{22}/g + W_2/g)V_o$$

The gross thrust, F_G, is the ideal level and must include corrections for the exhaust system velocity coefficient during VTO operation.

The performance in the transitional mode may employ the increased performance levels associated with the short time VTO ratings as given in Table IV. The maximum operating point during VTO operation is established by the tabulated levels of engine discharge temperature, T_{51}. This temperature level, with appropriate ambient temperature corrections, establishes the maximum gross thrust level of the particular fan design.

The transitional performance of fans designed for cruise may be achieved by operating with either 360 degrees or 240 degrees of scroll arc. For the case with 360 degree arc operation, two engines are used to deliver gas flow to the two cruise fans only. This is an abnormal mode of operation since the fan systems normally operate with two engines feeding three lift fans with 240 degree partial turbine arc. The performance for the 360 degree arc operation may be obtained from the conventional cruise data in a manner similar to that used for VTO fan designs. For operation with 240 degrees of turbine arc, performance data was generated for a range of flight speeds and altitudes for hot day operation. This performance for fan systems with design pressure ratios of 1.3 and 1.5 is tabulated in Tables XX and XXI.

Installation and Weights

The base point single stage fan design includes a three strut front frame with a cylindrical outer casing. The scroll is a single circular bubble scroll with double radial inlets. The fan exit is at the stator frame. The annular fan exhaust flow is separated from the turbine exhaust by a cylindrical case or mid-box splitter. The exhaust nozzle flowpath must blend into the two coaxial annular flowpaths of the fan exhaust. Figure 24 shows a typical single stage fan cross-section and identifies the significant geometric dimensions. The fan planform is shown in Figure 25. Figures 26 through 29 show the effects of design pressure on the installation dimensions. Data are provided for the two basic single stage fan design concepts.

Figure 30 gives the estimated weights for the single stage fan systems. These weights are for the basic fan as shown in the cross-section of Figure 24. The system does not include exit louvers or any exhaust section downstream of the stator exit plane. The weights are given for the two basic fan designs. Two weights are given for the cruise type design. The lowest or base weight represents a fan configuration which is driven by the J101 gas generator and which does not have the capability of operating with partial arc and at engine power levels above the two minute rating. The fan weights for the cruise type design, with the partial arc capability, represent a system design which operates in the VTO mode with three fans and two gas generators. The fan operates with 240 degrees of arc and can absorb all engine power available during three second rating point operation. The weight includes those design changes required for partial arc operation and an allowance for scroll shut-off valves and actuators as required to convert the system between 360 and 240 degree scroll arc operation.

Fan Scaling

The aircraft weight and number of engines being used for the NASA military transport studies are presently undefined. Therefore, as part of this study, fan weight scaling factors were derived. Figure 31 presents the appropriate weight ratios for scaling over a range of flow or thrust sizes. The appropriate scaling factors for the fan installation dimensions are given in Figure 32.

TWO STAGE FAN SYSTEMS

As the aircraft systems require higher pressure ratio fans, greater than 1.4, the single stage turbotip life fan becomes less attractive because of the small attendant reductions in fan tip diameter. For the single stage concept, the rotor tip speed is established by the turbine operating conditions and a limitation on the turbine exit swirl levels. Mechanical design considerations also tend to influence the design fan tip speed selection, which at present has a limit of about 1125-1150 feet per second. For this type of fan tip speed limit, as the design pressure ratio increases, the hub radius ratio must also increase for an established hub aerodynamic loading limit. Since the hub radius ratio increases with increasing design pressure ratio, the desired reductions in fan tip diameter and consequently fan weight are not achieved.

This desire for higher design pressure ratios established the need to investigate a turbotip lift fan concept which incorporates additional fan compressor stages or hub boosters for relief of the high fan hub loadings. Several different approaches were considered and the full two-stage concept appeared the most promising. This concept includes the following general design features as shown in Figure 33.

- A conventional first stage rotor without inlet guide vanes.
- An exit stator for the first stage rotor which also acts as an inlet guide vane for the second stage rotor.
- A second stage rotor containing the tip turbine system and employing design features similar to the LF460 fan derivatives. The aerodynamic design of the second rotor is established by a swirl-free exhaust flow without exit stators.
- A single stage tip turbine which operates with low (less than 10 degrees) exit swirl angles. For this low level of swirl, turbine exit stators are not required.

The cross-section of a typical two stage fan concept in Figure 33 shows the mechanical simplicity of this concept. The shrouded first stage and LF460 type second stages are interconnected and cantilevered from a two-bearing arrangement located between the rotors. The stationary exit stator-inlet guide vane row incorporates long chord, low aspect ratio blading, and thus is employed as the support frame for the two rotors. The scroll assembly is attached to this single mid-frame by swinging links. The mid-frame design approach permits both first and second stage rotor removal without further fan disassembly, a desirable maintenance feature. The bearing system may incorporate either grease-packed or lubricated sumps depending on the fan application.

Parametric Performance

The two stage fan design studies covered a range of fan pressure ratios between 1.3 and 1.7. The lower regions of design pressure ratio were extended to 1.3 for a direct comparison with the single stage fan concepts. At each fan design pressure ratio, fans were sized for both VTO and cruise operation. The fan design criteria for each system are derived from the conceptual design studies of a 1.55 fan which is described in a later section of this report.

Fan sizing was performed using the uninstalled gas conditions as given in Table VI. These gas conditions agree with those used for the single stage fan designs and represent intermediate power setting for the cruise designs and the three second hot day rating for the VTO designs. The designs assumptions used in sizing the two stage fan system were as follows:

- The fan tip speed is established by ten degrees of forward running swirl in the tip turbine exhaust flow.

- The fans are designed for confluent flow of the fan and turbine exhaust flows. The Mach numbers at the mixing station are 0.55 for both flows.

- The first stage hub radius ratio is based on a loading criteria established by the aerodynamic design studies of the 1.55 pressure ratio fan. The hub loading parameter for the first stage rotor is 2.28, based on fan exit radius ratio. The pressure rise at the first stage hub is defined by the following relationship as derived from the 1.55 fan design.

  $$PR\ (hub) = 1 + 0.6397\ (PR - 1) - 0.1099$$

  The 0.6397 parameter represents the ratio of average Stage 1 to total pressure rise of the two stages. The 0.1099 parameter corrects the hub pressure rise for the first stage pressure rise distribution.

- The fan inlet specific flow at the design point is 39.2 $lb/sec\text{-}ft^2$.

Application of this design criteria to both the designed for VTO and cruise fan systems produced the family of two stage fans as given in Tables XXII and XXIII. The significant fan design parameters are presented graphically in Figures 34 through 38. The difference in fan tip speed for the two fan designs as shown in Figure 36 is established by the 10 degree turbine exit swirl limit and the higher turbine pressure ratio for the VTO design. This difference is reflected in the first stage inlet radius ratio as shown in Figure 34. The radius ratio limit of 0.34 is established by the mechanical design limitations for insertion of the blade dovetails into the first stage disk.

The ten fan designs were used as the basis for estimating VTO and cruise performance for one J101 gas generator driving the tip turbine of one lift/cruise fan. The VTO performance is estimated for sea level static operation at the 90° F (308° K) ambient air temperature condition as established for the design criteria in the NASA VTOL transport studies. The gas generator short time ratings were used during the development of this performance data using the assumed installation factors given in Table IX.

The VTO performance for the two stage fans reflecting the two types of design criteria is listed in Tables XXIV and XXV. All performance for the VTO designs is presented for 360 degrees of turbine arc operation. The performance for the fans designed for cruise is presented for 240 degree turbine arc operation. Standard day performance at full and 2/3 arc is given to show the effects of partial arc operation for these two stage fan designs.

Cruise performance for the range of fan design pressure ratios is given in Tables XXVI through XXXV. Representative performance for the two fan designs with a pressure ratio of 1.7 is shown in Figures 39 through 44. The curves in these figures represent a single characteristic of the calculated performance covering the range of altitudes and Mach numbers.

Installation and Weights

The base point two stage fan includes a cylindrical inlet to the first stage rotor. The fan scroll assembly includes a double entry with a single bubble flowpath. The fan exhaust is at the exit plane of the second stage turbotip rotor where the outer casing flange is provided for transition into the fan exhaust system. The outer casing is not designed to accept the structural loads associated with the fan exhaust and thrust deflection configuration. The second stage fan rotor hub is terminated in a blunt base. In the actual fan installation, the base fairing may be a rotating centerbody attached to the second stage disk. Because of the dependency of the hub flowpath on the particular nozzle system, this component is not included as a fan system component.

Figure 45 shows the cross-section of a two stage fan system and identifies the significant fan dimensions. The fan planform and extreme installation dimensions are as shown in Figure 46. Figures 47 through 50 show the effects of fan design criteria and pressure ratio on these significant fan dimensions.

Fan weight for the full size fan being powered by the J101 gas generator are shown in Figure 51. The weights are given for the following three design concepts:

- Fans designed for cruise without the capability of operating partial arc in the VTO mode.
- Fans designed for cruise but including the design modification required for 240 degrees of partial arc operation in the VTO mode. During VTO operation, the fan is designed to sustain the operating conditions associated with the gas generator short-time ratings.
- Fans designed for cruise and capable of operating with 360 degree of turbine arc and under the environment established by the engine short-time ratings.

Fan Scaling

Figures 52 and 53 present the scale factors required for estimation of the weight and installation dimensions for variable size two stage fan systems. Figure 52 gives the weight scaling factors while Figure 53 presents the dimension scale factor based on the full size fan system operating with the full J101 gas generator exhaust flow.

OPERATING LIMITS

The range of cruise operation for the turbotip lift/cruise fan systems is established by the following limits:

- Altitude - Mach number envelope as given in Figure 54.
- A 105 percent physical speed limit for the J101 gas generator.
- A 114 percent corrected speed limit for the J101 gas generator.
- A 100 percent physical speed limit for the lift/cruise fan.
- A 105 percent corrected speed limit for the lift/cruise fan.

The envelope established by the physical and corrected speed limits of the J101 gas generator are given in Figure 55. These limits are presented as a function of previously used corrected fan turbine inlet temperature parameter. The envelope established by the fan physical and corrected speed limits are given in Figure 56.

PERFORMANCE DERIVATIVES

The cruise performance developed for the parametric fan system was based on a set of assumed installation parameters. These parameters were selected as being typical for the engine installed in a VSTOL aircraft system. Corrections to the fan performance for different installation conditions may be obtained through the use of derivatives of performance with respect to changes in the particular parameter. The most significant installation parameters that affect performance are:

- Engine inlet recovery
- Engine customer bleed
- Interconnect ducting pressure loss
- Fan inlet recovery
- Fan nozzle velocity coefficient

Fan performance was evaluated for variation of each of the installation parameters and the appropriate derivatives were determined. Some derivatives are independent of fan design condition while others vary with both fan design pressure and type of fan design. Figures 57 through 63 present the performance derivatives applicable to the fan systems developed during this study.

ALTERNATE DESIGN STUDIES

During the design studies, derivatives of the base point single and two stage fans were considered for investigation of the effects of several alternate design approaches. The following discussions present the results of several of these design studies.

Effects of Control Margin on Fan Designs

During the initial phases of the system study, the short-time engine ratings were established based on engine speed, turbine temperature and fan stall margins. This study identified the 2 minute and 3 second rating points. These ratings, when considered in the fan designs, produced thrust control margins of about 19 to 20 percent. The required level of control margin is actually established by the aircraft requirements based on propulsion system locations within the aircraft planform, control design criteria and aircraft geometry. A 20 percent lift control level was selected to be representative of typical aircraft requirements. Later in the program, a special study was undertaken to investigate effects of higher lift control margins on fan sizing, performance and weight.

For the J101 engine, the method employed to increase the control margins is to derate the engine during nominal operation. This derate method is required since the maximum lift conditions are set by the engine 3 second and emergency ratings, which are fixed limitations. The nominal rated operation of the engine is derated by increasing the discharge flow function or fan turbine nozzle area. Figures 64 through 66 present the gas conditions at the engine discharge for a typical range of engine discharge flow function. The discharge flow shown in Figure 64 includes the flow addition associated with the levels of flow transfer required to achieve engine operation equivalent to the 3 second and emergency rating points.

The fan design point, or maximum power condition, is established by normal maximum control operation. The engine discharge gas conditions were used to size a series of fans, all designed for VTO operation and a fan pressure ratio of 1.4. The effects of engine operating point on fan size and fan static thrust is shown in Figures 67 and 68. The lift control capability for this matrix of fan designs and engine operation is given in Figure 69. The control levels attendant with normal and emergency operation as identified by the dashed lines in the figure. Only one level of normal and emergency operation can be achieved for a selected set of engine operating conditions.

The fan weight increments associated with fans designed for these levels of control margin was determined and is shown in Figure 70.

Effects of Control Margin on Cruise Performance

During the design studies of the two stage fan systems, a study was performed to determine the effects of control margin on cruise performance. Normal design control margins were established at 20 percent. A higher level of about 30 percent was selected for this comparison. In order to achieve this level of control, the J101 gas generator must be derated during normal operation by increasing the engine discharge flow function or fan turbine nozzle area. The 30 percent control margin required a 4.9 percent increase in engine flow function. The estimated installed gas generator discharge conditions for this level of operation are listed in Table XXXVI. These gas generator conditions were used to estimate sea level static and 36,000 feet cruise performance for a group of two stage fan designs. The fans were first resized to reflect the increased turbine flow at the 3 second rating, with power transfer. The gas conditions used for the fan sizing are given in Table XXXVII and the fan design parameters are listed in Table XXXVIII. Two fan systems were studied with design pressure ratios of 1.4 and 1.6.

The cruise performance for these VTO fan designs was determined for a range of flight speeds at an altitude of 36,000 feet. The fan cruise performance is listed in Tables XXXIX and XL. A comparison was made between this performance and similar fan systems designed for a 20 percent control margin. Thrust, fuel flow and fan airflow ratios were determined and are presented in Figures 71 through 78.

At high power settings, the increased levels of control margins, 20 to 30 percent, produce a fan net thrust decrease of 6 to 8 percent with an engine fuel flow decrease of about 5.5 percent. Thus, the fans designed for higher control levels will have a specific fuel consumption increase of about 2 percent. The trends are fairly consistent for the range of lift fan pressure ratios.

Alternate Scroll Configurations

The maximum installation diameter of the fan system is established by the boundaries of the scroll ducting. In an effort to reduce the maximum installation dimensions, a multiple feed scroll configuration was considered. This configuration provides two auxiliary scroll inlets which supply the gas flow to the extreme 120 degree of turbine arc. A sketch of the fan planform is shown in Figure 79. Each of the two auxiliary inlets carry one sixth of the engine flow and require an inside diameter of 9.5 inches. The remaining engine flow is delivered by the two main inlets with a diameter of 13.5 inches. These inlets may either be oriented as an axial or radial type of inlet duct.

The planform installation dimensions for this alternate scroll configuration are given in Figure 80 for the single stage fan system. A comparison of the dimensions with the conventional design shows a diameter decrease of about 5 inches in the plane perpendicular to the main scroll inlets, dimension "A". Planform dimensions for two stage fan concepts employing the same scroll design concept are given in Figure 81. The design changes for this type of scroll are estimated to represent a weight increase of 10 pounds for each lift fan, regardless of the fan design.

CONCEPTUAL DESIGN STUDIES

Coincident with the parametric performance studies, conceptual design studies were performed to investigate those fan design features that differ significantly from existing fan technology. Two basic fan designs were selected for these studies, a single stage fan with a 1.4 design pressure ratio and a two stage fan with a 1.55 pressure ratio. Both fan systems were designed for cruise and operate with the full gas flow of the J101 gas generator.

Fan Aerodynamic Design

The fan aerodynamic design parameters for the two designs are given in Table XLI. The values of many of the designs were chosen during the initial studies and, in some cases, were the results of previous design studies made in an attempt to obtain the best compromise of high performance and low weight. Selection of the fan pressure ratios was based on trends of the concurrent aircraft studies, with airflow and size established by the available gas generator power. Aerodynamic design consideration strongly influenced the selection of many of the design parameters. The fan discharge static pressure was established by a fan exit Mach number requirement. Since these fan systems were considered for operation as both a lift and a cruise type fan, it is desirable to maintain low fan exit Mach numbers at the fan exit or inlet to the thrust vectoring system. A maximum Mach number of 0.55 was established by this criteria, which in turn, established the fan exit static pressure variation with fan design pressure ratio.

The aerodynamic design of the fan systems was accomplished using a computer program which numerically solves the axisymmetric differential equations of compressible flow along desired calculation boundaries. The theory is a modification and extension of the equation derived by Theodore Katsanis, Reference 6. The program is capable of handling flows with or without blade rows, variable total pressure profiles and leaned or unleaned stators.

The design of the blade rows was accomplished using a second computational procedure which uses the air and streamline inclination angles generated during the aerodynamic design. Airfoil definition data, blade coordinates, stall and choke margins, and other important blade parameters are generated.

The previously described aerodynamic design procedures were used to established the two stage fan flowpath and blade geometry in a unified study with the appropriate mechanical design activities. This level of detailed aerodynamic design was not warranted for the single stage fan design because of the close similarity to previous designs such as the LF460 as defined in Reference 1. The LF460 fan system was designed to develop a fan pressure ratio of 1.35 at a fan tip speed at 1125 feet per second. The differences of blading design between the 1.35 and 1.40 pressure ratio, at the same tip speed, are not sufficient to require a complete aerodynamic design process for use in the mechanical weight and geometry studies.

The two stage fan represented a new concept and a complete aerodynamic design was necessary to establish the blading geometry based on the overall fan performance parameters for the 1.55 pressure ratio design. Figures 82 through 84 show the total and static pressure distribution across the flowpath at the inlet and exit of each of the rotors and the single stator. The associated absolute and relative inlet Mach numbers are shown in Figure 85. The blade loading factors, difusion factors and static pressure rise coefficients are presented in Figures 86 and 87. Moderate blade loadings, less than 0.5, are maintained through appropriate blading design.

Figure 88 through 90 show the blade inlet and exit air angles along with the appropriate blade leading and trailing edge angles. Design levels of incidence and deviation angles can be observed by comparing the blade and air angles.

The significant rotor and stator blading design parameters, such as thickness, chord, solidity, and stagger and camber angles, are given in Figures 91 through 95. Figure 96 gives the relationship between the stream function parameters, used to present the aerodynamic data, and the radial location at the inlet and exit plane for each blade row.

Turbine Aerodynamic Design

The turbine designs used in both the single and two stage fans are impulse designs with 360 degrees of active admission arc. The flowpath is basically an axial flow type with small levels of radially inward slope for compatibility with the fan rotor outer flowpath. The scrolls used to feed the tip turbine are a "single bubble" design with double inlets that each supply 180 degrees of the turbine arc. The scroll diameters are established by about a 0.35 flow Mach number around the circumference except during the last 60 degrees where the scroll bubble diameter remains constant.

The tip turbine is driven by the exhaust gases of the J101 engine, and therefore, the design point was established by the sea level static intermediate power setting for this cruise type fan design. The design gas conditions and the appropriate turbine design parameters are listed in Table XLII. The single and two stage turbine designs reflect two basic design differences. The turbine pressure ratio for the two stage fan is lower than the single stage fan because of the increased fan back pressure or turbine exit static pressure. In addition, the single stage fan is permitted to operate at a higher exit swirl level since the single stage design incorporated an exit stator row. The ten degree exit swirl level for the two stage design was established as the limiting residual swirl and thus establishes the maximum fan tip speed.

The pitch line velocity diagrams for the two reference turbine designs are given in Figures 97 and 98. These turbine designs are representative of designs employed in previous tip turbine driven lift fans. The turbine overall pressure ratio is relatively moderate for a single stage impulse turbine and the bucket relative Mach numbers are reasonable.

Single Stage Fan Mechanical Design

The extent of the design studies for the single stage fan concept was limited to analysis of those design features that differ from the LF460 fan, Reference 1, the modified LF460 configuration, Reference 4, and the military versions, Reference 5. The original LF460 fan design incorporated a triple bubble scroll and four strut front frame. These design features were established by a design requirement of minimum installation depth coupled with minimum installation diameters. In addition, the fan design incorporated acoustic features such as two chord rotor-stator spacing, acoustic suppression and leaned or non radial exit stator vanes. These features represented penalties in both fan weight and performance that are not required for a military lift/cruise fan configuration. The first phase of the design evaluation was to simplify the scroll and front frame design. The scroll was modified to a single bubble design and the front frame was changed to a non-radial three strut configuration. These design features provided a significant weight reduction from an original weight of 789 pounds (358 kg) to 717 pounds (325 kg) or about a 10 percent weight reduction. A further weight reduction and performance improvement was obtained by removal of the two chord spacing and exhaust suppression features as required for low noise generation. This configuration represented the military fan version of the LF460. A comparison of the fan geometries for these two phases of fan design evolution is shown in Figure 99. The fan weight for a comparable military lift fan with this configuration would be about 670 pounds (304 kg). The weight improvement realized by these changes was significant.

The performance and weights of this military lift fan that used the J97 engine as the gas generator were used as the reference designs for these studies. The configuration changes considered and the reasons for these changes are as follows:

- <u>Front Frame Changed to a Cylindrical Casing</u>:

  Lift fan designs have normally incoporated the fan inlet bellmouth as part of the fan configuration. Since the study fans were considered primarily as a cruise propulsion component, a nacelle installation represents the normal case. Thus, an integral bellmouth was no longer required, and the bellmouth was replaced with a cylindrical casing for a more axial fan inlet flowpath.

- <u>Lubricated Fan Rotor Bearings</u>:

  Previous lift fan designs have incorporated grease packed bearings. Successful fan operation has been demonstrated for this type of lubrication. The fan bearing inspection and regrease cycle was about 50 to 100 hours of fan operation. This level of operating time was acceptable for fan systems used exclusively for VTOL operation. Fan systems required for operation as a cruise device require a much longer operating life, and thus a conventional forced feed oil system is required. Such a system was incorporated in the fan designs considered during this study. A description of this lubrication system, which operates using the engine driven pumps, will be given later in the text of this report.

- Reduced Fan Exit Velocities:

  Fan components utilized in cruise systems require an exhaust nozzle system that maintains design fan operation for a large range of altitudes, flight Mach number and power setting. This requirement establishes the need for an exhaust system with some method of nozzle area control. Since the fans are also used for vertical thrust operation, the exhaust nozzle must additionally include some method of thrust vectoring. Exhaust nozzle systems of this type require moderate inlet velocities for reasonable pressure losses and levels of performance. For these studies, the maximum Mach number at the nozzle inlet was set at 0.55. This level of exhaust velocity required the fan system to operate at fan exit pressures greater than the ambient static pressures. The nozzle systems also include the confluent flow feature, that is, the turbine and fan discharge flows are mixed prior to entering the exhaust nozzle minimum area or throat. At the mixing station of the two flows, equal pressure levels are maintained. Thus, the turbine exit pressure is established by the pressure levels of the fan exit flow. For a turbine exit Mach number of 0.55, the turbine design exit pressure levels are established as a function of fan design conditions. The effects of this design criteria on fan and turbine discharge pressures are given in Figure 100 for the range of fan design pressure ratios between 1.2 and 1.7. These design criteria were consistent for both the single and two stage fan designs.

A cross-section drawing of the reference single stage fan design is shown in Figure 101. This fan design includes those special features as established during this study for application in the NASA military transport. A description of the design features is as follows:

Front Frame

The principal components of the front frame assembly are the struts, hub, dome and casing. The front frame is the main structural support for the rotor, transferring all rotor loads, gyroscopic moments and inertial forces through the scroll to the airframe mounts. The front frame incorporates a center hub for mounting the rotor bearings and three structural struts oriented 120 degrees apart. These struts restrict the relative axial deflections between the rotor and adjacent structure. The struts are pinned at the hub and scroll allowing the struts to follow radial movement due to thermal growth of the scroll.

The machined hub provides a load-carrying structure to transfer rotor loads to the three struts. The hub is a machined titanium forging with lugs for attachement to the struts.

Three equally spaced 9.0 inch cord struts provide the hub and rotor load-path to the scroll mounts. The struts are structural spars utilizing top and bottom cap strips supported by a continuous shear web. A honeycomb filler between the cap strips on each side of the web forms the required airfoil contour. The honeycomb is adhesive-bonded between the web and the aluminum face sheets.

The titanium honeycomb casing provides the aerodynamic outer flowpath at the fan inlet and provides the necessary structural rigidity for the forward air seal attachment. The casing is mounted to the scroll with 36 "A" frame brackets and is fabricated in two cylindrical sections to allow assembly to the scroll.

A flange at the forward edge provides for mating with the airframe bellmouth or nacelle. A formed "U" channel brazed to the aft edge provides for mounting of the forward air seal. Axial holes within the casing admit air from the fan cavity to the "U" channel and eject it through metering slots forward of the honeycomb seal. A 0.25 inch thick insulation blanket is attached on the scroll side of the casing to limit soak back temperatures at shutdown.

At the three locations where the scroll mount brackets penetrate the casing, the honeycomb is crushed to provide a flange with six anchor nuts riveted to the back side. These are used to mount a slip seal around each scroll mount bracket.

The dome provides the aerodynamic contour over the hub region of the front frame. The dome has cutouts at each strut location to allow unrestricted strut motion during fan operation. The dome is formed from 0.25 inch thick aluminum honeycomb sandwich.

The forward air seal assembly is attached to the aft inner surface of the casing. This seal assembly utilizes segmented open faced honeycomb mating with a single tooth seal lip on the rotor to restrict the hot gas leakage from the turbine inlet into the fan stream. A segmented slip seal brazed to the scroll and bolted to the casing controls leakage from the fan cavity, between the casing and scroll, into the turbine rotor inlet. The air deflector directs the hot gas seal leakage rearward to minimize effects on the incoming fan air stream.

<u>Scroll</u>

The turbine scroll distributes the engine exhaust gases through two 180 degree arms to feed the turbine nozzle annulus. The gas leaves the scroll through the nozzle partitions at a constant exit angle to drive the tip turbine. To minimize weight, a simple single bubble scroll is utilized. The scroll provides a load path to transfer front frame and casing loads to the airframe mounts. The scroll assembly incorporates the inlet elbows, bubble, nozzle partitions and exhaust section.

Two inlet elbows direct the inlet gas tangentially. These elbows provide a controlled area change to maintain a constant Mach number as the flow is turned and fed to the first section of nozzle partitions. The elbows have a flange at the inlet for bolting to the gas duct system. A partition separates the two inlets and provides the structural load path from the front frame strut to the airframe mount beneath the scroll inlets.

The bubble cross-sectional area decreases to maintain a constant Mach flow condition as the gas is distributed to the first 120 degree segment of the nozzle partitions. For structural reasons, the diameter remains constant from 120 degree to the 180 degree point, opposite the inlets.

The scroll exhaust consists of an inner flowpath to which the slip seal is brazed, and an outer flowpath which incorporates the rear frame flange. Both flowpaths are eloxed prior to brazing to accept the nozzle partitions.

Variation of the gas flow angles inside the scroll requires three different families of nozzle partitions to turn the gas and provide a constant nozzle discharge angle. Each cast nozzle partition has a local protuberance on the pressure side which establishes the throat area for the convergent-divergent supersonic nozzle design. The nozzles are twisted slightly because of the required canting relative to the buckets. The canted position is necessary in order to carry the bubble membrane loads across the partitions.

The three fan mounts, spaced 120 degrees apart, are machined brackets having a 1 inch diameter uniball for airframe mounting. A drag link mount clevis welded to the bubble is provided 180 degrees from the scroll inlet to accept one half of the fore and aft fan inertia loads and half of any residual scroll nozzle torque loads.

The outer surface of the scroll is covered with 0.50 inch thick Min-K insulation bagged in a quartz cloth blanket.

Rotor

The rotor incorporates a single stage fan and tip turbine. The fan stage has 88 high aspect ratio blades. Each has two part-span shrouds to control blade vibrations and torsional flutter. Torque transmission is accomplished through these part-span shrouds and a blade tip lockup. Each blade has a brazed turbine sector at its tip, and a single hook dovetail at the blade root for disk attachment. The fan blades are multiple circular arc airfoils. The inner fan flowpath is established by integral platforms on the blade root and the adjacent disk dovetail posts. The outer fan flowpath is defined by the fan blade tip shroud.

The turbine consists of 88 sectors, each containing three hollow uncooled shrouded buckets having integral tip shrouds with each turbine sector brazed to the tip of each fan blade.

The disk and shaft transmit blade and bucket loads to the bearings, and must have sufficient strength to limit rotor tip deflection to reasonably small clearance variations with the non-rotating parts. The titanium disk halves are electron beam welded together with the stud shaft an integral part of the forward disk. The disk rim is contour-machined to form the hub flowpath with blade retainer hooks located on the aft face of the rim.

The rotor is supported by two oil lubricated bearings, one deep-trough, angular-contact thrust bearing and one preloaded roller bearing. The roller bearing employs an out-of-round inner ring which loads the rollers to prevent skidding. The sump is a self-contained removable subassembly allowing the rotor to be balanced on its own bearings prior to fan assembly. The bearings and sump maintain rotor concentricity and alignment with non-rotating parts while transmitting rotor thrust, maneuver loads and other dynamic loads to the front frame. The bearing sump is sealed fore and aft with an air purged piston ring type seal. An oil slinger centrifuges the oil for discharge back to the gas generator oil tank. All oil is provided by the gas generator. The proposed bearing sump configuration may be modified into a grease packed configuration by replacement of minor components such as the seals and seal runners.

Rear Frame

The major components of the rear frame include the fan and turbine stator vanes, the fan and turbine exit flowpaths and the mid-box structure. Air loads induced on the fan stators are transferred through the mid-box and the turbine struts to the rear frame casing and then to the scroll. The rear frame accepts all stator aerodynamic and maneuver loading. A spherically shaped cover provides a seal across the hub of the fan, allows access to the rotor instrumentation and is flanged at the outer radius for bolting to the hub ring. A honeycomb filled structural box forms the hub ring to retain the inboard end of the fan stator vanes providing structural stiffness while its outer diameter provides the inner fan flowpath.

Fifty-six fan stator vanes are incorporated into the rear frame. The vanes are hollow titanium, double circular arc airfoil sections with a thickness to chord ratio of 5.0 percent. Actual vane chord is 3.83 inches and has a die formed internal stiffener brazed into each hollow vane. Two full-span hat sections provide stability for the vane skins to preclude buckling. A circumferential splitter at mid-span precludes an adverse flutter parameter.

The mid-box separates the fan and turbine exhaust streams and transfers vane loads through the mid-box to the turbine vanes. The structural portion of the titanium mid-box is a brazed circumferential box section with "U" channel stiffeners into which the stator vanes are brazed. The steel inner turbine flowpath is brazed to each of the 56 steel turbine vanes which in turn are brazed to the steel outer turbine casing. The inner and outer flowpaths provide the flow passage for the turbine exhaust. The aft edge of the inner flowpath is riveted to flexible leaves which bolt to the forward side of the mid-box. The turbine struts transfer the rear frame loads into the scroll.

A 0.25 inch thick Min-K insulation blanket bagged in a quartz cloth attaches to the inner surface of the inner flowpath to protect the mid-box from the turbine exhaust temperatures. The 16 segments of the aft air seal restrict the flow of hot gas from the turbine stream into the fan stream. The aft air seal bolts to the forward end of the mid-box. The open face honeycomb mates with a single tooth lip on the aft side of the rotor carrier.

Two Stage Fan Mechanical Design

The two stage fan concept represents a departure from the conventional single stage turbotip lift fan system. The single stage fan concept was derived to meet the requirements of high augmentation ratio, lightweight and low overall thickness as established for pod or wing mounted lift fans in VTOL aircraft systems. During the more recent evolution in VTOL aircraft systems, the trends of propulsion has been directed more towards higher fan pressure ratios with an associated reduction in augmentation ratios. One of the dominent factors pressing for higher pressure ratio has been the use of the turbotip lift fan for cruise, as well as the normal VTOL operation. The remote fan is usually installed in a conventional nacelle configuration where installed diameter and frontal area are significant factors. The single stage fan system has been an attractive configuration where the fan pressure ratios are below about 1.4. For higher pressure ratios, the fan inlet hub becomes excessively large because of rotor hub aerodynamic loading and limitations of fan tip speed of the tip turbine rotor. A comparison of possible method for reduction of fan tip speed and hub radius ratio showed that the two stage fan concept has the potential for an attractive high pressure remote fan system. The first stage rotor of the two stage fan is a conventional stage which is employed to develop about two-thirds of the overall system pressure rise. For the range of design pressure ratios considered, the first stage rotor can accept low inlet radius ratios with moderate fan tip speeds compatible with the levels for turbotip rotors. The overall installation dimensions are further reduced since the tip turbine is located on the second stage rotor and partially shielded behind the first stage rotor tip diameter.

A conceptual design study of this turbotip fan configuration was performed as part of this study. The fan configuration developed during this study is shown in Figure 102. The fan consists of two major static components, the scroll and the mid-frame, in addition to the two rotor systems. The following discussion describes the design features of the major components of the two stage fan system.

Frame

The principal components of the front frame are the hub, stator vanes, and outer flowpath ring structure. The frame is the structural support for the rotor, transferring all rotor loads, gyroscopic moments and inertia forces to the scroll from which they are transferred to the airframe mounts. The frame incorporates a center hub for mounting the rotor bearing housings and 27 stator vanes which act as struts to transfer hub loading to the scroll. The vanes restrict the relative axial deflections between the rotor components and the adjacent structure. On the pressure side of each vane at its intersection with the outer flowpath ring structure is an air scoop which picks up air for cooling the second stage air seal. The outer end of each stator vane is attached to an "A" frame link which is attached to the scroll thus allowing the rotor and frame assembly to remain concentric with the scroll during scroll thermal excursions.

The hub portion of the frame is a titanium fabricated assembly composed of a stationary shaft, upper and lower cover plates and 27 outer ring sectors. The hub is machined on the inside to accept the rotor bearing housing. The outer surface has machined circumferential flanges which accept the two cover plates and axial slots which accept the stator vane ends.

The 27 stator vanes are double circular arc airfoil sections having a 6.9 inch chord, 6.0 percent thickness and a 1.5 percent leading and trailing edge thickness. The vanes are fabricated from titanium using a hollow core section with solid leading and trailing edges. The hollow core consists of titanium honeycomb with.020 inch thick face sheets. Each vane section has machined ends for attachment to the scroll links. The outer flowpath casing is brazed to each of the vane assemblies.

The outer flowpath casing is an assembly composed of an upper and a lower section, as shown in Figure 103. The upper casing contains the honeycomb seal for the first stage rotor. The forward edge of the casing is flanged for attachment of the fan inlet flowpath casing, an aircraft component. The lower flange is provided for access during installation of the "A" frames for attachment of the scroll to the fan casing.

The lower section of the lower casing ring contains a fabricated cavity. This cavity provides a flowpath for directing cooling air over the second stage rotor tip seal. Cooling air is obtained from the scoops located on the pressure side of each of the stator vanes. This pressurized air is directed over the backside of the honeycomb seal and returned to the main flow just forward of the second rotor inlet plane. A laminated seal covers the gap between the frame casing and the scroll structure. This seal is required to prevent leakage of the hot turbine gases into the aircraft cavity that surrounds the fan. The seal assembly is fabricated to the scroll flow deflector and bolted to the frame casing during assembly.

Scroll

The turbine scroll distributes the engine exhaust gases through two 180 degree arms to feed the turbine nozzle annulus. To minimize weight, a simple single bubble scroll was considered for this reference design study. An alternate scroll configuration can be provided to further reduce the fan installation dimensions with attendent increases of fan weight. A typical alternate multi-feed scroll has previously been described. Other more specialized configurations are possible but will require a coordinated study and evaluation of the fan weight trade-off when compared to overall aircraft performance and weights.

The scroll assembly is a high temperature pressure vessel that makes use of circular cross-sections whenever possible. The scroll structural members are fabricated from cast or sheet metal René 41 material. This turbine inlet stators or nozzles are hollow vanes, cast to a 0.040 inch wall thickness. Each nozzle partition is brazed into the inner and outer bands of the scroll. This completed assembly provides the basic structure for attachment of the scroll bubble or flowpath.

The scroll flowpath, including the two inlets, is fabricated from 0.060 inch thick material. The fabricated structure is then chemically-milled to the required metal thickness, except at the areas of weldments.

The exhaust flowpath is formed by the two machined rings that contain the turbine inlet stators. The contours of these rings are established by the turbine design flowfield between the stator exit and rotor inlet. An interwoven leaf seal is riveted and brazed to the exhaust inner rings. This loop seal is required to span the scroll to frame gap that varies with scroll metal temperature. The total scroll assembly is then enclosed in an insulation blanket that consists of two layers of 0.002 inch foil and one-half inch of insulation.

General Rotor

The rotor assembly as shown in Figure 102 includes two compressor or fan stage operating on a single stub shaft with an integral concentric tip turbine located on the second stage rotor. The first stage rotor contains 50 blades with an aspect ratio of about 4.2. This first stage rotor presents a possible application of composite blade designs. For this case, the number of rotor blades would be reduced to 28 without either tip or mid-span shrouds.

The second stage rotor employs lightweight design and advanced fabrication methods as developed for the single stage fan systems. The second stage rotor contains 70 blades with an integral tip turbine assembly containing three turbine blades per fan blade. The second stage disk utilizes twin web geometry proven by operation in previous lift fan systems. An integral electron beam welded design is used to eliminate the need for through-bolted construction. The bearings employ inner race rotation and a preloaded roller bearing for skidding prevention. The preloaded bearing concept employs an out-of-round outer race for maintaining roller bearing pressure loads during operation when the external applied bonds are low. Previous lift fan experience has shown that a preloaded roller bearing design is required for fan systems that have a full 360 degeee turbine arc of admission.

The rotor offers the following design features:

- Integral blade and tip turbine sector.
- New high-strength blade alloy (René 95).
- Torque transmission by two blade part-span shrouds and a blade tip lockup.
- One-piece turbine bucket and tip shroud.
- Buckets designed for improved FOD resistance.
- High temperature bucket alloy, Udimet 700.
- Turbine assembly requires only one braze cycle.

- Electron beam welded disk with integral shaft and integral webs.

- Sump is a self-contained removable subassembly.

- Rotor that can be balanced on its own bearings prior to fan assembly.

Other design features include:

- Seventy high-aspect ratio fan blades each integrally joined to three low-aspect ratio turbine buckets.

- Single-hook blade dovetail design.

- Dovetail contact surfaces coated with copper-nickel-indium and Aquadag to minimum fretting and galling.

- Part-span and tip lockup contact surfaces hard-coated to minimize wear.

- Overhung disk.

- Hub flowpath formed by integrally contoured disk platform.

- Rotor supported by two bearings (one angular-contact thrust bearing and one preloaded roller bearing).

Stage 1 Rotor-Titanium

The first stage rotor, for the titanium design, contains 50 blades. The definition of these blades, chord, camber, stagger and thickness has been described in the previous section of the report covering the fan aerodynamic design. The blade material was selected to be 6-4 titanium, and with a 4 percent thickness, both tip and mid-span shrouds are required. The mid-span requirement was established by the torsional stability criteria of the rotor. The proposed design results in a reduced velocity parameter of 1.5 which is satisfactory for safe flutter-free operation.

The titanium design first stage rotor is a high flexural design having considerable margins over potential two and four per revolution stimulus. The mode shapes were determined for this design and are depicted in Figure 104. Stress levels were determined for design operation of the rotor and are summarized in Figures 105 through 107. Peak blade stresses of 40 to 50,000 psi (275 to 345 kN/mm^2) in the root region are acceptable for the selected blade material. The blades are attached to the disk by a single tang dovetail, with the hub flowpath formed by integral blade platforms.

Stage 1 Rotor-Composite

In view of the complexity and expense of the 50 Stage 1 titanium blades, which require a tip and midspan shroud, a study was undertaken to use hybrid composite blades. The advantages of such blades are many. First of all, it is a simple cantilevered blade of which fewer are required. In addition, composite materials are less notch sensitive thus maintaining high fatigue strength. Many different number of blades, blade thicknesses and material layups were explored to establish the best composite blade design. This study showed that the 28 blade design with a root thickness of 8 percent emerged as an excellent candidate. The blade is a "high flex" design which means the first flexural frequency crosses the 2 per rev line at 115 percent speed as shown in Figure 108. The first torsional reduced velocity is only 1.32 which is lower than that of the titanium blade and is representative of a higher stability margin. The blade airfoil geometry was scaled from that for the 50 blade titanium design and is plotted in Figure 109. A comparison of important data for the 50 blade titanium design and the 28 blade composite design is shown in Table XLIII. Average steady state centrifugal stresses at 100 percent speed are shown in Figure 110. They are quite low due to the low density of the composite material. For these blades, a hybrid polymetric composite material consisting of 50 volume percent graphite at $\pm 22°$ layup angle for transverse strength and torsional stiffness. Additional material properties are shown in Table XLIV.

The lower aspect ratio composite blade combined with its increased mass per blade should offer improved bird impact resistance over the metal blade. A fan layout with composite blades is shown on Figure 111.

Stage 2 Rotor

The second rotor contains 70 blades, each having an integrally attached turbine sector at the tip. The blade configuration is shown in Figure 112, and identifies the radial location of the two part span shrouds. The blades employ multiple circular arc airfoil designs with the geometry as previously defined. The outer fan flowpath is established by the fan blade tip shroud geometry with hub flowpath determined by the blade platforms combined with the adjacent dovetail posts.

Blade rigidity for frequency control and torque transmission is provided at the root by the dovetail, along the airfoil by part-span lockups near the 1/3 and 2/3 span points, and at the tip by the tip shroud lockup. Axial blade retention is provided in the forward direction by an integral hook on the dovetail aft face and in the aft direction by a blade retainer ring.

The exhaust gas temperature produces metal temperatures in the blade-turbine attachment region above the maximum design allowable temperature of any titanium alloy. For this reason, the blades are made of René 95, a relatively new nickel-base alloy. René 95 offers strength margins higher than other candidate blade materials at room temperature and at elevated temperatures.

The blade root attachment to the disk is made using a straight, single-hook dovetail with a 55° flank angle. Straight, single-hook dovetails are employed for ease of manufacture and reliability. Strength levels even at overspeed conditions are adequate. The dovetail and the dovetail shank extension to the airfoil are progressively stronger than the blade root, as required for good rotor design practices.

Airfoil centrifugal stress levels were evaluated at design speed and are shown in Figure 113. Mises-Hencky stresses are shown in Figure 114 and blade airfoil resultant spanwise stresses in Figure 115. Fundamental frequencies, node shapes and reduced velocity calculations are shown in Figure 116. This blade design yields a velocity parameter of 1.0 which is quite acceptable for good flutter stability margins.

The blade part-span shrouds are triangular platform extensions from the airfoil surface. The shrouds are located near the 1/3 and 2/3 span blade locations. Cross-sections through the shroud taken along flow streamlines are elliptical to reduce flow losses. Flat contact surfaces provide lockup between adjacent blades. The contact faces are set at 40 degrees from tangential to balance steady state and dynamic loading. A hard coating will be flame-sprayed onto the contact surface for long life. Torque transmission is provided by the part-span shrouds and the tip lockups during crossflow and partial scroll arc. Contact is assured between the blades at all times by installing the blades with pretwist at assembly. The upper part-span shroud is more highly stressed than the lower shroud. The combined stress in the upper shroud under total loading (centrifugal bending, assembly preload, airload untwist and torque transmission) is relatively low.

The blade tip section transitions from an airfoil into the blade tip shroud which forms the fan tip flowpath and supports the seal. The siderails support the turbine blades and transmit torque loads to the blade. The tip shroud and the siderails are machined as integral parts of the blade. The blade tip shroud, like the siderails, is tapered for better utilization of the René 95 material. No rupture life is consumed in the blade shroud; therefore, the limiting design criteria is fatigue. The seal is 0.015 inch thick and is formed from René 41 sheet. This single-tooth running seal rubs the stationary honeycomb seal strip on the front frame-bellmouth assembly, blocking hot gas leakage from the tip turbine into the fan. This seal supports only its own weight and is, therefore, not highly stressed. The seal is brazed to the fan tip shroud and is replaceable. The siderails are tapered along the tangential surface to obtain maximum material utilization and to reduce weight. The upper part of the siderails is in the same temperature environment as the braze. At these temperatures, only 25 percent of rupture life is consumed; therefore, fatigue is the limiting design criteria for the siderails.

Fan Weight Summery

At the conclusion of the conceptual design studies, the overall fan weight was estimated for the two base point designs. The total estimated weight of the single stage fan assembly was 998 pounds (453 kg) and 718 pounds (326 kg) for the two stage fan. Tables XLX and XLVI present the weight of the major fan components that contribute to the estimated total fan weight.

The weights of these referenced designs were used as the basis for estimating the parametric fan weights. The parametric weights were determined by scaling the major fan subassemblies.

TRANSIENT ANALYSIS

The response of lift fans to changes of inlet gas conditions is of prime importance when the thrust from the lift fans is used for aircraft altitude control. Therefore, as part of this study, a simplified transient analysis was performed to compare the response rates of the various fan designs including single and two stage fan systems.

Generalized Transient Response

The transient analysis is based on an idealized case where the response rates of the gas generator, ducting and control valves are treated as instantaneous functions. This type of analysis is representative of fan alone response, which has been shown in previous transient analysis to represent the major contribution to the overall system response. The analysis assumes a change of fan inlet gas conditions as would be experienced by the fan during power transfer with an ETC type control. The initial and final gas conditions are given in Table XLVII. These changes of gas conditions produce fan thrust excursions of about 20 percent of nominal lift.

In the study, only the fan experiencing the increased power levels was analyzed. During each control excursion, the corresponding opposite fan will experience small changes of gas energy and, consequently, small speed or thrust changes. The response of this opposite fan is an insignificant contribution to the overall system response. In addition, the opposite fan is subjected to thrust spoiling by an exit louver or nozzle system. The thrust spoiling method of control is very rapid with limits imposed only by the actuator rate. This fast thrust spoiling response, coupled with the slower increasing fan thrust, yields an effective control time constant intermediate between the response of the two fans.

This combination of power transfer and thrust spoiling for aircraft attitude control is demonstrated by the general type of performance characteristics shown in Figures 117 and 118. Figure 117 shows the typical variation of the thrusts of the two fans during power transfer. During the control excursion within the range of zero to maximum, the one fan experiences an increase of thrust while the opposite fan undergoes only small changes. In order to achieve constant total lift from the two fan systems, the fan thrust is spoiled on the low level fan by an amount equal to the thrust increase of the high level device.

The previous discussion represents the steady state performance for the system. Figure 118 shows the typical transient response of the system during ideal or instantaneous changes of fan inlet gas conditions. The lower figure shows the representative transients of both the increasing fan and the fan with thrust spoiling. Typical time constants for the response of the increasing fan are between 0.2 and 0.3 seconds, where the time constant, τ, is defined as the time required to achieve 63 percent of the steady state input control level. The time required to achieve thrust spoiling on the opposite fan is in the range of 0.1 to 0.15 seconds. These different response rates can be observed in the sketches. The total control moment is the thrust difference between the two fans taking into account the distance between fans as determined by the aircraft installation. The development of this moment is depicted in the figure. The effective time constant, or the time required to develop 63 percent of the commanded control moment, is indicated to be shorter than the increasing fan thrust change. Present aircraft control criteria requires a fan response representative of a time constant of less than 0.2 seconds. Through this combined system, control moment time constants, as required to meet the aircraft criteria, can be achieved.

The analysis procedure will employ an approximate method based on steady state fan aerodynamic performance in combination with transient changes of fan rotor speed.

The analysis procedure used was as follows:

- Initially, the fan is operating at some steady state condition.
- At some time interval, the gas conditions of the fan are instantaneously changed.
- This change of gas conditions produces a change of turbine power.
- Since the rotor speed cannot change instantaneously, this increased turbine power is utilized to change the rotor speed. The power required to drive the fan blading is simply a function of the fan rotational speed, thus

  Turbine Power = Fan Power + Rotor Inertia Power

- This torque balance is evaluated for a series of very small time increments throughout the complete transient. This analysis yields a variation of fan speed and thrust on a time basis.

This type of analysis was performed for both the single and two stage fan concepts. Figure 119 shows a typical set of fan steady state data used as input to the transient analysis. The gas conditions assumed at the fan turbine inlet are for the 3 second rating point, and are representative of the final conditions for a fan system receiving a maximum control input, The final steady state speed of 3788 RPM and thrust of 17,580 pounds are represented by the balanced power condition. The initial steady state conditions are established by the gas conditions prior to the control input. For this analysis, the initial operating point was established by the comparable 2 minute operating point. Table XLVIII gives the initial and final steady state conditions for the reference single and two stage fans used during the transient analyses.

Rotor Moment of Inertia

An essential input for the transient analysis is the rotor polar moment of inertia, since the excess energy during the transient is absorbed by this rotor inertia during the speed change. The rotor polar moment of inertia was evaluated for both single and two stage fan designs. The effects of fan pressure ratio and rotor design criteria are shown in Figures 120 and 121. The three rotor design criteria were:

- Fan Designed for Cruise with no requirement to operate with partial turbine admission arc. This is a reference design for comparison with other fan systems and does not represent a practical system design since the fan cannot absorb power transfer for control.

- Fan Designed for Cruise with requirement to operate with 240 degree arc during VTO and power transfer operation. The fan size is the same as the fan above, but the rotor inertia has increased because of the added requirement for partial arc operation. Partial arc operation requires a lower turbine bucket design stress criteria because of expected increased vibratory stress levels.

- Fan Designed for VTO with no requirement for partial arc operation. This rotor design criteria is similar to previous fan designs like the LF460. This rotor has larger inertias because of the increased diameters required to provide the control margin while operating with a 360 degree turbine admission arc.

During the transient analysis, the effects of fan scale factors on response were investigated. This analysis required estimates of effects of diameter on rotor inertias with all other design criteria fixed. The estimated effects of fan scale factor are shown in Figure 122.

Single Stage Fans

The transient analysis was performed for the two design types of single stage fans. Each fan was designed to develop a fan pressure ratio of 1.4 at the design point. The analysis was performed for fan operation at sea level static, hot day conditions.

The analysis procedures defined in the previous discussion were used to determine the fan transient characteristics as shown in Figures 123 and 124. These data show the time variation of fan speed during an increasing and decreasing thrust command. The effective time constant for both fan speed and thrust is identified in the figures. The fan thrust characteristics exhibit an unusual behavior at the beginning of the transients. This initial change of thrust, in unison with the changes of turbine inlet gas conditions, contributes to the smaller time constant for the thrust change as compared to the rotor speed. The estimated time constants, both thrust and speed, for the single stage fan systems are given in Table XLIX.

As part of the single stage fan transient analysis, a study was performed to investigate the effects of fan scaling on transient response. The fan system designed for VTO was selected for this analysis. All performance data were corrected to represent the scaled fan system. The rotor inertias were also corrected for fan size using the scale factors given in Figure 122. The results of this study, covering a large range of fan scaling, are shown in Figure 125. Increasing the fan size by a factor of two produces a fan time constant increase of about 40 percent. This change is small considering the rotor inertia has increased by a factor of about 22 to 1.

Two Stage Fans

A similar analysis was performed for the two design types of two stage fans. The reference fan design with a pressure ratio of 1.55 was used for the study. The estimated time constants for these fan system are listed in Table L. A comparison of a single and two stage time constants shows the improvements exhibited by the two stage fan concept. This improvement in time response can be attributed to the higher design pressure ratio and the attendent higher percentage of turbine residual thrust. In addition, the two stage fan concept operates at lower turbine wheel speeds that have a significant effect on reducing the response times because of the higher levels of turbine torque.

NOISE PREDICTIONS

The fan systems considered during this study were selected based on mechanical and performance qualities without concern for the levels of noise generation. For the selected configurations, the fan noise levels were generated as input study data for use during the concurrent aircraft studies. Noise levels were determined for representative designs including both single and twin stage fan systems, a range of design pressure ratios and systems designed for either cruise or VTO modes of operation. For each configuration, a vertical takeoff flight path was used to evaluate the noise levels on a 500 foot sideline. Systems were modeled to be representative of installations as either a pure lift or a lift plus cruise system. Figure 126 presents a schematic of the fan orientation used during these two analytical techniques.

The noise prediction procedures and techniques used for these lift fans were consistent with those used during previous studies of advanced commercial integral and remote lift fans and the LF460 lift fan systems. The following summarizes the procedures.

Noise Prediction Technique

The lift fan has several noise sources which must be evaluated to obtain the total system noise. Each source is predicted separately and a noise spectrum defined. The spectra are then added together to arrive at the total noise. The following summarizes the methods for predicting the noise constituents:

- Fan

  This is the major noise source in the fan and is made up of a puretone at the blade passing frequency and broadband noise. The puretone level is predicted analytically from the physical and aerodynamic fan characteristics. It is based on the interaction of the fan rotor wakes with the outlet guide vanes. Reference 7 describes the analysis in detail. Directivity patterns for the puretone are based on CF6 measured levels.

  The broadband noise is based on CF6 measurements correlated with rotor tip relative Mach number for level and tip physical Mach number for directivity.

- Fan Jet

  NASA large scale fan test acoustic data and GE scale model cold jet data were used to define a level of overall sound power level as a function of jet velocity. This curve was approximately 5 dB below the SAE line for jet noise extrapolated to velocities below 1000 ft/sec. The SAE spectrum shape was used along with GE cold jet directivity indices to define the noise at each angle.

- Turbine Jet

  The SAE jet noise curve was extrapolated to velocities below 1000 ft/sec for the hot turbine jet predictions. As with the cold fan jet, the SAE spectrum and GE directivity indices were used to define the noise at each angle.

- Turbine

  A puretone level is defined using the same type rotor-stator interaction as used in the fan noise analysis. The directivity indices are based on Rolls Royce and GE data. The associated broadband noise was also estimated from Rolls Royce and GE engine data.

Figure 127 shows graphically the procedure used in defining the spectrum for each noise source and the summation to obtain total system noise. The fan systems modeled in this analysis did not include normal noise reduction features such as suppression, rotor-stator vane ratio optimization, stator lean or rotor-stator spacing.

Estimated Noise Levels

Noise levels were estimated for six specific fan configurations. Single stage fans with design pressure ratios of 1.4 were considered. Twin stage fans at design pressure ratios of 1.4 and 1.55 were included in the analysis to show the effects of both design pressure and number of fan stages. Table LI summarizes the significant feature of each of the fan designs, and includes the fan operating conditions at the 2 minute operation point where the VTO noise estimates were generated.

Noise levels were predicted on a 500 foot (152.4 meters) for a vertical takeoff trajectory. Operation as a pure lift fan and a lift plus cruise fan was modeled during the analysis. Based on the flyover prediction techniques, the maximum perceived noise levels occur at an altitude of about 250 feet. For the lift fan configuration, the maximum occurs at a ground angle of 90 degrees. The lift plus cruise fan configuration exhibited the higher maximum noise level at a 70 degree angle because of the higher levels of inlet radiated noise. The estimated maximum sideline perceived noise levels for the six fan configurations operating in both the lift and lift/cruise installation are given in Table LII. The estimate for the single fan configurations include variations in overall fan thrust. A more representative comparison is at an equal thrust level. This comparison is also included in the table for a total fan system thrust of 60,000 pounds (267 kN). The individual constituents included in the total noise at the maximum perceived noise level location are given in Figure 128.

CONCLUSIONS

1. Parametric design and performance data were provided for use in concurrent aircraft studies for a system that meets the Carrier On-Board Delivery (COD) mission of the sea control ship. These aircraft studies have shown that the remote turbotip lift fan propulsion system is an attractive system for this application. The typical aircraft for this mission employed three or four lift fans and gas generators. All fans were operating during VTO with a two fan/engine system used for conventional cruise operation. The aircraft gross weight was about 40,000 pounds (178 kN).

2. The conceptual design studies included both single and two stage fan systems. A comparison of the two concepts showed that the two stage system requires a smaller installation diameter at all design pressure ratios. The smaller diameter exists because of a smaller fan inlet hub, relative to the single stage system, and smaller overall scroll diameter. Comparison of fan plus engine weight shows that the two stage system is lighter for fan design pressure ratios above about 1.4. At lower pressure ratios, the single stage fan is the lighter weight system.

3. The two stage fan concept is a potential system for application of composite first stage rotor blading. A comparison of composite and titanium rotor designs showed little difference in overall weight. The application of composites must be justified based on reduced costs and improved bird strike capability.

4. An analysis of the transient response of single and two stage fan systems showed that both fan systems exhibit similar levels of time constant. Fan only time constants of 0.15 to 0.25 were calculated. This level of response should be adequate for meeting the aircraft systems requirements when used with the ETC type control method which also includes thrust spoiling for rapid thrust control.

5. The scroll designs used in the generation of these parametric data were established for minimum weight. Scroll modification to reduce installation dimensions, at some increase in weight, should be evaluated relative to the complete aircraft systems weight and performance.

6. The turbotip rotor used as the basis for these studies employs integral fan turbine blade assemblies. The number of rotor blades was established by minimum rotor weight and, therefore, require double mid-span shrouds for acceptable torsional flutter stability. The reliability and ruggedness of these thin complex blades are items of concern for the application as a cruise fan system. Additional studies are required to determine the weight trade-off for reduced numbers of blades for reduced costs and improved ruggedness.

7. Noise levels were determined for six fan configurations operating as either pure lift fans (fan axis vertical), and lift plus cruise fans (fan axis horizontal). Normalized to a total system thrust of 60,000 pounds (267 kN), the fans designed for a 1.4 pressure ratio are quietest with a maximum sideline perceived noise level of 117 PNdB for the cruise type design. The loudest fan was the 1.55 pressure ratio designed for VTO where the estimated perceived noise level was 122.7 PNdB.

NOMENCLATURE

Symbol	Definition	Units
A	Area	in^2 (m^2)
C	Blade Chord	in (cm)
C_V	Nozzle Velocity Coefficient	-----
D	Diameter	in (m)
D-F	Diffusion Factor	-----
E	Tensile Modulus	psi (kN/mm^2)
F	Thrust, Force	lb (kN)
g	Gravitational Constant	ft/sec^2 (m/sec^2)
G	Shear Modulus	psi (kN/mm^2)
h	Enthalpy	BTU/lb (Joules/kg)
HP	Horsepower	HP (kW)
Ip	Polar Moment of Inertia	lb ft sec^2 (kg m sec^2)
J	Joule's Constant	ft lb/BTU (---)
L	Lift	lb (kg)
LC	Lift Control	pct (pct)
M	Mach Number	-----
n	Weight Scaling Exponent	-----
N	Rotational Speed	pct (pct)
P	Pressure	psi (kN/m^2)
PNdB	Precieved Noise Level	dB (dB)
PS	Gas Generator Power Setting	-----
R	Radius	in (cm)
t	Time	sec (sec)
tm	Blade Maximum Thickness	in (cm)
T	Temperature	° R (° K)
U	Tangential Speed	ft/sec (m/sec)
W	Flow Rate	lb/sec (kg/sec)
WT	Gas Generator Weight	lb (kg)
β_{1C}	Angle of Gas Entering Blade Row	deg (deg)
β_{2C}	Angle of Gas Leaving Blade Row	deg (deg)
β^*_{1C}	Blade Leading Edge Angle	deg (deg)
β^*_{2C}	Blade Trailing Edge Angle	deg (deg)

Symbol	Definition	Units
β_S	Stagger Angle	deg (deg)
δ	Standard Pressure Correction	-----
η	Efficiency	pct (pct)
θ	Standard Temperature Correction	-----
σ	Stress	ksi (kN/mm^2)
τ	Time Constant	sec (sec)

Subscripts

B	Gas Generator Bleed
DR	Ram
F	Fan, Fuel, Thrust
G	Gross, Gas Generator
N	Speed, Net, Nozzle
r	Recovery
SLS	Sea Level Static
T	Tip, Total
W	Water
0	Ambient
2	Gas Generator Compressor Inlet
4	Gas Generator Turbine Inlet
51	Gas Generator Turbine Discharge
54	Fan Turbine Inlet
22	Fan Compressor Inlet

REFERENCES

1. General Electric Company, Aircraft Engine Group, Cincinnati, Ohio 45215: LF460 Detail Design, NASA Contractor Report NASA CR-120787, September 1971.

2. McDonnell Aircraft Company, Saint Louis, Missouri, 63166: A Full Scale Test of a New V/STOL Control System, Energy Transfer Control (ETC), Report No. MDC A1588, June 1972.

3. General Electric Company, Aircraft Engine Group, Cincinnati, Ohio 45215: Engine, Aircraft, Turbojet, J101-GE-100, Model Specification E1193, May 1971.

4. General Electric Company, Aircraft Engine Group, Cincinnati, Ohio 45215: LF460 Detail Design Final Technical Report on Aircraft Support Activity, NASA Contractor Report NAS CR-121146.

5. General Electric Company, Aircraft Engine Group, Cincinnati, Ohio 45215: RLF-J97 Turbotip Lift Fan Propulsion System, Report No. R72AEG153, April 1972.

6. Katsanis, T.; National Aeronautics and Space Administration, Washington, D.C.: Use of Quasi-Orthogonals for Calculating Flow Distributions in the Meridional Plane of a Turbomachine, NASA Report TN D-2546, December 1964.

7. Phipps, W.H., and Kazin, S.B.; General Electric Company, Aircraft Engine Group, Cincinnati, Ohio 45215: FAINT - A Computer Program to Predict Aerodynamically Produced Noise Transmission, Report No. R69AEG129, February 1969.

Table I. Lift Fan Gas Generator Comparison.

Gas Generator	W_2 (lb/sec)	W_2 (kg/sec)	T_4 (°R)	T_4 (°K)	T_{51} (°R)	T_{51} (°K)	P_{51} (lb/in^2)	P_{51} (kN/m^2)	(HP)	(kW)	HP/W2		HP/WT		$(\sqrt{T}/P)5.1$	
T58-3	12.4	5.62	2170	1205	1693	940	36.3	350	1524	1136	123	202	5.3	8.6	1.14	0.123
T58-16	13.9	6.30	2450	1361	1905	1058	42.0	290	2380	1775	171	282	8.2	13.5	1.04	0.112
T64-6	24.5	11.1	2200	1222	1600	889	39.5	272	3340	2491	136	224	6.1	10.0	1.01	0.110
T64-16	28.2	12.8	2434	1352	1785	992	47.1	325	4940	3684	175	288	9.0	14.8	0.90	0.097
J85-5	43.7	19.8	2100	1167	1711	950	34.6	239	5640	4206	129	212	16.1	26.5	1.04	0.129
J85-21	51.9	23.5	2256	1253	18.5	1008	39.8	274	8210	6122	158	261	18.9	31.0	1.07	0.116
YJ97	70.0	31.8	2494	1385	1833	1018	51.4	354	13450	10030	192	315	18.7	30.7	0.83	0.090
J101	126.7	57.5	2935	1630	1773	985	54.6	376	24820	18510	195	322	17.6	28.9	0.77	0.083

Table II. "Short-Time" VTO Ratings.
(Sea Level Static, Uninstalled)

Rating	T_O (°R)	T_O (°K)	N_G (Percent)	W_W (lb/sec)	W_W (kg/sec)	W_F (lb/hr)	W_F (kg/hr)
Intermediate	518.7	288.2	105	0	0	8415	3816
Intermediate	549.7	305.4	103.85	0	0	7808	3542
VTO (Nom)	549.7	305.4	106	0	0	8416	3817
VTO (Max)	549.7	305.4	106	0	0	9532	4324
VTO (Emer)	549.7	305.4	110	0	0	9082	4120
VTO (Nom)	549.7	305.4	110	3	1.36	10085	4574
VTO (Max)	549.7	305.4	110	3	1.36	11087	5029
VTO (Emer)	549.7	305.4	115	6	2.72	11837	5369

Rating	P_{51} (lb/in^2)	P_{51} (kN/m^2)	T_{51} (°R)	T_{51} (°K)	W_{51} (lb/sec)	W_{51} (kg/sec)	HP_{51} (HP)	HP_{51} (kW)
Intermediate	54.60	376.5	1773	985	128.6	58.33	24817	18506
Intermediate	50.35	347.1	1775	986	121.9	55.39	22307	16634
VTO (Nom)	53.51	368.9	1845	1025	123.5	56.02	24511	18278
VTO (Max)	61.32	422.8	1998	1110	123.6	56.06	28944	21584
VTO (Emer)	55.63	383.6	1912	1062	126.0	57.15	26607	19841
VTO (Nom)	58.92	406.2	1899	1055	129.3	58.64	28098	20953
VTO (Max)	65.22	449.7	2026	1125	129.4	58.69	31905	23792
VTO (Emer)	62.86	433.4	1960	1089	134.7	61.10	31426	23434

Table III. Gas Generator Installation Assumptions.

Engine Inlet Total Pressure Recovery	0.99
Customer Bleed	0.5%
Power Extraction	20 HP (15 kW)

Table IV. "Short-Time" VTO Ratings.
(Sea Level Static, Installed)

Rating	T_o (°R)	T_o (°K)	N_G (Percent)	W_W (lb/sec)	W_W (kg/sec)	W_F (lb/hr)	W_F (kg/hr)	P_{51} (lb/in^2)	P_{51} (kN/m^2)	T_{51} (°R)	T_{51} (°K)	W_{51} (lb/sec)	W_{51} (kg/m^2)	HP_{51} (HP)	HP_{51} (kW)
Intermediate	518.7	288.2	105	0	0	8324	3776	53.63	369.8	1773	985	126.8	57.51	24186	18035
Intermediate	549.7	305.4	103.85	0	0	7706	3495	49.29	339.8	1773	985	120.2	54.52	21644	16140
VTO (Nom)	549.7	305.4	106	0	0	8332	3779	52.60	362.7	1846	1026	121.8	55.25	23913	17832
VTO (Max)	549.7	305.4	106	0	0	9419	4272	60.22	415.2	1997	1109	121.9	55.29	28277	21086
VTO (Emerg)	549.7	305.4	110	0	0	8987	4076	54.67	376.9	1913	1063	124.3	56.38	25971	19366
VTO (Nom)	549.7	305.4	110	3	1.36	9970	4522	57.85	398.9	1898	1054	127.5	57.83	27383	20420
VTO (Max)	549.7	305.4	110	3	1.36	10945	4965	64.01	441.3	2073	1124	127.6	57.88	31083	23179
VTO (Emerg)	549.7	305.4	115	6	2.75	11695	5305	61.68	425.3	1957	1087	132.8	60.24	30595	22815

Table V. Estimated Installed Gas Generator Performance.

Altitude (ft)	Altitude (m)	M_0	$NF/\sqrt{\theta}$ (pct)	$W_2\sqrt{\theta_0}/\delta$ (lb/sec)	$W_2\sqrt{\theta_0}/\delta$ (kg/sec)	$W_F/\delta_0\sqrt{\theta_0}$ (lb/hr)	$W_F/\delta_0\sqrt{\theta_0}$ (kg/hr)	P_{51}/δ_0 (lb/in^2)	P_{51}/δ_0 (kN/m^2)	T_{51}/θ_0 (°R)	T_{51}/θ_0 (°K)	$W_{51}\sqrt{\theta_0}/\delta_0$ (lb/sec)	$W_{51}\sqrt{\theta_0}/\delta_0$ (kg/sec)	T_B/θ_0 (°R)	T_B/θ_0 (°K)	P_B/δ_0 (lb/in^2)	P_B/δ_0 (kN/m^2)
0	0	0	105	125.4	56.88	8324	3776	53.63	369.8	1773	986	126.8	57.51	1203	668	177	1220
			97.80	118.0	53.52	6943	3159	48.36	333.4	1642	912	119.0	53.98	1154	641	156	1076
			91.83	105.0	47.62	5259	2385	40.67	280.4	1484	824	105.7	47.94	1089	605	131	903
			84.50	87.9	39.87	3497	1586	31.67	218.3	1297	720	88.2	40.01	1010	561	102	903
			75.00	71.4	32.38	2141	971	23.67	163.2	1114	619	71.5	32.43	928	516	77	531
0	0	0.2	104.8	128.0	58.06	8512	3861	54.84	378.1	1779	988	129.4	58.69	1208	671	181	1248
			97.69	120.0	54.43	7043	3195	49.18	339.1	1643	913	121.0	54.68	1158	643	159	1096
			91.79	106.4	48.26	5311	2409	41.24	284.3	1484	824	107.1	48.58	1092	607	133	917
			84.53	89.4	40.55	3559	1614	32.27	222.5	1301	723	89.7	40.69	1015	564	103	710
			75.14	72.8	33.02	2196	996	24.26	167.3	1121	823	73.0	33.11	934	519	78	538
0	0	0.4	104.4	136.0	61.69	9087	4122	58.55	403.7	1794	997	137.5	62.37	1225	680	193	1331
			97.37	126.0	57.15	7350	3334	51.69	356.4	1648	916	127.1	57.65	1169	649	166	1144
			91.66	110.7	50.21	5452	2493	42.89	295.7	1484	824	111.4	50.53	1102	612	138	952
			84.63	93.9	42.59	3741	1697	34.07	234.9	1313	729	94.3	42.77	1029	572	109	751
			75.56	77.4	35.11	2363	1072	26.02	179.4	1140	633	77.6	35.20	952	529	84	579
0	0	0.6	103.11	149.2	67.68	9939	4508	64.46	444.4	1809	1005	150.8	69.40	1249	694	210	1448
			96.83	134.7	61.10	7714	3499	55.24	380.9	1647	915	135.8	61.60	1185	658	177	1221
			91.44	118.8	53.89	5783	2623	46.15	318.2	1493	829	119.5	54.20	1121	623	148	1020
			84.80	101.7	46.13	4051	1837	37.17	256.3	1332	740	102.1	46.31	1053	585	119	820
			76.26	85.5	38.78	2663	1208	29.14	200.9	1171	650	85.6	38.82	981	545	94	648
15000	4572	0.2	110.9	131.1	59.46	9333	4233	57.58	397.0	1880	1044	132.4	60.05	1255	697	191	1317
			106.4	129.0	58.51	8608	3904	55.33	381.5	1800	1000	130.1	59.01	1225	680	184	1269
			98.8	121.9	55.29	7219	3274	50.12	345.6	1665	925	122.8	55.70	1174	652	163	1124
			89.8	101.3	45.95	4669	2118	38.28	293.9	1427	793	101.7	46.13	1074	597	123	848
			77.7	76.5	34.70	2468	1119	25.96	179.0	1166	648	76.6	34.75	958	532	84	579
15000	4572	0.4	110.9	140.1	63.55	10045	4556	61.90	426.7	1900	1056	141.5	64.23	1273	707	206	1420
			106.0	137.3	62.27	9208	4177	59.21	407.6	1817	1009	138.6	62.87	1243	691	196	1351
			98.3	127.7	57.92	7501	3402	52.54	362.2	1667	926	128.7	58.38	1185	658	170	1172
			89.7	105.9	48.03	4854	2202	40.10	276.4	1433	796	106.4	48.36	1087	604	129	889
			78.0	81.2	36.83	2640	1197	27.75	191.3	1183	657	81.3	36.88	976	542	90	621
15000	4572	0.6	110.9	155.8	70.67	11335	5141	69.56	479.6	1938	1077	157.4	71.40	1307	726	231	1593
			104.7	151.0	68.49	10121	4591	65.46	451.3	1835	1019	152.4	69.13	1268	704	215	1482
			97.7	137.2	62.33	7928	3596	56.47	389.3	1669	927	138.2	62.68	1202	668	182	1255
			89.5	113.4	51.44	5129	2326	43.10	297.6	1441	801	113.9	51.66	1106	614	139	958
			79.6	89.4	40.55	2956	1341	30.96	213.4	1213	694	89.5	40.60	1005	558	100	689

Table V. Estimated Installed Gas Generator Performance. (Continued)

Altitude (ft)	Altitude (m)	M_0	$NF/\sqrt{\theta}$ (pct)	$W_2\sqrt{\theta_o}/\delta$ (lb/sec)	$W_2\sqrt{\theta_o}/\delta$ (kg/sec)	$W_F/\delta_o\sqrt{\theta_o}$ (lb/hr)	$W_F/\delta_o\sqrt{\theta_o}$ (kg/hr)	P_{51}/δ_o (lb/in^2)	P_{51}/δ_o (kN/m^2)	T_{51}/θ_o (°R)	T_{51}/θ_o (°K)	$W_{51}\sqrt{\theta_o}/\delta_o$ (lb/sec)	$W_{51}\sqrt{\theta_o}/\delta_o$ (kg/sec)	T_B/θ_o (°R)	T_B/θ_o (°K)	P_B/δ_o (lb/in^2)	P_B/δ_o (kN/m^2)
36000	10973	0.2	114.4	132.0	59.87	9893	4487	58.98	406.6	1970	1094	133.0	60.33	1301	723	195	1344
			111.2	131.1	59.46	9256	4198	57.38	395.6	1890	1050	132.1	59.92	1269	705	191	1317
			103.4	126.9	57.56	8002	3926	53.28	376.3	1756	976	127.6	57.88	1217	676	176	1213
			93.1	109.3	49.58	5566	2525	42.62	293.9	1531	851	109.6	49.71	1123	624	138	951
			79.7	78.4	35.56	2940	1334	27.20	187.5	1224	680	78.5	35.61	979	544	87	600
36000	10973	0.4	115.8	141.6	64.22	10890	4940	64.11	442.0	2017	1121	142.8	64.77	1331	739	212	1462
			112.4	140.7	63.82	10155	4606	62.23	429.1	1931	1073	141.7	64.27	1296	720	207	1427
			104.5	136.1	61.74	8793	3988	57.82	398.7	1795	997	136.9	62.10	1245	692	191	1316
			94.1	117.1	53.12	6100	2967	46.23	318.7	1564	869	117.5	53.29	1147	637	149	1027
			80.5	84.2	38.19	3166	1436	29.47	203.2	1248	693	84.2	38.19	1002	557	95	655
36000	10973	0.6	118.0	158.7	71.98	12730	5774	73.33	505.6	2096	1164	160.1	72.62	1381	767	242	1668
			114.3	157.6	71.49	11870	5384	71.07	490.0	2000	1111	158.8	72.03	1342	746	237	1634
			106.4	152.5	69.17	10263	4655	66.07	455.5	1862	1034	153.4	69.58	1290	717	218	1503
			95.9	131.1	59.47	7082	3212	52.70	363.3	1620	890	131.6	59.69	1189	661	171	1179
			82.0	94.4	42.82	3567	1622	33.61	231.7	1288	716	94.5	48.86	1038	577	108	745
36000	10973	0.8	121.0	184.9	83.87	15674	7110	87.83	605.6	2203	1223	186.7	84.68	1450	806	290	1999
			116.9	183.5	83.23	14467	6562	84.93	585.5	2097	1165	185.1	83.96	1406	781	283	1951
			109.0	177.6	80.56	21617	5723	79.05	545.0	1958	1088	178.8	81.10	1354	752	261	1799
			98.2	152.5	69.17	8670	3933	62.91	433.7	1700	944	153.2	69.49	1248	693	203	1400
			84.0	110.1	49.94	4219	1913	40.17	277.0	1349	749	110.3	50.03	1091	606	129	889
36000	10973	1.0	121.0	221.0	100.24	18835	8543	106.2	732.2	2245	1247	233.4	101.33	1495	831	353	2434
			116.2	217.6	98.70	17370	7879	102.0	703.3	2149	1194	219.6	99.61	1460	811	338	2330
			107.8	205.7	93.30	14610	6627	92.46	637.5	1991	1106	207.2	93.98	1401	778	300	2068
			98.0	170.5	77.34	9446	4284	70.53	486.3	1708	948	171.3	77.70	1281	717	227	1565
			84.8	128.7	58.38	5016	2275	47.79	329.5	1393	774	128.9	58.46	1143	635	154	1062
45000	13716	0.2	114.5	131.3	59.56	10160	4605	59.37	409.3	2010	1117	132.3	60.01	1305	725	196	1351
			111.2	130.5	59.19	9505	4311	57.66	397.6	1927	1070	131.4	59.60	1274	708	190	1311
			103.4	125.3	56.83	8227	3731	53.56	369.3	1793	996	126.7	57.47	1222	679	173	1193
			93.1	107.8	48.89	5774	2619	42.68	294.3	1575	876	108.2	49.08	1127	626	136	938
			88.1	94.9	43.05	4536	2057	35.91	247.6	1446	803	95.2	43.18	1069	594	114	786
45000	13716	0.4	115.8	140.9	63.91	11138	5052	64.43	444.2	2052	1140	142.1	64.45	1334	741	213	1468
			112.4	140.0	62.52	16389	4734	62.52	431.1	1964	1091	141.0	63.96	1301	723	207	1427
			104.5	135.2	61.33	9016	4090	58.00	399.9	1829	1016	136.0	61.69	1250	694	189	1303
			94.2	115.5	52.39	6303	2859	46.23	318.7	1605	892	116.0	52.62	1152	640	148	1020
			87.0	96.6	43.82	4457	2022	36.25	249.9	1423	790	96.9	43.95	1069	594	115	792

Table V. Estimated Installed Gas Generator Performance. (Concluded)

Altitude (ft)	Altitude (m)	M_o	$NF/\sqrt{\theta}$ (pct)	$W_2\sqrt{\theta_o}/\delta$ (lb/sec)	$W_2\sqrt{\theta_o}/\delta$ (kg/sec)	$W_F/\delta_o\sqrt{\theta_o}$ (lb/hr)	$W_F/\delta_o\sqrt{\theta_o}$ (kg/hr)	P_{51}/δ_o (lb/in^2)	P_{51}/δ_o (kN/m^2)	T_{51}/θ_o (°R)	T_{51}/θ_o (°K)	$W_{51}\sqrt{\theta_o}/\delta_o$ (lb/sec)	$W_{51}\sqrt{\theta_o}/\delta_o$ (kg/sec)	T_B/θ_o (°R)	T_B/θ_o (°K)	P_B/δ_o (lb/in^2)	P_B/δ_o (kN/m^2)
45000	13716	0.6	118.1	157.9	71.62	12937	5868	73.60	507.5	2123	1179	159.4	72.30	1383	768	243	1675
			114.3	156.9	71.17	12006	5446	71.27	491.4	2026	1126	158.1	71.27	1346	748	237	1634
			106.4	151.4	68.67	10460	4744	66.28	457.0	1890	1050	152.5	69.04	1295	719	216	1489
			95.9	129.5	58.74	7265	3295	52.66	363.1	1655	919	130.1	59.01	1193	663	169	1165
			85.0	99.5	45.13	4331	1965	36.87	254.2	1391	773	99.7	45.22	1072	596	117	807
45000	13716	0.8	121.1	184.0	83.45	15840	7185	87.96	606.4	2224	1235	185.9	84.32	1451	806	290	1999
			116.9	182.7	82.87	14609	6626	84.88	585.2	2115	1175	184.4	83.64	1408	782	281	1937
			109.1	176.6	80.10	12771	5193	79.07	545.2	1978	1099	177.9	80.69	1358	754	259	1786
			98.3	150.9	68.45	8834	4007	62.79	432.9	1728	960	151.7	68.81	1252	896	203	1400
			84.1	108.2	49.08	4496	2039	40.08	276.3	1387	771	108.5	49.21	1095	608	128	882
45000	13716	1.0	121.1	220.2	99.88	18956	8298	106.1	731.5	2246	1248	222.4	100.88	1498	832	352	2427
			116.2	216.7	98.29	17512	7943	101.9	702.6	2164	1202	218.7	99.20	1463	813	337	2323
			107.9	204.4	92.71	14712	6673	92.27	636.2	2006	1114	205.9	93.39	1403	779	298	2055
			98.1	168.8	76.57	9553	4333	70.18	483.9	1726	959	169.6	76.93	1283	713	225	1551
			84.9	126.8	57.52	5175	2347	47.67	328.7	1430	794	127.0	57.60	1145	636	153	1055

Table VI. Engine Discharge and Fan Turbine Inlet Design Point Parameters.

	Design for Cruise (1)	Design for VTO (2)
Ambient Temperature, °R (°K)	518.69 (288.2)	549.69 (305.4)
Ambient Pressure, psia (kN/m^2)	14.696 (101.33)	14.696 (101.33)
Engine Discharge Flow, lb/sec (kg/sec)	128.58 (58.32)	123.55 (56.04)
Engine Discharge Temperature, °R (°K)	1772.5 (985)	1997.9 (1110)
Engine Discharge Pressure, psia (kN/m^2)	54.60 (376.5)	61.32 (422.8)
Engine Main Fuel Flow, lb/hr (kg/hr)	8415 (3817)	9532 (4323)
Fan Turbine Inlet Flow, lb/sec (kg/hr)	128.58 (58.32)	135.88 (61.50)
Fan Turbine Inlet Pressure, psia (kN/m^2)	50.23 (346.3)	56.41 (388.9)

(1) J101 engine at intermediate power setting.

(2) J101 engine at three second, VTO rating. Fan flow includes power transfer.

Table VII. Design Point Parameters for Single Stage Fans Designed for VTO, SLS, 90° F (305° K) Day, Uninstalled.

Fan Pressure Ratio	1.2	1.3	1.4	1.5
Fan Tip Speed, ft/sec (m/sec)	1158 (353.0)	1158 (353.0)	1158 (353.0)	1158 (353.0)
Fan Tip Diameter, inches (m)	103.05 (2.62)	83.43 (2.12)	73.72 (1.87)	67.08 (1.70)
Fan Inlet Radius Ratio	0.400	0.412	0.471	0.522
Fan Exit Mach Number	0.55	0.55	0.55	0.55
Fan Efficiency	0.843	0.843	0.843	0.843
Fan Airflow, lb/sec (kg/sec)	1846.5 (837.6)	1215.7 (551.4)	888.8 (403.1)	687.8 (312.0)
Turbine Inlet Temperature, °R (°K)	1998 (1110)	1998 (1110)	1998 (1110)	1998 (1110)
Turbine Inlet Pressure, lb/in^2 (kN/m^2)	56.41 (388.9)	56.41 (388.9)	56.41 (388.9)	56.41 (388.9)
Turbine Inlet Flow, lb/sec (kg/sec)	135.58 (61.50)	135.58 (61.50)	135.58 (61.50)	135.58 (61.50)
Turbine Exit Static Pressure Ratio	0.98	1.06	1.14	1.22
Turbine Exit Mach Number	0.55	0.55	0.55	0.55
Interconnect Duct Pressure Loss (Engine Exit to Scroll Inlet), pct.	3	3	3	3
Scroll Pressure Loss, pct.	5	5	5	5
Ideal Thrust, lbs (kN)	37166 (165.3)	31205 (138.8)	27466 (122.2)	24825 (110.4)
Nozzle Area, sq. in. (m^2)	7114 (4.590)	4098 (2.644)	2781 (1.794)	2069 (1.335)

Table VIII. Design Point Parameters for Single Stage Fans Designed for Cruise, SLS, Standard Day, Uninstalled.

Fan Pressure Ratio	1.2	1.3	1.4	1.5
Fan Tip Speed, ft/sec (m/sec)	1125 (342.9)	1125 (342.9)	1125 (342.9	1125 (342.9)
Fan Tip Diameter, inches (m)	92.27 (2.34)	74.22 (1.89)	64.96 (1.65)	58.47 (1.49)
Fan Inlet Radius Ratio	0.400	0.412	0.471	0.522
Fan Exit Mach Number	0.55	0.55	0.55	0.55
Fan Efficiency	0.843	0.843	0.843	0.843
Fan Airflow, lb/sec (kg/sec)	1527.3 (692.8)	992.4 (450.1)	712.2 (323.0)	529.5 (242.9)
Turbine Inlet Temperature, °R (°K)	1773 (985)	1773 (985)	1773 (985)	1773 (985)
Turbine Inlet Pressure, lb/in^2 (kN/m^2)	50.23 (346.3)	50.23 (346.3)	50.23 (346.3)	50.23 (346.3)
Turbine Inlet Flow, lb/sec (kg/sec)	128.58 (58.32)	128.58 (58.32)	128.58 (58.32)	128.58 (58.32)
Turbine Exit Static Pressure Ratio	0.98	1.06	1.14	1.22
Turbine Exit Mach Number	0.55	0.55	0.55	0.55
Interconnect Duct Pressure Loss, pct (Engine Exit to Scroll Inlet)	3	3	3	3
Scroll Pressure Loss, pct.	5	5	5	5
Ideal Thrust, lbs (kN)	30249 (134.6)	25263 (112.4)	22054 (98.1)	19762 (87.9)
Nozzle Area, sq in (m^2)	5786 (3.733)	3316 (2.139)	2232 (1.440)	1647 (1.063)

Table IX. Gas Generator and Fan Installation Parameters.

Engine Inlet Recovery	0.99
Customer Bleed	0.5 percent
Power Extraction	20 horsepower (15 kilowatts)
Interconnect Duct Loss (Engine Exit to Scroll Inlet)	3 percent
Scroll Pressure Loss	5 percent
Fan Inlet Recovery	0.985
Exhaust Nozzle Velocity Coefficient	0.98

Table X. VTO Performance of Single Stage Fans Designed for VTO, SLS, 90° F (305° K) Day, Installed.

	Intermediate Std Day, 360°	Intermediate Hot Day, 360°	2 Min VTO (Dry) Hot Day, 360°	3 Sec VTO (Dry) Hot Day, 360°	Emergency (Dry) Hot Day, 360°
NE	105	105	106	106	110
W5.4, lb/sec(kg/sec)	126.8(57.50)	120.2(54.54)	121.8(55.24)	133.8(60.69)	124.3(58.36)
P5.1, lb/in^2(kN/m^2)	53.63(369.8)	51.34(354.0)	52.60(362.7)	60.22(415.2)	54.67(376.9)
T5.4, °R(°K)	1773(985)	1814(1008)	1847(1026)	1997(1109)	1913(1063)
P5.4, lb/in^2(kN/m^2)	49.34(340.2)	47.23(325.6)	48.39(333.6)	55.40(392.)	50.30(346.8)
WF, lb/hr(kg/hr)	8324(3775)	7990(3624)	8247(3741)	9323(4229)	8895(4035)
Fan Design Pressure Ratio = 1.2					
P/P	1.169	1.159	1.165	1.200	1.175
NF	93.62	94.10	95.31	102.91	97.55
W10, lb/sec(kg/sec)	1788(811.0)	1705(773.4)	1721(780.6)	1818(824.6)	1753(795.1)
Fn, lb(kN)	29707(132.1)	28047(124.7)	28938(128.7)	34377(152.9)	30549(135.9)
Fn Ratio	1.000	0.944	0.974	1.157	1.028
Fan Design Pressure Ratio = 1.3					
P/P	1.255	1.239	1.248	1.300	1.263
NF	93.29	93.61	94.90	102.89	97.25
W10, lb/sec(kg/sec)	1164(52.80)	1105(501.2)	1119(507.6)	1197(542.9)	1144(518.9)
Fn, lb(kN)	25206(112.1)	23754(105.7)	24534(109.1)	29258(180.1)	25935(115.4)
Fn Ratio	1.000	0.942	0.973	1.161	1.029

Table X. VTO Performance of Single Stage Fans Designed for VTO, SLS, 90° F (305° K) Day, Installed. (Concluded)

Fan Design Pressure Ratio = 1.4

	Intermediate Std Day, 360°	Intermediate Hot Day, 360°	2 Min VTO (Dry) Hot Day, 360°	3 Sec VTO (Dry) Hot Day, 360°	Emergency (Dry) Hot Day, 360°
P/P	1.341	1.319	1.331	1.399	1.351
NF	93.01	93.29	94.60	102.87	96.99
W10, lb/sec (kg/sec)	843.6(382.7)	798.6(362.2)	809.8(396.8)	874.8(396.8)	830.3(376.6)
Fn, lb (kN)	22246(98.95)	20943(93.16)	21638(96.25)	25914(115.3)	22901(101.9)
Fn Ratio	1.000	0.941	0.973	1.165	1.029

Fan Design Pressure Ratio = 1.5

	Intermediate Std Day, 360°	Intermediate Hot Day, 360°	2 Min VTO (Dry) Hot Day, 360°	3 Sec VTO (Dry) Hot Day, 360°	Emergency (Dry) Hot Day, 360°
P/P	1.428	1.401	1.415	1.499	1.441
NF	92.73	92.96	94.29	102.87	96.75
W10, lb/sec (kg/sec)	648.0(293.9)	611.8(277.5)	621.2(281.8)	626.9(307.0)	638.8(289.7)
Fn, lb (kN)	20145(89.61)	18950(84.29)	19587(87.13)	23517(104.6)	20750(92.30)
Fn Ratio	1.000	0.941	0.972	1.167	1.030

Table XI. VTO Performance of Single Stage Fans Designed for Cruise, SLS, Standard Day, Installed.

	Intermediate Std Day, 360°	Intermediate Std Day, 240°	Intermediate Hot Day, 240°	2 Min VTO (Dry) Hot Day, 240°	3 Sec VTO (Dry) Hot Day, 240°	Emergency (Dry) Hot Day, 240°
NE	105	105	105	106	106	110
W5.4,lb/sec(kg/sec)	126.8(57.51)	84.5(38.33)	80.2(36.38)	81.2(36.83)	89.2(40.46)	82.8(37.56
P5.1,lb/m^2(kN/m^2)	53.63(369.8)	53.63(369.8)	51.34(354.0)	52.60(362.7)	60.22(415.2)	54.67(376.9)
T5.4,°R(°K)	1773(985)	1773(985)	1814(1008)	1847(1026)	1997(1109)	1913(1063)
P5.4,lb/in^2(kN,m^2)	49.34(340.2)	49.34(340.2)	47.23(325.6)	48.39(333.6)	55.40(382.0)	50.30(346.8)
WF,lb/hr(kg/hr)	8324(3776)	5549(2516)	5329(2417)	5498(2493)	6824(3095)	5930(2690)
Fan Design Pressure Ratio = 1.2						
P/P	1.200	1.142	1.133	1.138	1.166	1.146
NF	99.96	87.70	88.26	89.34	95.67	91.31
W10,lb/sec(kg/sec)	1503(681.7)	1365(619.2)	1300(589.7)	1314(596.0)	1387(629.1)	1338(606.9)
Fn, lb(kN)	27973(130.5)	20814(143.5)	19669(135.6)	20280(139.8)	24038(165.7)	21396(147.5)
Fn Ratio	1.000	0.744	0.703	0.725	0.859	0.765
Fan Design Pressure Ratio = 1.3						
P/P	1.300	1.215	1.203	1.209	1.252	1.221
NF	99.93	87.22	87.67	88.79	95.52	90.84
W10,lb/sec(kg/sec)	977.0(443.1)	869.0(394.1)	824.9(374.2)	835.1(378.8)	892.7(404.9)	853.5(387.1)
Fn, lb(kN)	23681(163.3)	17395(119.9)	16431(113.2)	16941(116.8)	20175(139.1)	17881(123.3)
Fn Ratio	1.000	0.735	0.694	0.715	0.852	0.755

Table XI. VTO Performance of Single Stage Fans Designed for Cruise, SLS, Standard Day, Installed. (Concluded)

	Intermediate Std Day, 360°	Intermediate Std Day, 240°	Intermediate Hot Day, 240°	2 Min VTO (Dry) Hot Day, 240°	3 Sec VTO (Dry) Hot Day, 240°	Emergency (Dry) Hot Day, 240°
Fan Design Pressure Ratio = 1.4						
P/P	1.399	1.290	1.273	1.282	1.339	1.298
NF	99.92	86.96	87.31	88.48	95.45	90.61
W10, lb/sec (kg/sec)	701.0(318.0)	613.8(278.4)	580.7(263.4)	588.8(267.1)	635.9(288.4)	603.7(273.8)
Fn, lb (kN)	20810(143.5)	15098(104.1)	14239(98.18)	14691(101.3)	17580(121.2)	15526(107.0)
Fn Ratio	1.000	0.726	0.684	0.706	0.845	0.746
Fan Design Pressure Ratio = 1.5						
P/P	1.499	1.368	1.347	1.358	1.429	1.378
NF	99.93	86.35	86.62	87.82	95.00	90.00
W10, lb/sec (kg/sec)	531.1(240.9)	458.4(207.9)	432.7(196.3)	439.2(199.2)	479.0(217.3)	451.7(204.9)
Fn, lb (kN)	18724(129.1)	13457(92.78)	12679(87.42)	13083(90.20)	15734(108.4)	13846(95.46)
Fn Ratio	1.000	0.719	0.677	0.699	0.840	0.739

Table XII. Cruise Performance for Single Stage Fans.
Designed for VTO, P/P = 1.2

Altitude (ft)	Altitude (m)	Mach	P/S	F_N/δ_o (lb)	F_N/δ_o (kN)	$N_F/\sqrt{\theta_o}$ (pct)	$W_{22}\sqrt{\theta_o}/\delta_o$ (ft/sec)	$W_{22}\sqrt{\theta_o}/\delta_o$ (m/sec)	A_N (in^2)	A_N (m^2)
0	0	0.	75	29707	1331.5	93.6	1788	811	7669	4.948
			62	25750	1154.2	88.3	1708	774	8017	5.172
			52	19862	890.3	79.5	1568	711	8723	5.628
			40	12566	563.2	65.9	1307	592	9686	6.249
			30	6370	285.5	50.3	986	447	9986	6.443
0	0	0.2	75	20033	897.9	93.7	1826	828	7152	4.614
			62	16529	740.9	88.1	1741	789	7357	4.746
			52	11662	522.7	78.9	1587	719	7638	4.928
			40	6451	289.1	65.6	1328	602	7670	4.948
			30	2561	114.8	50.3	1006	456	7152	4.614
0	0	0.4	75	15122	677.8	93.9	1945	882	6216	4.010
			62	11795	528.7	87.5	1839	834	6201	4.001
			52	7690	344.7	77.2	1651	748	6023	3.886
			40	4132	185.2	64.9	1391	630	5526	3.565
			30	1596	71.5	50.2	1063	482	4607	2.972
0	0	0.6	75	12620	565.7	93.7	2147	973	5508	3.554
			62	9061	406.1	85.7	1995	904	5318	3.431
			52	5777	258.9	75.4	1778	806	4544	2.932
			40	3135	140.5	63.6	1496	678	4338	2.799
			30	1292	57.9	50.0	1163	527	3521	2.272
15000	4572	0.2	75	21864	980.0	96.6	1868	847	7061	4.555
			62	20374	913.2	94.2	1835	832	7137	4.605
			62	17092	766.1	89.1	1756	796	7324	4.725
			52	9862	442.0	74.6	1506	683	7653	4.937
			30	3372	151.1	54.1	1084	491	7293	4.705
15000	4572	0.4	75	16897	757.4	97.1	1996	905	6217	4.011
			62	15465	693.2	94.5	1955	886	6216	4.010
			52	12187	546.2	88.3	1854	840	6208	4.005
			40	6481	290.5	73.6	1578	715	5910	3.813
			30	2116	94.8	53.9	1143	518	4843	3.125
15000	4572	0.6	75	14779	662.4	97.9	2220	1006	5577	3.598
			62	13005	582.9	94.5	2160	979	5518	3.560
			52	9488	425.3	86.8	2016	914	5345	3.448
			40	4755	213.1	71.5	1688	765	4769	3.077
			30	1671	74.9	53.4	1247	565	3734	2.409

Table XII. (Continued)

Altitude (ft)	Altitude (m)	Mach	P/S	F_N/δ_o (lb)	F_N/δ_o (kN)	$N_F/\sqrt{\theta_o}$ (pct)	$W_{22}\sqrt{\theta_o}/\delta_o$ (ft/sec)	$W_{22}\sqrt{\theta_o}/\delta_o$ (m/sec)	A_N (in^2)	A_N (m^2)
36000	10972	0.2	75	22893	1026.1	98.3	1890	857	7007	4.521
			62	21730	974.0	96.5	1866	846	7070	4.561
			52	19086	855.5	92.2	1804	818	7204	4.648
			40	12564	563.1	80.9	1625	737	7625	4.919
			30	3972	178.0	56.7	1141	517	7410	4.781
36000	10972	0.4	75	18221	816.7	99.6	2029	920	6204	4.003
			62	17102	766.5	97.5	2002	908	6216	4.010
			52	14766	661.8	93.3	1936	878	6219	4.012
			40	9224	413.4	81.8	1743	790	6165	3.977
			30	2639	118.3	57.3	1222	554	5081	3.278
36000	10972	0.6	75	16647	746.2	101.7	2276	1032	5617	3.624
			62	15484	694.0	99.5	2244	1017	5595	3.610
			52	13272	594.9	95.1	2170	984	5527	3.566
			40	8083	362.3	83.3	1952	885	5264	3.396
			30	2274	101.9	58.3	1366	619	4032	2.601
36000	10972	0.8	75	17080	765.6	104.3	2654	1203	5369	3.464
			62	15769	706.8	101.9	2613	1185	5325	3.435
			52	13527	606.3	97.8	2530	1147	523	0.337
			40	8119	363.9	85.4	2273	1031	4862	3.137
			30	2318	103.9	59.7	1591	721	3600	2.323
36000	10972	1.0	75	18065	809.7	105.6	3155	1431	5318	3.431
			62	16509	740.0	102.9	3098	1405	5257	3.392
			52	13348	598.3	97.3	2967	1345	5103	3.292
			40	7066	316.7	81.5	2543	1153	4514	2.912
			30	2323	104.1	59.1	1830	830	3359	2.167

Table XII. (Concluded)

Altitude (ft)	Altitude (m)	Mach	P/S	F_N/δ_o (lb)	F_N/δ_o (kN)	$N_F/\sqrt{\theta_o}$ (pct)	$W_{22}\sqrt{\theta_o}/\delta_o$ (ft/sec)	$W_{22}\sqrt{\theta_o}/\delta_o$ (m/sec)	A_N (in^2)	A_N (m^2)
45000	13716	0.2	75	23269	1043.0	99.1	1892	858	6983	4.505
			62	22066	989.0	97.2	1867	846	7046	4.546
			52	19364	867.9	92.8	1805	818	7180	4.632
			40	12770	572.4	81.4	1626	737	7601	4.904
			30	8659	388.1	71.8	1447	656	7692	4.963
45000	13716	0.4	75	18516	829.9	100.2	2029	920	6201	4.001
			62	17373	778.7	98.3	2002	908	6211	4.007
			52	15007	672.6	93.9	1935	877	6216	4.010
			40	9378	420.3	82.2	1741	789	6166	3.978
			30	5068	227.2	68.9	1472	667	5730	3.697
45000	13716	0.6	75	16860	755.7	102.2	2274	1031	5622	3.627
			62	15677	702.7	100.0	2240	1016	5600	3.613
			52	13461	603.3	95.6	2168	983	5533	3.570
			40	8194	367.3	83.7	1949	884	5271	3.401
			30	3167	142.0	63.9	1496	678	4354	2.809
45000	13716	0.8	75	17216	771.7	104.7	2648	1201	5376	3.468
			62	15876	711.6	102.3	2607	1182	5331	3.439
			52	13625	610.7	98.0	2525	1145	5230	3.374
			40	8201	367.6	85.7	2268	1028	4870	3.142
			30	2387	107.0	60.1	1594	723	3620	2.335
45000	13716	1.0	75	18140	813.1	105.9	3091	1402	5264	3.396
			62	16607	744.4	103.2	3091	1402	5264	3.396
			52	13379	599.7	97.5	2957	1341	5107	3.295
			40	7086	317.6	81.5	2534	1149	4517	2.914
			30	2380	106.7	59.4	1830	830	3373	2.176

Table XIII. Cruise Performance for Single Stage Fans.

Designed for VTO, P/P = 1.3

Altitude (ft)	Altitude (m)	Mach	P/S	F_N/δ_o (lb)	F_N/δ_o (kN)	$N_F/\sqrt{\theta_o}$ (pct)	$W_{22}\sqrt{\theta_o}/\delta_o$ (ft/sec)	$W_{22}\sqrt{\theta_o}/\delta_o$ (m/sec)	A_N (in^2)	A_N (m^2)
0	0	0.	75	25206	1129.8	93.3	1164	527	4165	2.687
			62	21812	977.7	87.7	1102	499	4366	2.817
			52	16792	752.7	78.3	990	449	4529	2.922
			40	10821	485.0	64.7	809	366	4667	3.011
			30	5794	259.7	49.4	602	273	4860	3.135
0	0	0.2	75	18477	828.2	93.3	1189	539	4094	2.641
			62	15380	689.4	87.5	1121	508	4147	2.675
			52	11079	496.6	77.7	1002	454	4192	2.705
			40	6496	291.2	64.4	821	372	4111	2.652
			30	2946	132.0	49.4	613	278	3858	2.489
0	0	0.4	75	14801	663.4	93.5	1264	573	3748	2.418
			62	11726	525.6	86.8	1181	535	3706	2.391
			52	7894	353.8	76.1	1040	471	3566	2.301
			40	4526	202.9	63.7	858	389	3257	2.101
			30	2012	90.2	49.4	648	293	2764	1.783
0	0	0.6	75	12850	576.0	93.2	1391	630	3453	2.228
			62	9437	423.0	84.8	1274	577	3312	2.137
			52	6256	280.4	74.3	1114	505	3056	1.972
			40	3633	162.8	62.5	921	417	2673	1.725
			30	1700	76.2	48.9	703	318	2177	1.405
15000	4572	0.2	75	20106	901.2	96.4	1223	554	4071	2.626
			62	18775	841.5	93.9	1196	542	4091	2.639
			52	15873	711.5	88.5	1133	513	4140	2.671
			40	9504	426.0	73.6	947	429	4179	2.696
			30	3679	164.9	53.1	662	300	3916	2.526
15000	4572	0.4	75	16456	737.6	96.8	1305	591	3764	2.428
			62	15114	677.4	94.1	1271	576	3749	2.419
			52	12084	541.6	87.5	1192	540	3714	2.396
			40	6762	303.1	72.4	988	448	3493	2.254
			30	2518	112.9	52.8	698	316	2889	1.864
15000	4572	0.6	75	14939	669.6	99.6	1449	657	3509	2.264
			62	13222	592.6	95.9	1401	635	3462	2.234
			52	9855	441.7	87.6	1289	584	3329	2.148
			40	5270	236.2	71.7	1053	477	2944	1.899
			30	2114	94.8	53.5	762	345	2317	1.495

Table XIII. (Continued)

Altitude (ft)	Altitude (m)	Mach	P/S	F_N/δ_o (lb)	F_N/δ_o (kN)	$N_F/\sqrt{\theta_o}$ (pct)	$W_{22}\sqrt{\theta_o}/\delta_o$ (ft/sec)	$W_{22}\sqrt{\theta_o}/\delta_o$ (m/sec)	A_N (in^2)	A_N (m^2)
36000	10972	0.2	75	21034	942.8	98.2	1241	562	4053	2.615
			62	20009	896.8	96.3	1221	553	4074	2.628
			52	17619	789.7	91.8	1172	531	4110	2.652
			40	11881	532.5	80.0	1032	468	4217	2.721
			30	4240	190.0	55.7	698	316	3973	2.563
36000	10972	0.4	75	17686	792.7	99.5	1332	604	3766	2.430
			62	16661	746.8	97.4	1310	594	3764	2.428
			52	14476	648.8	92.9	1257	570	3747	2.417
			40	9336	418.5	80.8	1107	502	3662	2.363
			30	3058	137.1	56.3	748	339	3015	1.945
3600	1097	0.6	75	16719	749.4	101.6	1494	677	3546	2.288
			62	15622	700.2	99.3	1468	665	3529	2.277
			52	13486	604.5	94.6	1409	639	3469	2.238
			40	8498	380.9	82.3	1238	561	3265	2.106
			30	8498	380.9	82.3	1238	561	2490	1.606
36000	10972	0.8	75	17539	786.1	104.2	1743	790	3479	2.245
			62	16259	728.8	101.7	1710	775	3445	2.223
			52	14053	629.9	97.3	1643	745	3365	2.171
			40	8752	392.3	84.3	1441	653	3090	1.994
			30	2898	129.9	58.7	973	441	2262	1.459
36000	10972	1.0	75	18819	843.5	105.4	2065	936	3451	2.226
			62	17289	774.9	102.6	2018	915	3406	2.197
			52	14191	636.1	96.7	1914	868	3296	2.126
			40	7949	356.3	80.3	1598	724	2880	1.858
			30	3027	135.7	58.0	1117	506	2126	1.372

Table XIII. (Concluded)

Altitude (ft)	(m)	Mach	P/S	F_N/δ_o (lb)	(kN)	$N_F/\sqrt{\theta_o}$ (pct)	$W_{22}\sqrt{\theta_o}/\delta_o$ (ft/sec)	(m/sec)	A_N (in^2)	(m^2)
45000	13716	0.2	75	21361	957.4	99.1	1243	563	4047	2.611
			62	20301	909.9	97.0	1223	554	4066	2.623
			52	17866	800.8	92.4	1173	532	4102	2.646
			40	12066	540.8	80.6	1035	469	4216	2.720
			30	8454	378.9	70.7	904	410	4171	2.691
45000	13716	0.4	75	17948	804.5	100.2	1333	604	3767	2.430
			62	16908	757.9	98.0	1311	594	3764	2.428
			52	14692	658.5	93.4	1257	570	3747	2.417
			40	9480	424.9	81.4	1109	503	3670	2.368
			30	5431	243.4	67.7	914	414	3380	2.181
45000	13716	0.6	75	16915	758.2	102.1	1494	677	3551	2.291
			62	15793	707.9	99.8	1467	665	3529	2.277
			52	13659	612.2	95.1	1409	639	3471	2.239
			40	8611	386.0	82.7	1239	562	3277	2.114
			30	3680	164.9	62.6	921	417	2682	1.730
45000	13716	0.8	75	17668	791.9	104.6	1740	789	3485	2.248
			62	16368	733.6	102.1	1706	773	3449	2.225
			52	14145	634.0	97.6	1639	743	3370	2.174
			40	8837	396.1	84.6	1441	653	3100	2.000
			30	2962	132.8	59.0	976	442	2273	1.466
45000	13716	1.0	75	18885	846.5	105.6	2059	933	3455	2.229
			62	17378	778.9	102.9	2015	913	3411	2.201
			52	14213	637.1	96.9	1909	865	3298	2.128
			40	7962	356.9	80.4	1593	722	2886	1.862
			30	3085	138.3	58.5	1117	506	2135	1.377

Table XIV. Cruise Performance for Single Stage Fans.
Designed for VTO, P/P = 1.4

Altitude (ft)	Altitude (m)	Mach	P/S	F_N/δ_o (lb)	F_N/δ_o (kN)	$N_F/\sqrt{\theta_o}$ (pct)	$W_{22}\sqrt{\theta_o}/\delta_o$ (ft/sec)	$W_{22}\sqrt{\theta_o}/\delta_o$ (m/sec)	A_N (in2)	A_N (m^2)
0	0	0.	75	22246	997.1	93.0	844	382	2833	1.828
			62	19196	860.4	87.3	791	358	2859	1.845
			52	14707	659.2	77.5	700	317	2885	1.861
			40	9478	424.8	63.9	561	254	2881	1.859
			30	5129	229.9	48.9	412	186	2926	1.888
0	0	0.2	75	17120	767.4	92.7	861	390	2757	1.779
			62	14294	640.7	86.7	805	365	2761	1.781
			52	10374	465.0	76.6	708	321	2737	1.766
			40	6208	278.3	63.4	570	258	2639	1.703
			30	2945	132.0	48.7	420	190	2488	1.605
0	0	0.4	75	14247	638.6	93.2	914	414	2598	1.676
			62	11356	509.0	86.3	845	383	2547	1.643
			52	7750	347.4	75.3	732	332	2426	1.565
			40	4567	204.7	62.9	595	269	2209	1.425
			30	2122	95.1	48.7	443	200	1899	1.225
0	0	0.6	75	12703	569.4	92.9	1002	454	2453	1.583
			62	9423	422.4	84.2	908	411	2337	1.508
			52	6351	284.7	73.4	781	354	2142	1.382
			40	8939	400.7	72.8	665	301	2714	1.751
			30	3617	162.1	52.4	454	205	2516	1.623
15000	4572	0.2	75	18625	834.8	96.2	889	403	2757	1.779
			62	17390	779.5	93.7	866	392	2757	1.779
			52	14742	660.8	88.1	814	369	2763	1.783
			40	8939	400.7	72.8	665	301	2714	1.751
			30	3617	162.1	52.4	454	205	2516	1.623
15000	4572	0.4	75	15807	708.5	96.6	949	430	2618	1.689
			62	14538	651.6	93.8	920	417	2601	1.678
			52	11696	524.2	87.1	854	387	2554	1.648
			40	6686	299.7	71.6	692	313	2373	1.531
			30	3619	162.2	52.2	478	216	1978	1.276
15000	4572	0.6	75	14707	659.2	97.4	1051	476	2502	1.614
			62	13066	585.6	93.8	1011	458	2462	1.588
			52	9828	440.5	85.3	920	417	2351	1.517
			40	5393	241.7	69.5	734	332	2062	1.330
			30	2275	102.0	52.0	523	237	1936	1.249

Table XIV. (Continued)

Altitude (ft)	Altitude (m)	Mach	P/S	F_N/δ_o (lb)	F_N/δ_o (kN)	$N_F/\sqrt{\theta_o}$ (pct)	$W_{22}\sqrt{\theta_o}/\delta_o$ (ft/sec)	$W_{22}\sqrt{\theta_o}/\delta_o$ (m/sec)	A_N (in²)	A_N (m²)
36000	10972	0.2	75	19487	873.4	98.1	928	420	2753	1.776
			62	18547	831.3	96.1	888	402	2758	1.779
			52	16535	741.1	91.5	847	384	2761	1.781
			40	11106	497.8	79.2	731	331	2757	1.779
			30	4133	185.2	55.0	480	217	2546	1.643
36000	10972	0.4	75	16973	760.8	99.4	972	440	2627	1.695
			62	16009	717.6	97.2	953	432	2619	1.690
			52	13955	625.5	92.6	909	412	2595	1.674
			40	9122	408.9	80.0	783	355	2494	1.609
			30	3152	141.3	55.6	514	233	2053	1.325
36000	10972	0.6	75	16420	736.0	101.4	1090	494	2537	1.637
			62	15368	688.8	99.0	1067	483	2517	1.624
			52	13321	597.1	94.4	1019	462	2468	1.592
			40	8529	382.3	81.5	876	397	2293	1.479
			30	2920	130.9	56.6	575	260	1747	1.127
36000	10972	0.8	75	17527	785.6	104.1	1271	576	2524	1.628
			62	16291	730.2	101.6	1243	563	2499	1.612
			52	14128	633.2	96.9	1188	538	2438	1.573
			40	8926	400.1	83.5	1020	462	2211	1.426
			30	3125	140.1	58.0	670	303	1611	1.039
36000	10972	1.0	75	18912	847.7	105.1	1503	681	2503	1.615
			62	17414	780.5	102.2	1463	663	2468	1.592
			52	14405	645.7	96.3	1377	624	2383	1.537
			40	8270	370.7	79.4	1123	509	2071	1.336
			30	3326	149.1	57.2	7667	3477	1527	0.985

Table XIV. (Concluded)

Altitude (ft)	Altitude (m)	Mach	P/S	F_N/δ_o (lb)	F_N/δ_o (kN)	$N_F/\sqrt{\theta_o}$ (pct)	$W_{22}\sqrt{\theta_o}/\delta_o$ (ft/sec)	$W_{22}\sqrt{\theta_o}/\delta_o$ (m/sec)	A_N (in^2)	A_N (m^2)
45000	13716	0.2	75	19781	886.6	99.0	907	411	2752	1.775
			62	18810	843.1	96.9	891	404	2755	1.777
			52	16580	743.1	92.1	849	385	2759	1.780
			40	11279	505.5	79.8	734	332	2763	1.783
			30	7975	357.5	69.9	633	287	2698	1.741
45000	13716	0.4	75	17216	771.7	100.1	974	441	2630	1.697
			62	16238	727.8	97.9	955	433	2622	1.692
			52	14152	634.3	93.2	910	412	2597	1.675
			40	9254	414.8	80.6	786	356	2502	1.614
			30	5431	243.4	66.8	636	288	2290	1.477
45000	13716	0.6	75	16601	744.1	102.1	1091	494	2541	1.639
			62	15534	696.3	99.6	1068	484	2521	1.626
			52	13488	604.6	94.9	1019	462	2473	1.595
			40	8632	386.9	81.9	878	398	2301	1.485
			30	3844	172.3	61.9	637	288	1877	1.211
45000	13716	0.8	75	17647	791.0	104.6	1270	576	2529	1.632
			62	16389	734.6	101.9	1242	563	2502	1.614
			52	14213	637.1	97.2	1186	537	2441	1.575
			40	9008	403.8	83.8	1020	462	2219	1.432
			30	3187	142.8	58.2	671	304	1619	1.045
45000	13716	1.0	75	18974	850.5	105.4	1499	679	2506	1.617
			62	17510	784.8	102.5	1461	662	2472	1.595
			52	14425	646.6	96.4	1373	622	2385	1.539
			40	8283	371.3	79.5	1119	507	2073	1.337
			30	3379	151.5	57.4	766	347	1531	0.988

Table XV. Cruise Performance for Single Stage Fans.

Designed for VTO, P/P = 1.5

Altitude (ft)	Altitude (m)	Mach	P/S	F_N/δ_o (lb)	F_N/δ_o (kN)	$N_F/\sqrt{\theta_o}$ (pct)	$W_{22}\sqrt{\theta_o}/\delta_o$ (ft/sec)	$W_{22}\sqrt{\theta_o}/\delta_o$ (m/sec)	A_N (in^2)	A_N (m^2)
0	0	0.	75	20145	902.9	92.7	648	293	2073	1.337
			62	17338	777.1	86.9	603	273	2069	1.335
			52	13200	591.7	76.8	526	238	2050	1.323
			40	8478	380.0	63.2	415	188	2003	1.292
			30	4599	206.1	48.3	300	136	1996	1.288
0	0	0.2	75	16032	718.6	97.8	661	299	2035	1.313
			62	13398	600.5	86.6	613	278	2017	1.301
			52	9730	436.1	76.2	531	240	1970	1.271
			40	5881	263.6	63.0	421	190	1874	1.209
			30	2856	128.0	48.3	305	138	1763	1.137
0	0	0.4	75	13709	614.5	92.9	701	317	1592	1.027
			62	10960	491.2	85.8	642	291	1900	1.226
			52	7533	337.6	74.7	548	248	1793	1.157
			40	4500	201.7	62.2	438	198	1626	1.049
			30	2134	95.7	47.9	320	145	1404	0.906
0	0	0.6	75	12464	558.7	92.5	767	347	1875	1.210
			62	9293	416.5	83.6	687	311	1776	1.146
			52	6325	283.5	72.8	583	264	1619	1.045
			40	3835	171.9	60.9	469	212	1415	0.913
			30	1903	85.3	47.2	344	156	1161	0.749
15000	4572	0.2	75	17439	781.7	96.1	686	311	3045	1.965
			62	16282	729.8	93.4	666	302	2037	1.314
			52	13817	619.3	87.6	621	281	2021	1.304
			40	8414	377.1	72.1	497	225	1946	1.255
			30	3482	156.1	51.8	332	150	1784	1.151
15000	4572	0.4	75	15192	680.9	96.5	731	331	1975	1.274
			62	13987	626.9	93.6	707	320	1956	1.262
			52	11285	505.8	86.7	650	294	1906	1.230
			40	6525	292.5	70.9	516	234	1751	1.130
			30	2630	117.9	51.5	349	158	1464	0.945
15000	4572	0.6	75	14391	645.0	97.1	809	366	1920	1.239
			62	12821	574.7	93.5	775	351	1884	1.215
			52	9688	434.2	84.8	697	316	1787	1.153
			40	5394	241.8	68.8	545	247	1557	1.005
			30	2341	104.9	51.3	381	172	1240	0.800

Table XV. (Continued)

Altitude (ft)	Altitude (m)	Mach	P/S	F_N/δ_o (lb)	F_N/δ_o (kN)	$N_F/\sqrt{\theta_o}$ (pct)	$W_{22}\sqrt{\theta_o}/\delta_o$ (ft/sec)	$W_{22}\sqrt{\theta_o}/\delta_o$ (m/sec)	A_N (in^2)	A_N (m^2)
36000	10972	0.2	75	18243	817.7	98.1	699	317	2046	1.320
			62	17370	778.6	95.9	685	310	2044	1.319
			52	15328	687.0	91.3	649	294	2032	1.311
			40	10410	466.6	78.4	549	249	1987	1.282
			30	3955	177.3	54.3	351	159	1803	1.163
36000	10972	0.4	75	16286	730.0	99.4	751	340	1986	1.281
			62	15381	689.4	97.1	734	332	1977	1.275
			52	13442	602.5	92.3	697	316	1948	1.257
			40	8828	395.7	79.2	589	267	1844	1.190
			30	3139	140.7	54.9	376	170	1515	0.977
36000	10972	0.6	75	16032	718.6	101.3	842	381	1953	1.260
			62	15029	673.6	98.9	823	373	1934	1.248
			52	13067	585.7	94.1	658	298	1733	1.118
			40	8422	377.5	80.6	658	298	1733	1.118
			30	2974	133.3	55.8	420	190	1320	0.852
36000	10972	0.8	75	17321	776.4	104.1	982	445	1953	1.260
			62	16135	723.2	101.3	959	434	1933	1.247
			52	14044	629.5	96.6	911	413	1884	1.215
			40	8939	400.7	82.7	766	347	1698	1.095
			30	3223	144.5	57.2	489	221	1233	0.795
36000	10972	1.0	75	18783	841.9	105.0	1160	526	1937	1.250
			62	17329	776.7	102.0	1124	509	1908	1.231
			52	14405	645.7	95.8	1050	476	1840	1.187
			40	8386	375.9	78.8	840	381	1594	1.028
			30	3473	155.7	56.6	560	254	1177	0.759

Table XV. (Concluded)

Altitude (ft)	Altitude (m)	Mach	P/S	F_N/δ_o (lb)	F_N/δ_o (kN)	$N_F/\sqrt{\theta_o}$ (pct)	$W_{22}\sqrt{\theta_o}/\delta_o$ (ft/sec)	$W_{22}\sqrt{\theta_o}/\delta_o$ (m/sec)	A_N (in^2)	A_N (m^2)
45000	13716	0.2	75	18516	829.9	99.0	702	318	2047	1.321
			62	17613	789.4	96.8	688	312	2044	1.319
			52	15540	696.5	91.9	651	295	2032	1.311
			40	10568	473.7	79.1	552	250	1991	1.285
			30	3473	155.7	56.6	560	254	1177	0.759
45000	13716	0.4	75	16512	740.1	100.1	753	341	1990	1.284
			62	15595	699.0	97.8	737	334	1979	1.277
			52	13625	610.7	92.9	699	317	1951	1.259
			40	8953	401.3	79.8	591	268	1850	1.194
			30	5328	238.8	66.2	472	214	1686	1.088
45000	13716	0.6	75	16204	726.3	101.9	843	382	1957	1.263
			62	15185	680.6	99.4	823	373	1938	1.250
			52	13228	592.9	94.6	782	354	1893	1.221
			40	8523	382.0	81.1	660	299	1739	1.122
			30	3378	173.8	61.1	468	212	1416	0.914
45000	13716	0.8	75	17435	781.5	104.5	982	445	1956	1.262
			62	16224	727.2	101.7	957	434	1935	1.248
			52	14125	633.1	96.9	910	412	1887	1.217
			40	9015	404.1	82.9	766	347	1703	1.099
			30	3283	147.2	57.5	490	222	1238	0.799
45000	13716	1.0	75	18837	844.3	105.3	1157	524	1935	1.248
			62	17415	780.6	102.3	1123	509	1911	1.233
			52	14425	646.6	96.0	1048	475	1842	1.188
			40	8399	376.5	78.9	837	379	1595	1.029
			30	3529	158.2	56.7	560	254	1180	0.761

Table XVI. Cruise Performance for Single Stage Fans.

Designed for Cruise, P/P = 1.2

Altitude (ft)	Altitude (m)	Mach	P/S	F_N/δ_o (lb)	F_N/δ_o (kN)	$N_F/\sqrt{\theta_o}$ (pct)	$W_{22}\sqrt{\theta_o}/\delta_o$ (ft/sec)	$W_{22}\sqrt{\theta_o}/\delta_o$ (m/sec)	A_N (in^2)	A_N (m^2)
0	0	0.	75	27973	1253.8	99.9	1503	681	5977	3.856
			62	24301	1089.2	93.8	1438	652	6230	4.019
			52	19123	857.1	85.2	1331	603	6694	4.319
			40	12278	550.3	70.9	1129	512	7495	4.835
			30	6339	284.1	54.2	854	387	8391	5.414
0	0	0.2	75	19607	878.8	100.0	1536	696	5657	3.650
			62	16272	729.3	93.5	1465	664	5821	3.755
			52	11886	532.8	84.7	1353	613	6071	3.917
			40	6711	300.8	70.6	1148	520	6255	4.035
			30	2781	124.6	54.1	870	394	5925	3.823
0	0	0.4	75	15211	681.8	100.2	1637	742	5046	3.255
			62	11943	535.3	92.9	1550	703	5061	3.265
			52	8115	363.7	83.4	1420	644	5018	3.237
			40	4420	198.1	69.9	1205	546	4696	3.030
			30	1784	80.0	54.0	919	416	3956	2.552
0	0	0.6	75	12920	579.1	99.8	1807	819	4558	2.941
			62	9396	421.1	91.3	1688	765	4440	2.865
			52	6236	279.5	81.6	1538	697	4228	2.728
			40	3400	152.4	68.6	1301	590	3761	2.426
			30	1462	65.5	53.6	1004	455	3053	1.970
15000	4572	0.2	75	21217	951.0	103.6	1584	718	5681	3.665
			62	19929	893.3	100.7	1544	700	5650	3.645
			52	16316	753.7	94.6	1479	670	5797	3.740
			40	10188	456.6	80.8	1304	591	6202	4.001
			30	3573	160.1	58.2	942	427	6067	3.914
15000	4572	0.4	75	16876	756.4	104.1	1689	766	5085	3.281
			62	15536	696.4	100.9	1645	746	5043	3.254
			52	12323	552.3	93.7	1561	708	5058	3.263
			40	6901	309.3	79.4	1362	617	4955	3.197
			30	2306	103.4	57.9	994	450	4173	2.692
15000	4572	0.6	75	15029	673.6	104.8	1873	849	4921	3.175
			62	13310	596.6	100.8	1818	824	4565	2.945
			52	9780	438.4	92.3	1703	772	4458	2.876
			40	5127	229.8	76.8	1453	659	4071	2.626
			30	1868	83.7	57.6	1084	491	3251	2.097
36000	10972	0.2	75	21801	977.2	105.1	1606	728	5730	3.697
			62	21132	947.2	103.4	1583	718	5679	3.664
			52	18734	839.7	98.4	1519	689	5697	3.675
			40	12711	569.7	86.6	1378	625	6024	3.886
			30	4195	188.0	61.1	989	448	6125	3.952

Table XVI. (Concluded)

Altitude (ft)	Altitude (m)	Mach	P/S	F_N/δ_o (lb)	F_N/δ_o (kN)	$N_F/\sqrt{\theta_o}$ (pct)	$W_{22}\sqrt{\theta_o}/\delta_o$ (ft/sec)	$W_{22}\sqrt{\theta_o}/\delta_o$ (m/sec)	A_N (in^2)	A_N (m^2)
36000	10972	0.4	75	17040	763.8	106.8	1729	784	5274	3.403
			62	17031	763.4	104.6	1697	769	5101	3.291
			52	14891	667.4	99.6	1630	739	5048	3.257
			40	9603	430.4	87.5	1477	669	5046	3.255
			30	2867	128.5	61.7	1059	480	4350	2.806
36000	10972	0.6	75	16161	724.4	108.8	1936	878	4763	3.073
			62	15635	700.8	106.6	1902	862	4667	3.011
			52	13580	608.7	101.5	1827	828	4571	2.949
			40	8538	382.7	89.1	1654	750	4395	2.835
			30	2506	112.3	62.8	1185	537	3496	2.255
36000	10972	0.8	75	16924	758.6	111.5	2254	1022	4567	2.946
			62	16063	720.0	109.3	2215	1004	4488	2.895
			52	13955	625.5	104.3	2131	966	4370	2.819
			40	8645	387.5	91.4	1926	873	4103	2.647
			30	2577	115.5	64.3	1380	625	3138	2.025
36000	10972	1.0	75	18431	826.1	113.1	2676	1213	4498	2.902
			62	17035	763.5	109.9	2608	1182	4406	2.843
			52	13874	621.9	103.4	2498	1133	4289	2.767
			40	7677	344.1	88.3	2202	998	3909	2.522
			30	2604	116.7	63.6	1591	721	2944	1.899
45000	13716	0.2	62	21313	955.3	104.1	1585	718	5698	3.676
			52	19015	852.3	99.1	1520	689	5680	3.665
			40	12921	579.1	87.1	1379	625	6010	3.877
			30	8953	401.3	77.3	1246	565	6205	4.003
45000	13716	0.4	62	17182	770.1	105.2	1699	770	5121	3.304
			52	15123	677.8	100.2	1630	739	5046	3.255
			40	9761	437.5	88.0	1478	670	5049	3.257
			30	5417	242.8	74.1	1269	575	4822	3.111
45000	13716	0.6	62	15746	705.8	107.1	1902	862	4684	3.022
			52	13769	617.2	102.1	1826	828	4576	2.952
			40	8653	387.8	89.5	1653	749	4403	2.841
			30	3441	154.2	68.9	1300	589	3772	2.434
45000	13716	0.8	62	16129	722.9	109.7	2211	1002	4500	2.903
			52	14049	629.7	104.6	2126	964	4374	2.822
			40	8735	391.5	91.7	1923	872	4110	2.652
			30	2647	118.6	64.8	1383	627	3155	2.035
45000	13716	1.0	75	8461	379.2	113.4	2669	1210	4506	2.907
			62	17134	768.0	110.4	2604	1181	4417	2.850
			52	13906	623.3	103.6	2490	1129	4293	2.770
			40	7709	345.5	88.4	2194	995	3912	2.524
			30	2668	119.6	63.9	1591	721	2956	1.907

Table XVII. Cruise Performance for Single Stage Fans.

Designed for Cruise, P/P = 1.3

Altitude (ft)	Altitude (m)	Mach	P/S	F_N/δ_o (lb)	F_N/δ_o (kN)	$N_F/\sqrt{\theta_o}$ (pct)	$W_{22}\sqrt{\theta_o}/\delta_o$ (ft/sec)	$W_{22}\sqrt{\theta_o}/\delta_o$ (m/sec)	A_N (in^2)	A_N (m^2)
0	0	0.	75	23681	1061.4	99.9	977	443	3378	2.179
			62	20495	918.6	93.4	924	419	3452	2.227
			52	16050	719.4	84.2	840	381	3579	2.309
			40	10415	466.8	69.6	695	315	3738	2.412
			30	5594	250.7	53.0	514	233	3851	2.485
0	0	0.2	75	17882	801.5	100.0	997	452	3273	2.112
			62	14917	668.6	93.1	940	426	3315	2.139
			52	11037	494.7	83.7	853	386	3377	2.179
			40	6545	293.4	69.4	706	320	3371	2.175
			30	3023	135.5	53.0	523	237	3173	2.047
0	0	0.4	75	14652	656.7	100.0	1061	481	3053	1.970
			62	11643	521.9	92.4	992	449	3034	1.957
			52	8116	363.8	82.5	894	405	2976	1.920
			40	4680	209.8	68.6	740	335	2759	1.780
			30	2110	94.6	52.8	553	250	2348	1.515
0	0	0.6	75	12912	578.7	99.4	1166	528	2859	1.845
			62	9640	432.1	90.8	1076	488	2764	1.783
			52	6506	291.6	80.1	954	432	2596	1.675
			40	3804	170.5	67.3	795	360	2307	1.488
			30	1818	81.5	52.5	604	273	1886	1.217
15000	4572	0.2	75	19233	862.1	103.6	1031	467	3310	2.135
			62	18161	814.0	100.6	1003	454	3272	2.111
			52	15398	690.2	94.2	951	431	3310	2.135
			40	9573	429.1	79.7	816	370	3410	2.200
			30	3764	168.7	57.1	570	258	3239	2.090
15000	4572	0.4	75	16160	724.3	104.1	1100	498	3090	1.994
			62	14955	670.3	100.7	1067	483	3054	1.970
			52	11992	537.5	93.2	1000	453	3035	1.958
			40	6936	310.9	78.0	845	383	2915	1.881
			30	2646	118.6	56.9	600	272	2465	1.590
15000	4572	0.6	75	14941	669.7	104.9	1219	552	2913	1.879
			62	13286	595.5	100.4	1175	532	2866	1.849
			52	10030	449.6	92.0	1088	493	2778	1.792
			40	5481	245.7	75.7	900	408	2506	1.617
			30	2251	100.9	56.5	653	296	2000	1.290
36000	10972	0.2	75	19675	881.9	105.4	1045	474	3354	2.164
			62	19175	859.5	103.5	1031	467	3308	2.134
			52	17080	765.6	98.1	983	445	3283	2.118
			40	11770	527.6	85.8	872	395	3365	2.171
			30	4316	193.5	59.8	599	271	3269	2.109

Table XVII. (Concluded)

Altitude (ft)	Altitude (m)	Mach	P/S	F_N/δ_o (lb)	F_N/δ_o (kN)	$N_F/\sqrt{\theta_o}$ (pct)	$W_{22}\sqrt{\theta_o}/\delta_o$ (ft/sec)	$W_{22}\sqrt{\theta_o}/\delta_o$ (m/sec)	A_N (in^2)	A_N (m^2)
36000	10972	0.4	75	16786	752.4	106.6	1123	509	3155	2.035
			62	16291	730.2	104.7	1105	501	3102	2.001
			52	14367	644.0	99.4	1055	478	3051	1.968
			40	9483	425.0	86.7	935	424	2999	1.935
			30	3197	143.3	60.4	642	291	2559	1.651
36000	10972	0.6	62	15479	693.8	106.6	1238	561	2945	1.900
			52	13549	607.3	101.2	1182	536	2871	1.852
			40	8752	392.3	88.3	1047	474	2725	1.758
			30	2911	130.5	61.4	718	325	2145	1.384
36000	10972	0.8	62	16286	730.0	109.4	1442	654	2903	1.873
			52	14244	638.4	104.0	1379	625	2817	1.817
			40	9073	406.7	90.5	1218	552	2159	1.393
			30	3076	137.9	63.1	836	379	1629	1.051
36000	10972	1.0	75	18827	843.9	113.2	1742	790	2381	1.536
			62	17526	785.6	110.0	1695	768	2332	1.505
			52	14445	647.5	102.9	1606	728	2272	1.466
			40	8355	374.5	87.1	1378	625	2071	1.336
			30	3237	145.1	62.4	963	436	1542	0.995
45000	13716	0.2	62	19302	865.2	104.3	1032	468	3323	2.144
			52	17312	776.0	98.8	984	446	3278	2.115
			40	11949	535.6	86.4	874	396	3361	2.168
			30	8482	380.2	76.1	774	351	3387	2.185
45000	13716	0.4	62	16402	735.2	105.3	1106	501	3118	2.012
			52	14549	652.1	99.9	1055	478	3051	1.968
			40	9624	431.4	87.2	935	424	3002	1.937
			30	5602	251.1	72.9	784	355	2836	1.830
45000	13716	0.6	62	15561	697.5	107.1	1238	561	2957	1.908
			52	13714	614.7	101.8	1182	536	2875	1.855
			40	8858	397.0	88.7	1046	474	2731	1.762
			30	3844	172.3	67.6	794	360	2313	1.492
45000	13716	0.8	62	16334	732.1	109.7	1440	653	2911	1.878
			52	14330	642.3	104.4	1376	624	2821	1.820
			40	9159	410.5	90.7	1217	552	2615	1.687
			30	3146	141.0	63.3	838	380	1972	1.272
45000	13716	1.0	75	18844	844.6	113.5	1739	788	2920	1.884
			62	17613	789.4	110.4	1695	768	2858	1.844
			52	14466	648.4	103.2	1603	727	2768	1.786
			40	8372	375.2	87.2	1374	623	2495	1.610
			30	3297	147.8	62.6	963	436	1866	1.204

Table XVIII. Cruise Performance for Single Stage Fans.

Designed for Cruise, P/P = 1.4

Altitude (ft)	Altitude (m)	Mach	P/S	F_N/δ_o (lb)	F_N/δ_o (kN)	$N_F/\sqrt{\theta_o}$ (pct)	$W_{22}\sqrt{\theta_o}/\delta_o$ (ft/sec)	$W_{22}\sqrt{\theta_o}/\delta_o$ (m/sec)	A_N (in^2)	A_N (m^2)
0	0	0.	75	20310	932.7	99.9	701	317	2258	1.457
			62	17945	804.3	93.1	657	298	2274	1.467
			52	13975	626.4	83.6	589	267	2303	1.486
			40	9040	405.2	68.7	476	215	2318	1.495
			30	4880	218.7	52.1	344	156	2313	1.492
0	0	0.2	75	16424	736.2	99.5	715	324	2213	1.428
			62	13721	615.0	92.4	668	302	2214	1.428
			52	10199	457.1	82.8	597	270	2214	1.428
			40	6149	275.6	68.5	483	219	2158	1.392
			30	2947	132.1	52.1	351	159	2020	1.303
0	0	0.4	75	13948	625.2	99.9	759	344	2115	1.365
			62	11162	500.3	92.1	704	319	2082	1.343
			52	7861	352.3	81.9	624	283	2020	1.303
			40	4632	207.6	67.7	505	229	1854	1.196
			30	2177	97.6	52.0	371	168	1592	1.027
0	0	0.6	75	12610	565.2	99.2	832	377	2027	1.308
			62	9482	425.0	90.3	758	343	1942	1.253
			52	6479	290.4	79.1	660	299	1807	1.166
			40	3891	174.4	66.3	540	244	1597	1.030
			30	1938	86.9	51.6	404	183	1316	0.849
15000	4572	0.2	75	17617	789.6	103.8	741	336	2251	1.452
			62	16676	747.5	100.6	720	326	2215	1.429
			52	14156	634.5	93.9	676	306	2214	1.428
			40	8850	396.7	78.7	565	256	2208	1.425
			30	3629	162.7	56.2	384	174	2055	1.326
1500	457	0.4	75	15334	687.3	104.3	791	358	2152	1.388
			62	14230	637.8	100.7	765	346	2118	1.366
			52	11646	522.0	92.9	710	322	2085	1.345
			40	6731	301.7	77.0	584	264	1967	1.269
			30	2692	120.7	56.0	404	183	1660	1.071
15000	4572	0.6	75	14537	651.6	105.0	876	397	2075	1.339
			62	12970	581.3	100.3	840	381	2033	1.312
			52	9878	442.8	91.6	769	348	1954	1.261
			40	5513	247.1	74.8	620	281	1742	1.124
			30	2364	106.0	55.5	438	198	1389	0.896
36000	10972	0.2	62	17570	787.5	103.7	741	336	2249	1.451
			52	15707	704.0	98.1	703	318	2213	1.428
			40	10852	486.4	85.1	611	277	2213	1.428
			30	4124	184.8	58.8	405	183	2078	1.341

Table XVIII. (Concluded)

Altitude (ft)	Altitude (m)	Mach	P/S	F_N/δ_o (lb)	F_N/δ_o (kN)	$N_F/\sqrt{\theta_o}$ (pct)	$W_{22}\sqrt{\theta_o}/\delta_o$ (ft/sec)	$W_{22}\sqrt{\theta_o}/\delta_o$ (m/sec)	A_N (in²)	A_N (m²)
36000	10972	0.4	62	15444	692.2	104.8	795	360	2161	1.394
			52	13674	612.9	99.3	755	342	2111	1.362
			40	9113	408.5	86.0	656	297	2043	1.318
			30	3223	144.5	59.5	434	196	1722	1.111
36000	10972	0.6	62	15020	673.2	106.9	891	404	2101	1.355
			52	13219	592.5	101.2	846	383	2037	1.314
			40	8631	386.9	87.6	734	332	1991	1.285
			30	3018	135.3	60.6	485	219	1489	0.961
36000	10972	0.8	62	16081	720.8	109.5	1037	470	2094	1.351
			52	14155	634.5	104.0	987	447	2027	1.308
			40	9104	408.1	89.8	854	387	1864	1.203
			30	3446	154.5	62.0	565	256	1384	0.893
36000	10972	1.0	75	18663	836.5	113.3	1253	568	2102	1.356
			62	17441	781.7	110.0	1216	551	2054	1.325
			52	14467	648.4	102.7	1144	518	1988	1.283
			40	8538	382.7	86.0	954	432	1773	1.144
			30	3478	155.9	61.4	648	293	1314	0.848
45000	13716	0.2	62	17661	791.6	104.4	741	336	2263	1.460
			52	15917	713.4	98.9	705	319	2212	1.427
			40	11006	493.3	85.7	613	278	2213	1.428
			30	7880	353.2	75.2	534	242	2187	1.411
45000	13716	0.4	62	15527	696.0	105.5	795	360	2173	1.402
			52	13858	621.1	99.9	756	342	2113	1.363
			40	9241	414.2	86.6	657	298	2045	1.319
			30	5499	246.5	71.9	539	244	1908	1.231
45000	13716	0.6	62	15082	676.0	107.4	890	403	2110	1.361
			52	13379	599.7	101.8	846	383	2041	1.317
			40	8735	391.5	88.0	734	332	1914	1.235
			30	3933	176.3	66.5	540	244	1601	1.033
45000	13716	0.8	62	16115	722.3	109.9	1035	469	2101	1.355
			52	14234	638.0	104.3	985	446	2031	1.310
			40	9186	411.7	90.1	853	386	1868	1.205
			30	3311	148.4	62.4	566	256	1390	0.897
45000	13716	1.0	75	18673	837.0	113.6	1249	566	2107	1.359
			62	17524	785.5	110.5	1216	551	2059	1.328
			52	14487	649.3	102.9	1140	517	1989	1.283
			40	8550	383.2	86.2	951	431	1775	1.145
			30	3536	158.5	61.7	649	294	1323	0.854

Table XIX. Cruise Performance for Single Stage Fans.

Designed for Cruise, P/P = 1.5

Altitude (ft)	Altitude (m)	Mach	P/S	F_N/δ_o (lb)	F_N/δ_o (kN)	$N_F/\sqrt{\theta_o}$ (pct)	$W_{22}\sqrt{\theta_o}/\delta_o$ (ft/sec)	$W_{22}\sqrt{\theta_o}/\delta_o$ (m/sec)	A_N (in^2)	A_N (m^2)
0	0	0.	75	18724	839.2	99.9	531	240	1659	1.070
			62	16100	721.6	92.7	493	223	1651	1.065
			52	12480	559.4	82.9	437	198	1641	1.059
			40	8034	360.1	67.9	346	156	1610	1.039
			30	4331	194.1	51.4	245	111	1582	1.021
0	0	0.2	75	15235	682.9	99.5	541	245	1637	1.056
			62	12744	571.2	92.1	502	227	1621	1.046
			52	9485	425.1	82.1	443	200	1594	1.028
			40	5761	258.2	67.7	351	159	1526	0.985
			30	2168	97.2	50.4	264	119	1173	0.757
0	0	0.4	75	13271	594.8	98.2	574	260	1588	1.025
			62	10696	479.4	90.5	528	239	1555	1.003
			52	7534	337.7	79.7	460	208	1484	0.957
			40	4507	202.0	65.8	366	166	1353	0.873
			30	2168	97.2	50.4	264	119	1173	0.757
0	0	0.6	75	12233	548.3	95.6	628	284	1546	0.997
			62	9241	414.2	89.6	564	255	1467	0.946
			52	6360	285.1	78.1	483	219	1353	0.873
			40	3876	173.7	65.3	389	176	1194	0.770
			30	1975	88.5	50.8	286	129	990	0.639
15000	4572	0.2	75	16167	724.6	103.7	559	253	1675	1.081
			62	15460	692.9	100.6	545	247	1640	1.058
			52	13137	588.8	93.6	508	230	1623	1.047
			40	8191	367.1	77.6	413	187	1574	1.015
			30	3438	154.1	55.5	274	124	1448	0.934
15000	4572	0.4	75	14446	647.5	104.2	597	270	1624	1.048
			62	13535	606.7	100.6	579	262	1591	1.026
			52	10980	492.1	92.7	533	241	1554	1.003
			40	6484	290.6	76.2	428	194	1441	0.930
			30	2656	119.0	55.2	288	130	1217	0.785
15000	4572	0.6	75	14012	628.0	105.1	663	300	1590	1.026
			62	15852	710.5	100.2	634	287	1552	1.001
			52	9626	431.5	91.0	574	260	1479	0.954
			40	5446	244.1	73.9	312	141	1044	0.674
			30	2394	107.3	54.7	312	141	1044	0.674
36000	10972	0.2	62	16126	722.8	103.6	559	253	1673	1.079
			52	14583	653.6	98.0	532	241	1632	1.053
			40	10085	452.0	84.5	454	205	1597	1.030
			30	3879	173.9	58.0	291	131	1463	0.944

Table XIX. (Concluded)

Altitude (ft)	Altitude (m)	Mach	P/S	F_N/δ_o (lb)	F_N/δ_o (kN)	$N_F/\sqrt{\theta_o}$ (pct)	$W_{22}\sqrt{\theta_o}/\delta_o$ (ft/sec)	$W_{22}\sqrt{\theta_o}/\delta_o$ (m/sec)	A_N (in^2)	A_N (m^2)
36000	10972	0.4	62	14521	650.9	104.8	599	271	1631	1.052
			52	13023	583.7	99.1	570	258	1584	1.022
			40	8729	391.3	85.4	487	220	1508	0.973
			30	3170	142.1	58.7	311	141	1259	0.812
36000	10972	0.6	62	14383	644.7	106.7	672	304	1611	1.039
			52	12822	574.7	101.2	639	289	1556	1.004
			40	8435	378.1	86.9	545	247	1441	0.930
			30	3032	135.9	59.6	348	157	1116	0.720
36000	10972	0.8	62	15604	699.4	109.4	782	354	1610	1.039
			52	13901	623.1	103.9	746	338	1556	1.004
			40	9033	404.9	88.9	634	287	1424	0.919
			30	3304	148.1	61.1	405	183	1052	0.679
36000	10972	1.0	75	18194	815.5	113.3	945	428	1617	1.043
			62	17151	768.7	110.1	922	418	1577	1.017
			52	14302	641.0	102.4	859	389	1524	0.983
			40	8520	381.9	84.7	698	316	1347	0.869
			30	3580	160.5	60.6	463	210	1007	0.650
45000	13716	0.2	62	16183	725.4	104.4	559	253	1684	1.086
			52	14767	661.9	98.7	533	241	1633	1.054
			40	10226	458.3	85.1	456	206	1598	1.031
			30	7339	328.9	74.4	391	177	1556	1.004
45000	13716	0.4	62	14576	653.3	105.4	600	272	1642	1.059
			52	13187	591.1	99.9	572	259	1586	1.023
			40	8844	396.4	85.9	488	221	1511	0.975
			30	5328	238.8	71.2	392	177	1395	0.900
45000	13716	0.6	62	14425	646.6	107.3	671	304	1619	1.045
			52	12696	569.1	101.7	640	290	1559	1.006
			40	8529	382.3	87.3	545	247	1443	0.931
			30	3912	175.3	65.7	389	176	1196	0.772
45000	13716	0.8	62	15629	700.5	109.8	781	354	1615	1.042
			52	13974	626.3	104.1	745	337	1559	1.006
			40	9111	408.4	89.4	634	287	1427	0.921
			30	3365	150.8	61.5	406	184	1056	0.681
45000	13716	1.0	75	18194	815.5	113.6	942	427	1620	1.045
			62	17216	771.7	110.5	921	417	1582	1.021
			52	14323	642.0	102.5	857	388	1526	0.985
			40	8536	382.6	84.8	696	315	1349	0.870
			30	3623	162.4	60.9	463	210	1010	0.652

Table XX. Low Speed VTO Performance, 90° F (305° K), Designed for Cruise, P/P=1.3

Altitude		Mp	PS	T54/Θo		FG/δo		NF/√Θo	W22√Θ/δo		WF/δ√Θ		FDR/δ	
ft	m			°R	°K	lbs	kN	PCT	lb/sec	kg/sec	lb/hr	kg/hr	lb	kN
0	0	0	2 min	1743	968	16922	75.27	86.3	858.8	389.5	5396	2448	0	0.00
			75	1711	950	16380	72.89	85.1	847.6	384.5	5174	2347	0	0.00
			62	1556	864	13223	58.81	77.5	776.1	352.0	4035	1830	0	0.00
			52	1406	781	9743	43.34	67.9	676.3	306.8	3003	1362	0	0.00
			40	1251	694	6428	28.59	56.6	554.4	251.5	2092	949	0	0.00
			30	1096	608	3542	15.76	44.1	417.9	189.6	1359	616	0	0.00
0	0	.0734	2 min	1744	968	17146	76.27	86.3	861.2	390.6	5415	2456	2404	10.69
			75	1712	951	16619	73.94	85.1	850.4	385.7	5189	2354	2374	10.56
			62	1556	864	13408	59.64	77.4	777.4	352.6	4038	1831	2168	9.64
			52	1406	781	9932	44.18	67.8	677.7	307.4	3008	1364	1891	8.41
			40	1252	695	6620	29.45	56.6	555.5	251.9	2097	951	1556	6.92
			30	1097	610	3741	16.64	44.1	419.0	190.1	1364	619	1185	5.27
0	0	.1469	2 min	1747	970	17814	79.24	86.3	868.8	394.1	5472	2482	4853	21.59
			75	1714	952	17269	76.82	85.2	857.6	389.0	5237	2375	4791	21.31
			62	1555	863	13950	62.05	77.2	781.4	354.4	4051	1837	4362	19.40
			52	1407	781	10490	46.66	67.7	681.6	309.2	3024	1372	3807	16.93
			40	1253	696	7173	31.91	56.5	558.8	253.5	2111	958	3133	13.94
			30	1100	611	4285	19.06	44.0	421.8	191.3	1378	635	2388	10.62
0	0	.2202	2 min	1752	973	18918	84.15	86.5	881.6	399.9	5565	2524	7381	32.83
			75	1717	954	18341	81.58	85.2	869.7	394.5	5317	2412	7282	32.39
			62	1554	868	14828	65.96	81.4	787.9	357.4	4071	1846	6593	29.33
			52	1408	782	11373	50.59	67.4	687.7	311.9	3049	1383	5758	25.61
			40	1256	698	8036	35.74	56.4	564.6	256.1	2135	968	4746	21.11
			30	1104	613	5083	22.61	43.9	426.3	193.4	1401	635	3670	16.10
1000	305	0	2 min	1748	971	16999	75.61	86.4	860.4	390.3	5425	2461	0	0.00
			75	1717	954	16500	73.40	85.4	850.1	385.6	5212	2364	0	0.00
			62	1567	870	13494	60.02	78.3	783.8	355.5	4114	1866	0	0.00
			52	1413	765	9914	44.10	68.4	681.8	309.3	3050	1383	0	0.00
			40	1257	698	6527	29.03	57.0	558.4	253.3	2119	961	0	0.00
			30	1099	610	3583	15.94	44.2	420.0	190.5	1368	621	0	0.00
1000	305	.0737	2 min	1747	971	17224	76.62	86.4	862.9	391.4	5444	2469	2018	10.76
			75	1718	954	16722	74.38	85.4	852.6	386.7	5229	2372	2389	10.63
			62	1567	871	13680	60.85	78.2	785.1	356.1	4119	1868	2198	9.78
			52	1413	785	10105	44.95	68.3	683.1	309.8	3055	1386	1810	8.05
			40	1257	698	6723	29.91	57.0	559.7	253.9	2123	963	1574	7.01
			30	1100	611	3781	16.82	44.2	421.1	191.0	1372	622	1196	5.32

Table XX. Low Speed VTO Performance, 90° F (305° K), Designed for Cruise, P/P=1.3 (concluded)

Altitude		Mp	PS	T54/Θo		FG/δo		NF/√Θo	W22√Θ/δo		WF/δ√Θ		FDR/δ	
ft	m			°R	°K	lbs	kN	PCT	lb/sec	kg/sec	lb/hr	kg/hr	lb	kN
1000	305	.1473	2 min	1752	973	17902	79.63	86.4	870.7	394.9	5500	2495	4877	21.69
			75	1720	955	17379	77.31	85.4	859.8	390.0	5278	2394	4817	21.43
			62	1566	870	14223	63.27	77.9	788.7	357.7	4132	1874	4414	19.63
			52	1414	785	10667	47.45	68.2	687.0	311.6	3071	1393	3849	17.12
			40	1258	699	7276	32.37	56.9	562.9	255.3	2138	970	3164	14.07
			30	1103	613	4334	19.28	44.2	424.3	192.5	1566	710	2409	10.72
1000	305	.221	2 min	1757	976	19011	84.57	86.5	883.3	400.7	5596	2538	7422	33.01
			75	1724	957	18460	82.11	85.5	872.0	395.5	5359	2431	7328	32.60
			62	1565	869	15111	67.21	77.5	795.3	360.7	4154	1884	6679	29.71
			52	1415	786	11564	51.44	67.9	693.6	314.6	3165	1436	5830	25.93
			40	1261	700	8147	36.24	56.8	568.7	258.0	2162	981	4797	21.34
			30	1106	614	5141	22.87	44.1	428.9	194.5	1410	670	3654	16.25
2000	610	0	2 min	1753	973	17082	75.99	86.6	862.0	391.0	5455	2747	0	0.00
			75	1724	958	16606	73.87	85.6	852.4	386.6	5254	2383	0	0.00
			62	1578	877	13768	61.24	79.0	791.8	359.1	4194	1903	0	0.00
			52	1421	789	10090	44.88	68.9	687.3	311.8	3098	1405	0	0.00
			40	1262	701	6630	29.49	57.4	562.6	255.2	2145	973	0	0.00
			30	1101	612	3621	16.11	44.5	422.2	191.5	1376	624	0	0.00
2000	610	.0739	2 min	1754	974	17309	76.99	86.6	864.7	392.2	5474	2083	2430	10.81
			75	1725	958	16829	74.86	85.6	854.8	387.7	5270	2390	2403	10.69
			62	1577	876	13952	62.06	78.9	792.1	359.2	4200	1905	2226	9.90
			52	1421	789	10282	45.74	68.8	688.6	312.3	3104	1408	1935	8.61
			40	1262	701	6822	30.35	57.4	563.6	255.6	2150	975	1590	7.07
			30	102	612	3821	17.00	44.5	423.3	192.0	1381	626	1205	5.36
2000	610	.1478	2 min	1757	976	17985	80.00	86.6	872.3	895.7	5531	2509	4902	21.81
			75	1727	959	17488	77.79	85.6	862.0	391.0	5319	2412	4845	21.59
			62	1577	876	14506	64.53	78.7	796.8	361.4	4215	1912	4475	19.91
			52	1422	789	10849	48.26	68.7	692.6	314.2	3120	1415	3893	17.32
			40	1264	702	7383	32.84	57.3	567.1	257.2	2165	982	3199	14.23
			30	1104	613	4373	19.45	44.5	426.3	193.3	1395	633	2427	10.80
2000	610	.2217	2 min	1762	979	19103	84.97	86.7	885.1	401.7	5627	2552	7462	33.19
			75	1730	961	18578	82.64	85.7	874.4	396.6	5400	2449	7372	32.79
			62	1577	876	15401	68.51	78.2	803.2	364.3	4237	1922	6765	30.09
			52	1424	791	11754	52.28	68.4	699.4	317.2	3148	1427	5895	26.22
			40	1267	703	8261	36.75	57.1	572.9	259.9	2190	2190	4848	21.56
			30	1109	616	5196	23.11	44.4	431.6	195.8	1419	1419	3687	16.40

Table XXI. Low Speed VTO Performance, 90° F (305° K), Designed for Cruise, P/P=1.5

Altitude ft	Altitude m	Mp	PS	T54/θo °R	T54/θo °K	FG/δo lbs	FG/δo kN	NF/√θo PCT	W22√θ/δo lb/sec	W22√θ/δo kg/sec	WF/δ√θ lb/hr	WF/δ√θ kg/hr	FDR/δ lb	FDR/δ kN
0	0	0	2 min	1743	968	13087	58.21	85.1	456.9	207.2	5396	2448	0	0.00
			75	1711	950	12664	56.33	83.8	444.3	201.5	5174	2347	0	0.00
			62	1556	864	10102	44.94	68.0	396.1	179.7	4035	1830	0	0.00
			52	1406	781	7407	32.95	66.2	336.3	152.5	3003	1362	0	0.00
			40	1251	694	4911	21.85	55.3	268.7	121.8	2092	949	0	0.00
			30	1096	608	2732	12.15	42.5	195.7	88.8	1359	616	0	0.00
0	0	.0734	2 min	1744	968	13204	58.73	85.1	452.6	205.3	5415	2456	1363	6.06
			75	1712	951	12789	56.89	83.9	445.9	202.3	5189	2354	1343	5.97
			62	1556	864	10183	45.30	75.7	396.8	180.0	4038	1831	1191	5.82
			52	1406	781	7488	33.31	66.2	336.9	152.8	3008	1364	1023	4.55
			40	1252	695	4992	22.21	55.3	269.2	122.1	2097	951	827	3.68
			30	1097	610	2812	12.51	42.5	196.3	89.0	1364	619	618	2.75
0	0	.1469	2 min	1747	970	13556	60.30	85.2	456.6	207.1	5472	2482	2751	12.24
			75	1714	952	13125	58.39	83.9	449.5	203.9	5237	2375	2710	12.05
			62	1555	863	10423	46.36	75.5	398.4	180.7	4051	1837	2409	10.72
			52	1407	781	7732	34.39	66.1	338.6	153.6	3024	1372	2058	9.15
			40	1253	696	5229	23.26	55.1	270.8	122.8	2111	958	1665	7.41
			30	1100	611	3037	13.51	42.4	197.3	89.5	1378	625	1244	5.53
0	0	.2202	2 min	1752	973	14145	62.92	85.2	463.0	210.0	5565	2524	4182	18.60
			75	1717	954	13685	60.88	83.9	455.6	206.7	5317	2412	4117	18.31
			62	1554	868	10818	48.12	68.3	401.3	182.0	4071	1846	3637	16.18
			52	1408	782	8128	13.91	65.8	341.3	154.8	3049	1383	3111	13.84
			40	1256	698	5612	24.96	55.1	273.5	124.0	2135	968	2521	11.21
			30	1104	613	3387	15.07	42.4	199.2	90.4	1401	635	1884	8.38
1000	305	0	2 min	1748	971	13151	58.50	85.3	452.6	205.2	5425	2461	0	0
			75	1717	954	12756	56.74	84.1	446.0	202.3	5212	2364	0	0
			62	1567	870	10308	45.85	76.5	400.4	181.6	4114	1866	0	0
			52	1413	765	7540	33.54	66.8	339.7	154.0	3050	1383	0	0
			40	1257	698	4981	22.16	55.6	270.7	122.8	2119	961	0	0
			30	1099	610	2764	12.29	42.8	197.1	89.4	1368	621	0	0
1000	305	0	2 min	1749	971	13268	59.02	85.3	453.8	205.8	5444	2469	1371	6.10
			75	1718	954	12869	57.24	84.1	447.2	202.8	5224	2372	1352	6.01
			62	1567	871	10398	46.25	76.4	400.9	181.8	4119	1868	1215	5.40
			52	1413	785	76228	33.93	66.7	340.3	154.3	3055	1386	1037	4.61
			40	1257	698	5064	22.52	55.6	271.3	123.0	2123	963	836	3.72
			30	1100	611	2842	12.64	42.7	197.4	89.5	1372	622	623	2.77
1000	304	.1473	2 min	1752	973	13626	60.61	85.4	457.7	207.6	5500	2495	2765	12.30
			75	1720	955	13211	58.77	84.2	450.9	204.5	5278	2394	2725	12.12
			62	1566	870	10633	47.30	76.2	402.7	182.7	4132	1874	2441	10.86
			52	1414	785	7868	35.00	66.5	341.9	155.1	3071	1393	2084	9.27
			40	1258	699	5302	28.58	55.5	272.9	123.8	2138	970	1681	7.48
			30	1103	613	3071	13.66	42.7	198.8	90.2	1566	710	1256	5.59

Table XXI. Low Speed VTO Performance, 90° F (305° K), Designed for Cruise, P/P=1.5 (concluded)

Altitude		Mp	PS	T54/Θo		FG/δo		NF/√Θo	W22√Θ/δo		WF/δ√Θ		FDR/δ	
ft	m			°R	°K	lbs	kN	PCT	lb/sec	kg/sec	lb/hr	kg/hr	lb	kN
1000	610	.221	2 min	1757	976	14216	63.24	85.4	464.2	210.6	5596	2538	4208	18.72
			75	1724	957	13778	61.29	84.2	457.1	207.4	5359	2431	4145	18.43
			62	1565	869	11037	49.10	75.8	405.7	184.0	4154	1884	3690	16.41
			52	1415	786	8269	36.78	66.3	344.6	156.3	3165	1436	3152	14.02
			40	1261	700	5691	25.31	55.4	275.7	125.0	2162	981	2652	11.80
			30	1106	614	3426	15.24	42.6	200.8	91.1	1410	670	1904	8.47
2000	610	0	2 min	1753	973	13218	58.80	85.5	453.6	205.7	5455	2747	0	0.00
			75	1724	958	12839	57.11	84.4	447.4	202.9	5254	2383	0	0.00
			62	1578	877	10517	46.78	77.1	404.7	183.6	4194	1903	0	0.00
			52	1421	789	7673	34.13	67.3	342.9	155.5	3098	1405	0	0.00
			40	1262	701	5053	22.48	55.9	272.8	123.7	2145	973	0	0.00
			30	1101	612	2798	12.45	43.0	198.4	89.99	1376	624	0	0.00
2000	610	.0739	2 min	1754	974	13337	59.33	85.5	454.9	206.3	5474	2083	1379	6.13
			75	1725	958	12955	57.63	84.4	448.7	203.5	5270	2390	1361	6.05
			62	1577	876	10597	47.14	77.0	405.2	183.8	4200	1905	1231	5.48
			52	1421	789	7756	34.50	67.2	343.5	155.8	3104	1408	1050	4.67
			40	1262	701	5134	22.84	55.8	273.2	123.9	2150	975	845	3.76
			30	1102	612	2877	12.80	43.0	198.9	90.2	1381	626	629	2.80
2000	610	.1478	2 min	1757	976	13692	60.91	85.6	458.9	208.2	5531	2509	2781	12.37
			75	1727	959	13297	59.15	84.3	452.3	205.1	5319	2412	2743	12.20
			62	1577	876	10848	48.25	76.9	407.0	189.1	4215	1912	2475	11.01
			52	1422	789	8007	35.62	67.1	345.3	156.7	3120	1415	2111	9.39
			40	1264	702	5376	23.91	55.8	275.0	124.7	2165	982	1699	7.56
			30	1104	613	3105	13.81	42.9	200.1	90.8	1345	633	1267	5.64
2000	610	.2217	2 min	1762	979	14287	63.55	85.6	465.4	211.1	5627	2552	4232	18.82
			75	1730	961	13869	61.69	84.4	458.6	208.0	5400	2449	4172	18.56
			62	1577	876	11258	50.08	76.5	410.1	186.0	4237	1922	3741	16.64
			50	1424	791	8414	37.43	66.8	348.1	157.8	3148	1427	3192	14.20
			40	1267	703	5770	25.67	55.7	277.7	126.0	2140	993	2577	11.46
			30	1109	616	3465	15.41	42.8	202.2	91.7	1419	644	1922	8.55

Table XXII. Design Point Parameters for Two Stage Fans Designed for VTO, SLS, 90° F (305° K) Day, Uninstalled.

Fan Pressure Ratio	1.3	1.4	1.5	1.6	1.7
Fan Tip Speed, ft/sec (m/sec)	1200(365.8)	1180(359.7)	1155(352.0)	1095(333.8)	1050(320.0)
Fan Tip Diameter, inches (meters)	82.17(2.087)	70.15(1.782)	6.175(1.568)	56.42(1.433)	52.67(1.338)
Fan Inlet Radius Ratio	0.340	0.340	0.340	0.388	0.444
Fan Exit Mach Number	0.55	0.55	0.55	0.55	0.55
Fan Efficiency	0.84	0.84	0.84	0.84	0.84
Fan Airflow, lb/sec (kg/sec)	1231.1(558.4)	896.5(406.6)	693.6(314.6)	556.6(242.5)	458.0(207.7)
Turbine Inlet Temperature, °R (° K)	1998(1110)	1998(1110)	1998(1110)	1998(1110)	1998(1110)
Turbine Inlet Pressure, psia (kN/m^2)	56.41(388.9)	56.41(388.9)	56.41(388.9)	56.41(388.9)	56.41(388.9)
Turbine Inlet Flow, lb/sec (kg/sec)	135.58(662.0)	135.58(662.0)	135.58(662.0)	135.58(662.0)	135.58(662.0)
Turbine Exit Static PRessure Ratio	1.058	1.140	1.222	1.303	1.384
Turbine Exit Mach Number	0.55	0.55	0.55	0.55	0.55
Interconnect Duct Pressure Loss (pct) (Engine Exit to Scroll Inlet)	3	3	3	3	3
Scroll Pressure Loss (pct)	5	5	5	5	5
Ideal Uninstalled Thrust, lb(kN)	3.532(140.3)	27652(123.0)	24981(111.1)	22978(102.2)	21412(95.25)
Nozzle Area, sq in (sq meters)	4141(2.671)	2800(1.806)	2077(1.339)	1633(1.054)	1336(0.862)

Table XXIII. Design Point Parameters for Two Stage Fans Designed for Cruise, SLS, Standard Day, Uninstalled.

Fan Pressure Ratio	1.3	1.4	1.5	1.6	1.7
Fan Tip Speed, ft/sec (m/sec)	1071(326.4)	1047(319.1)	1000(304.8)	950(289.6)	900(274.3)
Fan Tip Diameter, inches (meters)	72.93(1.852)	61.99(1.575)	54.92(1.395)	50.62(1.286)	47.71(1.212)
Fan Inlet Radius Ratio	0.340	0.340	0.370	0.440	0.511
Fan Exit Mach Number	0.55	0.55	0.55	0.55	0.55
Fan Efficiency	0.84	0.84	0.84	0.84	0.84
Fan Airflow, lb/sec(kg/sec)	99.9(453.5)	721.7(327.4)	552.5(250.6)	438.4(198.9)	356.5(161.7)
Turbine Inlet Temperature, °R (°K)	1773(985)	1773(985)	1773(985)	1773(985)	1773(985)
Turbine Inlet Pressure, psia (kN/m^2)	50.23(346.3)	50.23(346.3)	50.23(346.3)	50.23(346.3)	50.23(346.3)
Turbine Inlet Flow, lb/sec(kg/sec)	128.58(627.8)	128.58(627.8)	128.58(627.8)	128.58(627.8)	128.58(627.8)
Turbine Exit Static Pressure Ratio	1.058	1.140	1.221	1.303	1.384
Turbine Exit Mach Number	0.55	0.55	0.55	0.55	0.55
Interconnect Duct Pressure Loss(pct) (Engine Exit to Scroll Inlet)	3	3	3	3	3
Scroll Pressure Loss (pct)	5	5	5	5	5
Ideal Uninstalled Thrust, lb(kN)	25417(113.1)	22276(99.09)	20095(89.39)	18463(82.13)	17190(76.46)
Nozzle Area, sq. in. (sq meters)	3336(2.152)	2256(1.455)	1671(1.078)	1312(0.846)	1073(0.692)

Table XXIV. VTO Performance of Two Stage Fans
Designed for VTO, SLS, 90° F (305° K) Day, Installed.

	Intermediate Std Day, 360°	Intermediate Hot Day, 360°	2 Min VTO (Dry) Hot Day, 360°	3 Sec VTO (Dry) Hot Day, 360°	Emergency (Dry) Hot Day, 360°
NE, pct	105	105	106	106	110
W5.4,lb/sec(kg/sec)	126.8(51.50)	120.2(54.54)	121.8(55.24)	133.8(60.68)	124.3(60.69)
P5.1,psi(kN/m^2)	53.63(396.8)	51.34(354.0)	52.60(362.7)	60.22(415.2)	54.67(376.9)
T5.4, °R(°K)	1773(985)	1814(1008)	1847(1026)	1997(1109)	1913(1063)
P5.4,psi,(kN/m^2)	49.34(340.2)	47.23(325.6)	48.39(333.6)	55.40(382.0)	50.30(346.8)
WF,lb/hr(kg/hr)	8324(3775)	7990(3624)	8247(3741)	9323(4229)	8895(4035)

<u>Fan Pressure Ratio = 1.3</u>

	Intermediate Std Day, 360°	Intermediate Hot Day, 360°	2 Min VTO (Dry) Hot Day, 360°	3 Sec VTO (Dry) Hot Day, 360°	Emergency (Dry) Hot Day, 360°
P/P	1.253	1.237	1.246	1.3	1.262
NF,pct	93.07	93.34	94.66	102.88	97.10
W10,lb/sec(kN/sec)	1176(533.8)	1117(506.6)	1130(513.0)	1212(549.8)	1157(525.9)
Fn, lb(kN)	25380(112.9)	23888(106.3)	24691(109.8)	29558(131.5)	26148(116.3)
Fn Ratio	1.0	0.941	0.972	1.164	1.030

<u>Fan Pressure Ratio = 1.4</u>

	Intermediate Std Day, 360°	Intermediate Hot Day, 360°	2 Min VTO (Dry) Hot Day, 360°	3 Sec VTO (Dry) Hot Day, 360°	Emergency (Dry) Hot Day, 360°
P/P	1.339	1.317	1.329	1.399	1.350
NF	92.75	92.97	94.32	102.86	96.77
W10	848.9(385.0)	803.4(364.4)	814.7(369.5)	882.4(400.2)	836.1(379.2)
Fn	22333(99.34)	21000(93.41)	21715(96.59)	26094(116.1)	23011(102.4)
Fn Ratio	1.0	0.940	0.972	1.168	1.030

Table XXIV. VTO Performance of Two Stage Fans Designed for VTO, SLS, 90° F Day, Installed. (Concluded)

	Intermediate Std Day, 360°	Intermediate Hot Day, 360°	2 Min VTO (Dry) Hot Day, 360°	3 Sec VTO (Dry) Hot Day, 360°	Emergency (Dry) Hot Day, 360°
	Fan Pressure Ratio = 1.5				
P/P	1.426	1.399	1.414	1.499	1.439
NF	92.41	92.58	93.95	102.85	96.45
W10	651.8(295.7)	615.1(279.0)	624.8(283.4)	682.6(309.6)	642.8(291.6)
Fn	20218(89.93)	18996(84.50)	19651(87.41)	23670(105.3)	20838(92.69)
Fn Ratio	1.0	0.939	0.971	1.170	1.030
	Fan Pressure Ratio = 1.6				
P/P	1.509	1.477	1.494	1.599	1.525
NF	92.29	92.49	93.85	102.85	96.31
W10	518.5(235.2)	488.2(221.4)	496.5(225.2)	547.7(248.4)	511.7(232.1)
Fn	18528(82.42)	17403(77.41)	18006(80.09)	21829(97.10	19097(84.95)
Fn Ratio	1.0	0.9393	0.971	1.178	1.030
	Fan Pressure Ratio = 1.7				
P/P	1.595	1.557	1.577	1.699	1.612
NF	92.21	92.35	93.76	102.85	96.16
W10	424.3(192.5)	398.5(180.8)	405.9(184.1)	450.7(204.4)	418.9(190.0)
Fn	17280(76.87)	16214(72.12)	16786(74.67)	20382(90.66)	17799(79.17)
Fn Ratio	1.0	0.938	0.971	1.179	1.030

Table XXV. VTO Performance of Two Stage Fans
Designed for Cruise, SLS, Standard Day, Installed.

	Intermediate Std Day, 360°	Intermediate Std Day, 240°	Intermediate Hot Day, 240°	2 Min VTO (Dry) Hot Day, 240°	3 Sec VTO (Dry) Hot Day, 240°	Emergency (Dry) Hot Day, 240°
NE, pct	105	105	105	106	106	110
W54, lb/sec (kg/sec)	126.8(57.50)	84.5(38.33)	80.2(36.37)	81.2(41.36)	89.2(40.46)	82.8(37.58)
P5.1, psia (kN/m^2)	63.63(369.8)	53.63(369.8)	51.34(354.0)	52.60(362.7)	60.22(415.2)	54.67(376.9)
T5.4, °R(°K)	1773(985)	1773(985)	1814(1008)	1847(1026)	1997(1109)	1913(1063)
P5.4, psia (kN/m^2	49.34(343.2)	49.34(340.2)	47.23(325.6)	48.39(333.6)	55.40(382.0)	50.30(346.8)
WF, lb/hr (kg/hr)	8324(3776)	5549(2517)	5239(2417)	5498(2494)	6824(3095)	5930(2690)
Fan Design Pressure Ratio = 1.3						
P/P	1.3	1.215	1.203	1.209	1.252	1.222
NF, pct	99.94	87.29	87.66	88.83	95.61	90.95
W10, lb/sec (kg/sec)	984.4(446.5)	876.2(397.4)	831.0(376.9)	841.6(381.8)	900.1(408.3)	860.8(390.5)
Fn, lb(kN)	23828(106.0)	17528(77.97)	16531(73.53)	17060(75.88)	20324(90.4)	18027(80.19)
Fn Ratio	1.0	0.735	0.693	0.716	0.853	0.756
Fan Design Pressure Ratio = 1.4						
P/P	1.4	1.291	1.273	1.282	1.34	1.299
NF	99.92	86.89	87.14	88.36	95.41	90.58
W10	710.4(322.2)	622.1(282.2)	587.9(266.7)	596.5(270.6)	644.9(292.5)	612.3(277.7)
Fn	21023(93.51	15276(67.95)	14383(63.98)	14854(66.07)	17793(79.15)	15722(69.93)
Fn Ratio	1.0	0.72	0.684	0.706	0.846	0.747

Table XXV. VTO Performance of Two Stage Fans Designed for Cruise, SLS, Standard Day, Installed. (Concluded)

	Intermediate Std Day, 360°	Intermediate Std Day, 240°	Intermediate Hot Day, 240°	2 Min VTO (Dry) Hot Day, 240°	3 Sec VTO (Dry) Hot Day, 240°	Emergency (Dry) Hot Day, 240°
Fan Design Pressure Ratio = 1.5						
P/P	1.499	1.366	1.347	1.356	1.427	1.377
NF	99.92	86.88	87.04	88.31	95.56	90.59
W10	543.7(246.7)	470.38(213.4)	443.1(201.0)	449.3(203.8)	491.2(222.8)	463.5(210.3)
Fn	19040(84.69)	13680(60.85)	12861(57.21)	13290(59.11)	15989(71.12)	14085(62.65)
Fn Ratio	1.0	0.718	0.675	0.698	0.839	0.739
Fan Design Pressure Ratio = 1.6						
P/P	1.599	1.443	1.416	1.446	1.534	1.472
NF	99.91	86.85	86.91	87.18	94.92	89.51
W10	431.4(195.7)	369.5(167.6)	348.8(158.2)	354.8(161.0)	391.8(177.7)	366.3(166.2)
FN	17540(78.02)	12489(55.55)	11724(52.15)	12122(53.92)	14641(65.13)	12860(57.20)
Fn Ratio	1.0	0.712	0.668	0.691	0.834	0.733
Fan Design Pressure Ratio = 1.7						
P/P	1.698	1.521	1.489	1.506	1.608	1.536
NF	99.88	86.90	86.92	88.25	95.83	90.65
W10	350.7(159.1)	298.2(135.3)	279.4(126.7)	284.7(129.1)	315.4(143.1)	294.5(133.6)
Fn	16361(72.78)	11566(51.48)	10849(48.26)	11224(49.93)	13594(60.47)	11912(51.65)
Fn Ratio	1.0	0.707	0.663	0.686	0.831	0.728

Table XXVI. Cruise Performance for Two Stage Fans. Designed for VTO, P/P = 1.3

Altitude (ft)	Altitude (m)	Mach	P/S	F_N/δ_o (lb)	F_N/δ_o (kN)	$N_F/\sqrt{\theta_o}$ (pct)	$W_{22}\sqrt{\theta_o}/\delta_o$ (ft/sec)	$W_{22}\sqrt{\theta_o}/\delta_o$ (m/sec)	A_N (in^2)	A_N (m^2)
0	0	0.	75	25380	1137.6	93.1	1176	533	4313	2.783
			62	21797	977.0	87.1	1108	502	4419	2.851
			52	16778	752.0	77.7	994	450	4569	2.948
			40	11129	498.8	65.2	826	374	4710	3.039
			30	5803	260.1	49.2	605	274	4906	3.165
0	0	0.2	75	18583	832.9	93.1	1201	544	4138	2.670
			62	15317	686.5	86.9	1127	511	4195	2.706
			52	11076	496.4	77.2	1008	457	4232	2.730
			40	6722	301.3	65.0	840	381	4161	2.685
			30	2937	131.6	49.1	616	279	4889	3.154
0	0	0.4	75	14866	666.3	93.2	1277	579	3788	2.444
			62	11614	520.6	86.1	1186	537	3743	2.415
			52	7932	355.5	75.9	1049	475	3600	2.323
			40	4722	211.6	64.5	881	399	3314	2.138
			30	1994	89.4	48.9	650	294	2778	1.792
0	0	0.6	75	12880	577.3	92.9	1404	636	3487	2.250
			62	9298	416.8	83.9	1278	579	3339	2.154
			52	6329	283.7	74.3	1127	511	3087	1.992
			40	3781	169.5	63.2	945	428	2715	1.752
			30	1697	76.1	46.9	707	320	2189	1.412
15000	4572	0.2	75	20300	909.9	101.4	1237	561	4114	2.654
			62	18839	846.6	98.5	1208	547	4134	2.667
			52	15832	709.6	92.5	1140	517	4189	2.703
			40	9596	430.1	77.3	957	434	4220	2.723
			30	3748	168.0	53.2	672	304	3958	2.554
15000	4572	0.4	75	16589	743.6	96.7	1320	598	3804	2.454
			62	15187	680.7	93.9	1285	582	3788	2.444
			52	11988	537.3	86.9	1197	542	3749	2.419
			40	6851	307.1	73.0	1000	453	3530	2.277
			30	2552	114.4	52.9	707	320	2921	1.885
15000	4572	0.6	75	15027	673.5	97.5	1465	664	3545	2.287
			62	13261	594.4	93.8	1415	641	3497	2.256
			52	9704	435.0	85.0	1292	586	3356	2.165
			40	5361	240.3	70.5	1068	484	2980	1.923
			30	2130	95.5	52.4	770	349	2340	1.510

Table XXVI. (Continued)

Altitude (ft)	Altitude (m)	Mach	P/S	F_N/δ_o (lb)	F_N/δ_o (kN)	$N_F/\sqrt{\theta_o}$ (pct)	$W_{22}\sqrt{\theta_o}/\delta_o$ (ft/sec)	$W_{22}\sqrt{\theta_o}/\delta_o$ (m/sec)	A_N (in^2)	A_N (m^2)
36000	10972	0.2	75	21302	954.8	98.3	1257	570	4096	2.643
			62	20192	905.0	96.2	1236	560	4116	2.655
			52	17704	793.5	91.5	1183	536	4157	2.682
			40	11828	530.2	79.3	1036	469	4251	2.743
			30	4374	196.1	56.1	713	323	4019	2.593
36000	10972	0.4	75	17905	802.5	99.6	1350	612	3806	2.455
			62	16799	753.0	97.3	1326	601	3804	2.454
			52	14530	651.3	92.6	1269	575	3786	2.443
			40	9287	416.3	80.1	1110	503	3687	2.379
			30	3152	141.3	56.6	763	346	3059	1.974
36000	10972	0.6	75	16919	758.3	101.7	1515	687	3584	2.312
			62	15738	705.4	99.1	1485	673	3562	2.298
			52	13527	606.3	94.4	1423	645	3504	2.261
			40	8457	379.1	81.6	1242	563	3284	2.119
			30	2827	126.7	57.6	853	386	2529	1.632
36000	10972	0.8	75	17735	794.9	104.4	1766	801	3517	2.269
			62	16371	733.8	101.6	1730	784	3480	2.245
			52	14093	631.7	97.0	1660	752	3398	2.192
			40	8716	390.7	83.6	1446	655	3106	2.004
			30	2960	132.7	59.0	993	450	2298	1.483
36000	10972	1.0	75	18947	849.2	105.3	2090	948	3487	2.250
			62	17356	777.9	102.4	2040	925	3439	2.219
			52	14142	633.9	96.1	1928	874	3322	2.143
			40	8016	359.3	80.2	1617	733	2913	1.879
			30	3067	137.5	58.1	1135	514	2155	1.390

Table XXVI. (Concluded)

Altitude (ft)	Altitude (m)	Mach	P/S	F_N/δ_o (lb)	F_N/δ_o (kN)	$N_F/\sqrt{\theta_o}$ (pct)	$W_{22}\sqrt{\theta_o}/\delta_o$ (ft/sec)	$W_{22}\sqrt{\theta_o}/\delta_o$ (m/sec)	A_N (in2)	A_N (m^2)
45000	13716	0.2	75	21676	971.6	99.2	1261	571	4088	2.637
			62	20527	920.1	97.0	1239	562	4108	2.650
			52	17989	806.3	92.2	1185	537	4147	2.675
			40	12038	539.6	80.0	1041	472	4259	2.748
			30	8625	386.6	70.9	919	416	4213	2.718
45000	13716	0.4	75	18201	815.8	100.4	1352	613	3807	2.456
			62	17079	765.5	98.0	1327	601	3804	2.454
			52	14774	662.2	93.2	1271	576	3787	2.443
			40	9446	423.4	80.8	1114	505	3701	2.388
			30	5595	250.8	68.1	933	423	3426	2.210
45000	13716	0.6	75	17141	768.3	102.2	1515	687	3589	2.315
			62	15937	714.3	99.7	1485	673	3566	2.301
			52	13721	615.0	95.0	1424	645	3510	2.265
			40	8577	384.4	82.1	1245	564	3298	2.128
			30	3824	171.4	63.5	945	428	2735	1.765
45000	13716	0.8	75	17880	801.4	104.9	1764	800	3523	2.273
			62	16484	738.8	102.0	1727	783	3485	2.248
			52	14193	636.2	97.3	1657	751	3403	2.195
			40	8810	394.9	84.0	1446	655	3117	2.011
			30	3037	136.1	59.4	997	452	2313	1.492
45000	13716	1.0	75	19029	852.9	105.6	2085	945	3491	2.252
			62	17462	782.7	102.7	2036	923	3445	2.223
			52	14179	635.5	96.3	1923	872	3325	2.145
			40	8037	360.2	80.4	1612	731	2917	1.882
			30	3140	140.7	58.5	1137	515	2167	1.398

Table XXVII. Cruise Performance for Two Stage Fans. Designed for VTO, P/P = 1.4

Altitude (ft)	(m)	Mach	P/S	F_N/δ_o (lb)	(kN)	$N_F/\sqrt{\theta_o}$ (pct)	$W_{22}\sqrt{\theta_o}/\delta_o$ (ft/sec)	(m/sec)	A_N (in^2)	(m^2)
0	0	0.	75	22333	1001.0	92.7	848	384	2850	1.839
			62	19132	857.5	86.7	792	359	2877	1.856
			52	14668	657.4	76.9	700	317	2900	1.871
			40	9748	436.9	64.4	572	259	2890	1.865
			30	5138	230.3	48.4	411	186	2902	1.872
0	0	0.2	75	17178	770.0	92.4	866	392	2774	1.790
			62	14210	636.9	86.0	805	365	2777	1.792
			52	10354	464.1	76.2	709	321	2749	1.774
			40	6426	288.0	64.2	581	263	2654	1.712
			30	2952	132.3	48.3	418	189	2469	1.593
0	0	0.4	75	14281	640.1	92.9	920	417	2613	1.686
			62	11243	503.9	85.5	845	383	2560	1.652
			52	7792	349.3	75.1	736	333	2437	1.572
			40	4767	213.7	63.7	609	276	2232	1.440
			30	2126	95.3	48.1	440	199	1885	1.216
0	0	0.6	75	12707	569.6	92.5	1007	456	2467	1.592
			62	9294	416.6	83.4	906	410	2346	1.514
			52	6438	288.6	73.4	788	357	2155	1.390
			40	3934	176.3	62.2	650	294	1895	1.223
			30	1869	83.8	47.7	477	216	1530	0.987
15000	4572	0.2	75	18740	840.0	101.1	896	406	2775	1.790
			62	17452	782.2	98.2	871	395	2774	1.790
			52	14678	657.9	92.0	816	370	2779	1.793
			40	9032	404.8	76.4	670	303	2725	1.758
			30	3695	165.6	52.4	458	207	2513	1.621
15000	4572	0.4	75	15887	712.1	96.5	955	433	2635	1.700
			62	14580	653.5	93.5	926	420	2616	1.688
			52	11591	519.5	86.4	854	387	2566	1.655
			40	6785	304.1	71.7	699	317	2385	1.539
			30	2669	119.6	52.1	482	218	1979	1.277
15000	4572	0.6	75	14758	661.5	97.2	1057	479	2517	1.624
			62	13084	586.5	93.4	1017	461	2476	1.597
			52	9686	434.1	84.5	918	416	2360	1.523
			40	5497	246.4	69.7	743	337	2077	1.340
			30	2307	103.4	51.6	524	237	1634	1.054

Table XXVII. (Continued)

Altitude (ft)	Altitude (m)	Mach	P/S	F_N/δ_o (lb)	F_N/δ_o (kN)	$N_F/\sqrt{\theta_o}$ (pct)	$W_{22}\sqrt{\theta_o}/\delta_o$ (ft/sec)	$W_{22}\sqrt{\theta_o}/\delta_o$ (m/sec)	A_N (in^2)	A_N (m^2)
36000	10972	0.2	75	19652	880.8	98.2	913	414	2769	1.786
			62	18654	836.1	95.9	895	405	2775	1.790
			52	16393	734.8	91.2	852	386	2778	1.792
			40	11039	494.8	78.4	729	330	2765	1.784
			30	4267	191.3	55.3	487	220	2553	1.647
36000	10972	0.4	75	17111	766.9	99.4	980	444	2643	1.705
			62	16095	721.4	97.0	960	435	2636	1.701
			52	13981	626.7	92.3	914	414	2610	1.684
			40	9064	406.3	79.3	782	354	2499	1.612
			30	3250	145.7	55.9	522	236	2066	1.333
36000	10972	0.6	75	16549	741.8	101.5	1100	498	2553	1.647
			62	15444	692.2	98.9	1076	488	2532	1.634
			52	13339	597.9	94.1	1024	464	2482	1.601
			40	8475	379.9	80.7	875	396	2296	1.481
			30	3005	134.7	56.8	584	264	1762	1.137
36000	10972	0.8	75	17659	791.5	104.2	1283	581	2541	1.639
			62	16358	733.2	101.4	1252	567	2513	1.621
			52	14146	634.1	96.6	1195	542	2451	1.581
			40	8881	398.1	82.7	1018	461	2213	1.428
			30	3201	143.5	58.2	679	307	1626	1.049
36000	10972	1.0	75	19001	851.7	105.0	1514	686	2518	1.625
			62	17459	782.5	102.0	1472	667	2482	1.601
			52	14342	642.8	95.6	1379	625	2392	1.543
			40	8359	374.7	79.4	1132	513	2084	1.345
			30	3388	151.9	57.2	774	351	1534	0.990

Table XXVII. (Concluded)

Altitude (ft)	Altitude (m)	Mach	P/S	F_N/δ_o (lb)	F_N/δ_o (kN)	$N_F/\sqrt{\theta_o}$ (pct)	$W_{22}\sqrt{\theta_o}/\delta_o$ (ft/sec)	$W_{22}\sqrt{\theta_o}/\delta_o$ (m/sec)	A_N (in^2)	A_N (m^2)
45000	13716	0.2	75	19986	895.8	99.1	945	428	2769	1.786
			62	18947	849.2	96.8	898	407	2772	1.788
			52	16642	745.9	91.9	854	387	2775	1.790
			40	11231	503.4	79.2	734	332	2772	1.788
			30	8146	365.1	70.1	641	290	2710	1.748
45000	13716	0.4	75	17380	779.0	100.3	983	445	2647	1.708
			62	16348	732.3	97.8	962	436	2638	1.702
			52	14200	636.5	92.9	916	415	2612	1.685
			40	9213	412.9	80.0	786	356	2508	1.618
			30	5601	251.0	67.3	647	293	2309	1.490
45000	13716	0.6	75	16758	751.1	102.1	1101	499	2558	1.650
			62	15622	700.2	99.5	1076	488	2537	1.637
			52	13523	606.1	94.6	1025	464	2486	1.604
			40	8591	385.1	81.3	878	398	2305	1.487
			30	3981	178.4	62.6	651	295	1901	1.226
45000	13716	0.8	75	17798	797.7	104.7	1282	581	2545	1.642
			62	16471	738.3	101.8	1251	567	2518	1.625
			52	14241	638.3	96.9	1193	541	2454	1.583
			40	8967	401.9	83.1	1019	462	2221	1.433
			30	3276	146.8	58.7	682	309	1636	1.055
45000	13716	1.0	75	19070	854.8	105.3	1511	685	2522	1.627
			62	17558	787.0	102.3	1470	666	2486	1.604
			52	14378	644.5	95.8	1376	624	2395	1.545
			40	8379	375.6	79.5	1129	512	2086	1.346
			30	3454	154.8	57.6	775	351	1541	0.994

Table XXVIII. Cruise Performance for Two Stage Fans. Designed for VTO, P/P = 1.5

Altitude (ft)	Altitude (m)	Mach	P/S	F_N/δ_o (lb)	F_N/δ_o (kN)	$N_F/\sqrt{\theta_o}$ (pct)	$W_{22}\sqrt{\theta_o}/\delta_o$ (ft/sec)	$W_{22}\sqrt{\theta_o}/\delta_o$ (m/sec)	A_N (in^2)	A_N (m^2)
0	0	0.	75	20185	904.7	92.6	651	295	2083	1.344
			62	17253	773.3	86.4	604	273	2079	1.341
			52	13154	589.6	76.4	526	238	2058	1.328
			40	8709	390.4	63.8	423	191	2007	1.295
			30	4600	206.2	47.7	298	135	1969	1.270
0	0	0.2	75	16052	719.5	92.6	664	301	2044	1.319
			62	13299	596.1	86.1	613	278	2026	1.307
			52	9705	435.0	76.0	533	241	1978	1.276
			40	6072	272.2	63.7	430	195	1882	1.214
			30	2861	128.2	47.7	303	137	1740	1.123
0	0	0.4	75	13711	614.6	92.7	705	319	1961	1.265
			62	10843	486.0	85.1	641	290	1906	1.230
			52	7551	338.5	74.6	552	250	1800	1.161
			40	4674	209.5	63.1	449	203	1638	1.057
			30	2153	96.5	47.4	319	144	1389	0.896
0	0	0.6	75	12446	557.9	92.3	770	349	1882	1.214
			62	9162	410.7	82.9	685	310	1779	1.148
			52	6377	285.8	72.9	588	266	1626	1.049
			40	3953	177.2	61.5	478	216	1424	0.919
			30	1941	87.0	47.1	345	156	1154	0.745
15000	4572	0.2	75	17501	784.4	96.0	690	312	2053	1.325
			62	16307	730.9	93.2	669	303	2045	1.319
			52	13734	615.6	91.7	622	282	2030	1.310
			40	8462	379.3	72.1	501	227	1953	1.260
			30	3548	159.0	51.7	334	151	1774	1.145
15000	4572	0.4	75	15226	682.5	96.4	735	333	1983	1.279
			62	13996	627.3	93.4	710	322	1964	1.267
			52	11173	500.8	86.1	649	294	1913	1.234
			40	6587	295.2	71.1	521	236	1758	1.134
			30	2674	119.9	51.4	351	159	1457	0.940
15000	4572	0.6	75	14411	645.9	97.0	813	368	1927	1.243
			62	12809	574.1	93.2	779	353	1891	1.220
			52	9545	427.8	84.0	695	315	1791	1.155
			40	5471	245.2	69.1	551	249	1564	1.009
			30	2371	106.3	50.9	381	172	1232	0.795

Table XXVIII. (Continued)

Altitude (ft)	Altitude (m)	Mach	P/S	F_N/δ_o (lb)	F_N/δ_o (kN)	$N_F/\sqrt{\theta_o}$ (pct)	$W_{22}\sqrt{\theta_o}/\delta_o$ (ft/sec)	$W_{22}\sqrt{\theta_o}/\delta_o$ (m/sec)	A_N (in^2)	A_N (m^2)
36000	10972	0.2	75	18350	822.5	75.1	705	319	2055	1.326
			62	17428	781.2	95.9	689	312	2052	1.324
			52	15332	687.2	91.1	652	295	2041	1.317
			40	10339	463.4	77.9	548	248	1990	1.284
			30	4075	182.6	54.7	356	161	1880	1.213
36000	10972	0.4	75	16380	734.2	99.4	757	343	1995	1.287
			62	15426	691.4	96.9	739	335	1985	1.281
			52	13433	602.1	92.1	700	317	1956	1.262
			40	8765	392.9	78.7	588	266	1847	1.192
			30	3232	144.9	55.2	382	173	1517	0.979
36000	10972	0.6	75	16121	722.6	101.4	849	385	1961	1.265
			62	15065	675.2	98.7	828	375	1942	1.253
			52	13054	585.1	93.9	785	356	1896	1.223
			40	8364	374.9	80.1	658	298	1735	1.119
			30	3054	136.9	56.2	426	193	1325	0.855
36000	10972	0.8	75	17414	780.5	104.2	990	449	1962	1.266
			62	16166	724.6	101.2	964	437	1939	1.251
			52	14035	629.1	96.5	916	415	1890	1.219
			40	8885	398.2	82.1	766	347	1698	1.095
			30	3304	148.1	57.5	496	224	1238	0.799
36000	10972	1.0	75	18832	844.1	104.9	1166	528	1944	1.254
			62	17343	777.3	101.8	1130	512	1915	1.235
			52	14329	642.3	95.3	1052	477	1844	1.190
			40	8431	377.9	78.8	864	391	1600	1.032
			30	3535	158.4	56.5	564	255	1176	0.759

Table XXVIII. (Concluded)

Altitude (ft)	Altitude (m)	Mach	P/S	F_N/δ_o (lb)	F_N/δ_o (kN)	$N_F/\sqrt{\theta_o}$ (pct)	$W_{22}\sqrt{\theta_o}/\delta_o$ (ft/sec)	$W_{22}\sqrt{\theta_o}/\delta_o$ (m/sec)	A_N (in^2)	A_N (m^2)
45000	13716	0.2	75	18653	836.1	99.1	708	321	2057	1.327
			62	17695	793.1	96.7	692	313	2053	1.325
			52	15561	697.5	91.7	655	297	2041	1.317
			40	10513	471.2	78.6	552	250	1996	1.288
			30	7640	342.4	69.6	477	216	1935	1.248
45000	13716	0.4	75	16635	745.6	100.3	759	344	1999	1.290
			62	15657	701.8	97.7	741	336	1988	1.283
			52	13639	611.3	92.8	702	318	1956	1.262
			40	8899	398.9	79.4	591	268	1854	1.196
			30	5472	245.3	66.8	480	217	1697	1.095
45000	13716	0.6	75	16313	731.2	102.1	851	386	1966	1.268
			62	15239	683.0	99.4	829	376	1946	1.255
			52	13229	593.0	94.5	786	356	1900	1.226
			40	8475	379.9	80.6	660	299	1741	1.123
			30	4001	179.3	61.8	478	216	1428	0.921
45000	13716	0.8	75	17538	786.1	104.7	990	449	1966	1.268
			62	16265	729.0	101.6	963	436	1943	1.254
			52	14125	633.1	96.8	914	414	1893	1.221
			40	8967	401.9	82.5	766	347	1704	1.099
			30	3372	151.1	58.0	498	225	1246	0.804
45000	13716	1.0	75	18899	847.1	105.2	1164	527	1947	1.256
			62	17435	781.5	102.2	1129	512	1918	1.237
			52	14357	643.5	95.6	1050	476	1846	1.191
			40	8447	378.6	78.9	844	382	1601	1.033
			30	3598	161.3	56.8	565	256	1181	0.762

Table XXIX. Cruise Performance for Two Stage Fans.

Designed for VTO, P/P = 1.6

Altitude (ft)	Altitude (m)	Mach	P/S	F_N/δ_o (lb)	F_N/δ_o (kN)	$N_F/\sqrt{\theta_o}$ (pct)	$W_{22}\sqrt{\theta_o}/\delta_o$ (ft/sec)	$W_{22}\sqrt{\theta_o}/\delta_o$ (m/sec)	A_N (in^2)	A_N (m^2)
0	0	0.	75	18528	830.5	92.3	518	234	1617	1.043
			62	15843	710.1	86.1	478	216	1600	1.032
			52	11987	537.3	75.9	411	186	1563	1.008
			40	7849	351.8	63.0	324	146	1497	0.966
			30	4185	187.6	47.2	225	102	1448	0.934
0	0	0.2	75	15100	676.8	92.3	528	239	1596	1.030
			62	12538	562.0	85.7	484	219	1569	1.012
			52	9125	409.0	75.4	415	188	1515	0.977
			40	5691	255.1	62.8	328	148	1422	0.917
			30	2755	123.5	47.2	229	103	1311	0.846
0	0	0.4	75	13169	590.3	92.4	560	254	1550	1.000
			62	10439	467.9	84.7	505	229	1497	0.966
			52	7285	326.5	74.1	429	194	1403	0.905
			40	4509	202.1	62.2	343	155	1268	0.818
			30	2148	96.3	47.0	241	109	1082	0.698
0	0	0.6	75	12144	544.3	92.0	610	276	1506	0.972
			62	8975	402.3	82.4	537	243	1415	0.913
			52	6524	292.4	72.3	455	206	1289	0.832
			40	3894	174.5	60.7	365	165	1126	0.726
			30	1976	88.6	46.7	262	118	919	0.593
15000	4572	0.2	75	16454	737.5	95.7	551	249	1609	1.038
			62	15334	687.3	92.9	532	241	1597	1.030
			52	12970	581.3	87.0	493	223	1574	1.015
			40	7955	356.6	71.6	388	175	1490	0.961
			30	3394	152.1	51.2	254	115	1337	0.863
15000	4572	0.4	75	14597	654.3	96.1	586	265	1572	1.014
			62	13440	602.4	93.1	565	256	1553	1.002
			52	10762	482.4	85.7	512	232	1503	0.970
			40	6351	284.7	70.5	403	182	1368	0.883
			30	2644	118.5	50.8	267	121	1133	0.731
15000	4572	0.6	75	14022	628.5	96.7	647	293	1548	0.999
			62	12495	560.1	93.0	618	280	1515	0.977
			52	9346	418.9	83.6	546	247	1427	0.921
			40	5383	241.3	68.4	425	192	1237	0.798
			30	2389	107.1	50.3	288	130	976	0.630

Table XXIX. (Continued)

Altitude (ft)	Altitude (m)	Mach	P/S	F_N/δ_o (lb)	F_N/δ_o (kN)	$N_F/\sqrt{\theta_o}$ (pct)	$W_{22}\sqrt{\theta_o}/\delta_o$ (ft/sec)	$W_{22}\sqrt{\theta_o}/\delta_o$ (m/sec)	A_N (in^2)	A_N (m^2)
36000	10972	0.2	75	17236	772.6	97.8	563	255	1613	1.041
			62	16384	734.4	95.6	550	249	1608	1.037
			52	14441	647.3	90.8	518	234	1590	1.026
			40	9733	436.3	77.4	429	194	1527	0.985
			30	3865	173.2	54.1	271	122	1357	0.875
36000	10972	0.4	75	15675	702.6	99.1	605	274	1585	1.023
			62	14784	662.6	96.6	590	267	1574	1.015
			52	12916	578.9	91.9	556	252	1545	0.997
			40	8453	378.9	78.3	460	208	1443	0.931
			30	3170	142.1	54.6	290	131	1176	0.759
36000	10972	0.6	75	15662	702.0	101.1	678	307	1577	1.017
			62	14655	656.9	98.5	661	299	1560	1.006
			52	12737	570.9	93.6	623	282	1519	0.980
			40	8199	367.5	79.6	514	233	1379	0.890
			30	3050	136.7	55.5	324	146	1047	0.675
36000	10972	0.8	75	17049	764.2	103.8	791	358	1578	1.018
			62	15867	711.2	100.9	769	348	1560	1.006
			52	13830	619.9	96.2	728	330	1520	0.981
			40	8814	395.1	81.7	598	271	1364	0.880
			30	3330	149.3	56.9	378	171	991	0.639
36000	10972	1.0	75	18542	831.1	104.6	931	422	1564	1.009
			62	17107	766.8	101.5	899	407	1540	0.994
			52	14231	637.9	95.1	833	377	1482	0.956
			40	8413	377.1	78.2	656	297	1283	0.828
			30	3607	161.7	55.9	429	194	945	0.610

Table XXIX. (Concluded)

Altitude (ft)	Altitude (m)	Mach	P/S	F_N/δ_o (lb)	F_N/δ_o (kN)	$N_F/\sqrt{\theta_o}$ (pct)	$W_{22}\sqrt{\theta_o}/\delta_o$ (ft/sec)	$W_{22}\sqrt{\theta_o}/\delta_o$ (m/sec)	A_N (in²)	A_N (m²)
45000	13716	0.2	75	17510	784.8	98.8	566	256	1616	1.043
			62	16628	745.3	96.4	552	250	1609	1.038
			52	14644	656.4	91.5	520	235	1591	1.026
			40	9884	443.0	78.1	431	195	1531	0.988
			30	7175	321.6	68.9	369	167	1472	0.950
45000	13716	0.4	75	15903	712.8	99.9	607	275	1589	1.025
			62	15000	672.3	97.4	592	268	1577	1.017
			52	13099	587.1	92.5	558	253	1548	0.999
			40	8577	384.4	78.8	462	209	1448	0.934
			30	5267	236.1	66.0	368	166	1316	0.849
45000	13716	0.6	75	15834	709.7	101.8	680	308	1581	1.020
			62	14815	664.0	99.1	662	300	1564	1.009
			52	12893	577.9	94.2	625	283	1523	0.983
			40	8297	371.9	80.1	515	233	1383	0.892
			30	3933	176.3	61.0	365	165	1128	0.728
45000	13716	0.8	75	17161	769.2	104.3	791	358	1581	1.020
			62	15964	715.5	101.3	769	348	1563	1.008
			52	13912	623.6	96.5	727	329	1523	0.983
			40	8892	398.6	82.0	599	271	1368	0.883
			30	3393	152.1	57.3	379	171	996	0.643
45000	13716	1.0	75	18598	833.6	104.9	929	421	1565	1.010
			62	17189	770.4	101.8	898	407	1543	0.995
			52	14254	638.9	95.3	832	377	1484	0.957
			40	8427	377.7	78.3	654	296	1285	0.829
			30	3666	164.3	56.2	430	195	949	0.612

Table XXX. Cruise Performance for Two Stage Fans.
Designed for VTO, P/P = 1.7

Altitude (ft)	Altitude (m)	Mach	P/S	F_N/δ_o (lb)	F_N/δ_o (kN)	$N_F/\sqrt{\theta_o}$ (pct)	$W_{22}\sqrt{\theta_o}/\delta_o$ (ft/sec)	$W_{22}\sqrt{\theta_o}/\delta_o$ (m/sec)	A_N (in^2)	A_N (m^2)
0	0	0.	75	17280	774.5	92.2	424	192	1311	0.846
			62	14731	660.3	85.9	388	175	1287	0.830
			52	11107	497.8	75.6	330	149	1245	0.803
			40	7217	323.5	62.6	256	116	1179	0.761
			30	3863	173.1	46.9	176	79	1131	0.730
0	0	0.2	75	14357	643.5	92.3	432	195	1299	0.838
			62	11919	534.2	85.5	393	178	1267	0.817
			52	8666	388.4	75.1	333	151	1213	0.783
			40	5389	241.5	62.4	260	117	1131	0.730
			30	2652	118.9	46.9	179	81	1041	0.672
0	0	0.4	75	12722	570.2	92.3	458	207	1273	0.821
			62	10112	453.2	84.5	410	185	1222	0.788
			52	7054	316.2	73.7	343	155	1138	0.734
			40	4350	195.0	61.6	270	122	1026	0.662
			30	2124	95.2	46.7	189	85	881	0.568
0	0	0.6	75	11884	532.7	91.8	498	225	1248	0.805
			62	8807	394.7	82.1	433	196	1166	0.752
			52	6149	275.6	71.9	363	164	1059	0.683
			40	3839	172.1	60.3	288	130	926	0.597
			30	1986	89.0	46.5	205	92	761	0.491
15000	4572	0.2	75	15619	700.1	95.6	451	204	1313	0.847
			62	14578	653.4	92.8	436	197	1300	0.839
			52	12312	551.8	86.7	400	181	1273	0.821
			40	7547	338.3	71.1	310	140	1190	0.768
			30	3237	145.1	50.7	199	90	1060	0.684
15000	4572	0.4	75	14075	630.9	95.9	480	217	1294	0.835
			62	12984	582.0	93.0	462	209	1276	0.823
			52	10423	467.2	85.5	416	188	1228	0.792
			40	6159	276.1	70.1	322	146	1108	0.715
			30	2589	116.0	50.4	208	94	918	0.592
15000	4572	0.6	75	13709	614.5	96.6	530	240	1283	0.828
			62	12232	548.3	92.8	505	229	1256	0.810
			52	9175	411.2	83.4	442	200	1178	0.760
			40	5287	237.0	67.9	337	152	1016	0.655
			30	2380	106.7	50.0	225	102	805	0.519

Table XXX. (Continued)

Altitude (ft)	Altitude (m)	Mach	P/S	F_N/δ_o (lb)	F_N/δ_o (kN)	$N_F/\sqrt{\theta_o}$ (pct)	$W_{22}\sqrt{\theta_o}/\delta_o$ (ft/sec)	$W_{22}\sqrt{\theta_o}/\delta_o$ (m/sec)	A_N (in^2)	A_N (m^2)
36000	10972	0.2	75	16357	733.2	97.7	462	209	1319	0.851
			62	15560	697.4	95.4	451	204	1311	0.846
			52	13727	615.3	90.7	423	191	1292	0.834
			40	9251	414.6	77.1	345	156	1225	0.790
			30	3700	165.8	53.7	213	96	1075	0.694
36000	10972	0.4	75	15100	676.8	99.0	496	224	1307	0.843
			62	14258	639.1	96.5	483	219	1296	0.836
			52	12478	559.3	91.8	454	205	1268	0.818
			40	8189	367.0	77.9	370	167	1173	0.757
			30	3107	139.3	54.3	228	103	952	0.614
36000	10972	0.6	75	15269	684.4	101.0	557	252	1307	0.843
			62	14316	641.7	98.3	542	245	1294	0.835
			52	12465	558.7	93.5	509	230	1260	0.813
			40	8052	360.9	79.3	414	187	1136	0.733
			30	3031	135.9	55.2	255	115	861	0.555
36000	10972	0.8	75	16714	749.2	103.7	649	294	1309	0.845
			62	15586	698.6	100.8	630	285	1294	0.835
			52	13629	610.9	96.1	594	269	1260	0.813
			40	8738	391.7	81.3	481	218	1130	0.729
			30	3339	149.7	56.6	297	134	822	0.530
36000	10972	1.0	75	18256	818.3	104.4	763	346	1297	0.837
			62	16879	756.6	101.4	736	333	1277	0.824
			52	14065	630.4	94.8	677	307	1229	0.793
			40	8368	375.1	77.7	525	238	1065	0.687
			30	3629	162.7	55.4	336	152	787	0.508

Table XXX. (Concluded)

Altitude (ft)	Altitude (m)	Mach	P/S	F_N/δ_o (lb)	F_N/δ_o (kN)	$N_F/\sqrt{\theta_o}$ (pct)	$W_{22}\sqrt{\theta_o}/\delta_o$ (ft/sec)	$W_{22}\sqrt{\theta_o}/\delta_o$ (m/sec)	A_N (in^2)	A_N (m^2)
45000	13716	0.2	75	16607	744.4	98.7	465	210	1322	0.853
			62	15786	707.6	96.3	453	205	1314	0.848
			52	13912	623.6	91.4	425	192	1293	0.834
			40	9384	420.6	77.2	347	157	1228	0.792
			30	6792	304.4	68.4	293	132	1173	0.757
45000	13716	0.4	75	15307	686.1	99.8	498	225	1312	0.846
			62	14459	648.1	97.3	485	219	1299	0.838
			52	12647	566.9	92.4	456	206	1271	0.820
			40	8304	372.2	78.5	372	168	1177	0.759
			30	5103	228.7	65.5	292	132	1064	0.686
45000	13716	0.6	75	15431	691.6	101.7	558	253	1311	0.846
			62	14466	648.4	98.9	543	246	1296	0.836
			52	12612	565.3	94.1	510	231	1263	0.815
			40	8139	364.8	79.7	415	188	1139	0.735
			30	3378	173.8	60.6	288	130	927	0.598
45000	13716	0.8	75	16819	753.9	104.1	650	294	1311	0.846
			62	15670	702.4	101.1	630	285	1296	0.836
			52	13700	614.1	96.4	594	269	1263	0.815
			40	8809	394.8	81.6	482	218	1134	0.732
			30	3399	152.3	57.0	298	135	826	0.533
45000	13716	1.0	75	18304	820.4	104.7	762	345	1298	0.837
			62	16956	760.0	101.7	735	333	1279	0.825
			52	14083	631.2	95.0	676	306	1230	0.794
			40	8378	375.5	77.8	523	237	1065	0.687
			30	3686	165.2	55.7	336	152	790	0.510

Table XXXI. Cruise Performance for Two Stage Fans.

Designed for Cruise, P/P = 1.3

Altitude (ft)	Altitude (m)	Mach	P/S	F_N/δ_o (lb)	F_N/δ_o (kN)	$N_F/\sqrt{\theta_o}$ (pct)	$W_{22}\sqrt{\theta_o}/\delta_o$ (ft/sec)	$W_{22}\sqrt{\theta_o}/\delta_o$ (m/sec)	A_N (in^2)	A_N (m^2)
0	0	0.	75	23825	1067.9	99.9	984	446	3398	2.192
			62	20565	921.8	99.2	929	421	3474	2.241
			52	15762	706.5	83.1	836	379	3618	2.334
			40	10440	467.9	69.4	698	316	3759	2.425
			30	5586	250.4	52.8	515	233	3874	2.499
0	0	0.2	75	17986	806.2	100.0	1005	455	3293	2.125
			62	14952	670.2	92.9	946	429	3336	2.152
			52	10766	482.6	82.6	849	385	3409	2.199
			40	6560	294.0	69.2	710	322	3389	2.186
			30	3011	135.0	52.7	525	238	3188	2.057
0	0	0.4	75	14734	660.4	100.0	1069	484	3071	1.981
			62	11653	522.3	92.2	998	452	3052	1.969
			52	7926	355.3	81.5	891	404	2994	1.932
			40	4717	211.4	68.6	746	338	2777	1.792
			30	2100	94.1	52.6	554	251	2357	1.521
0	0	0.6	75	12971	581.4	99.4	1174	532	2877	1.856
			62	9504	426.0	90.0	1075	487	2773	1.789
			52	6430	288.2	79.3	953	432	2601	1.678
			40	3875	173.7	67.7	806	365	2329	1.503
			30	1808	81.0	52.2	605	274	1891	1.220
15000	4572	0.2	75	19374	868.4	103.8	1041	472	3333	2.150
			62	18267	818.8	100.6	1011	458	3292	2.124
			52	15439	692.0	94.0	956	433	3331	2.149
			40	9396	421.1	78.7	810	367	3419	2.206
			30	3798	170.2	57.1	575	260	3259	2.103
15000	4572	0.4	75	16268	729.2	104.3	1109	503	3111	2.007
			62	15040	674.1	100.8	1075	487	3072	1.982
			52	12003	538.0	93.1	1006	456	3053	1.970
			40	6871	308.0	77.4	845	383	2926	1.888
			30	2658	119.1	56.8	605	274	2479	1.599
15000	4572	0.6	75	15022	673.3	104.9	1228	557	2931	1.891
			62	13348	598.3	100.4	1183	536	2884	1.861
			52	9931	445.1	91.3	1089	493	2790	1.800
			40	5467	245.0	75.4	904	410	2516	1.623
			30	2251	100.9	56.4	657	298	2009	1.296

Table XXXI. (Continued)

Altitude (ft)	Altitude (m)	Mach	P/S	F_N/δ_o (lb)	F_N/δ_o (kN)	$N_F/\sqrt{\theta_o}$ (pct)	$W_{22}\sqrt{\theta_o}/\delta_o$ (ft/sec)	$W_{22}\sqrt{\theta_o}/\delta_o$ (m/sec)	A_N (in^2)	A_N (m^2)
36000	10972	0.2	75	19777	886.4	105.6	1055	478	3383	2.183
			62	19309	865.5	103.6	1039	471	3329	2.148
			52	17178	770.0	98.1	990	449	3303	2.131
			40	11529	516.8	84.7	868	393	3393	2.189
			30	4418	198.0	60.2	608	275	3290	2.123
36000	10972	0.4	75	16870	756.1	106.9	1132	513	3180	2.052
			62	16398	735.0	104.8	1115	505	3123	2.015
			52	14423	646.5	99.3	1062	481	3068	1.979
			40	9269	415.5	85.6	931	422	3014	1.945
			30	3268	146.5	60.8	652	295	2583	1.666
36000	10972	0.6	75	16099	721.6	109.2	1270	576	3027	1.953
			62	15568	697.8	106.8	1249	566	2965	1.913
			52	13607	609.9	101.2	1191	540	2889	1.864
			40	8551	383.3	87.1	1042	472	2733	1.763
			30	2965	132.9	61.8	729	330	2167	1.398
36000	10972	0.8	75	17044	763.9	112.1	1481	671	2989	1.928
			62	16371	733.8	109.5	1455	659	2923	1.886
			52	14307	641.3	104.0	1389	630	2833	1.828
			40	8881	398.1	89.3	1213	550	2612	1.685
			30	3125	140.1	63.4	848	384	1984	1.280
36000	10972	1.0	75	18921	848.1	113.4	1758	797	2935	1.894
			62	17593	788.6	110.0	1708	774	2868	1.850
			52	14467	648.4	102.8	1616	733	2781	1.794
			40	8243	369.5	85.9	1369	620	2486	1.604
			30	3250	145.7	62.4	971	440	1871	1.207

Table XXXI. (Concluded)

Altitude (ft)	Altitude (m)	Mach	P/S	F_N/δ_o (lb)	F_N/δ_o (kN)	$N_F/\sqrt{\theta_o}$ (pct)	$W_{22}\sqrt{\theta_o}/\delta_o$ (ft/sec)	$W_{22}\sqrt{\theta_o}/\delta_o$ (m/sec)	A_N (in^2)	A_N (m^2)
45000	13716	0.2	75	19679	382.1	106.6	1055	478	3427	2.211
			62	19432	871.0	104.4	1041	472	3347	2.159
			52	17428	781.2	98.9	992	449	3297	2.127
			40	11731	525.8	85.4	871	395	3388	2.186
			30	8440	378.3	75.7	776	351	3406	2.197
45000	13716	0.4	75	16792	752.7	107.8	1131	513	3213	2.073
			62	16505	739.8	105.5	1116	506	3139	2.025
			52	14644	656.4	100.0	1064	482	3070	1.981
			40	9432	422.8	86.2	932	422	3016	1.946
			30	5609	251.4	72.7	788	357	2851	1.839
45000	13716	0.6	75	16047	719.3	109.9	1268	575	3048	1.966
			62	15657	701.8	107.4	1249	566	2978	1.921
			52	13796	618.4	101.9	1191	540	2893	1.866
			40	8680	389.1	87.6	1042	472	2738	1.766
			30	3919	175.7	68.0	806	365	2337	1.508
45000	13716	0.8	75	17004	762.2	112.6	1477	669	3002	1.937
			62	16423	736.1	109.9	1452	658	2932	1.892
			52	14398	645.3	104.3	1386	628	2838	1.831
			40	8974	402.2	89.7	1212	549	2617	1.688
			30	3201	143.5	63.8	850	385	1994	1.286
45000	13716	1.0	75	18940	848.9	113.6	1753	795	2940	1.897
			62	17681	792.5	110.4	1706	773	2875	1.855
			52	14501	650.0	103.1	1612	731	2784	1.796
			40	8263	370.4	86.1	1365	619	2489	1.606
			30	3317	148.7	62.7	973	441	1881	1.214

Table XXXII. Cruise Performance for Two Stage Fans.

Designed for Cruise, P/P = 1.4

Altitude (ft)	Altitude (m)	Mach	P/S	F_N/δ_o (lb)	F_N/δ_o (kN)	$N_F/\sqrt{\theta_o}$ (pct)	$W_{22}\sqrt{\theta_o}/\delta_o$ (ft/sec)	$W_{22}\sqrt{\theta_o}/\delta_o$ (m/sec)	A_N (in^2)	A_N (m^2)
0	0	0.	75	21019	942.1	99.9	710	322	2282	1.472
			62	18090	810.8	92.8	664	301	2296	1.481
			52	13822	619.5	82.4	589	267	2331	1.504
			40	9135	409.4	68.5	481	218	2334	1.506
			30	4922	220.6	51.8	347	157	2321	1.497
0	0	0.2	75	16586	743.4	99.9	725	328	2237	1.443
			62	13821	619.5	92.5	676	306	2236	1.443
			52	10039	450.0	81.9	579	262	2239	1.445
			40	6220	278.8	68.3	489	221	2174	1.403
			30	2974	133.3	51.8	354	160	2028	1.308
0	0	0.4	75	14075	630.9	99.9	769	348	2136	1.378
			62	11208	502.4	91.8	711	322	2103	1.357
			52	7732	346.6	80.6	623	282	2032	1.311
			40	4719	211.5	67.7	513	232	1870	1.206
			30	2197	98.5	51.6	373	169	1598	1.031
0	0	0.6	75	12712	569.8	99.1	843	382	2046	1.320
			62	9413	421.9	89.4	761	345	1954	1.261
			52	6453	289.2	78.4	663	300	1816	1.172
			40	3992	178.9	66.6	551	249	1618	1.044
			30	1949	87.4	51.2	406	184	1319	0.851
15000	4572	0.2	75	17728	794.6	103.9	751	340	2281	1.472
			62	16835	754.6	100.6	729	330	2238	1.444
			52	14263	639.3	93.7	684	310	2236	1.443
			40	8763	392.8	77.7	564	255	2220	1.432
			30	3693	165.5	56.2	389	176	2070	1.335
15000	4572	0.4	75	15431	691.6	104.4	801	363	2178	1.405
			62	14361	643.7	100.7	775	351	2139	1.380
			52	11533	516.9	92.7	718	325	2105	1.358
			40	6719	301.2	76.4	587	266	1980	1.277
			30	2734	122.5	55.9	409	185	1673	1.079
15000	4572	0.6	75	14648	656.6	105.0	880	399	2097	1.353
			62	13078	586.2	100.2	851	386	2053	1.325
			52	9826	440.4	90.8	773	350	1969	1.270
			40	5534	248.0	74.3	625	283	1755	1.132
			30	2395	107.3	55.3	442	200	1399	0.903

Table XXXII. (Concluded)

Altitude (ft)	Altitude (m)	Mach	P/S	F_N/δ_o (lb)	F_N/δ_o (kN)	$N_F/\sqrt{\theta_o}$ (pct)	$W_{22}\sqrt{\theta_o}/\delta_o$ (ft/sec)	$W_{22}\sqrt{\theta_o}/\delta_o$ (m/sec)	A_N (in^2)	A_N (m^2)
36000	10972	0.2	62	17677	792.3	103.8	750	340	2278	1.470
			52	15853	710.6	98.0	713	323	2235	1.442
			40	10722	480.6	84.0	612	277	2235	1.442
			30	4244	190.2	59.1	413	187	2094	1.351
36000	10972	0.4	62	15532	696.2	105.0	805	365	2188	1.412
			52	13794	618.3	99.1	765	346	2132	1.375
			40	8987	402.8	84.9	656	297	2059	1.328
			30	3313	148.5	59.7	442	200	1790	1.155
36000	10972	0.6	62	15086	676.2	106.9	902	409	2126	1.372
			52	13326	597.3	101.1	857	388	2058	1.328
			40	8511	381.5	86.4	735	333	1922	1.240
			30	3094	138.7	60.8	495	224	1506	0.972
36000	10972	0.8	62	16148	723.8	109.6	1050	476	2119	1.367
			52	14258	639.1	103.8	1000	453	2048	1.321
			40	8979	402.5	88.5	855	387	1873	1.208
			30	3317	148.7	62.3	576	261	1403	0.905
36000	10972	1.0	75	18733	839.7	113.5	1269	575	2128	1.373
			62	17552	786.7	110.0	1233	559	2075	1.339
			52	14539	651.7	102.4	1156	524	2007	1.295
			40	8462	379.3	84.8	657	298	1777	1.146
			30	3522	157.9	61.4	490	222	1332	0.859
45000	13716	0.2	62	17763	796.2	104.5	751	340	2293	1.479
			52	16081	720.8	98.8	715	324	2234	1.441
			40	10897	488.4	84.7	614	278	2234	1.441
			30	7900	354.1	74.8	539	244	2204	1.422
45000	13716	0.4	62	15602	699.3	105.6	805	365	2201	1.420
			52	13995	627.3	99.9	766	347	2136	1.378
			40	9131	409.3	85.5	658	298	2062	1.330
			30	5547	248.6	71.6	544	246	1923	1.241
45000	13716	0.6	62	15144	678.8	107.5	901	408	2136	1.378
			52	13495	604.9	101.7	858	389	2062	1.330
			40	8625	386.6	86.9	735	333	1926	1.243
			30	4035	180.9	67.0	551	249	1623	1.047
45000	13716	0.8	62	16183	725.4	110.0	1048	475	2126	1.372
			52	14343	642.9	104.1	998	452	2051	1.323
			40	9070	406.5	88.9	855	387	1877	1.211
			30	3386	151.8	62.7	578	262	1409	0.909
45000	13716	1.0	75	18741	840.0	113.8	1265	573	2133	1.376
			62	17633	790.3	110.4	1232	558	2081	1.343
			52	14562	652.7	102.7	1154	523	2008	1.295
			40	8482	380.2	85.0	951	431	1778	1.147
			30	3584	160.6	61.7	658	298	1338	0.863

Table XXXIII. Cruise Performance for Two Stage Fans.

Designed for Cruise, P/P = 1.5

Altitude (ft)	Altitude (m)	Mach	P/S	F_N/δ_o (lb)	F_N/δ_o (kN)	$N_F/\sqrt{\theta_o}$ (pct)	$W_{22}\sqrt{\theta_o}/\delta_o$ (ft/sec)	$W_{22}\sqrt{\theta_o}/\delta_o$ (m/sec)	A_N (in^2)	A_N (m^2)
0	0	0.	75	19037	853.3	99.9	543	246	1683	1.086
			62	16330	731.9	92.7	504	228	1677	1.082
			52	12427	557.0	82.0	441	200	1672	1.079
			40	8147	365.2	68.0	354	160	1638	1.057
			30	4393	196.9	51.1	250	113	1592	1.027
0	0	0.2	75	15476	693.7	99.9	554	251	1661	1.072
			62	12900	578.2	92.4	513	232	1645	1.061
			52	9396	421.1	81.6	447	202	1623	1.047
			40	5838	261.7	67.7	359	162	1552	1.001
			30	2850	127.7	51.0	254	115	1435	0.926
0	0	0.4	75	13461	603.3	99.8	588	266	1611	1.039
			62	10754	482.0	91.6	538	244	1574	1.015
			52	7461	334.4	80.0	464	210	1502	0.969
			40	4589	205.7	67.1	376	170	1376	0.888
			30	2192	98.2	50.8	268	121	1178	0.760
0	0	0.6	75	12379	554.9	99.0	642	291	1568	1.012
			62	9220	413.3	89.1	573	259	1487	0.959
			52	6367	285.4	77.9	492	223	1373	0.886
			40	3969	177.9	65.9	402	182	1216	0.785
			30	1994	89.4	50.3	290	131	996	0.643
15000	4572	0.2	75	16580	743.1	104.0	577	261	1699	1.096
			62	15713	704.3	69.0	558	253	1663	1.073
			52	13310	596.6	93.6	520	235	1647	1.063
			40	8196	367.4	77.1	419	190	1600	1.032
			30	3504	157.1	55.5	281	127	1464	0.945
15000	4572	0.4	75	14774	662.2	104.5	615	278	1648	1.063
			62	13736	615.7	100.7	593	268	1615	1.042
			52	11063	495.9	92.5	544	246	1578	1.018
			40	6502	291.4	76.0	436	197	1464	0.945
			30	2701	121.1	55.1	295	133	1230	0.794
15000	4572	0.6	75	14254	638.9	105.1	680	308	1612	1.040
			62	12738	570.9	100.1	649	294	1574	1.015
			52	9623	431.3	90.6	583	264	1500	0.968
			40	5476	245.4	73.9	462	209	1325	0.855
			30	2421	108.5	54.5	318	144	1053	0.679

Table XXXIII. (Continued)

Altitude (ft)	Altitude (m)	Mach	P/S	F_N/δ_o (lb)	F_N/δ_o (kN)	$N_F/\sqrt{\theta_o}$ (pct)	$W_{22}\sqrt{\theta_o}/\delta_o$ (ft/sec)	$W_{22}\sqrt{\theta_o}/\delta_o$ (m/sec)	A_N (in^2)	A_N (m^2)
36000	10972	0.2	75	16866	756.0	106.1	584	264	1734	1.119
			62	16536	741.2	103.9	576	261	1696	1.094
			52	14802	663.5	97.9	544	246	1655	1.068
			40	10027	449.4	83.6	459	208	1625	1.048
			30	4004	179.5	58.3	299	135	1483	0.957
36000	10972	0.4	75	15234	682.8	107.5	627	284	1695	1.094
			62	14868	666.4	105.1	618	280	1655	1.068
			52	13201	591.7	99.1	584	264	1607	1.037
			40	8663	388.3	84.6	493	223	1531	0.988
			30	3246	145.5	58.9	321	145	1278	0.825
36000	10972	0.6	75	15140	678.6	109.7	703	318	1677	1.082
			62	14704	659.1	107.0	692	313	1635	1.055
			52	12978	581.7	101.0	654	296	1578	1.018
			40	8364	374.9	86.1	551	249	1459	0.941
			30	3099	138.9	59.9	358	162	1133	0.731
36000	10972	0.8	75	16509	740.0	112.6	819	371	1679	1.083
			62	15916	713.4	109.7	806	365	1635	1.055
			52	14057	630.1	103.8	763	346	1579	1.019
			40	8952	401.2	88.2	642	291	1442	0.930
			30	3362	150.7	61.4	417	189	1069	0.690
36000	10972	1.0	75	18524	830.3	113.7	974	441	1642	1.059
			62	17343	777.3	110.0	944	428	1600	1.032
			52	14423	646.5	102.3	879	398	1546	0.997
			40	8502	381.1	84.3	709	321	1365	0.881
			30	3616	162.1	60.6	475	215	1019	0.657

Table XXXIII. (Concluded)

Altitude (ft)	Altitude (m)	Mach	P/S	F_N/δ_o (lb)	F_N/δ_o (kN)	$N_F/\sqrt{\theta_o}$ (pct)	$W_{22}\sqrt{\theta_o}/\delta_o$ (ft/sec)	$W_{22}\sqrt{\theta_o}/\delta_o$ (m/sec)	A_N (in^2)	A_N (m^2)
45000	13716	0.2	75	16853	755.4	107.0	584	264	1758	1.134
			62	16614	744.7	104.7	577	261	1708	1.102
			52	15007	672.6	98.8	546	247	1656	1.068
			40	10185	456.5	84.3	462	209	1626	1.049
			30	7401	331.7	74.3	399	180	1584	1.022
45000	13716	0.4	75	15233	682.8	108.2	626	283	1710	1.103
			62	14952	670.2	105.8	618	280	1666	1.075
			52	13386	600.0	99.9	585	265	1609	1.038
			40	8789	393.9	85.2	494	224	1534	0.990
			30	5376	241.0	71.2	401	181	1418	0.915
45000	13716	0.6	75	15144	678.8	110.3	701	317	1688	1.089
			62	14761	661.6	107.6	692	313	1644	1.061
			52	13140	589.0	101.7	655	297	1582	1.021
			40	8468	379.6	86.6	552	250	1463	0.944
			30	4015	180.0	66.2	402	182	1220	0.787
45000	13716	0.8	75	16505	739.8	113.0	817	370	1686	1.088
			62	15951	715.0	110.1	805	365	1640	1.058
			52	14138	633.7	104.1	762	345	1581	1.020
			40	9036	405.0	88.6	642	291	1444	0.932
			30	3434	153.9	61.3	418	189	1074	0.693
45000	13716	1.0	75	18529	830.5	114.0	971	440	1646	1.062
			62	17421	780.8	110.5	944	428	1604	1.035
			52	14446	647.5	102.5	877	397	1547	0.998
			40	8516	381.7	84.4	707	320	1366	0.881
			30	3680	164.9	60.9	475	215	1023	0.660

Table XXXIV. Cruise Performance for Two Stage Fans.

Designed for Cruise, P/P = 1.6

Altitude (ft)	Altitude (m)	Mach	P/S	F_N/δ_o (lb)	F_N/δ_o (kN)	$N_F/\sqrt{\theta_o}$ (pct)	$W_{22}\sqrt{\theta_o}/\delta_o$ (ft/sec)	$W_{22}\sqrt{\theta_o}/\delta_o$ (m/sec)	A_N (in^2)	A_N (m^2)
0	0	0.	75	17537	786.0	99.9	431	195	1318	0.850
			62	15010	672.8	92.5	397	180	1301	0.839
			52	11386	510.3	81.7	344	156	1281	0.826
			40	7416	332.4	67.4	270	122	1231	0.794
			30	3988	178.8	50.3	187	84	1180	0.761
0	0	0.2	75	14576	653.3	99.9	440	199	1306	0.843
			62	12156	544.9	92.2	404	183	1284	0.828
			52	8867	397.4	81.2	348	157	1251	0.807
			40	5519	247.4	67.2	274	124	1179	0.761
			30	2723	122.1	50.2	190	86	1085	0.700
0	0	0.4	75	12919	579.1	99.7	466	211	1281	0.826
			62	10347	463.8	91.4	423	191	1242	0.801
			52	7208	323.1	79.6	359	162	1175	0.758
			40	4455	199.7	66.5	286	129	1069	0.690
			30	2163	96.9	50.0	200	90	918	0.592
0	0	0.6	75	12067	540.9	98.8	507	229	1260	0.813
			62	9018	404.2	88.8	448	203	1187	0.766
			52	6258	280.5	77.4	379	171	1091	0.704
			40	3924	175.9	65.2	305	138	961	0.620
			30	2004	89.8	49.6	217	98	791	0.510
15000	4572	0.2	75	15600	699.2	104.2	458	207	1342	0.866
			62	14800	663.4	100.6	443	200	1309	0.845
			52	12541	562.1	93.4	409	185	1287	0.830
			40	7732	346.6	76.7	324	146	1227	0.792
			30	3335	149.5	54.9	211	95	1107	0.714
15000	4572	0.4	75	14157	634.5	104.6	489	221	1314	0.848
			62	13183	590.9	100.6	470	213	1288	0.831
			52	10645	477.1	92.3	428	194	1246	0.804
			40	6291	282.0	75.5	336	152	1143	0.737
			30	2651	118.8	54.4	221	100	956	0.617
15000	4572	0.6	75	13883	622.3	105.1	540	244	1297	0.837
			62	12415	556.5	100.0	513	232	1266	0.817
			52	9410	421.8	90.3	457	207	1199	0.774
			40	5393	241.7	73.3	354	160	1051	0.678
			30	2423	108.6	53.8	239	108	836	0.539

Table XXXIV. (Continued)

Altitude (ft)	Altitude (m)	Mach	P/S	F_N/δ_o (lb)	F_N/δ_o (kN)	$N_F/\sqrt{\theta_o}$ (pct)	$W_{22}\sqrt{\theta_o}/\delta_o$ (ft/sec)	$W_{22}\sqrt{\theta_o}/\delta_o$ (m/sec)	A_N (in^2)	A_N (m^2)
36000	10972	0.2	75	15863	711.0	106.3	464	210	1372	0.885
			62	15555	697.2	104.0	458	207	1339	0.864
			52	13946	625.1	97.8	431	195	1299	0.838
			40	9461	424.1	83.2	358	162	1254	0.809
			30	3794	170.1	57.7	226	102	1122	0.724
36000	10972	0.4	75	14592	654.0	107.7	498	225	1355	0.874
			62	14249	638.7	105.2	491	222	1321	0.852
			52	12675	568.1	99.0	462	209	1276	0.823
			40	8359	374.7	84.2	384	174	1202	0.775
			30	3170	142.1	58.2	242	109	993	0.641
36000	10972	0.6	75	14726	660.0	109.9	558	253	1353	0.873
			62	14302	641.0	107.2	550	249	1317	0.850
			52	12648	566.9	100.9	518	234	1268	0.818
			40	8194	367.3	85.6	430	195	1164	0.751
			30	3076	137.9	59.2	270	122	897	0.579
36000	10972	0.8	75	16166	724.6	112.8	651	295	1355	0.874
			62	15586	698.6	109.9	640	290	1316	0.849
			52	13807	618.9	103.7	604	273	1270	0.819
			40	8872	397.7	87.8	500	226	1158	0.747
			30	3375	151.3	60.7	315	142	856	0.552
36000	10972	1.0	75	18199	815.7	113.8	774	351	1323	0.854
			62	17066	764.9	110.0	749	339	1287	0.830
			52	14240	638.3	102.1	693	314	1243	0.802
			40	8475	379.9	83.8	548	248	1096	0.707
			30	3665	164.3	59.9	357	161	820	0.529

Table XXXIV. (Concluded)

Altitude (ft)	Altitude (m)	Mach	P/S	F_N/δ_o (lb)	F_N/δ_o (kN)	$N_F/\sqrt{\theta_o}$ (pct)	$W_{22}\sqrt{\theta_o}/\delta_o$ (ft/sec)	$W_{22}\sqrt{\theta_o}/\delta_o$ (m/sec)	A_N (in^2)	A_N (m^2)
45000	13716	0.2	75	15876	711.6	107.2	463	210	1387	0.895
			62	15629	700.5	104.8	458	207	1349	0.870
			52	14138	633.7	98.7	433	196	1301	0.839
			40	9596	430.1	84.0	360	163	1256	0.810
			30	6977	312.7	73.8	308	139	1211	0.781
45000	13716	0.4	75	14603	654.5	108.4	497	225	1367	0.882
			62	14323	642.0	105.9	491	222	1330	0.858
			52	12845	575.7	99.8	464	210	1279	0.825
			40	8475	379.9	84.8	385	174	1204	0.777
			30	5212	233.6	70.6	307	139	1104	0.712
45000	13716	0.6	75	14740	660.7	110.5	557	252	1363	0.879
			62	14357	643.5	107.8	550	249	1324	0.854
			52	12804	573.9	101.6	519	235	1272	0.821
			40	8290	371.6	86.1	430	195	1166	0.752
			30	3967	177.8	65.5	305	138	963	0.621
45000	13716	0.8	75	16170	724.8	113.2	649	294	1361	0.878
			62	15616	699.9	110.2	639	289	1321	0.852
			52	13885	622.4	104.0	604	273	1272	0.821
			40	8947	401.0	88.1	500	226	1161	0.749
			30	3441	154.2	61.1	316	143	860	0.555
45000	13716	1.0	75	18201	815.8	114.1	772	350	1326	0.855
			62	17141	768.3	110.5	749	339	1291	0.833
			52	14261	639.2	102.3	691	313	1244	0.803
			40	8488	380.4	83.9	547	248	1097	0.708
			30	3721	166.8	60.3	358	162	823	0.531

Table XXXV. Cruise Performance for Two Stage Fans.

Designed for Cruise, P/P = 1.7

Altitude (ft)	Altitude (m)	Mach	P/S	F_N/δ_o (lb)	F_N/δ_o (kN)	$N_F/\sqrt{\theta_o}$ (pct)	$W_{22}\sqrt{\theta_o}/\delta_o$ (ft/sec)	$W_{22}\sqrt{\theta_o}/\delta_o$ (m/sec)	A_N (in^2)	A_N (m^2)
0	0	0.	75	16358	733.2	99.9	350	158	1076	0.694
			62	13983	626.7	92.4	321	145	1055	0.681
			52	10575	474.0	81.4	275	124	1026	0.662
			40	6860	307.5	67.0	212	96	974	0.628
			30	3682	165.0	49.8	144	65	925	0.597
0	0	0.2	75	13834	620.1	99.9	357	161	1070	0.690
			62	11543	517.4	92.1	326	147	1044	0.674
			52	8430	377.8	80.9	278	126	1008	0.650
			40	5255	235.5	66.8	215	97	939	0.606
			30	2613	117.1	49.8	146	66	862	0.556
0	0	0.4	75	12446	557.9	99.7	378	171	1057	0.682
			62	9986	447.6	91.2	341	154	1019	0.657
			52	6979	312.8	79.2	285	129	955	0.616
			40	4334	194.3	66.1	224	101	866	0.559
			30	2131	95.5	49.6	154	69	747	0.482
0	0	0.6	75	11779	528.0	98.7	411	186	1045	0.674
			62	8818	395.2	88.4	359	162	983	0.634
			52	6148	275.6	77.0	301	136	898	0.579
			40	3873	173.6	64.8	238	107	791	0.510
			30	2005	89.9	49.2	167	75	655	0.423
15000	4572	0.2	75	14793	663.1	104.3	373	169	1102	0.711
			62	14049	629.7	100.7	360	163	1072	0.692
			52	11907	533.7	93.2	331	150	1048	0.676
			40	7347	329.3	76.3	257	116	984	0.635
			30	3188	142.9	54.4	164	74	880	0.568
15000	4572	0.4	75	13622	610.6	104.7	398	180	1088	0.702
			62	12700	569.2	100.6	382	173	1060	0.684
			52	10275	460.5	92.2	345	156	1023	0.660
			40	6101	273.5	75.1	266	120	928	0.599
			30	2598	116.4	53.9	171	77	776	0.501
15000	4572	0.6	75	13526	606.3	105.2	440	199	1076	0.694
			62	12116	543.1	99.9	416	188	1049	0.677
			52	9206	412.6	90.0	367	166	993	0.641
			40	5307	237.9	72.9	280	127	865	0.558
			30	2412	108.1	53.3	185	83	690	0.445

Table XXXV. (Continued)

Altitude (ft)	Altitude (m)	Mach	P/S	F_N/δ_o (lb)	F_N/δ_o (kN)	$N_F/\sqrt{\theta_o}$ (pct)	$W_{22}\sqrt{\theta_o}/\delta_o$ (ft/sec)	$W_{22}\sqrt{\theta_o}/\delta_o$ (m/sec)	A_N (in^2)	A_N (m^2)
36000	10972	0.2	75	15042	674.2	106.6	377	171	1129	0.728
			62	14752	661.2	104.2	373	169	1099	0.709
			52	13241	593.5	97.8	349	158	1062	0.685
			40	8988	402.9	81.8	287	130	1012	0.653
			30	3620	162.3	57.2	176	79	892	0.575
36000	10972	0.4	75	14039	629.3	107.9	405	183	1124	0.725
			62	13709	614.5	105.3	399	180	1093	0.705
			52	12216	547.5	98.9	375	170	1052	0.679
			40	8083	362.3	83.9	307	139	981	0.633
			30	3094	138.7	57.8	188	85	805	0.519
36000	10972	0.6	75	14342	642.8	110.1	454	205	1126	0.726
			62	13923	624.1	107.3	448	203	1093	0.705
			52	12340	553.1	100.8	420	190	1052	0.679
			40	8025	359.7	85.3	344	156	962	0.621
			30	3049	136.7	58.8	210	95	739	0.477
36000	10972	0.8	75	15831	709.6	113.0	530	240	1127	0.727
			62	15256	683.8	110.0	521	236	1093	0.705
			52	13548	607.2	103.6	491	222	1052	0.679
			40	8770	393.1	87.5	400	181	961	0.620
			30	3370	151.1	60.3	245	111	739	0.477
36000	10972	1.0	75	17860	800.5	113.9	630	285	1127	0.727
			62	16772	751.8	110.0	609	276	1093	0.705
			52	14035	629.1	101.9	560	254	1052	0.679
			40	8422	377.5	83.4	435	197	961	0.620
			30	3687	165.3	59.4	277	125	712	0.459

Table XXXV. (Concluded)

Altitude (ft)	Altitude (m)	Mach	P/S	F_N/δ_o (lb)	F_N/δ_o (kN)	$N_F/\sqrt{\theta_o}$ (pct)	$W_{22}\sqrt{\theta_o}/\delta_o$ (ft/sec)	$W_{22}\sqrt{\theta_o}/\delta_o$ (m/sec)	A_N (in^2)	A_N (m^2)
45000	13716	0.2	75	15068	675.4	107.5	377	171	1098	0.708
			62	14322	664.4	105.0	373	169	1067	0.688
			52	13470	603.8	98.7	351	159	1030	0.665
			40	9118	408.7	83.6	288	130	908	0.586
			30	6627	297.0	73.4	243	110	684	0.441
45000	13716	0.4	75	14063	630.3	108.7	405	183	1141	0.736
			62	13775	617.4	106.1	400	181	1108	0.715
			52	12373	554.6	99.7	376	170	1063	0.686
			40	8194	367.3	84.4	308	139	1013	0.654
			30	5061	226.8	70.2	242	109	969	0.625
45000	13716	0.6	75	14357	643.5	110.8	453	205	1134	0.732
			62	13974	626.3	107.9	448	203	1102	0.711
			52	12489	559.8	101.5	421	190	1055	0.681
			40	8119	363.9	85.8	344	156	983	0.634
			30	3906	175.1	65.0	238	107	894	0.577
45000	13716	0.8	75	15834	709.7	113.5	528	239	1133	0.731
			62	15287	685.2	110.4	520	235	1099	0.709
			52	13168	590.2	103.9	490	222	1054	0.680
			40	8837	396.1	87.9	398	180	984	0.635
			30	3433	153.9	60.6	245	111	792	0.511
45000	13716	1.0	75	17866	800.8	114.3	628	284	1133	0.731
			62	16846	755.1	110.5	609	276	1097	0.708
			52	14056	630.0	102.1	559	253	1054	0.680
			40	8434	378.0	83.5	428	194	963	0.621
			30	3714	166.5	59.7	277	125	715	0.461

Table XXXVI. Estimated Installed Gas Generator Performance With Derate Operating Line for 30 Percent Control Margin.

Altitude (ft)	Altitude (m)	M_0	PS	$N_F/\sqrt{\theta}$ (pct)	$W_2\sqrt{\theta_0}/\delta_0$ (lb/sec)	$W_2\sqrt{\theta_0}/\delta_0$ (kg/sec)	$W_F/\sqrt{\theta_0}\delta_0$ (lb/hr)	$W_F/\sqrt{\theta_0}\delta_0$ (kg/hr)	P_{51}/δ_0 (psia)	P_{51}/δ_0 (kN/m^2)	T_{51}/θ_0 (°R)	T_{51}/θ_0 (°K)	$W_{51}\sqrt{\theta_0}/\delta_0$ (lb/sec)	$W_{51}\sqrt{\theta_0}/\delta_0$ (kg/sec)
0	0	0	75	105	125.4	56.88	7894	3581	50.19	346.0	1715	953	126.7	57.47
			62	97.80	118.1	56.88	6568	2979	45.23	311.9	1585	881	119.0	53.98
			52	91.83	105.2	47.72	4972	2255	38.15	263.0	1433	796	105.8	47.99
			40	84.50	88.2	40.01	3289	1492	29.69	185.8	1251	695	88.5	40.16
36000	10972	0.2	75	114.4	132.0	59.87	9374	4252	55.16	380.3	1899	1055	132.9	60.28
			62	111.2	131.1	59.47	8783	3984	53.66	370.0	1825	1014	132.0	59.87
			52	103.4	126.9	57.56	7590	3443	49.87	343.8	1696	942	127.5	57.83
			40	93.1	109.5	49.67	5273	2392	39.96	275.5	1478	821	109.8	49.80
			30	79.6	78.5	35.61	2800	1270	25.51	175.9	1184	658	78.6	35.65
36000	10972	0.4	75	115.8	141.6	64.23	10309	4676	59.93	413.2	1943	1079	142.7	64.73
			62	112.3	140.7	63.82	9636	4371	58.22	401.4	1864	1036	141.6	64.22
			52	104.5	136.1	61.73	8341	3783	54.14	373.3	1734	963	136.8	62.05
			40	94.1	117.3	53.21	5771	2618	43.32	298.7	1510	839	117.6	53.34
			30	80.5	84.3	38.23	3014	1367	27.66	190.7	1207	670	84.4	38.28
36000	10972	0.6	75	118.0	158.7	71.99	12046	5464	68.56	472.7	2019	1122	160.0	72.57
			62	114.3	157.6	71.49	11203	5082	66.47	458.3	1931	1073	158.8	72.03
			52	106.4	152.5	69.17	9734	4415	61.87	426.6	1799	999	153.3	69.54
			40	95.9	131.3	59.51	6696	3037	49.40	340.6	1563	869	131.8	59.78
			30	82.0	94.6	42.90	3395	1540	31.55	217.5	1246	692	94.7	42.96
36000	10972	0.8	75	121.0	184.9	83.87	14827	6725	82.10	566.1	2122	1179	186.6	84.64
			62	116.9	183.5	83.23	13727	6226	79.42	547.6	2025	1125	185.0	83.91
			52	109.0	177.5	80.51	11974	5431	74.01	510.3	1892	1051	178.7	81.06
			40	98.2	152.8	69.31	8197	3718	58.94	406.4	1640	911	153.4	69.58
			30	84.0	110.3	50.03	4001	1815	37.67	259.7	1303	723	110.5	50.12
36000	10972	1.0	75	121.0	121.0	100.3	17858	8100	99.30	684.7	2167	1204	223.2	101.2
			62	116.2	217.6	98.70	16492	7481	95.47	658.3	2078	1154	219.4	99.52
			52	107.8	205.8	99.34	13824	6270	86.48	596.3	1922	1068	207.1	93.94
			40	98.0	170.9	77.52	8917	4045	66.10	455.8	1647	915	171.6	77.84
			30	84.8	128.9	58.49	4715	2139	44.84	309.2	1351	751	129.0	58.51

Table XXXVII. Engine Discharge and Fan Turbine Inlet Design Point Parameters, Derated for 30 Percent Control Margin.

	Designed for VTO
Ambient Temperature, °R (°K)	549.69 (305.4)
Ambient Pressure, psia (kN/m^2)	14.696 (101.33)
Engine Discharge Flow, lb/sec(kg/sec)	123.55 (56.04)
Engine Discharge Temperature, °R (°K)	1997.9 (1110)
Engine Discharge Pressure, psia (kN/m^2)	61.32 (422.8)
Engine Main Fuel Flow, lb/hr (kg/hr)	9532 (4324)
Fan Turbine Inlet Airflow, lb/sec (kg/sec)	142.22 (64.51)
Fan Turbine Inlet Pressure, psia (kN/m^2)	56.41 (388.9)

Table XXXVIII. Design Point Parameters for Two Stage Fans Designed for VTO with 30 Percent Control Margin.

Fan Pressure Ratio	1.4	1.6
Fan Tip Speed, ft/sec (m/sec)	1180(359.7)	1095(333.8)
Fan Tip Diameter, inches (m)	71.86(1.825)	57.79(1.468)
Fan Inlet Radius Ratio	0.340	0.388
Fan Exit Mach Number	0.55	0.55
Fan Efficiency	0.84	0.84
Fan Airflow, lb/sec (kg/sec)	940.6(426.6)	583.9(264.9)
Turbine Inlet Temperature, °R (°K)	1998(1110)	1998(1110)
Turbine Inlet Pressure, psia (kN/m^2)	56.41(388.9)	56.41(388.9)
Turbine Inlet Airflow, lb/sec (kg/sec)	142.22(64.51)	142.22(64.51)
Turbine Exit Static Pressure Ratio	1.058	1.140
Turbine Exit Mach Number	0.55	0.55
Interconnect Duct Pressure Loss, pct	3	3
Scroll Pressure Loss, pct	5	5
Ideal Uninstalled Thrust, lb(kN)	29008(129.0)	24107(107.2)

Table XXXIX. Performance of Two Stage Fans Designed for VTO, With 30 Percent Control Margin, P/P=1.4.

Altitude (ft)	Altitude (m)	Mach	P/S	F_N/δ_o (lb)	F_N/δ_o (kN)	$N_F/\sqrt{\theta_o}$ (pct)	$W_{22}\sqrt{\theta_o}/\delta_o$ (ft/sec)	$W_{22}\sqrt{\theta_o}/\delta_o$ (m/sec)	A_N (in^2)	A_N (m^2)
0	0	0.	75	17396	779.7	89.3	498	225	1620	1.045
			62	14700	658.9	82.6	455	206	1600	1.032
			52	11228	503.3	73.4	393	178	1558	1.005
			40	7263	325.5	60.4	307	139	1489	0.961
			30	3612	161.9	43.6	203	92	1455	0.939
36000	10972	0.2	75	16126	722.8	94.4	542	245	1610	1.039
			62	15292	685.4	92.3	528	239	1603	1.034
			52	13384	599.9	87.4	496	224	1585	1.023
			40	9042	405.3	74.7	410	185	1517	0.979
			30	3397	152.3	50.7	251	113	1344	0.867
36000	10972	0.4	75	14597	654.3	95.6	582	263	1575	1.016
			62	13741	615.9	93.3	566	256	1562	1.008
			52	11922	534.4	88.5	532	241	1532	0.988
			40	7811	350.1	75.6	440	199	1425	0.919
			30	2769	124.1	51.3	269	122	1148	0.741
36000	10972	0.6	75	14543	651.8	97.5	653	296	1561	1.007
			62	13589	609.1	95.1	634	287	1541	0.994
			52	11757	527.0	90.2	597	270	1499	0.967
			40	7575	339.5	76.9	492	223	1353	0.873
			30	2679	120.1	52.1	301	136	1012	0.653
36000	10972	0.8	75	15863	711.0	100.1	762	345	1562	1.008
			62	14735	660.5	97.5	738	334	1541	0.994
			52	12760	571.9	92.6	696	315	1498	0.966
			40	8145	365.1	78.8	572	259	1334	0.861
			30	2951	132.3	53.3	350	158	949	0.612
36000	10972	1.0	75	17272	774.2	101.0	894	405	1545	0.997
			62	15934	714.2	98.2	865	392	1523	0.983
			52	13085	586.5	91.2	793	359	1456	0.939
			40	7762	347.9	75.4	627	284	1253	0.808
			30	3210	143.9	52.2	394	178	899	0.580

Table XXXX. Performance of Two Stage Fans Designed for VTO With 30 Percent Control Margin, P/P=1.6.

Altitude (ft)	Altitude (m)	Mach	P/S	F_N/δ_o (lb)	F_N/δ_o (kN)	$N_F/\sqrt{\theta_o}$ (pct)	$W_{22}\sqrt{\theta_o}/\delta_o$ (ft/sec)	$W_{22}\sqrt{\theta_o}/\delta_o$ (m/sec)	A_N (in^2)	A_N (m^2)
0	0	0.	75	20921	937.7	90.4	821	372	2873	1.854
			62	17792	797.5	83.9	763	346	2893	1.866
			52	13710	614.5	74.8	675	306	1907	1.230
			40	9003	403.5	62.5	548	248	2906	1.375
			30	4417	198.0	45.5	379	171	2958	1.908
36000	10972	0.2	75	18306	820.5	95.4	885	401	2780	1.794
			62	17330	776.8	93.4	865	392	2779	1.793
			52	15154	679.2	88.7	822	372	2787	1.798
			40	10201	457.2	76.2	702	318	2755	1.777
			30	3700	165.8	52.6	458	207	2536	1.636
36000	10972	0.4	75	15827	709.4	96.6	950	430	2637	1.701
			62	14860	666.1	94.4	928	420	2634	1.699
			52	12840	575.5	89.7	882	400	2598	1.676
			40	8319	372.9	77.0	753	341	2496	1.610
			30	2800	125.5	53.1	490	222	2012	1.298
36000	10972	0.6	75	15270	684.4	98.6	1066	483	2531	1.633
			62	14222	637.5	96.2	1039	471	2505	1.616
			52	12243	548.8	91.5	989	448	2454	1.583
			40	7766	348.1	78.4	842	381	2254	1.454
			30	2604	116.7	54.0	548	248	1679	1.083
36000	10972	0.8	75	16291	730.2	101.2	1243	563	2512	1.621
			62	15056	674.8	98.6	1210	548	2478	1.599
			52	12960	580.9	93.9	1153	522	2414	1.557
			40	8141	364.9	80.3	980	444	2164	1.396
			30	2800	125.5	55.3	637	288	2558	1.650
36000	10972	1.0	75	17570	787.5	102.2	1465	664	2458	1.586
			62	16117	722.4	99.3	1424	645	2450	1.581
			52	13130	588.5	92.7	1327	601	2348	1.515
			40	7601	340.7	77.2	1090	494	2036	1.314
			30	2978	133.5	54.2	725	328	1466	0.946

Table XLI. Fan Design Parameters for Conceptual Design Studies.

	Single Stage	Two Stage
Rotor Inlet Total Temperature, °R (°K)	518.7(288.2)	518.7(288.2)
Rotor Inlet Total Pressure, psia (kN/m^2)	14.696(101.3)	14.696(101.3)
Total Pressure Ratio	1.4	1.55
Exit Static Pressure Ratio	1.14	1.262
Inlet Tip Diameter, inches (meters)	64.96(1.650)	52.47(1.333)
Inlet Hub Radius Ratio	0.471	0.419
Inlet Airflow, lb/sec (kg/sec)	716(325)	495(225)
Tip Speed, ft/sec (m/sec)	1125(342.9)	1018(310.3)
Inlet Specific flow, lb/sec-ft^2(kg/sec-m^2)	40(1.686)	40.0(1.686)
Hub Loading Coefficient	2.14	2.16
Exit Tip Diameter, inches (meters)	60.98(1.549)	48.00(1.219)
Exit Radius Ratio	0.567	0.505
Fan Exit Mach Number	0.55	0.55
Rotor Speed, rpm	3969	4452
Number of Blades, Stage 1	88	50
Stage 2	---	70
Number of Vanes	56	27
Aspect Ratio		
Rotor 1	5.8	4.2
Stator	4.0	1.9
Rotor 2	---	5.8
Tip Solidity		
Rotor 1	1.6	1.2
Stator	1.2	1.2
Rotor 2	---	1.0
Hub Solidity		
Rotor 1	3.2	2.2
Stator	2.8	2.5
Rotor 2	---	1.9

Table XLII. Turbine Design Parameters for Conceptual Design Studies.

	Single Stage	Two Stage
Inlet Total Temperature, °R (°K)	1773(985)	1773(985)
Inlet Total Pressure, psia (kN/m^2)	50.35(347.2)	50.35(347.2)
Inlet Gas Flow, lb/sec (kg/sec)	128.6(58.33)	128.6(58.33)
Total to Static Pressure Ratio	3.02	2.72
Total to Total Pressure Ratio	2.47	2.23
Speed, rpm	3969	4452
Design Power, HP (kilowatts)	15770(11760)	13961(10411)
Design Energy, BTU/lb(Joules/grams)	86.7(202)	76.7(178)
Design Exit Mach Number	0.55	0.55
Overall Efficiency	0.844	0.864
Pitch Wheel Speed, ft/sec (m/sec)	1223(554.7)	1023(464.0)
Stage Velocity Ratio	0.55	0.50
Stage Work Function; $gJ\Delta h/2U^2$	0.73	0.92
Turbine Tip Diameter, inches (meters)	67.83(1.723)	56.10)1.425)
Turbine Hub Diameter, inches (meters)	73.42(1.865)	49.23(1.250)
Bucket Length, inches (cm)	2.80(7.11)	3.44(8.74)
Admission Arc	360	360
Turbine Exit Rotor Swirl, degrees	-22.7	-10.0
Exit Stators	Yes	No

Table XLIII. Comparison of Titanium and Composite Blade Designs for Two Stage Fan.

	Titanium	Composite
Tip Radius, in (m)	25.9(0.658)	25.9(0.658)
Root Radius, in (m)	10.8(0.274)	10.8(0.274)
Hub/Tip Radius	0.417	0.417
Blade Length, in (m)	15.1(0.384)	15.1(0.384)
Root Solidity	2.321	2.321
Tip Chord, in (cm)	3.64(9.25)	6.50(16.51)
Root Chord, in (cm)	3.15(8.00)	5.63(14.30)
Pitch Aspect Ratio	4.15	2.32
Airfoil Weight, lb (kg)	1.0(0.454)	1.353(0.614)
Centrifugal Force at Root, lb (kg)	9274(4207)	7469(3388)
Area at Root, in^2 (cm^2)	0.294(1.90)	1.808(11.67)
Centrifugal Stress, psi (kN/mm^2)	31500(210)	7750(53.4)
First Flexural Frequency, Hz	507	173
First Torsional Frequency, Hz	793	504
Reduced Velocity Parameter	1.50	1.32

Table XLIV. Material Properties for Stage 1 Composite Blades.

Hybrid Polymetric

50% PRD 491 Epoxy	0 degree layup
50% Graphite 1 Epoxy	±22 degrees layup

$E = 11x10^6$ psi ($75.8x10^3$ kN/mm^2)

$G = 1.36x10^6$ psi ($9.38x10^3$ kN/mm^2)

Poisson's Ratio = 0.664

Density = 0.053 lb/in^3 (0.39 kg/cm^3)

Tensile Strength = 169,000 psi (1165 kN/mm^2)

Flexural Strength = 167,000 psi (1151 kN/mm^2)

Shear Strength = 10,000 psi (68.9 kN/mm^2)

Table XLV. Single Stage Fan Weight Summary.
(P/P = 1.4, designed for cruise, no partial arc)

Front Frame, lbs (kg)	165(74.8)
Rear Frame, lbs (kg)	161(73.0)
Scroll, lbs (kg)	318(144.2)
Rotor, lbs (kg)	354(160.6)
Total Fan Weight, lbs (kg)	998(452.6)

Table XLVI. Two Stage Fan Weight Summary.
(P/P = 1.55, designed for cruise, no partial arc)

Rotor 1, lb (kg)	139(63.0)
Rotor 2, lb (kg)	184(83.5)
Scroll, lb (kg)	234(106.1)
Mid-frame, lb (kg)	161(73.0)
Total, lb (kg)	718(325.6)

Table XLVII. Fan Turbine Inlet Gas Conditions Used for Transient Analysis.

	Nominal Lift	Maximum Control
Flow, lb/sec (kg/sec)	121.8(55.25)	133.8(60.69)
Fuel Flow, lb/hr (kg/hr)	8247(3741)	9323(4229)
Temperature, °R (°K)	1847(1026)	1997(1109)
Pressure, psia (kN/m^2)	48.39(336.6)	55.40(382.0)

Table XLVIII. Steady State Conditions for Fans Used in Transient Analysis.

Fan Design	2 Min Rating			3 Sec Rating		
	RPM	Thrust lbs	kN	RPM	Thrust lbs	kN
Single Stage, P/P = 1.4 (Designed for Cruise)	3511	14689	65.34	3788	17579	78.20
Single Stage, P/P = 1.4 (Designed for VTO)	3406	21638	96.25	3704	25914	115.27
Two Stage, P/P = 1.55 (Designed for Cruise)	3721	12657	56.30	4030	15255	67.86
Two Stage, P/P = 1.55 (Designed for VTO)	4094	18859	83.89	4469	22700	100.97
Two Stage, P/P = 1.4 (Designed for Cruise)	3420	14854	66.07	3693	17793	79.15
Two Stage, P/P = 1.4 (Designed for VTO)	3636	21718	96.61	3965	26094	116.07

Table XLIX. Summary of Time Constants for Single Stage, 1.4 Pressure Ratio Fans.

Fan Design	Increasing τ_N	Increasing τ_F	Decreasing τ_N	Decreasing τ_F
VTO	0.35	0.24	0.34	0.25
Cruise with Partial Arc	0.32	0.24	0.33	0.23

Table L. Summary of Time Constants for Two Stage, 1.55 Pressure Ratio Fans.

Pressure Ratio	Fan Design	τ_N Increasing	τ_F Increasing	τ_N Decreasing	τ_F Decreasing
1.55	VTO	0.23	0.15	0.20	0.15
1.55	Cruise with Partial Arc	0.20	0.14	0.21	0.14
1.4	VTO	0.32	0.24	0.30	0.24
1.4	Cruise with Partial Arc	0.28	0.21	0.30	0.21

Table LI. Fan Parameters Used for Inputs to Acoustic Analysis

Type of Design	Cruise	VTO	Cruise	VTO	Cruise	VTO
Number of Stages	1	1	2	2	2	2
Design Pressure	1.4	1.4	1.4	1.4	1.55	1.55
Ambient Temp at Design Point, °R (°K)	5.8.7(288)	549.7(305)	518.7(288)	549.7(305)	518.7(288)	549.7(305)
Design Corrected Tip Speed, ft/sec (m/sec)	1125(343)	1125(343)	1047(319)	1180(360)	965(294)	1110(338)
Fan Tip Diameter, in (m)	64.96(1.649)	73.72(1.872)	61.99(1.575)	70.16(1.782)	52.43(1.332)	58.57(1.448)
Design Fan Speed, rpm	3968	3600	3870	3854	4218	4344
Number of Blades	88	88	50/70	50/70	50/70	50/70
Number of Vanes	56	56	27	27	27	27
Number of Turbine Blades	264	264	210	210	210	210
Scroll Arc at NRP, degrees	240	360	240	360	240	360
Fan Pressure Ratio at NRP	1.28	1.33	1.28	1.33	1.39	1.46
Fan Speed @ NRP, rpm	3512	3406	3420	3635	3610	4094
Fan Airflow @ NRP, lb/sec (kg/sec)	589(267)	810(367)	597(271)	815(369)	397(180)	556(252)
Fan Jet Velocity, ft/sec (m/sec)	680(207)	736(224)	681(207)	734(224)	799(244)	857(261)
Fan Jet Area, in^2 (m^2)	1758(1.134)	224(1.446)	1780(1.148)	2260(1.458)	1016(0.655)	1330(0.858)
Turbine Airflow, lb/sec (kg/sec)	81.2(368)	121.8(55.2)	81.2(36.8)	121.8(55.2)	81.2(36.8)	121.8(55.2)
Turbine Jet Velocity, ft/sec (m/sec)	1190(3631)	1125(343)	1190(363)	1126(343)	1374(419)	1325(404)
Turbine Exit Area, in^2 (m^2)	354(0.228)	559(0.361)	353(0.228)	558(0.360)	304(0.196)	471(0.304)
Total Thrust, lb (kN)	15143(67.37)	22307(99.23)	15313(68.11)	22387(99.58)	13049(58.04)	18859(83.89)

Table LII. Maximum 500 Foot (152 meters) Sideline PNL's for Six Military VTOL Lift Fans.

			Single Fan		Normalized to 60,000 pounds (267 kN)	
P/P	Stage	Design	Lift	Lift/Cruise	Lift	Lift/Cruise
1.4	1	Cruise	111.0	112.5	117.0	118.5
1.4	1	VTO	113.0	114.8	117.3	119.1
1.4	2	Cruise	113.8	113.6	119.7	119.5
1.4	2	VTO	115.1	116.6	119.4	121.1
1.55	2	Cruise	114.2	113.6	120.8	122.5
1.55	2	VTO	117.5	117.7	120.3	122.7

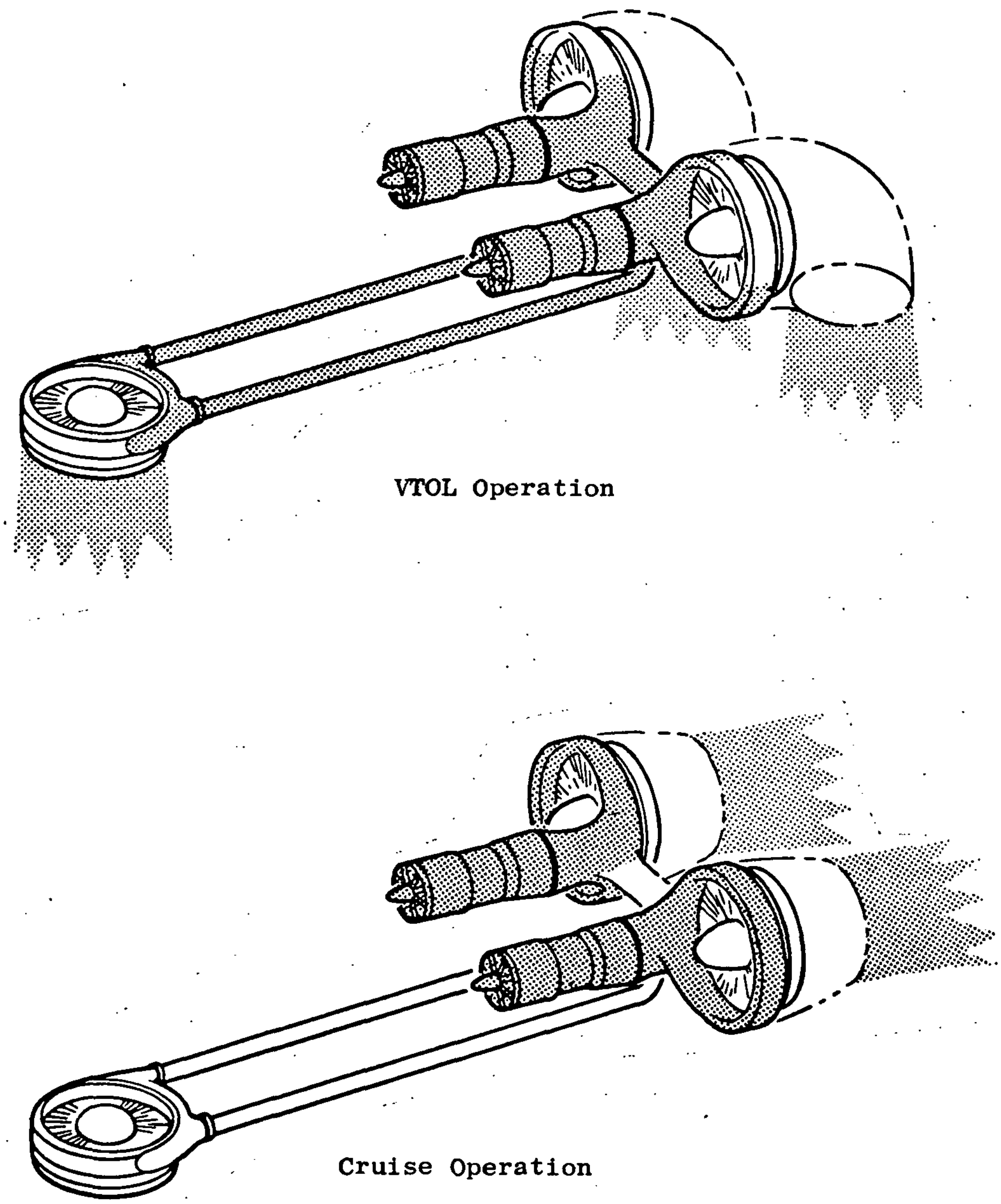

Figure 1 - Flow Schematic of Lift Fans Designed for Cruise

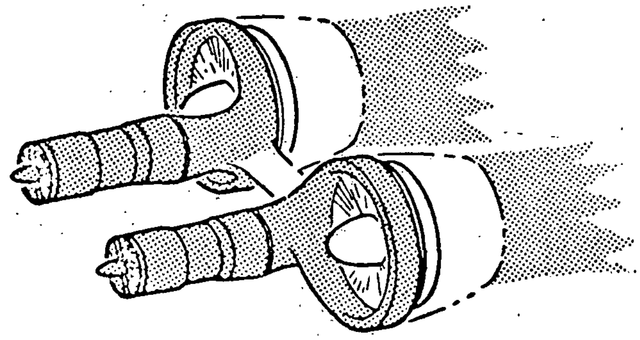

CRUISE OPERATION

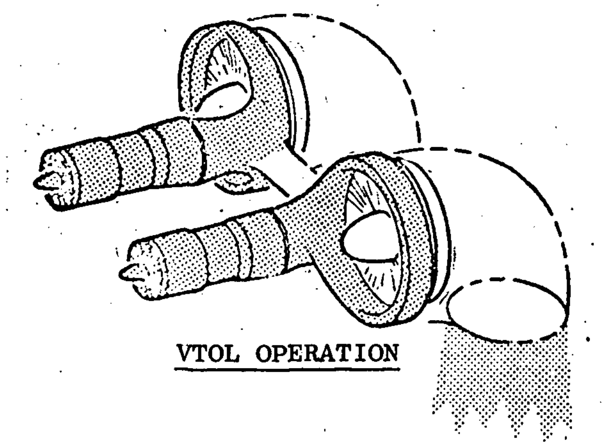

VTOL OPERATION

Figure 2 - Flow Schematic of Lift Fans Designed for VTOL

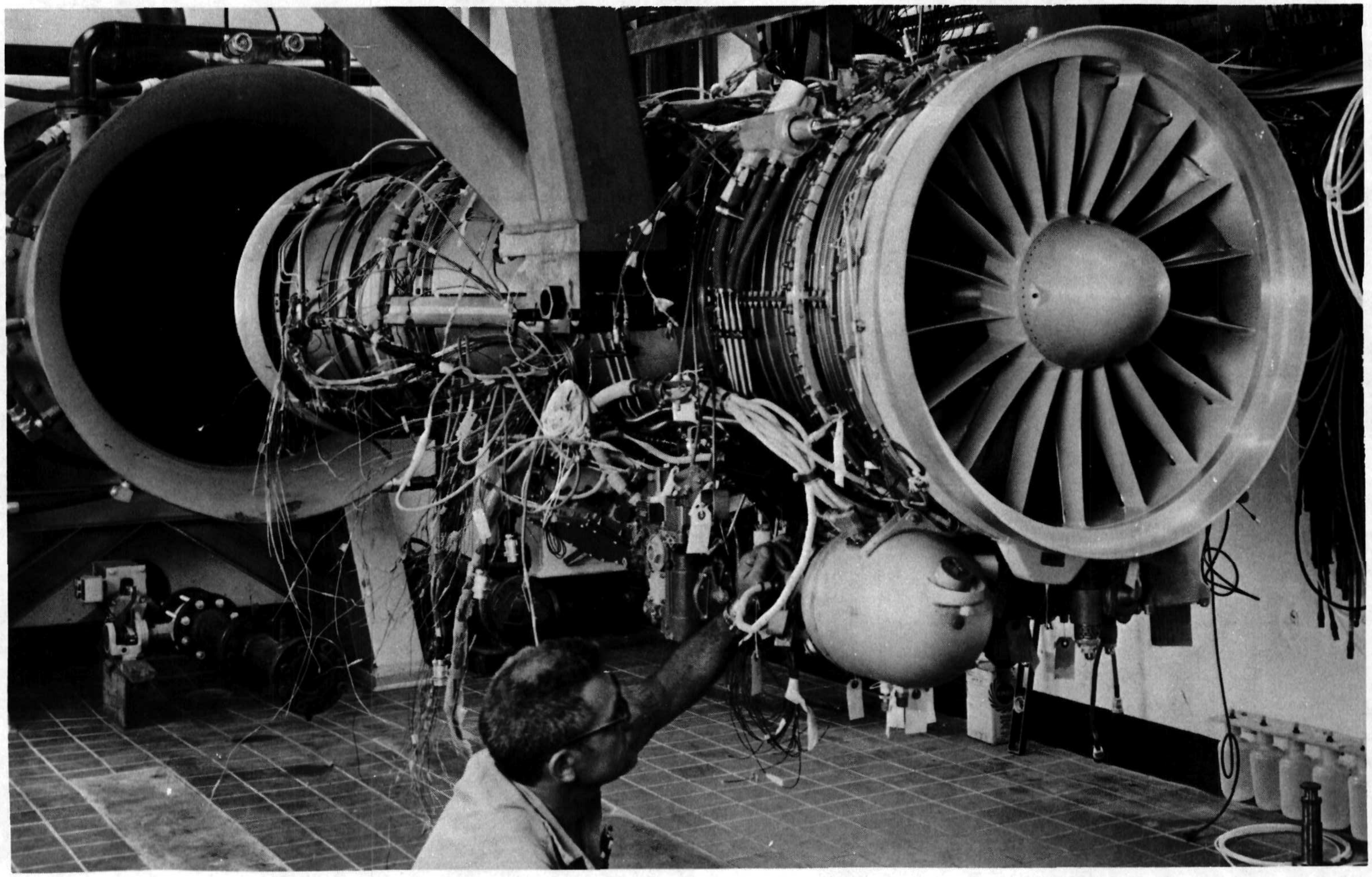

Figure 3 - YJ101-GE-100 Engine on Test

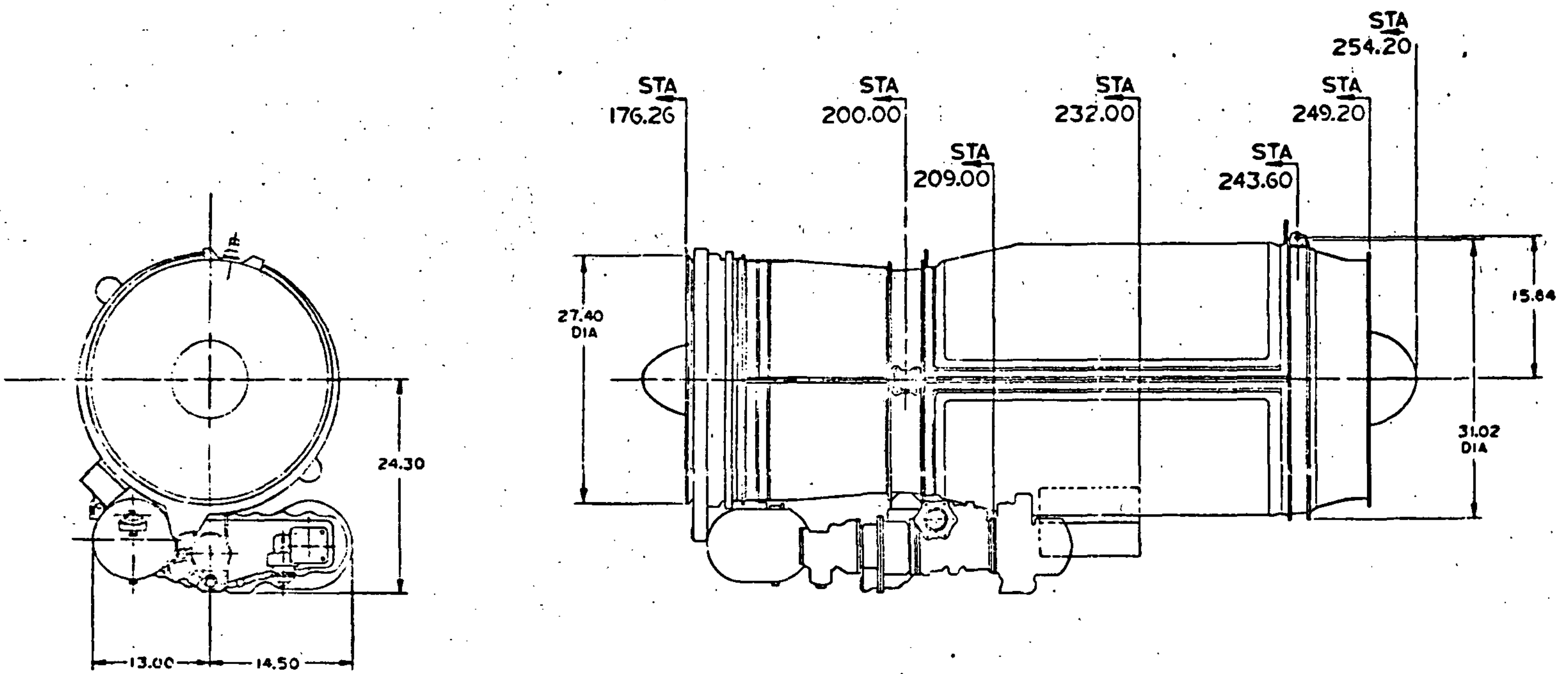

Figure 4 - J101 Engine Installation Drawing

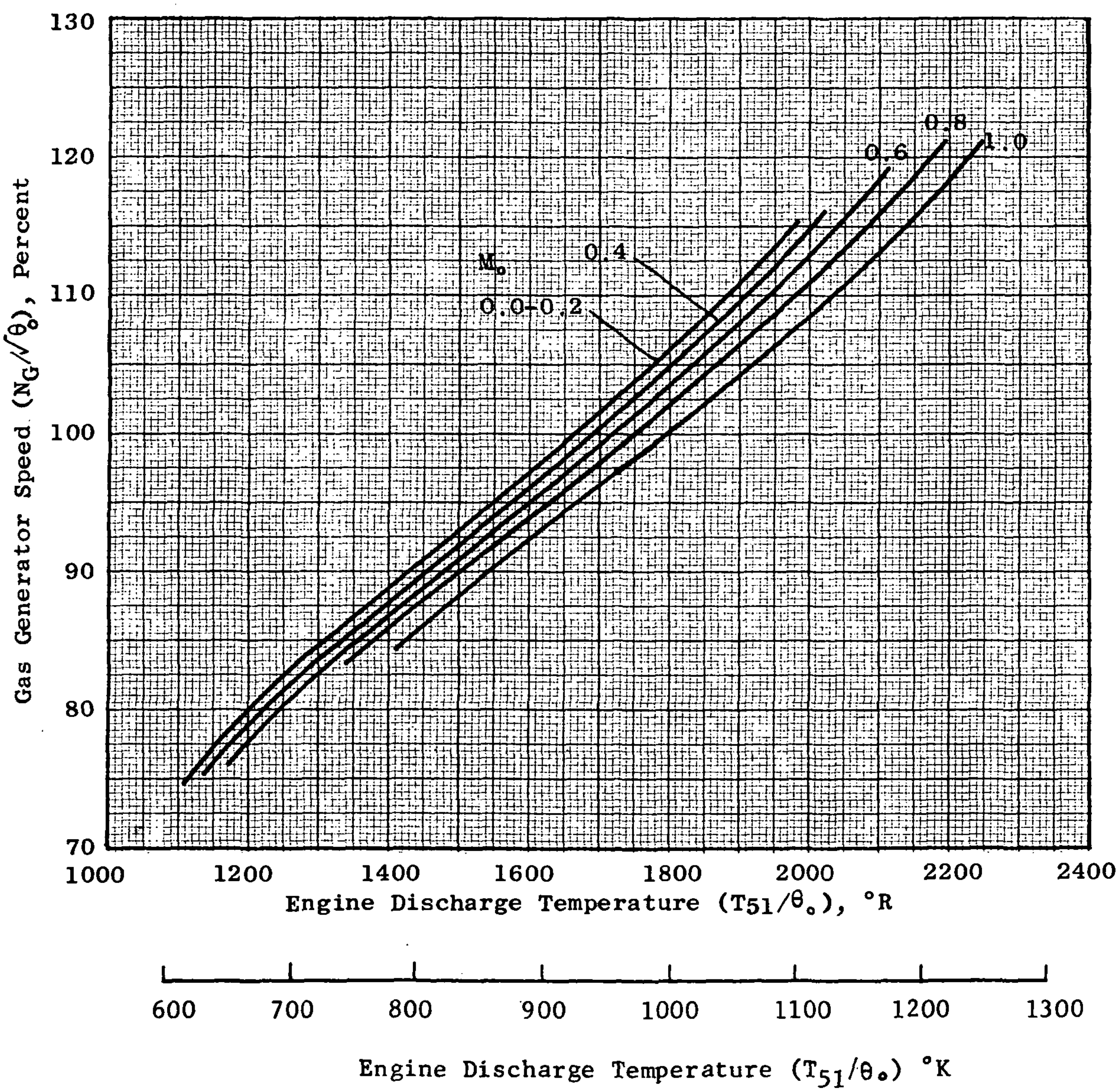

Figure 5 - J101 Gas Generator Fan Speed

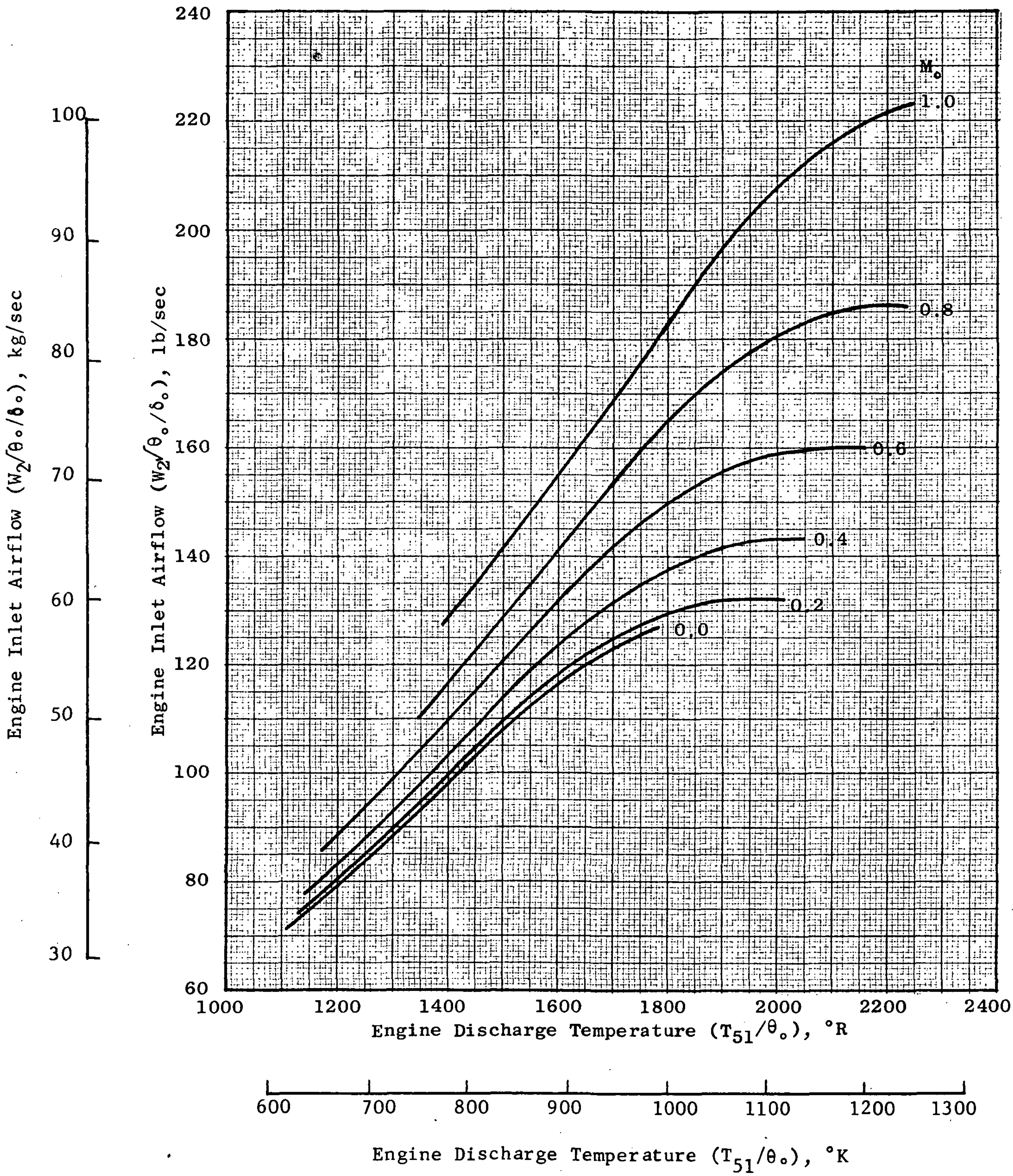

Figure 6 - J101 Gas Generator Inlet Airflow

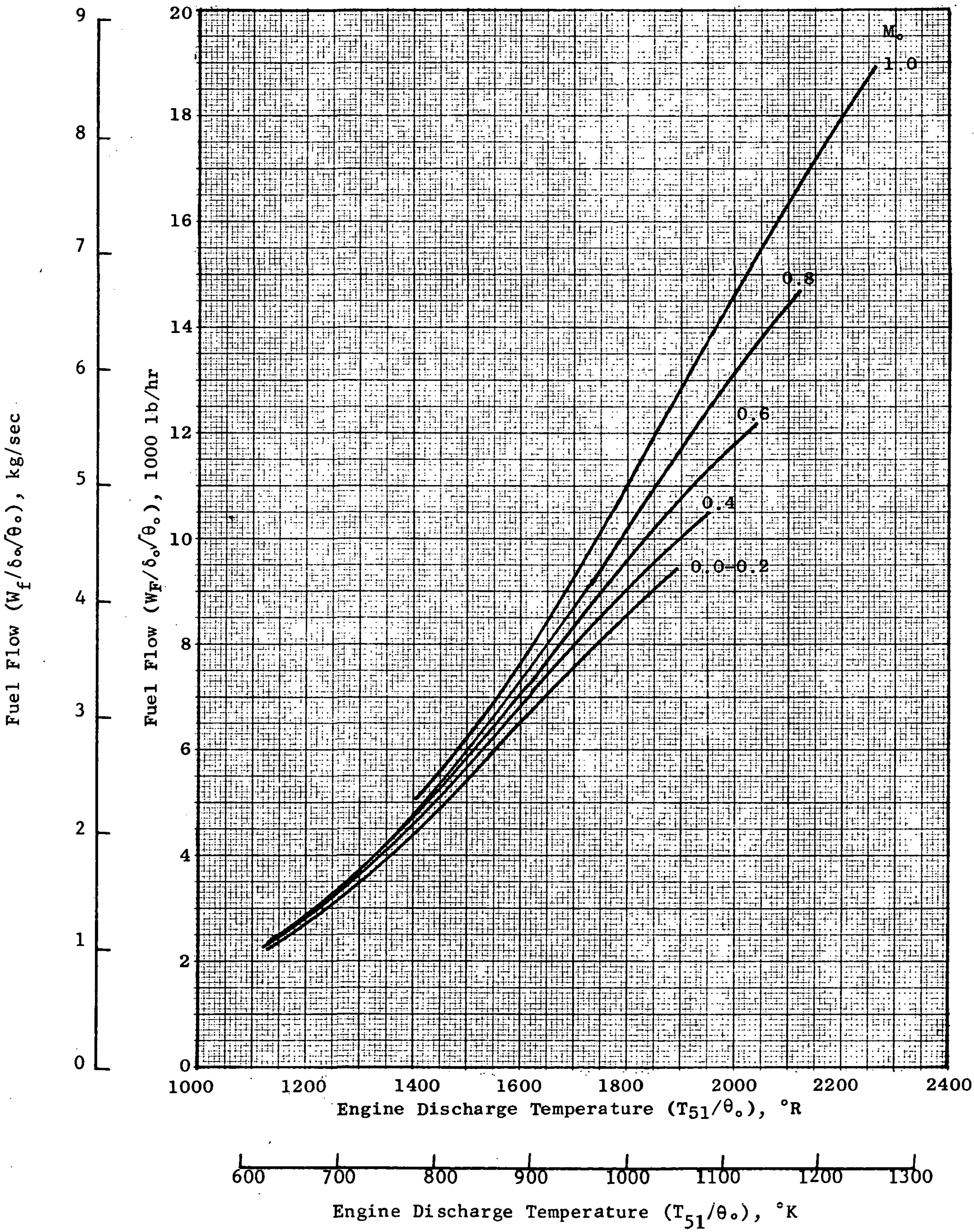

Figure 7 - J101 Gas Generator Fuel Flow

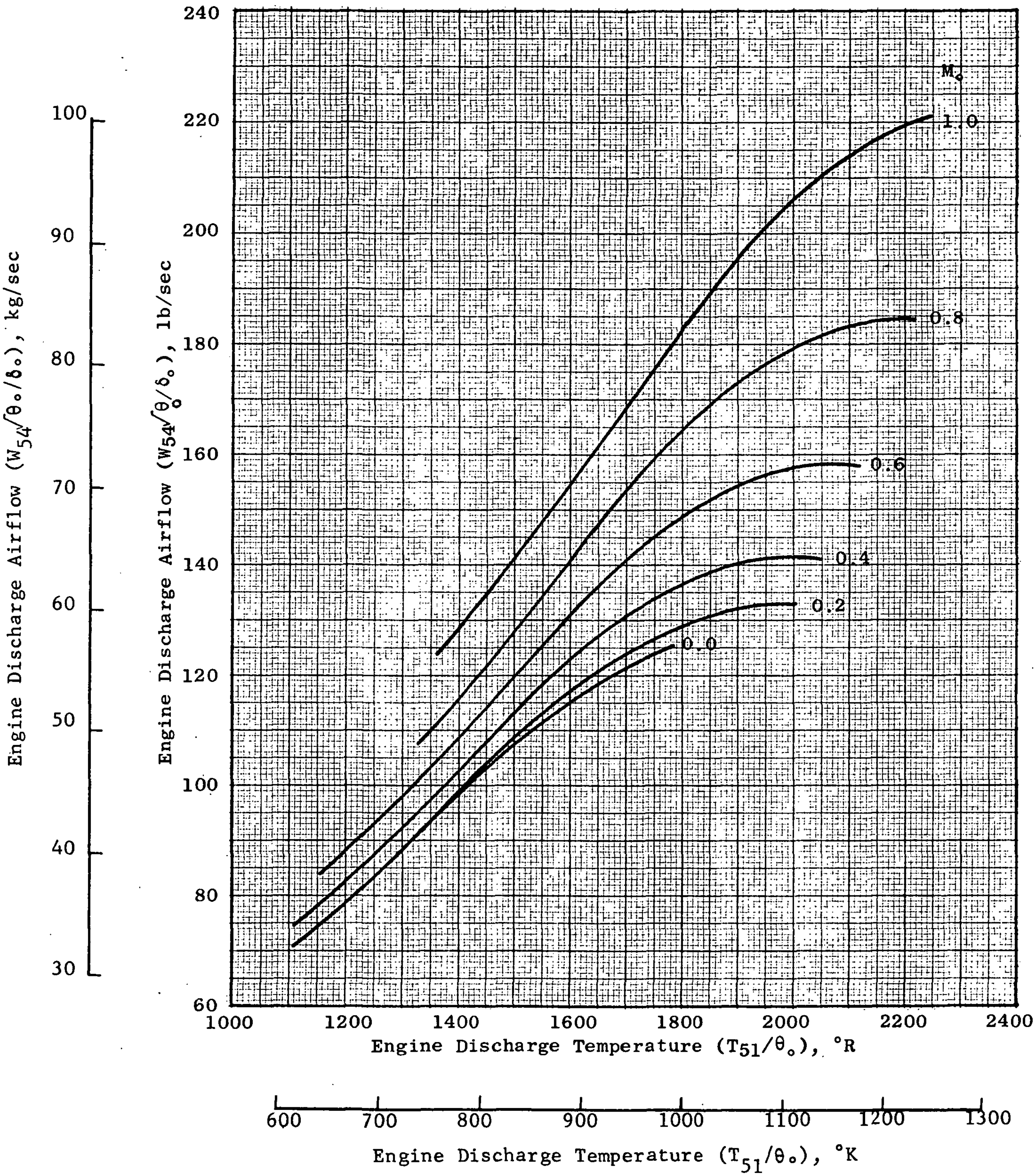

Figure 8 - J101 Gas Generator Discharge Flow

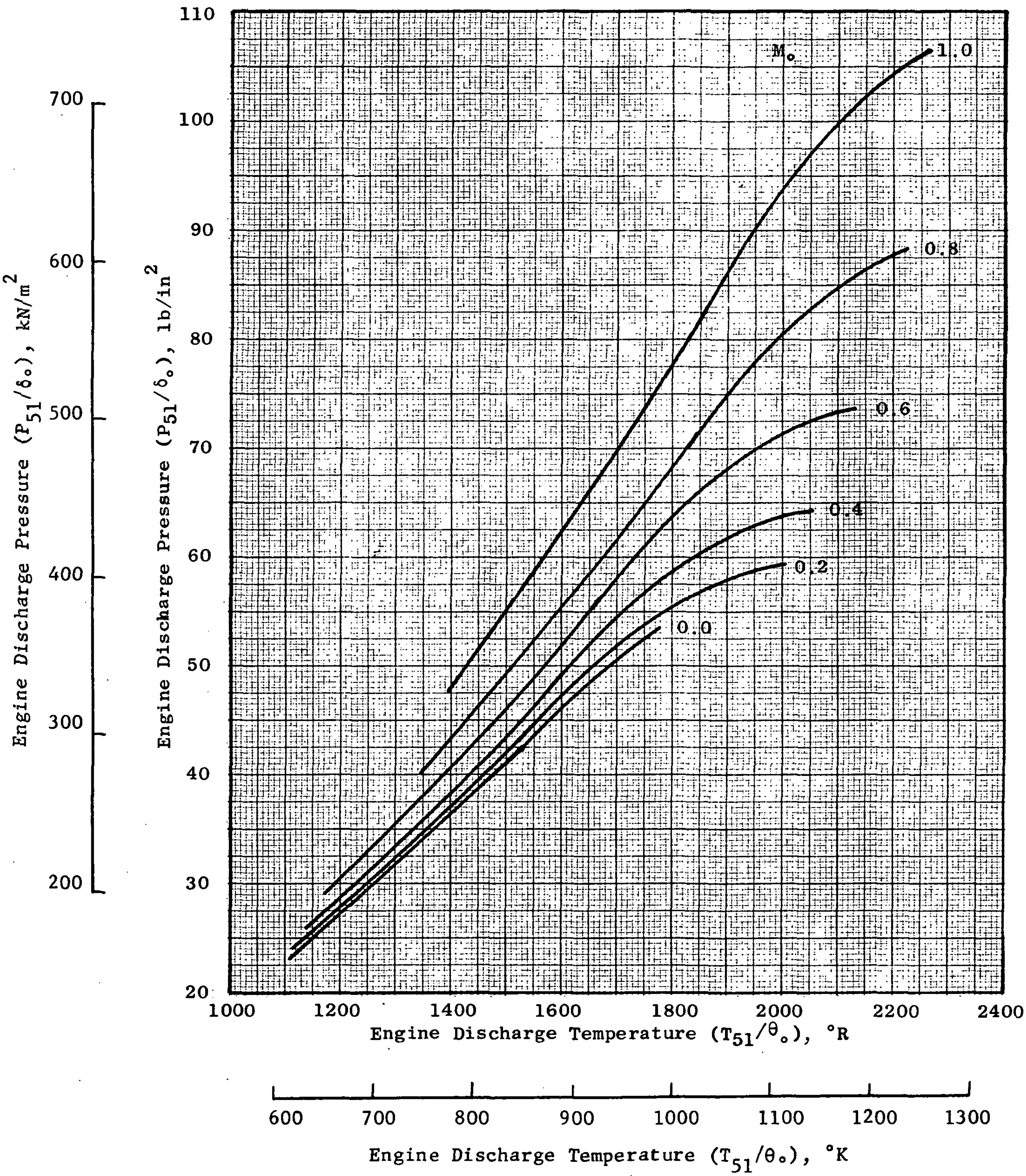

Figure 9 - J101 Gas Generator Discharge Pressure

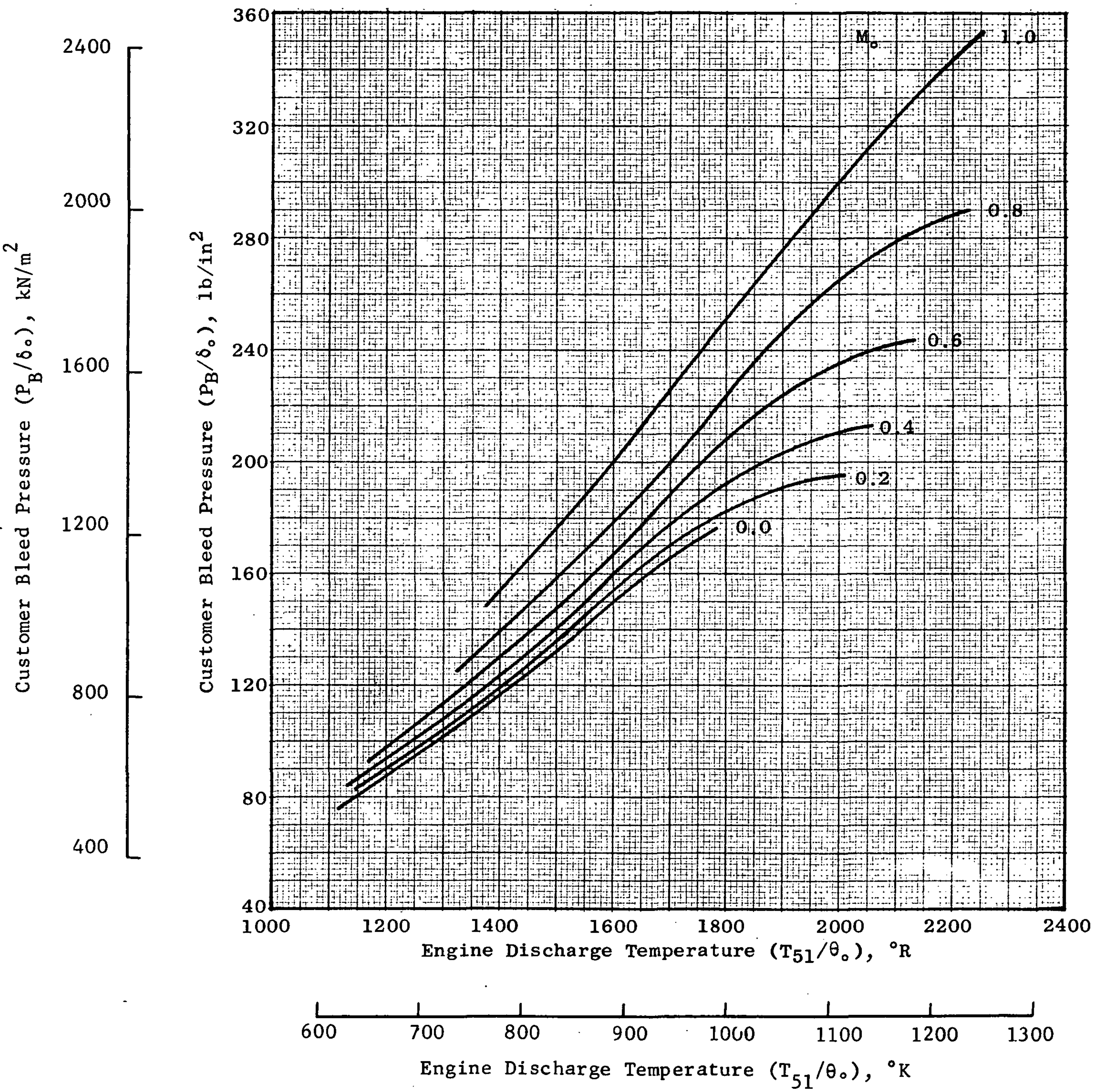

Figure 10 - J101 Gas Generator Bleed Pressure

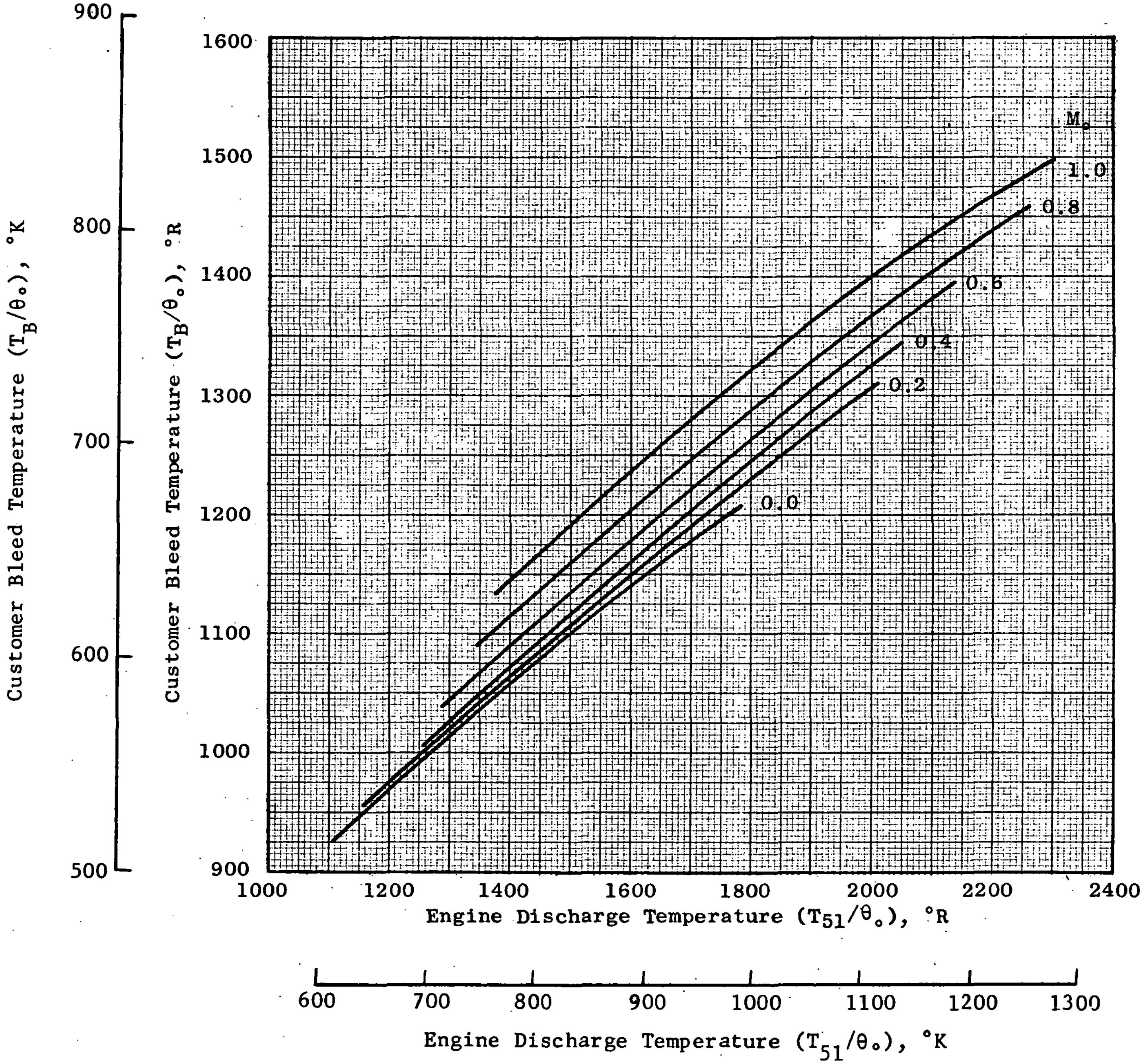

Figure 11 - J101 Gas Generator Customer Bleed Temperature

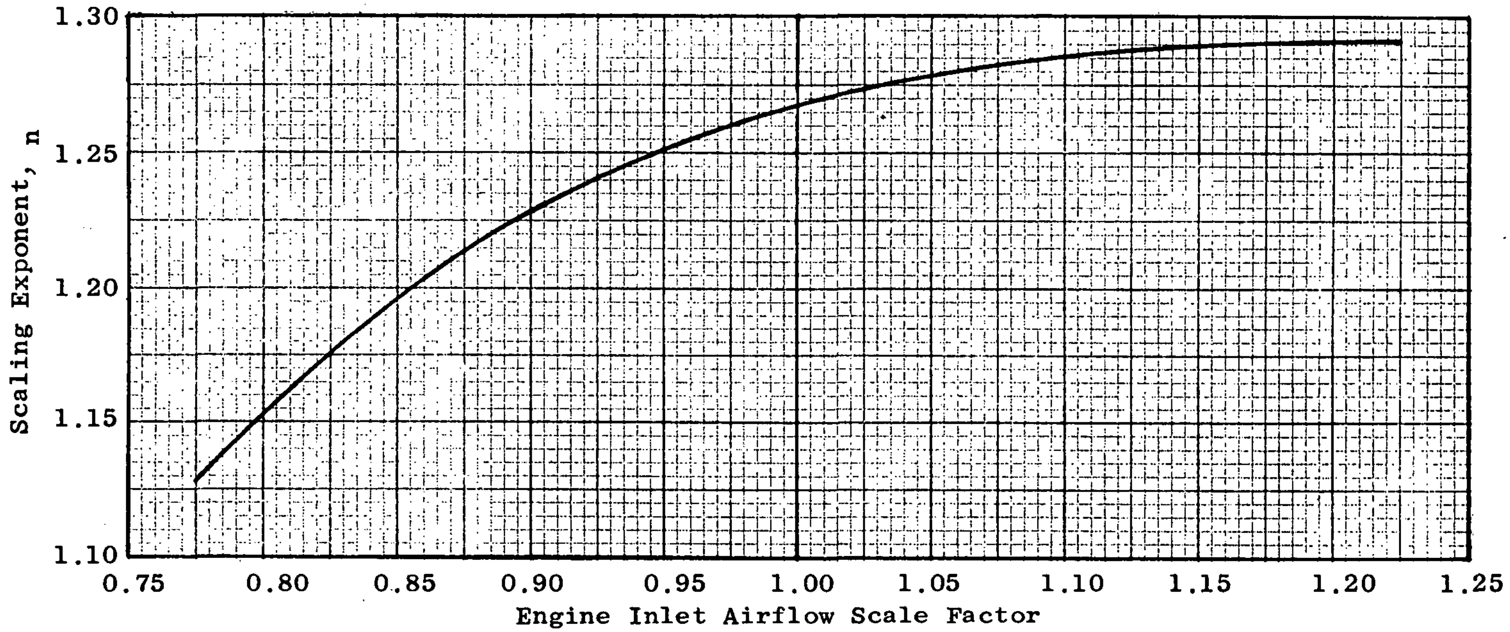

Weight (Ref) = 1480 lbs (671 kg)

$$\frac{\text{Weight}}{\text{Weight (Ref)}} = \left[\frac{\text{Airflow}}{\text{Airflow (Ref)}}\right]^n$$

Figure 12 - J101 Gas Generator Scaling Factor

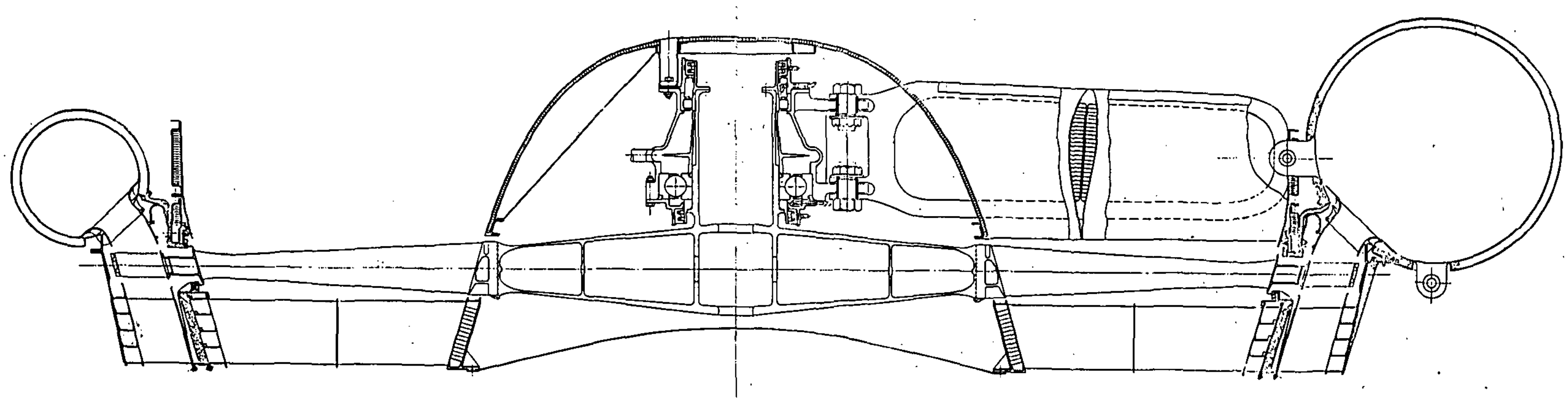

Figure 13 - Cross-Section of Single Stage Lift/Cruise Fan

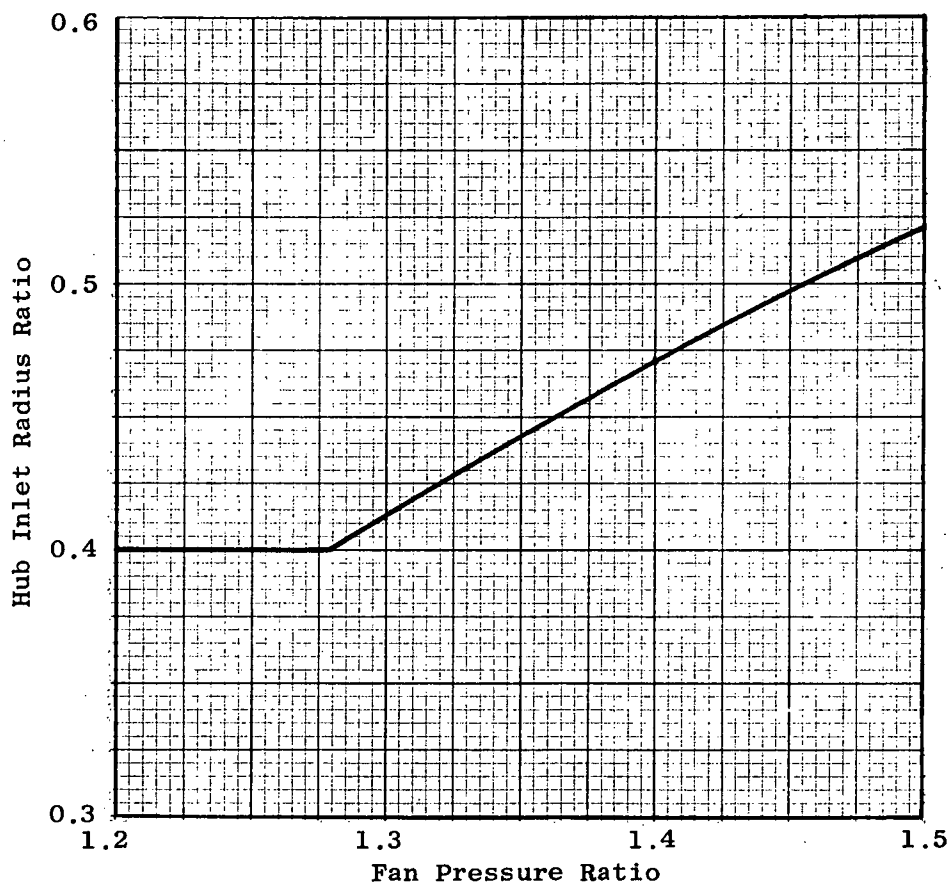

Figure 14 - Single Stage Fan Hub Radius Ratio Criteria

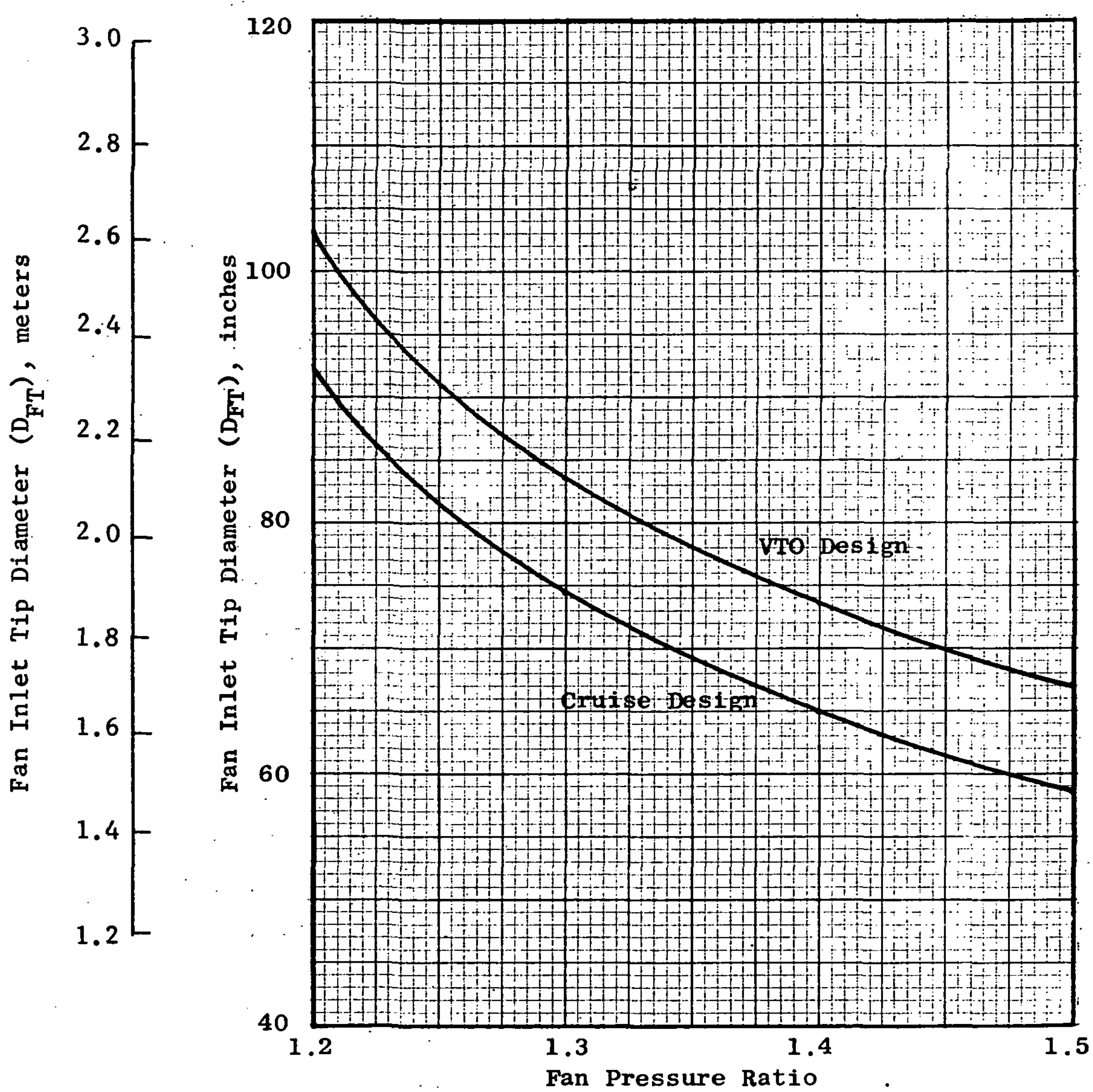

Figure 15 - Single Stage Fan Tip Diameter

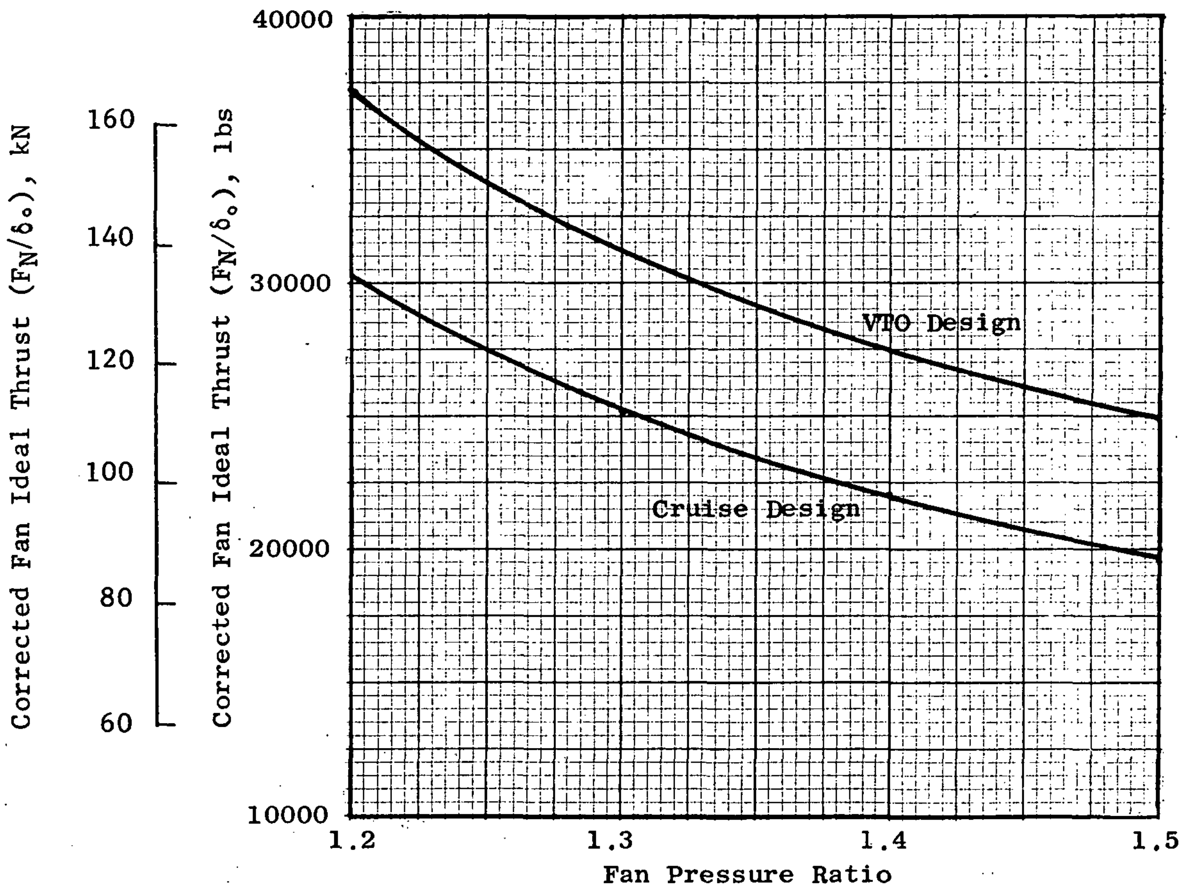

Figure 16 - Single Stage Fan Design Point Thrust

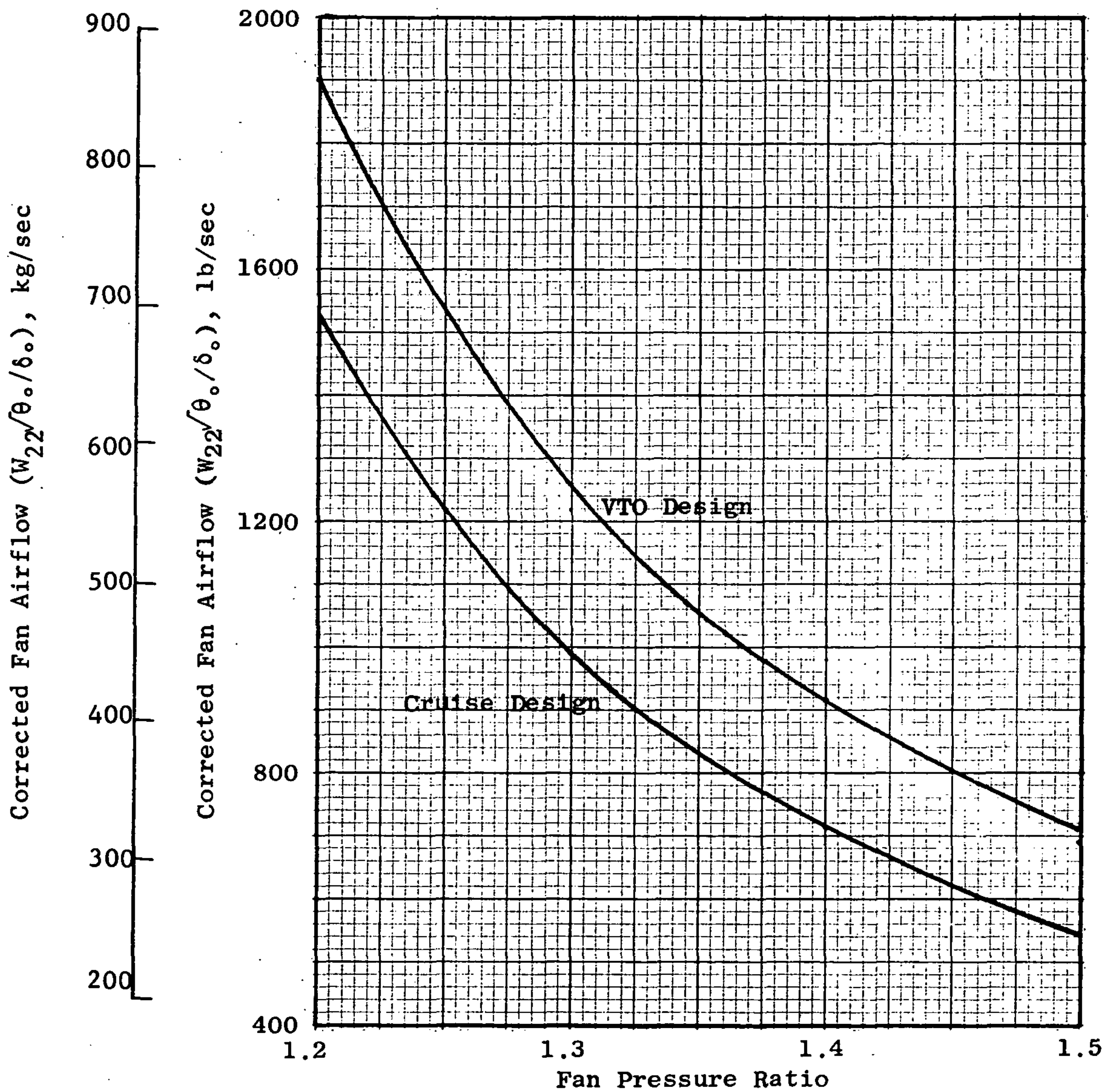

Figure 17 - Single Stage Fan Design Point Airflow

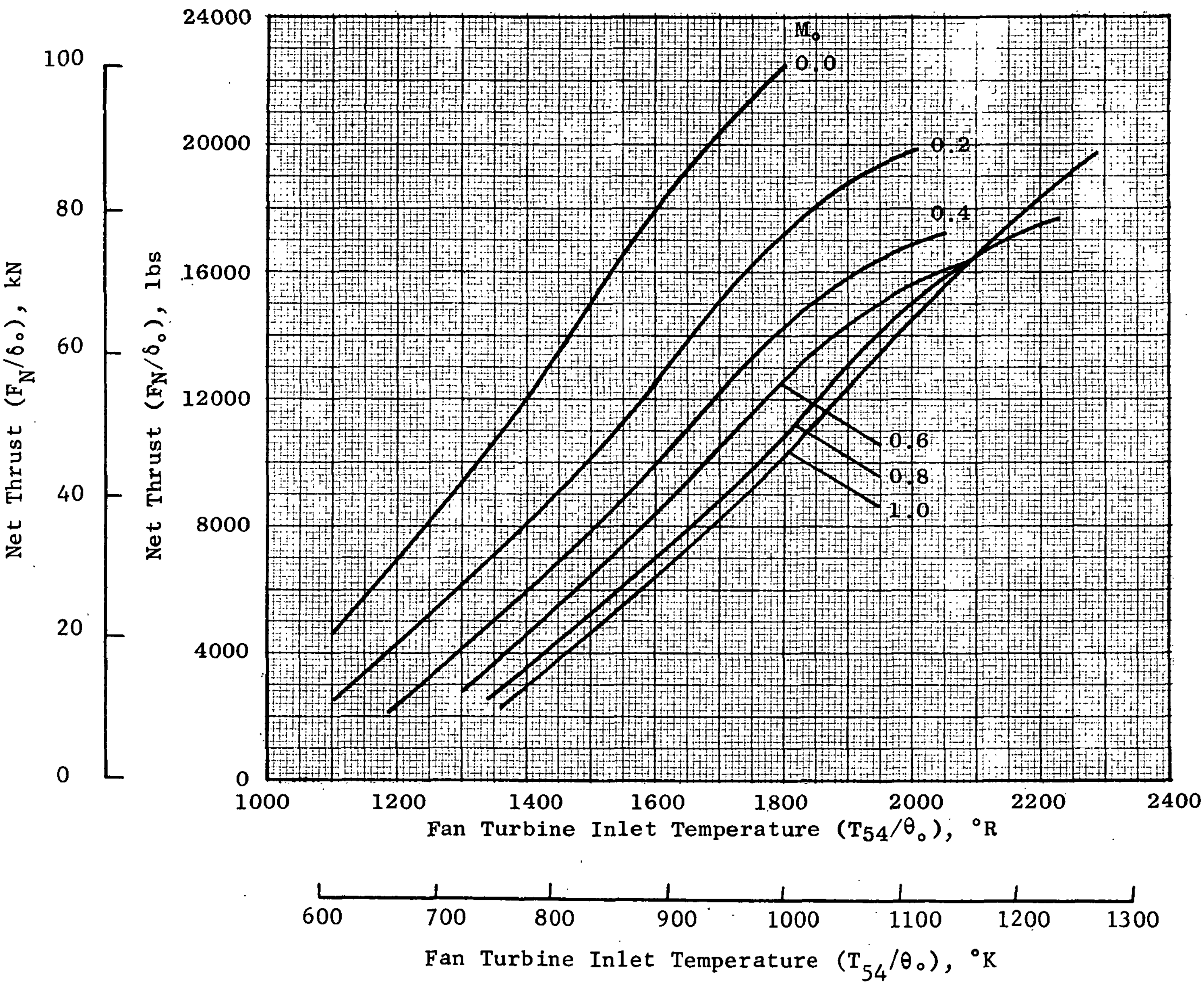

Figure 18 - Fan Net Thrust, Designed for VTO, P/P = 1.4

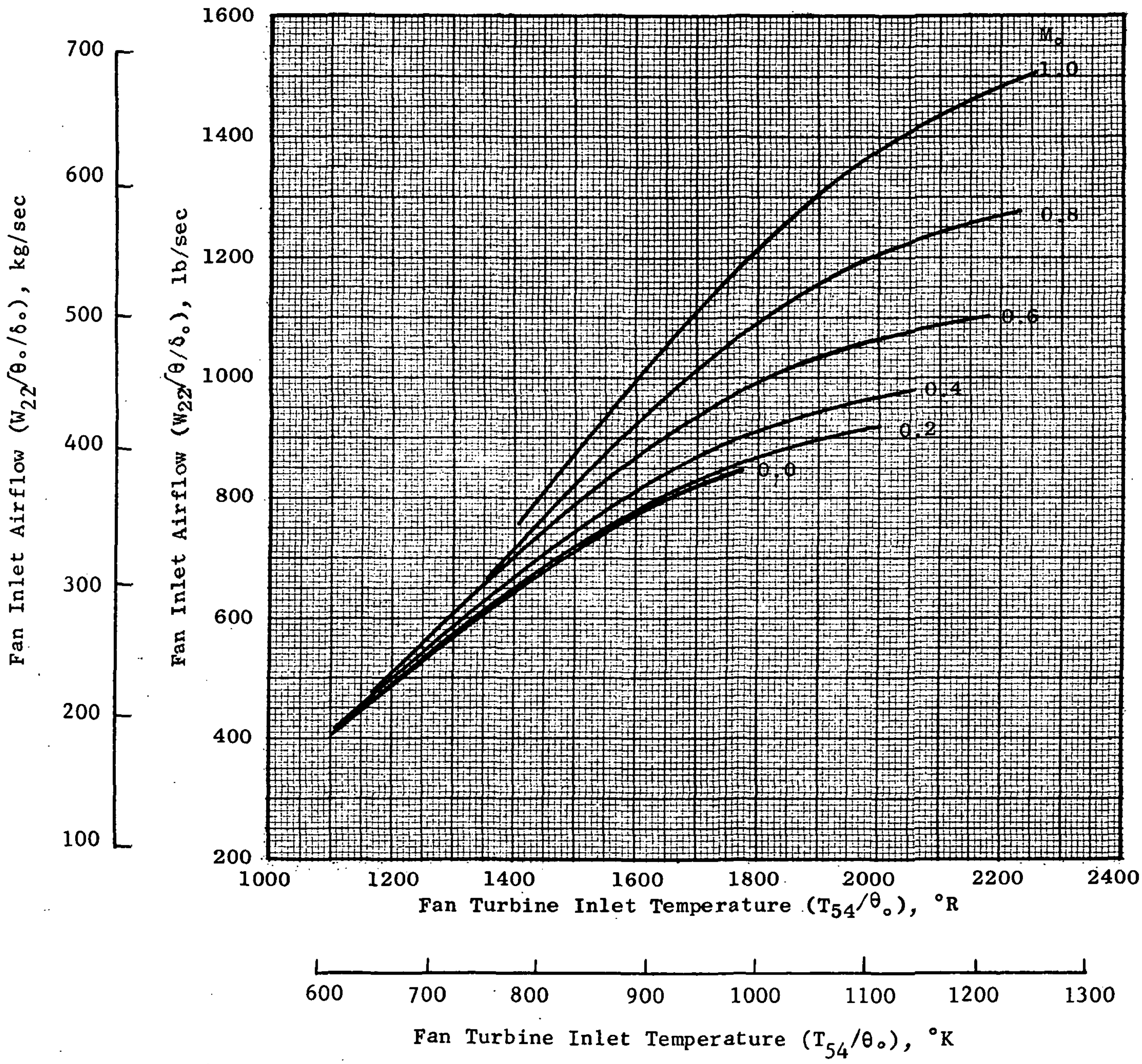

Figure 19 - Fan Inlet Airflow, Designed for VTO, P/P = 1.4

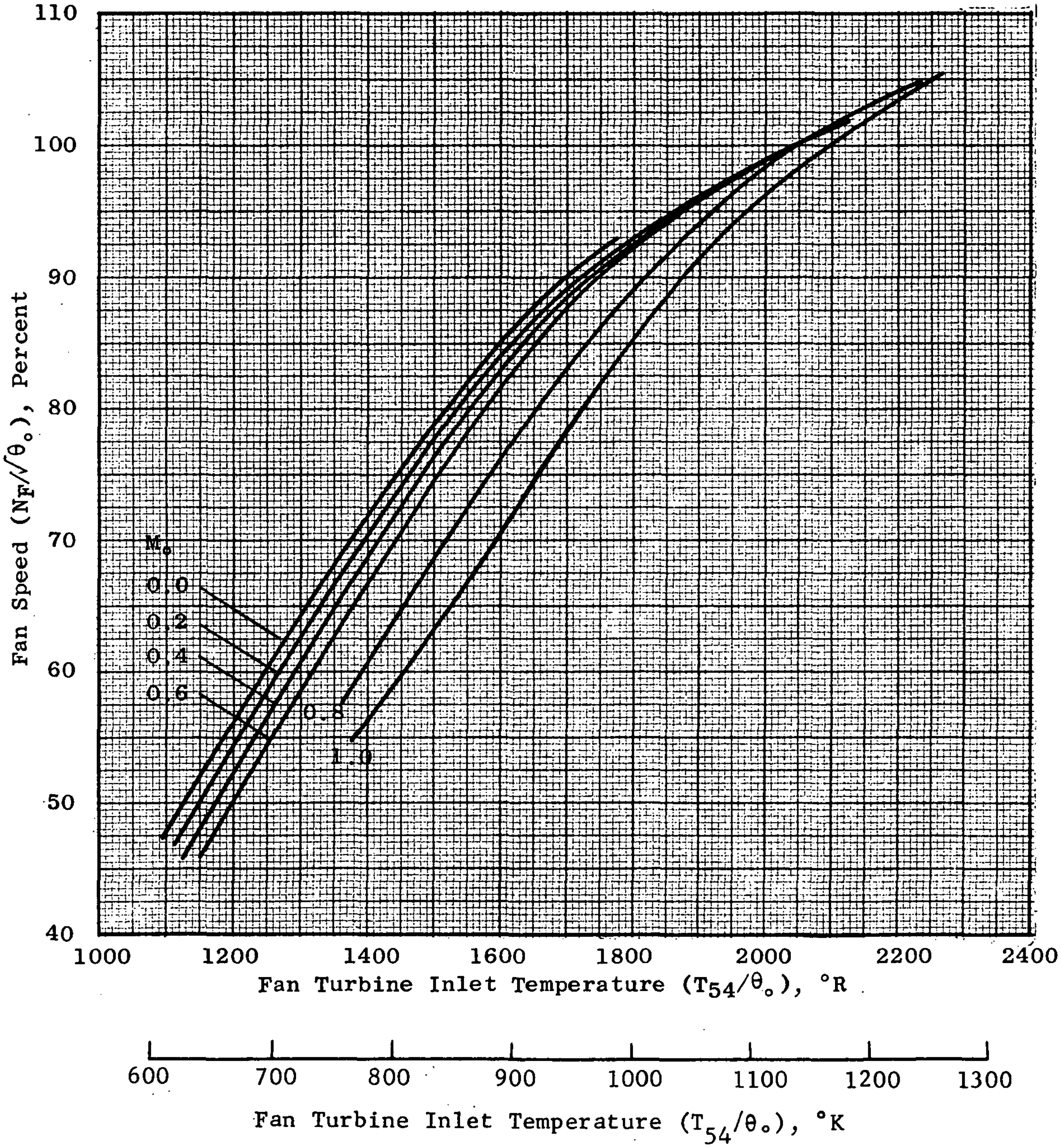

Figure 20 - Fan Speed, Designed for VTO, P/P = 1.4

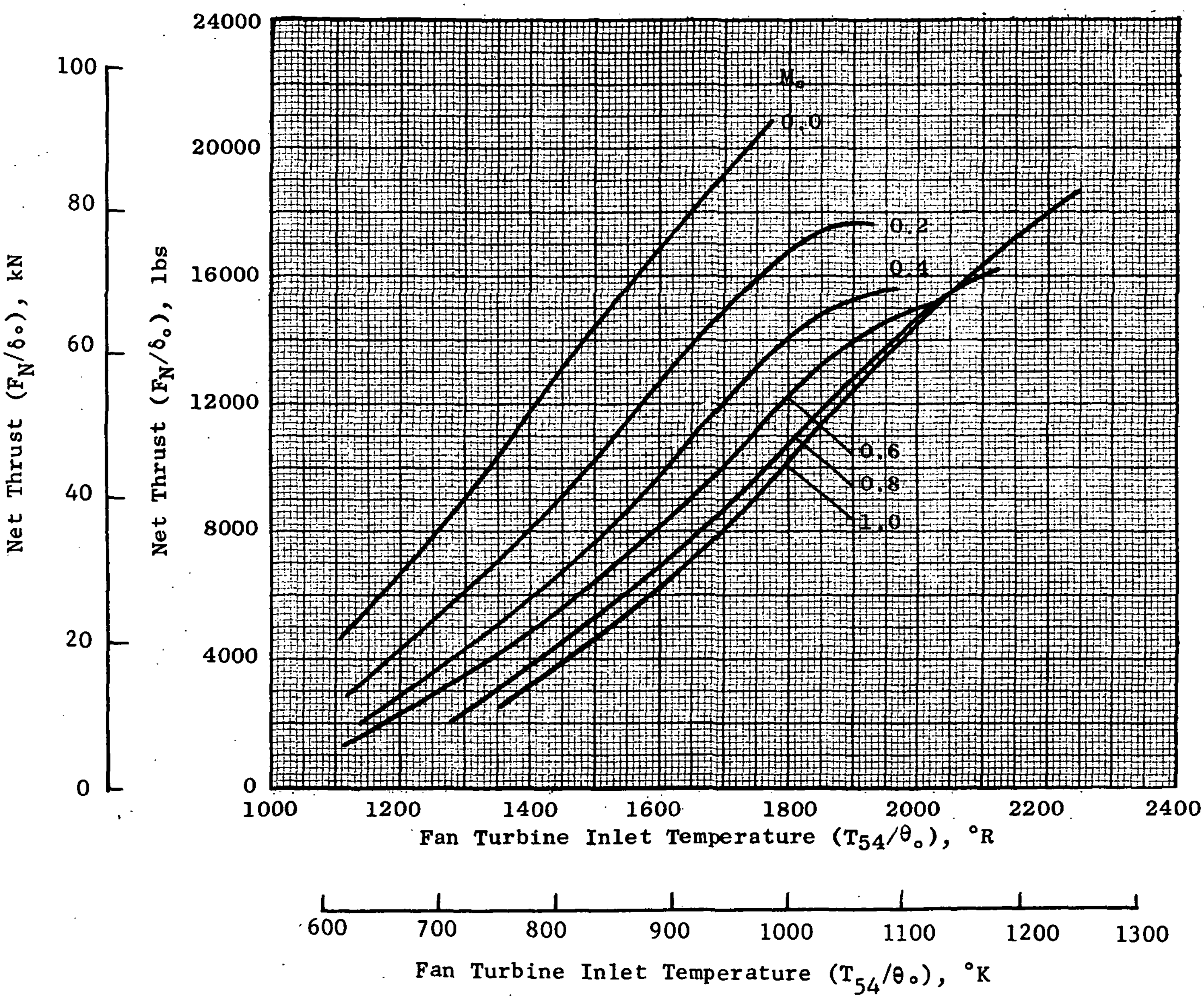

Figure 21 - Fan Net Thrust, Designed for Cruise, P/P = 1.4

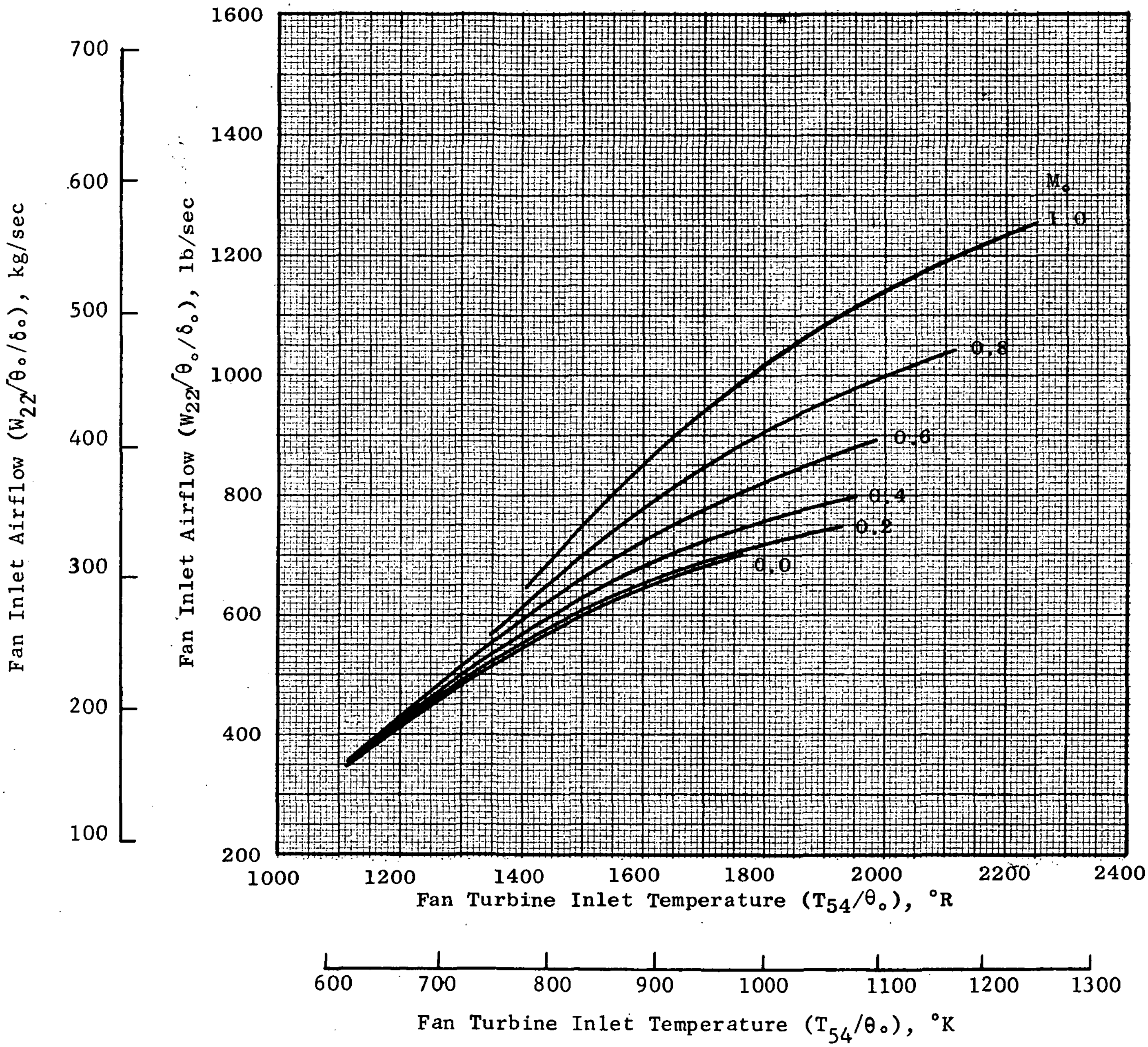

Figure 22 - Fan Inlet Airflow, Designed for Cruise, P/P = 1.4

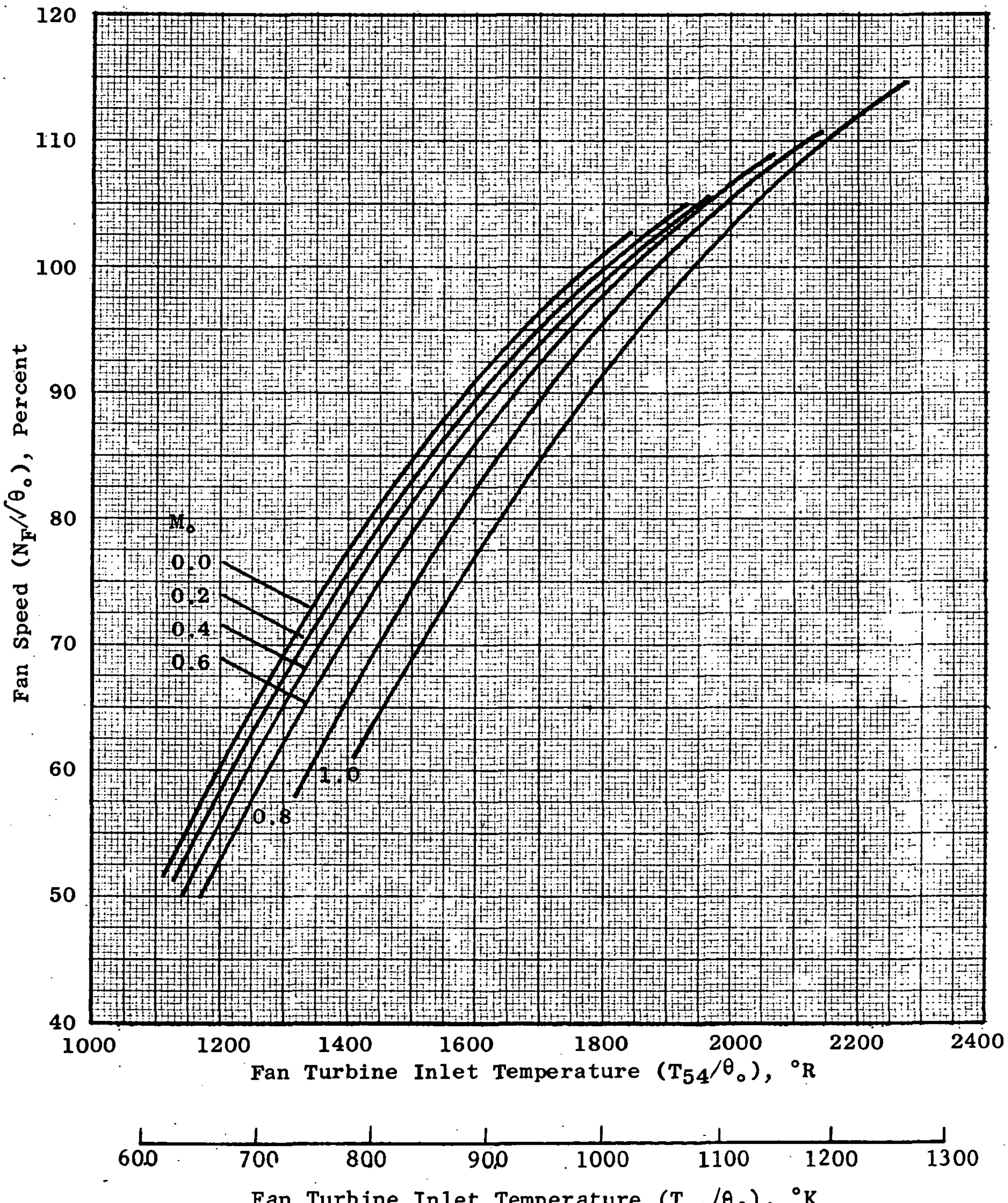

Figure 23 - Fan Speed, Designed for Cruise, P/P = 1.4

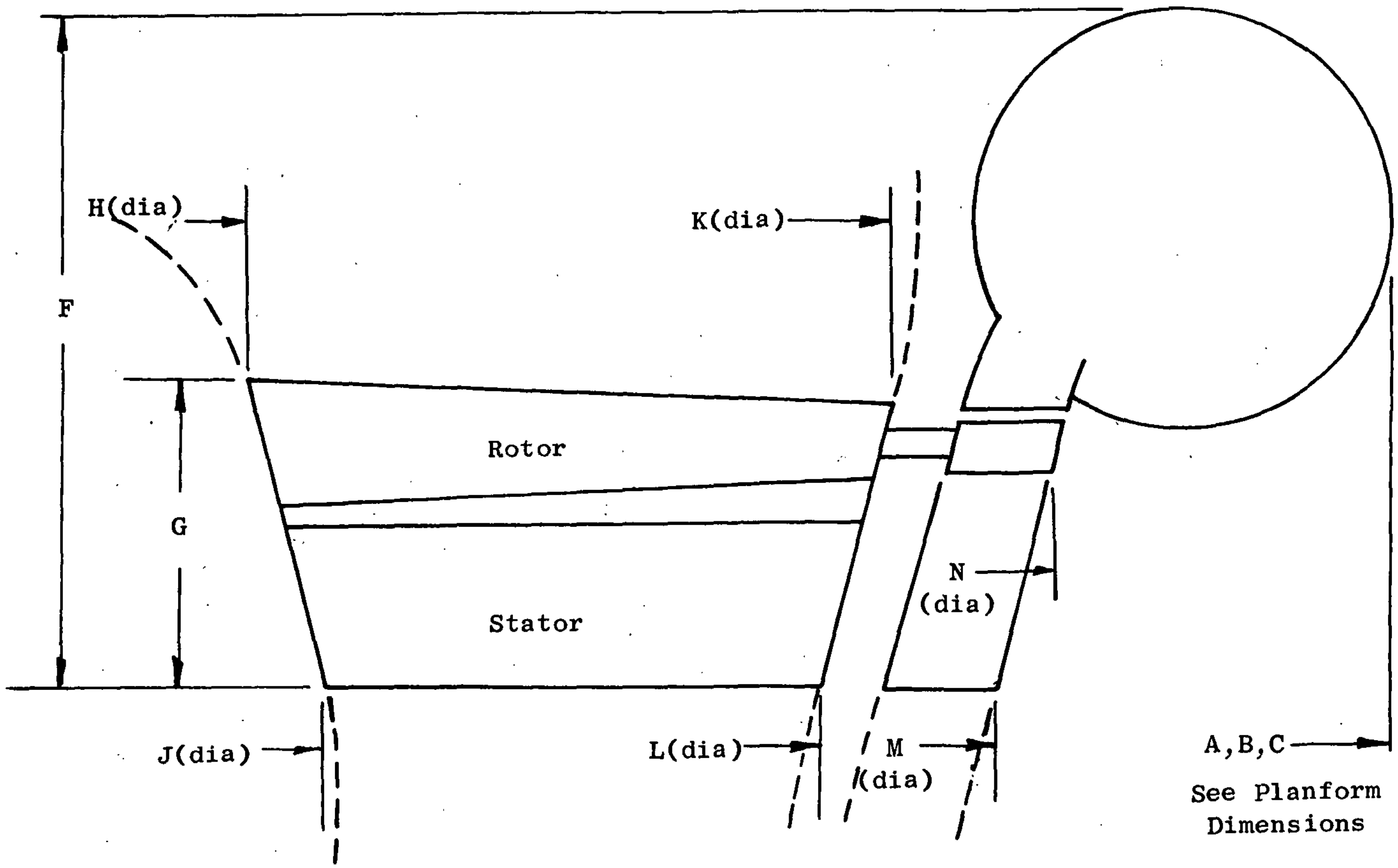

Figure 24 - One Stage Lift Fan Cross-Section Dimensions

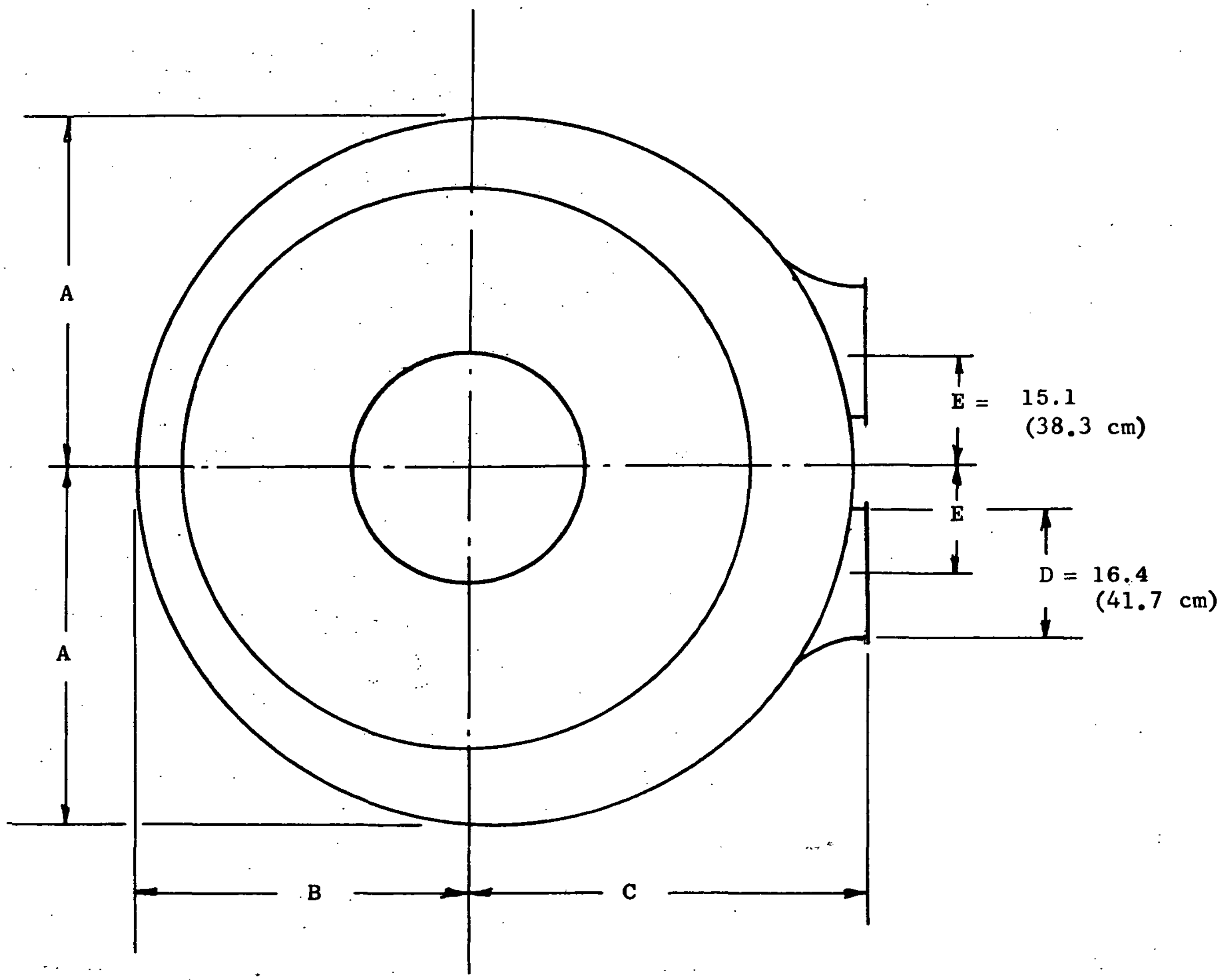

Figure 25 - Single Stage Fan Planform Dimensions

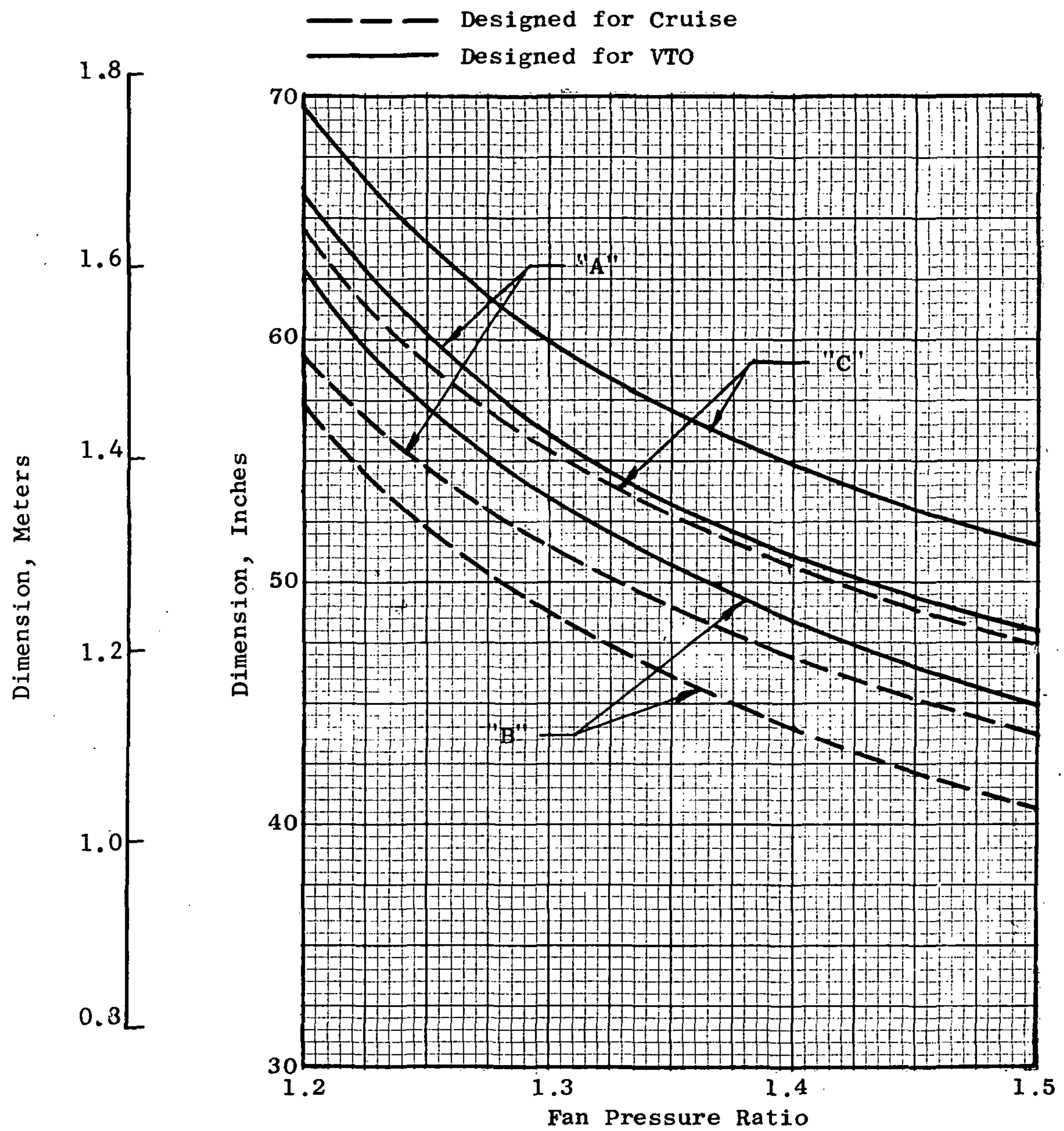

Figure 26 - Single Stage Fan Installation Dimensions - "A", "B" and "C"

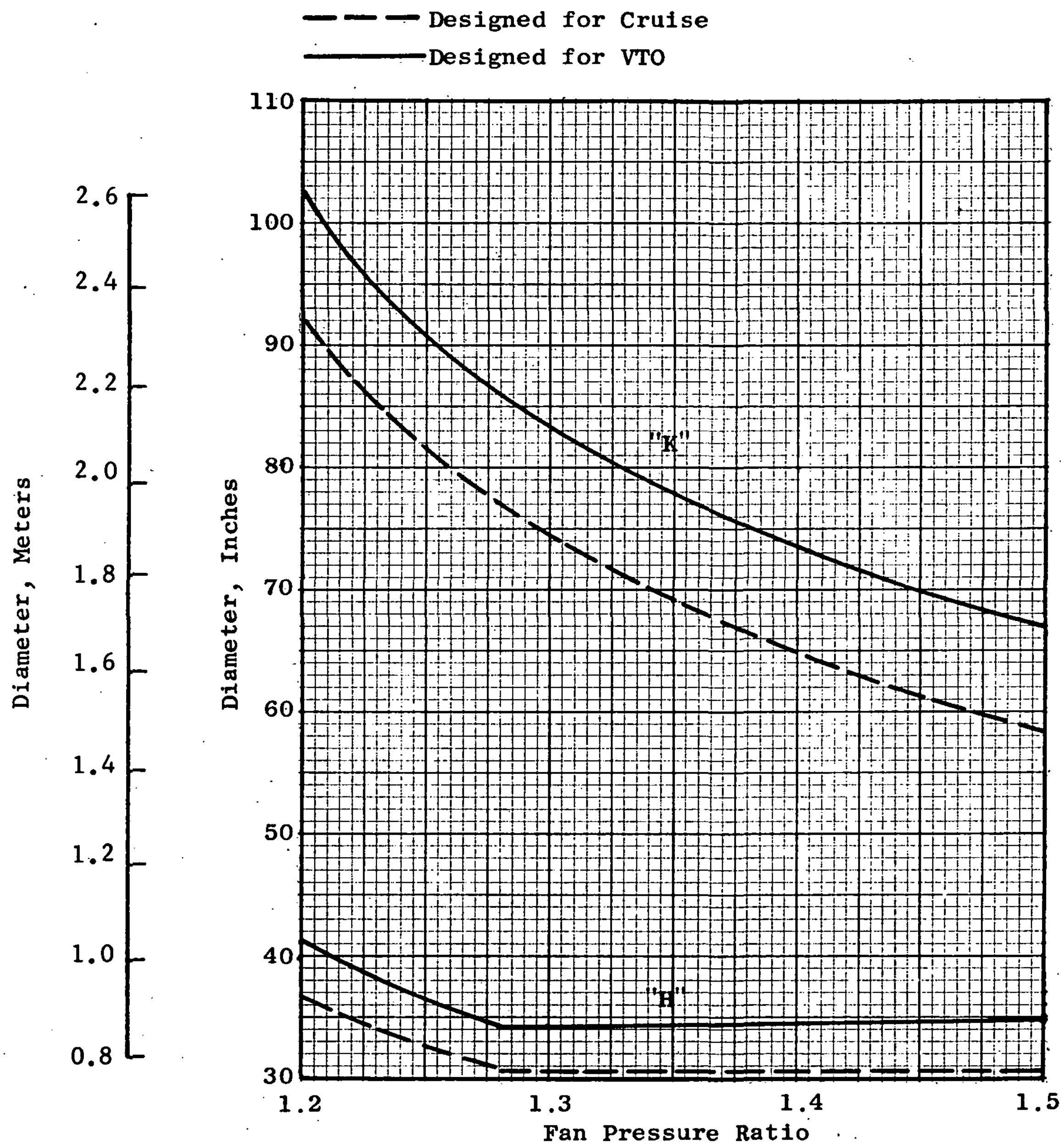

Figure 27 - Single Stage Fan Installation Dimensions "H" and "K"

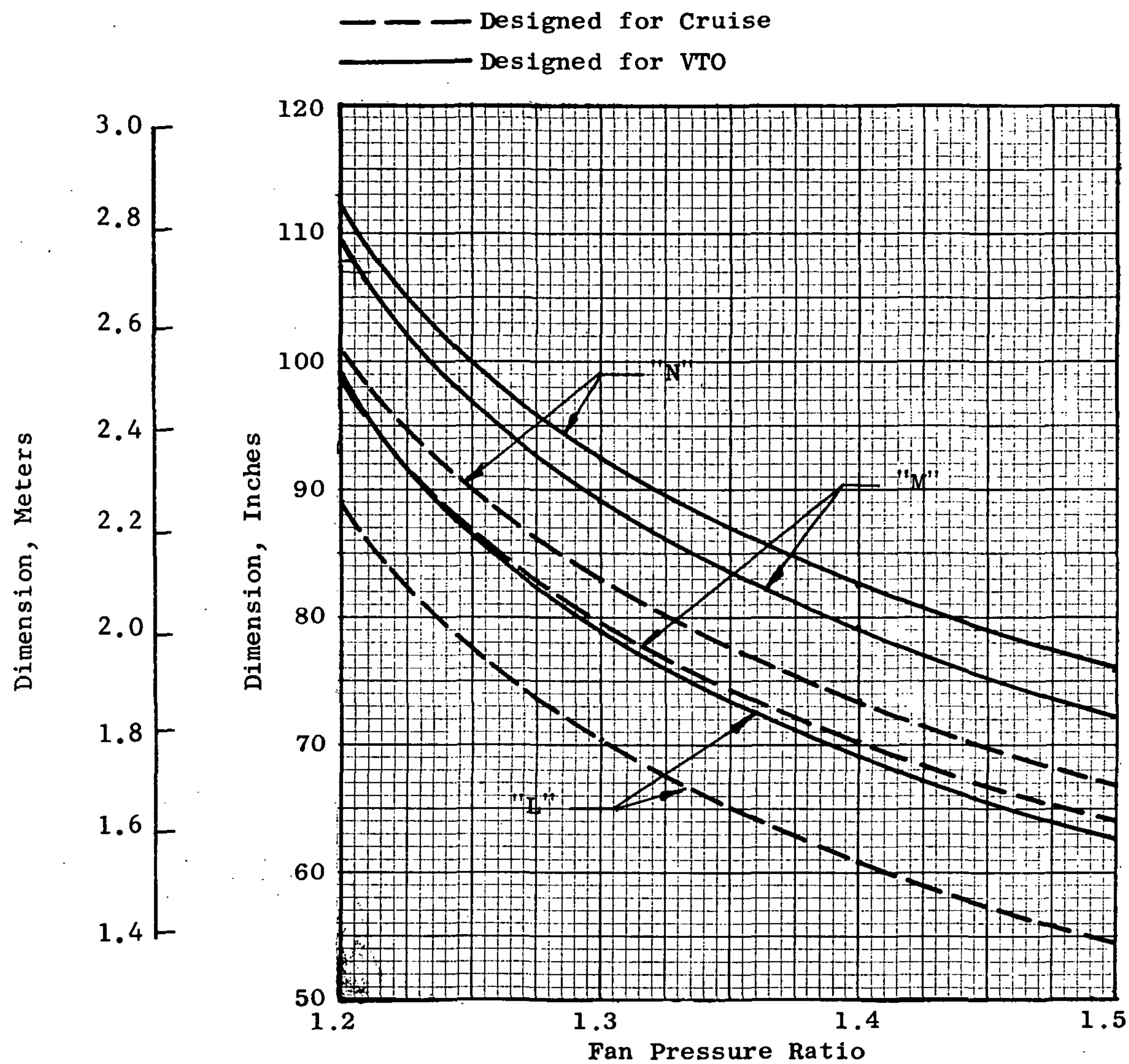

Figure 28 - Single Stage Fan Installation Dimensions "L", "M" and "N"

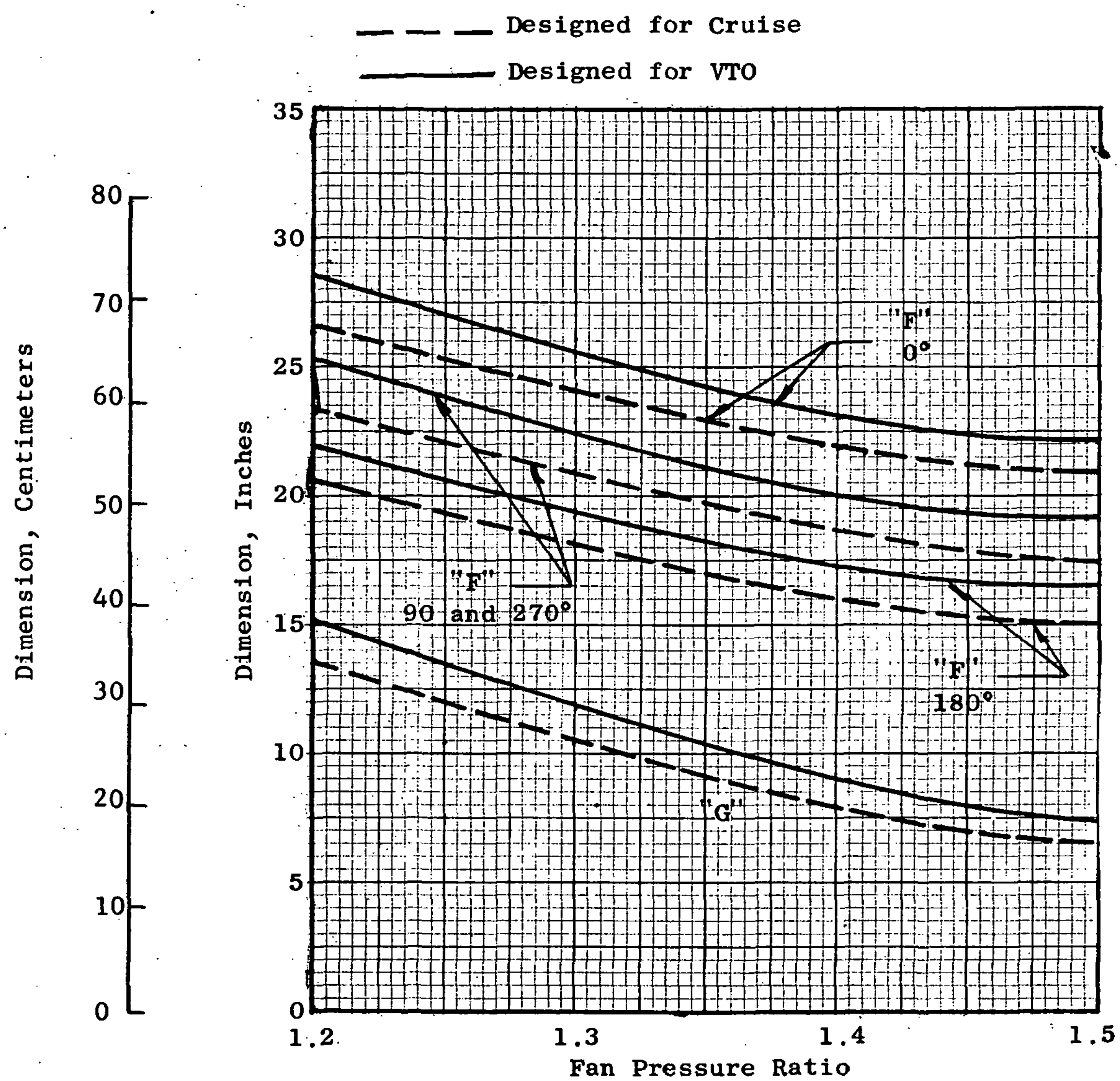

Figure 29 - Single Stage Installation Dimensions "F" and "G"

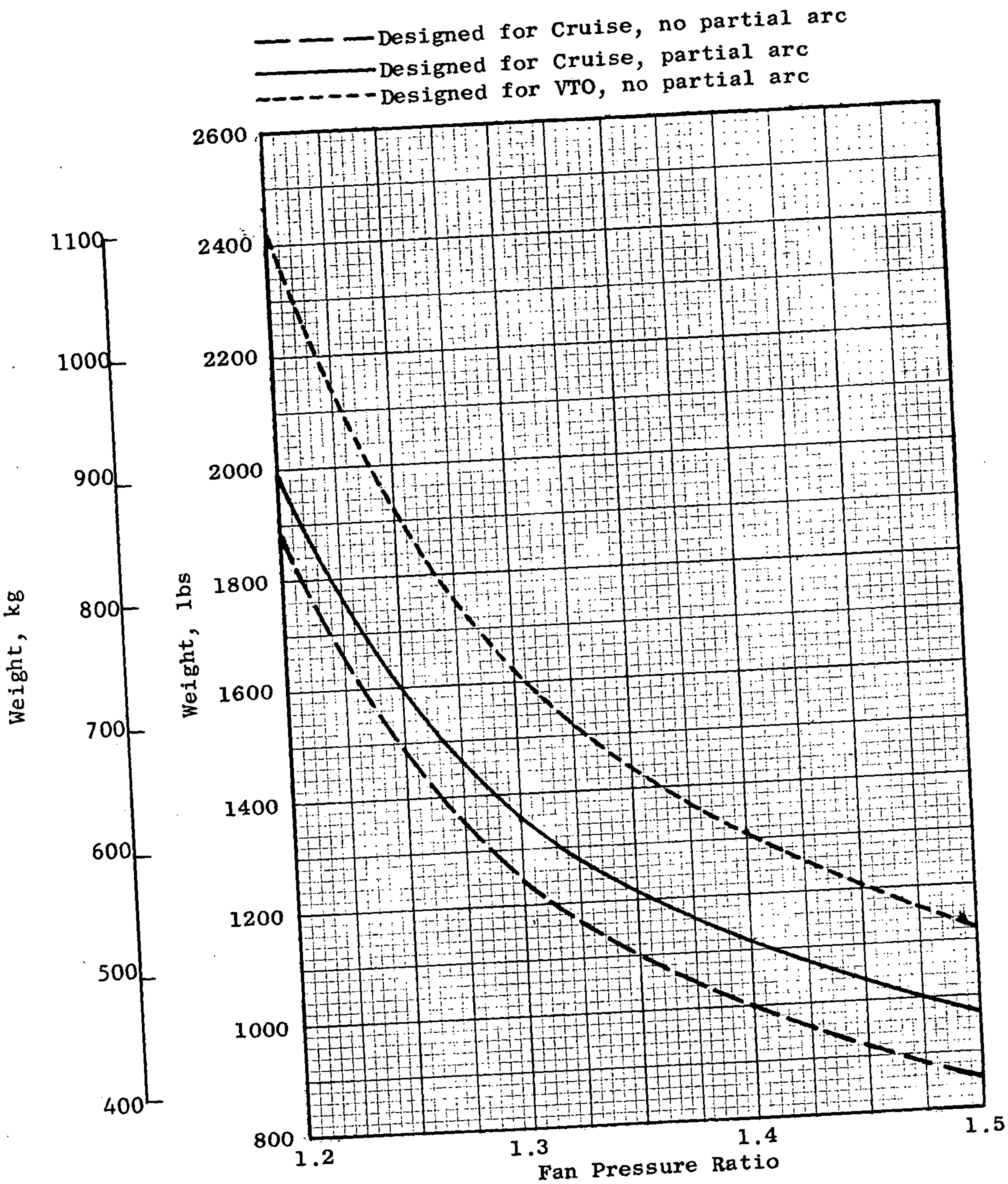

Figure 30- Single Stage Fan Weights

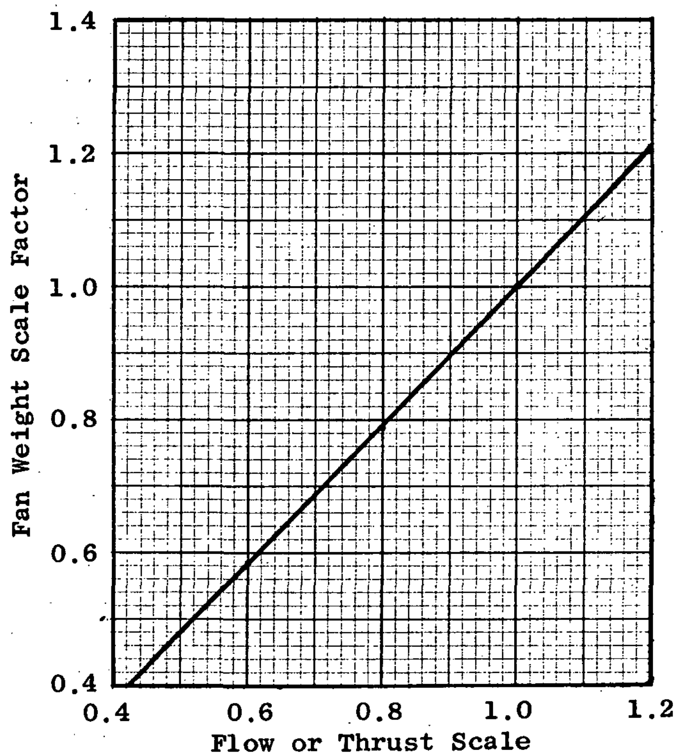

Figure 31 - Single Stage Weight Scaling Factor for Changes in Fan Thrust Size

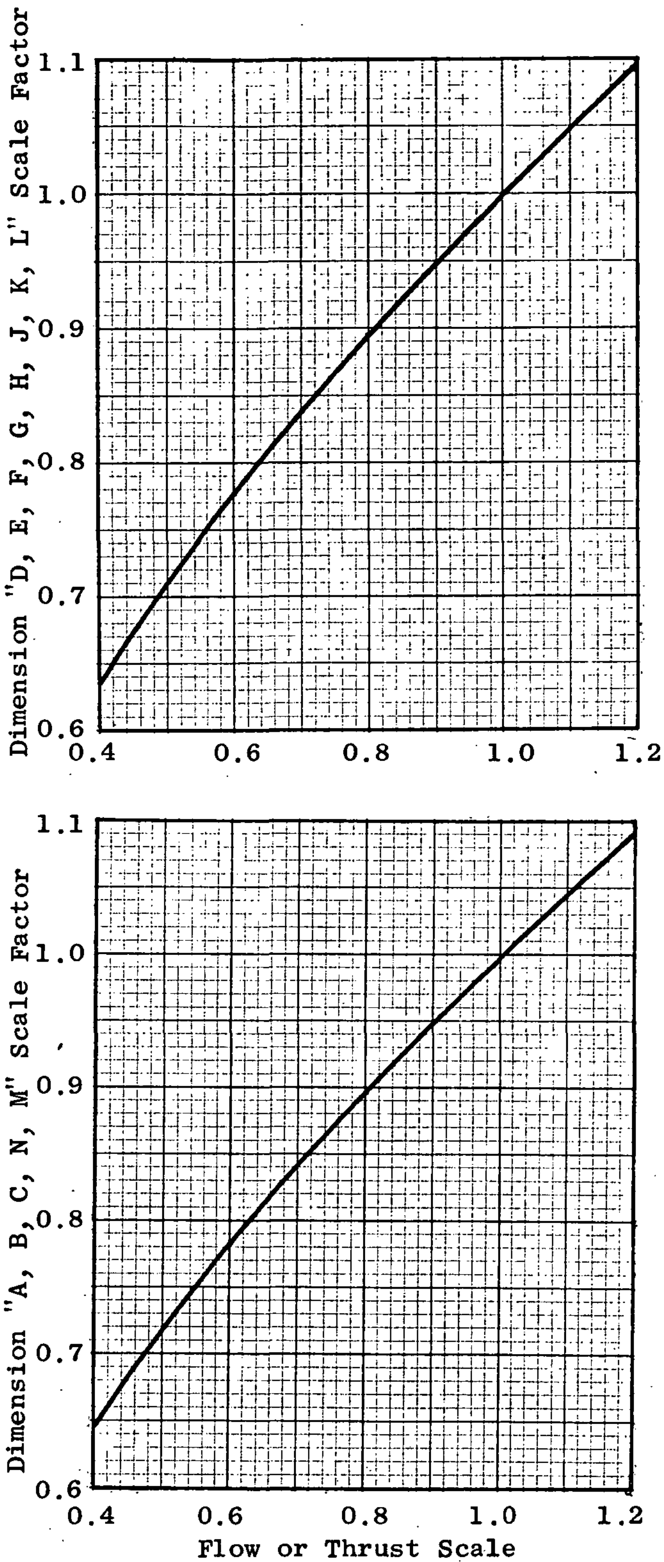

Figure 32 - Single Stage Dimension Scale Factors for Changes in Fan Thrust Size

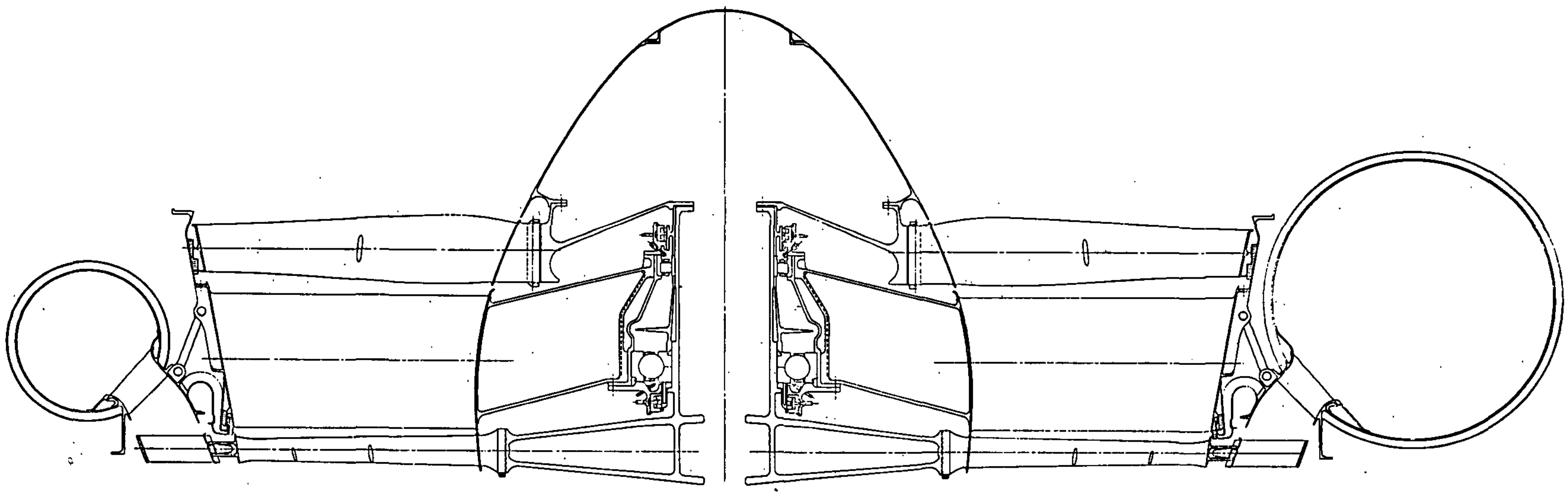

Figure 33 - Cross-Section of Two Stage Fan

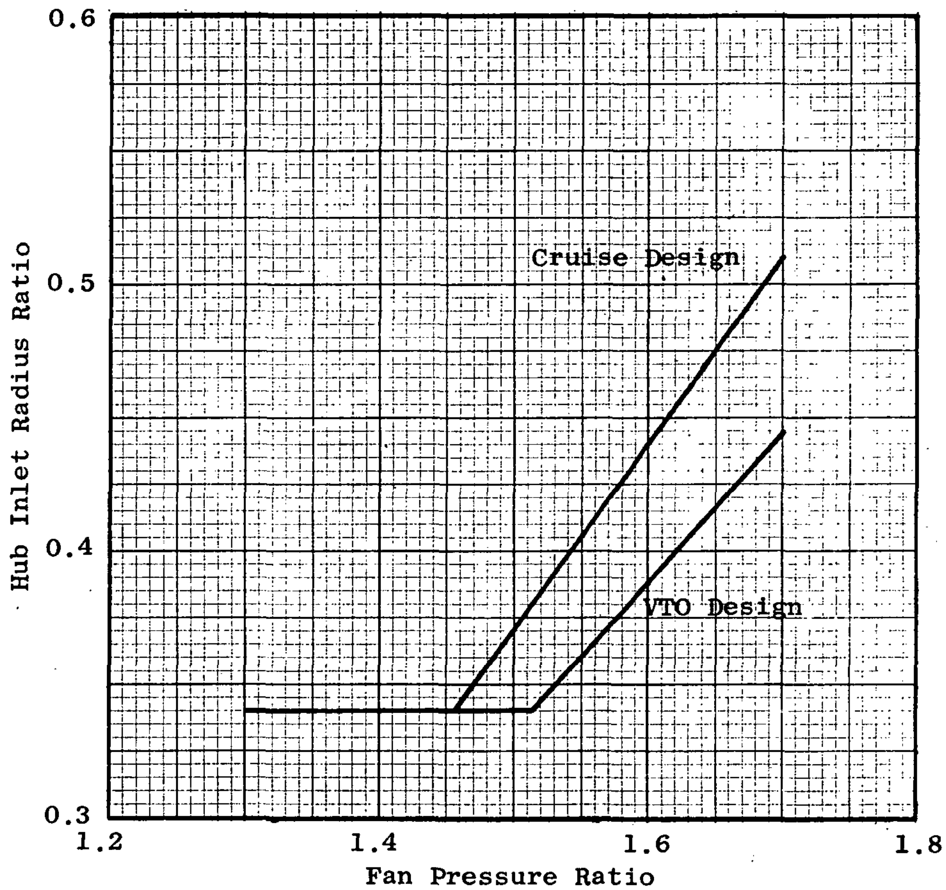

Figure 34 - Two Stage Fan Hub Radius Ratio Criteria

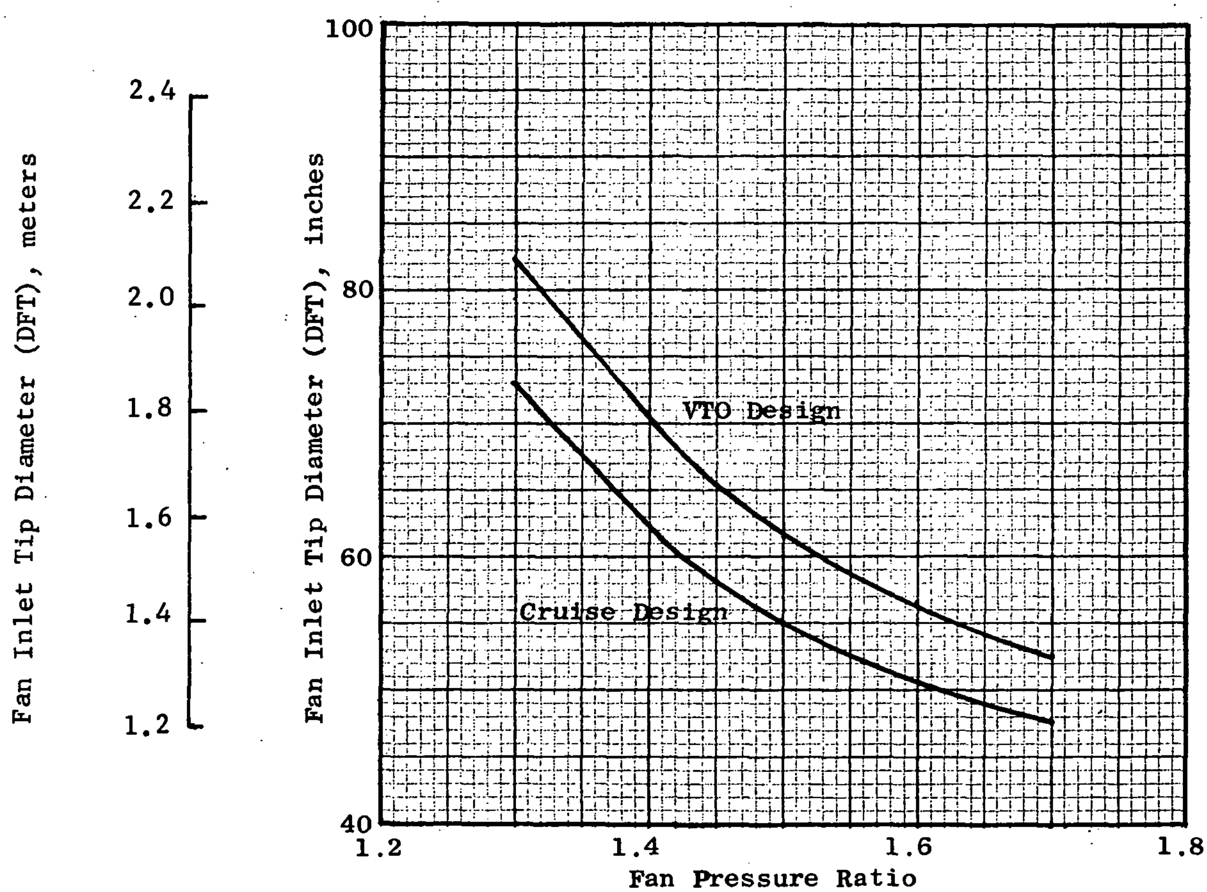

Figure 35 - Two Stage Fan Tip Diameter

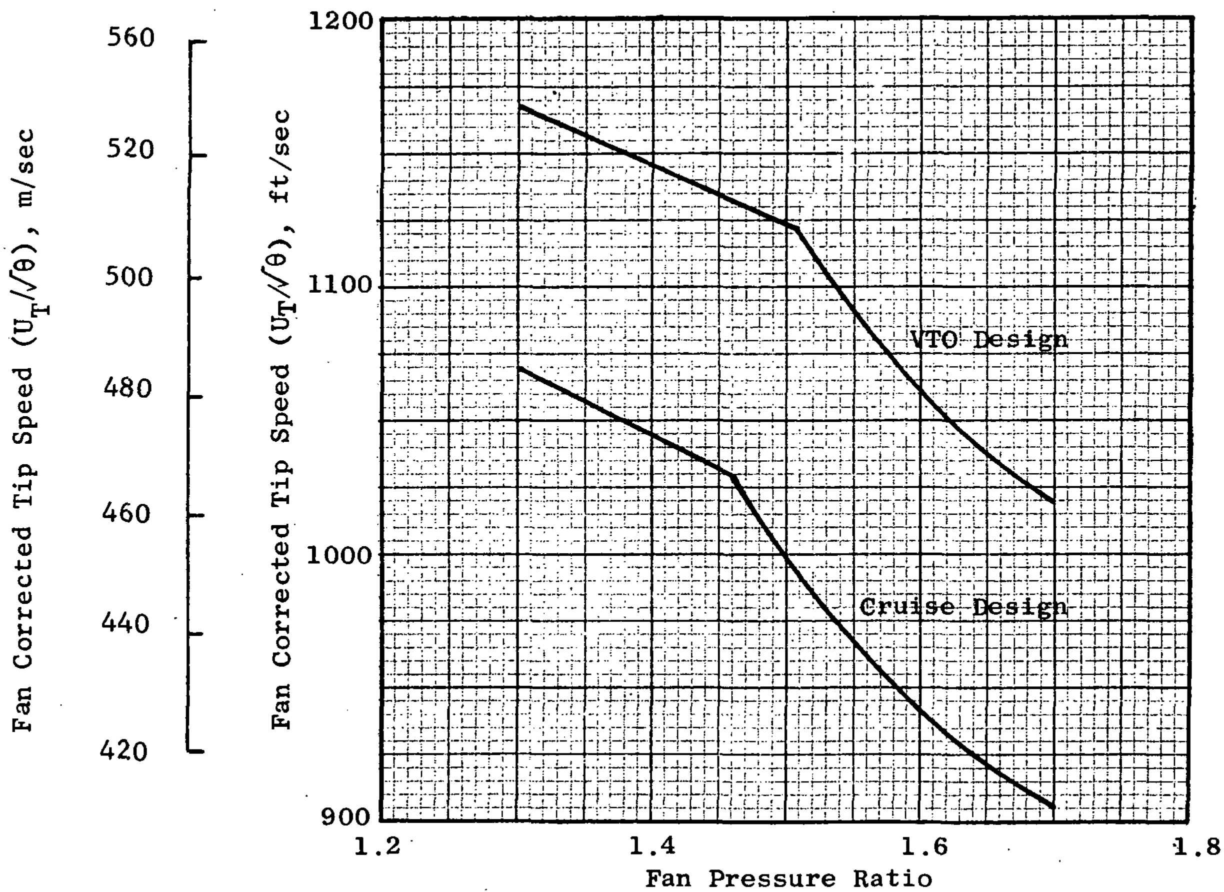

Figure 36 - Two Stage Fan Tip Speed Criteria

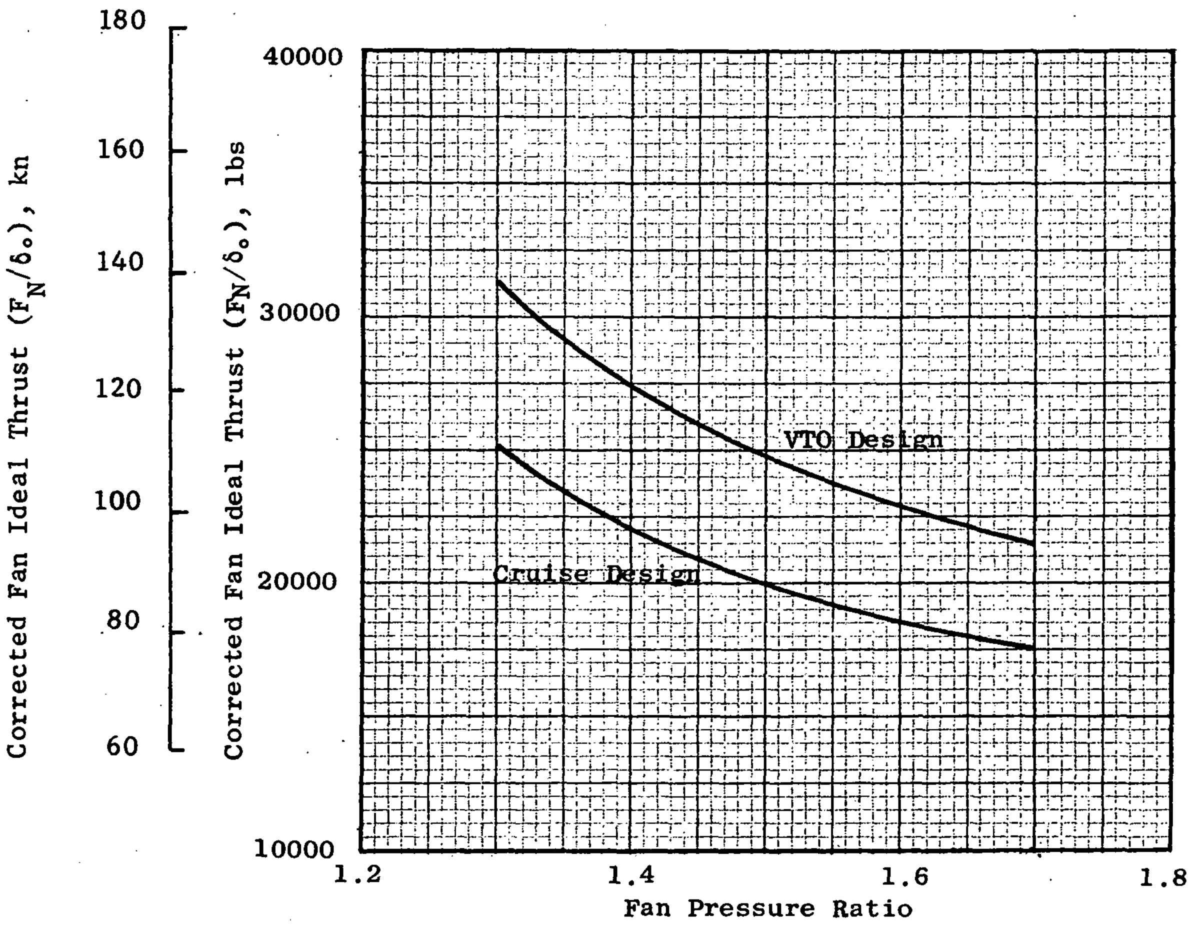

Figure 37 - Two Stage Fan Design Point Thrust

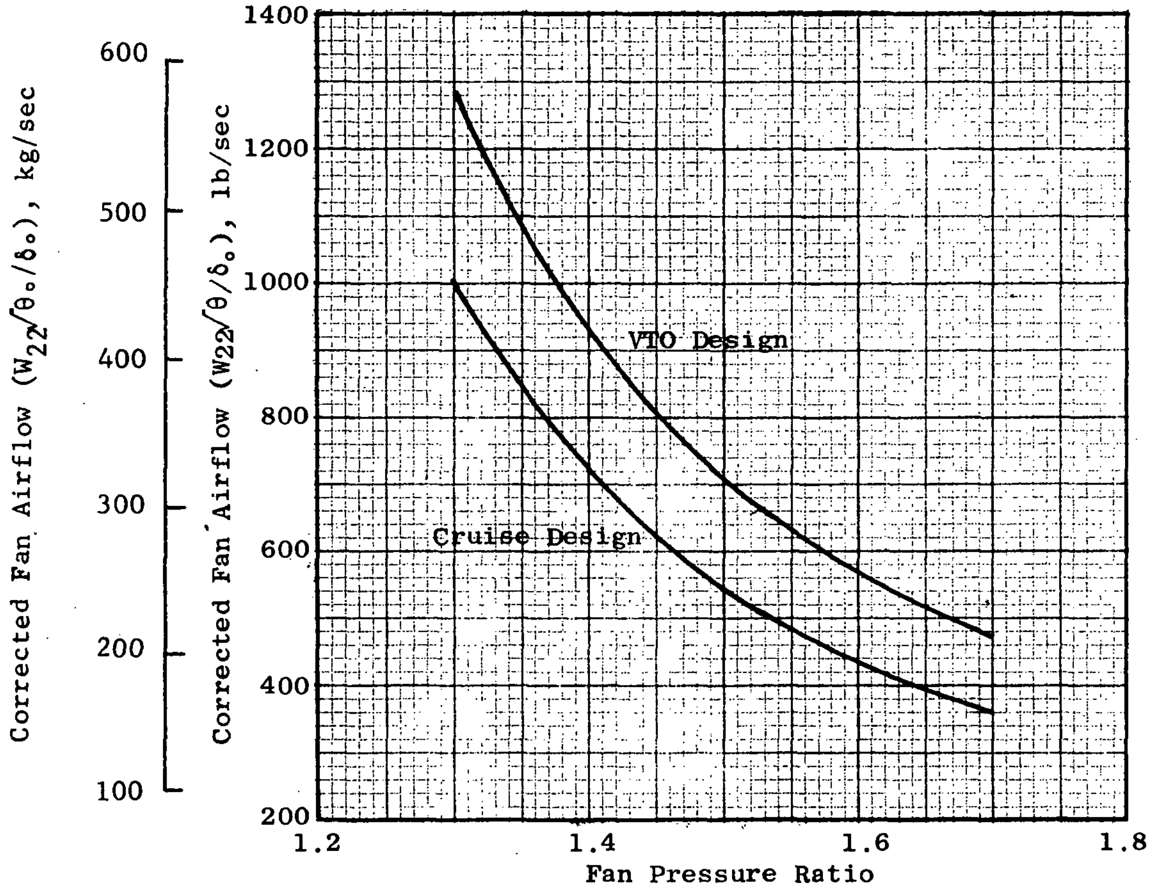

Figure 38 - Two Stage Fan Design Point Airflow

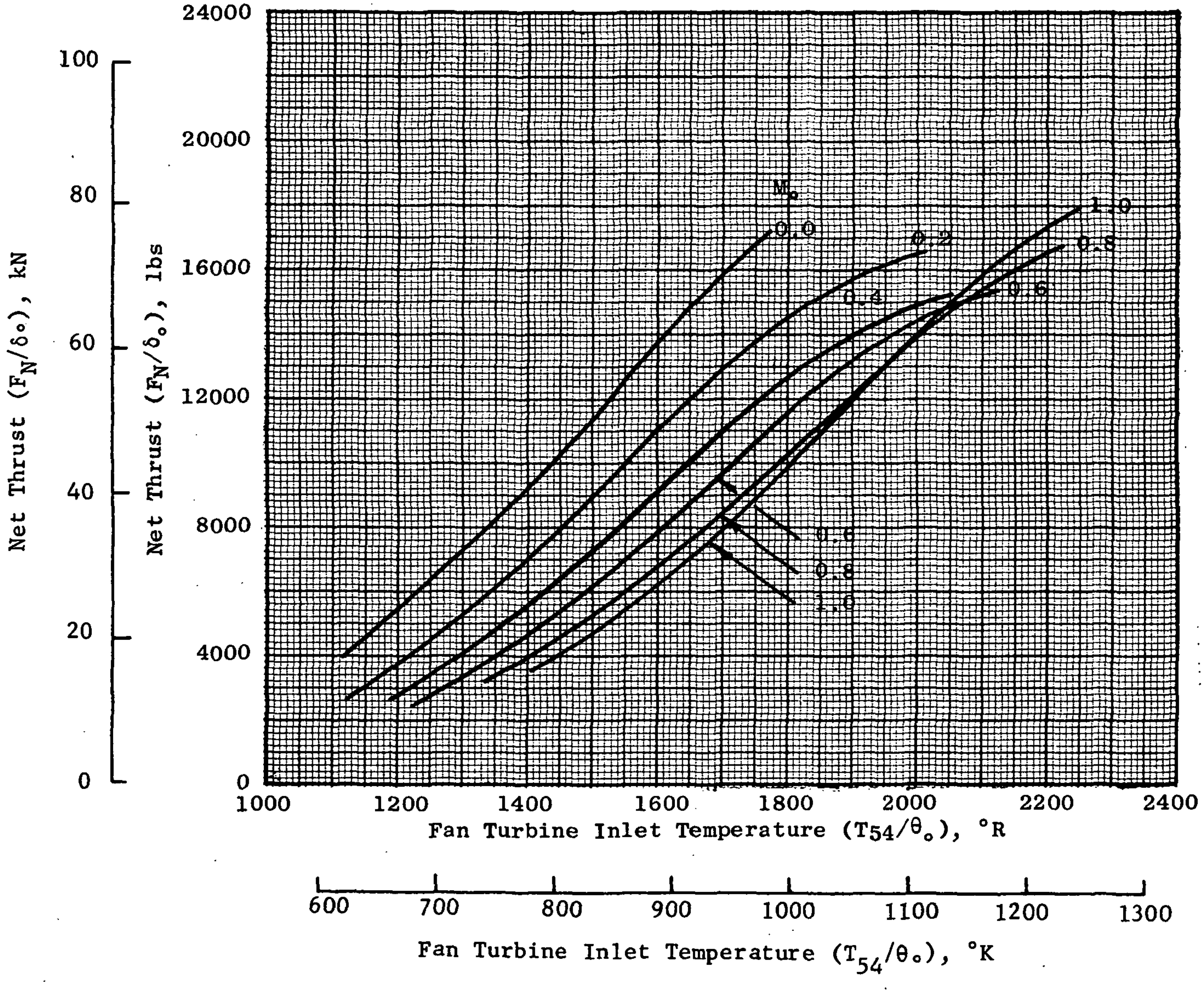

Figure 39 - Fan Net Thrust, Designed for VTO, P/P =1.7

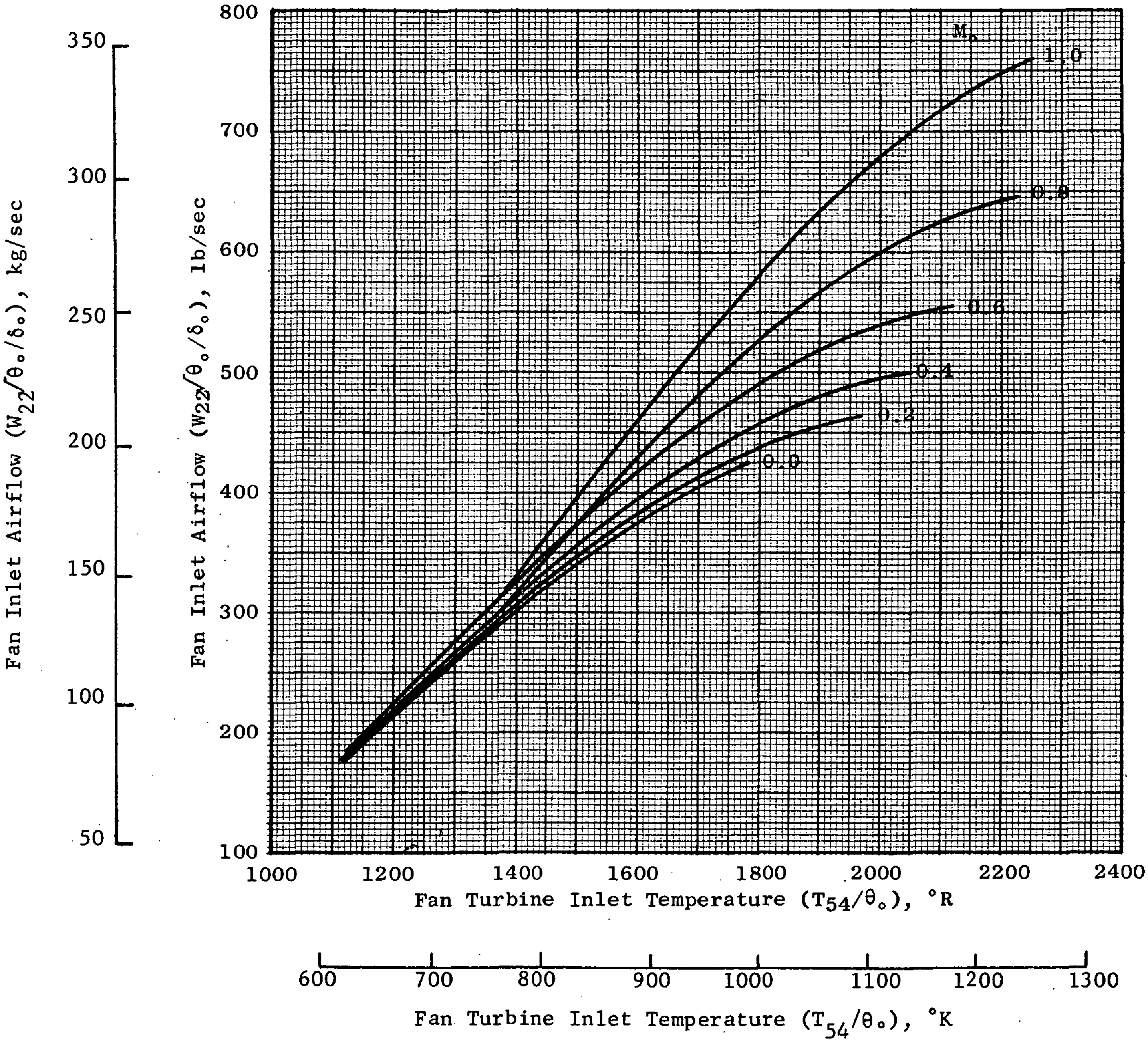

Figure 40 - Fan Inlet Airflow, Designed for VTO, P/P = 1.7

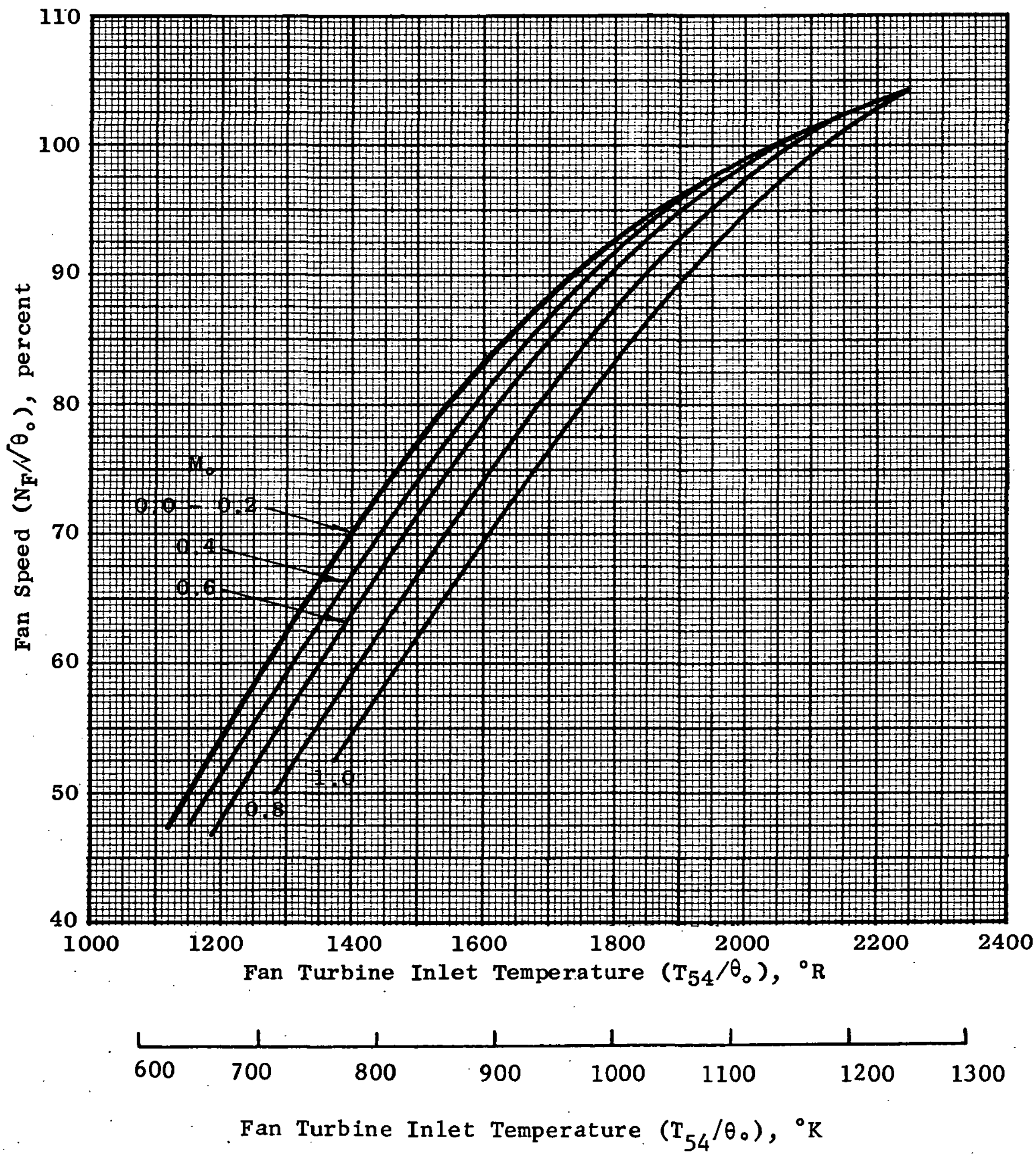

Figure 41 - Fan Speed, Designed for VTO, P/P = 1.7

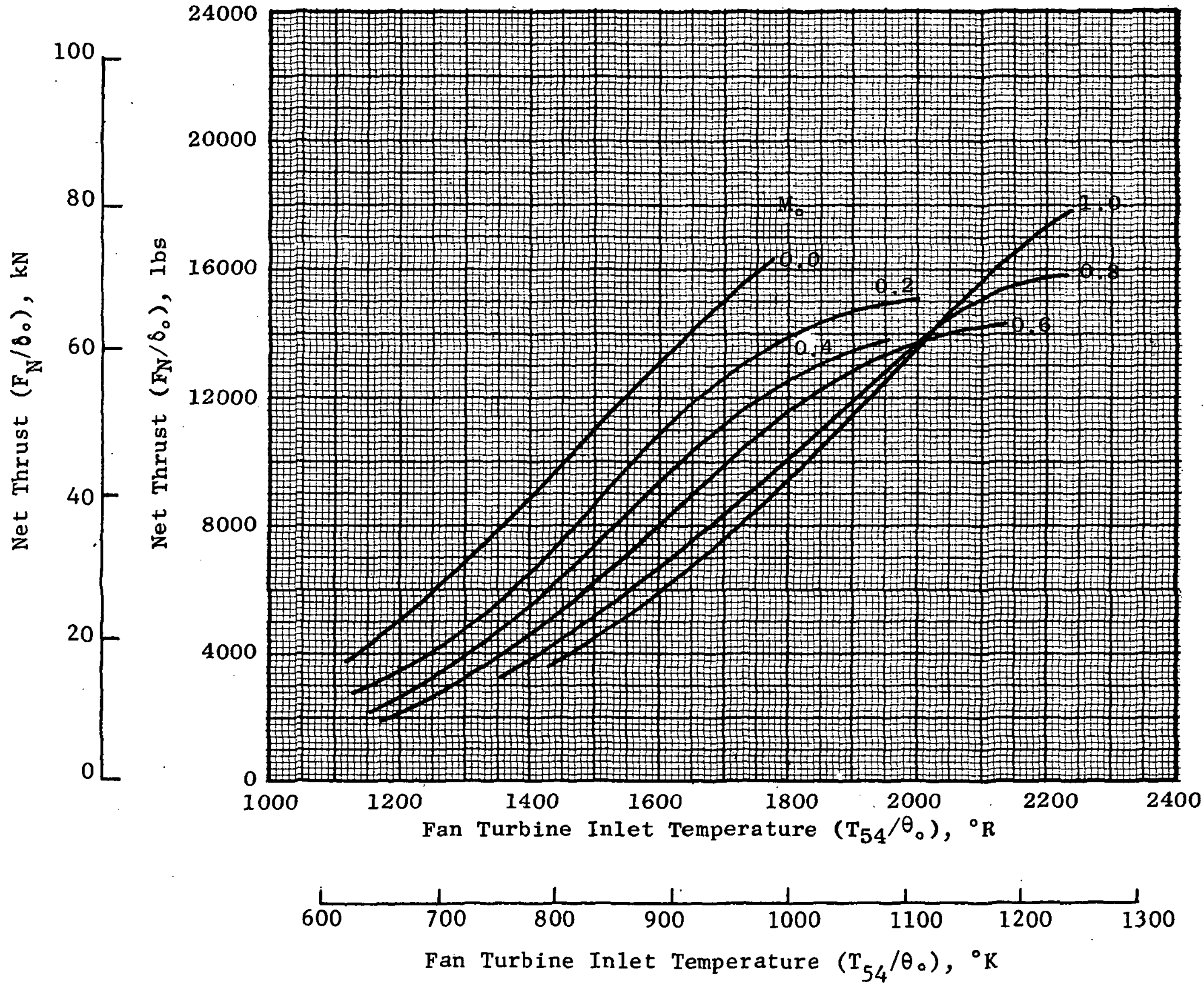

Figure 42 - Fan Net Thrust, Designed for Cruise, P/P = 1.7

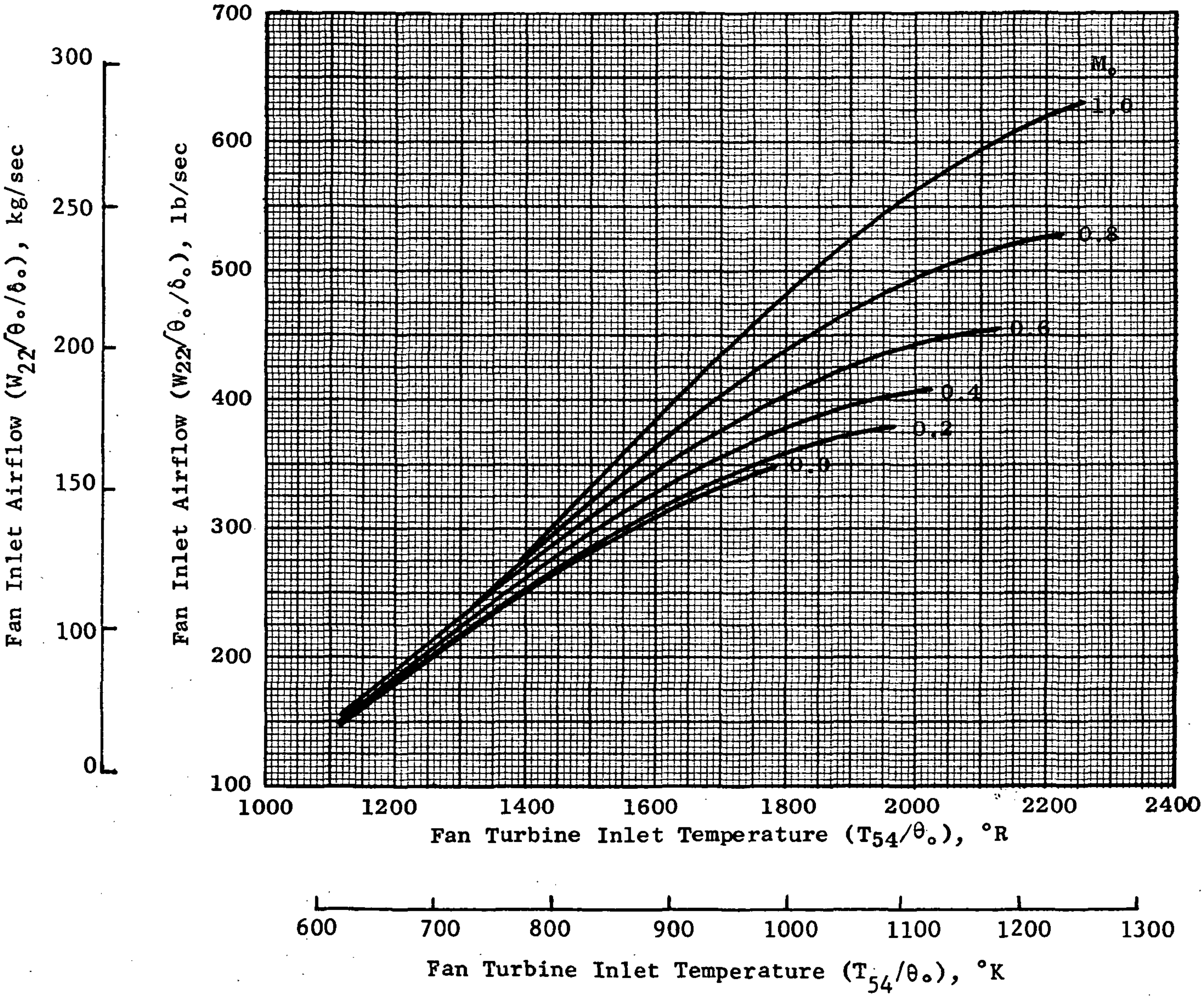

Figure 43 - Fan Inlet Airflow, Designed for Cruise, P/P = 1.7

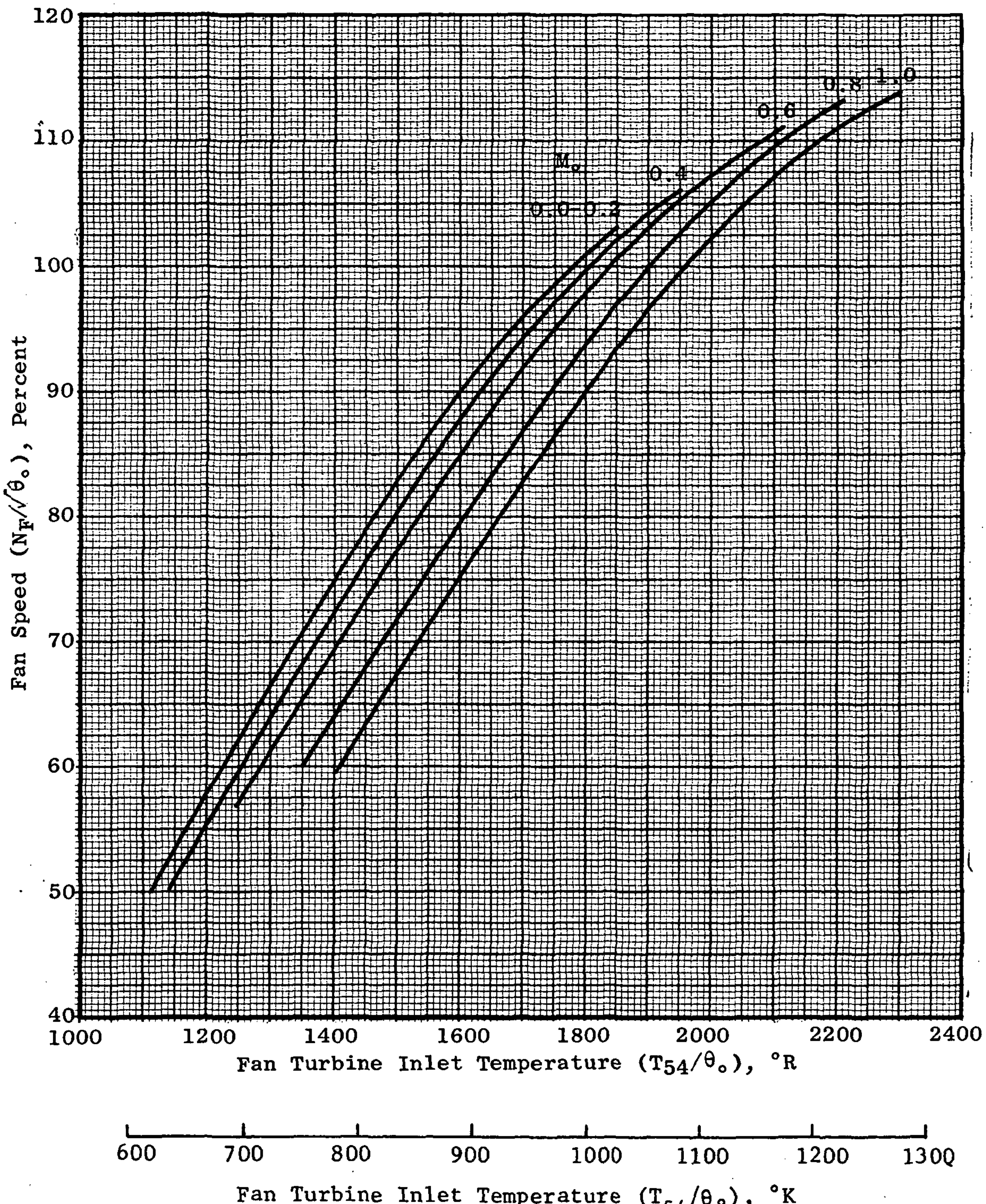

Figure 44 - Fan Speed, Designed for Cruise, P/P = 1.7

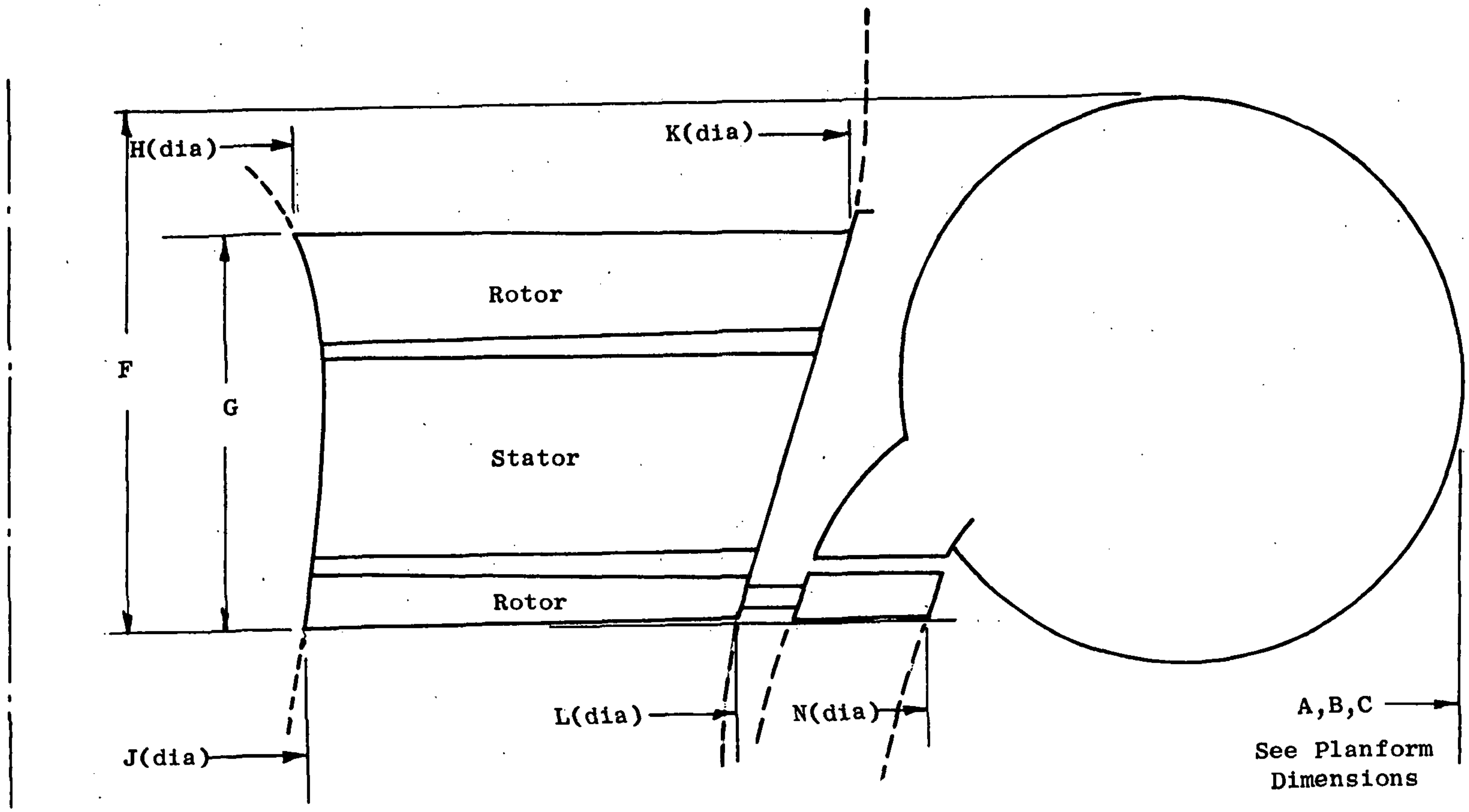

Figure 45 - Two Stage Lift Fan Cross-Section Dimensions

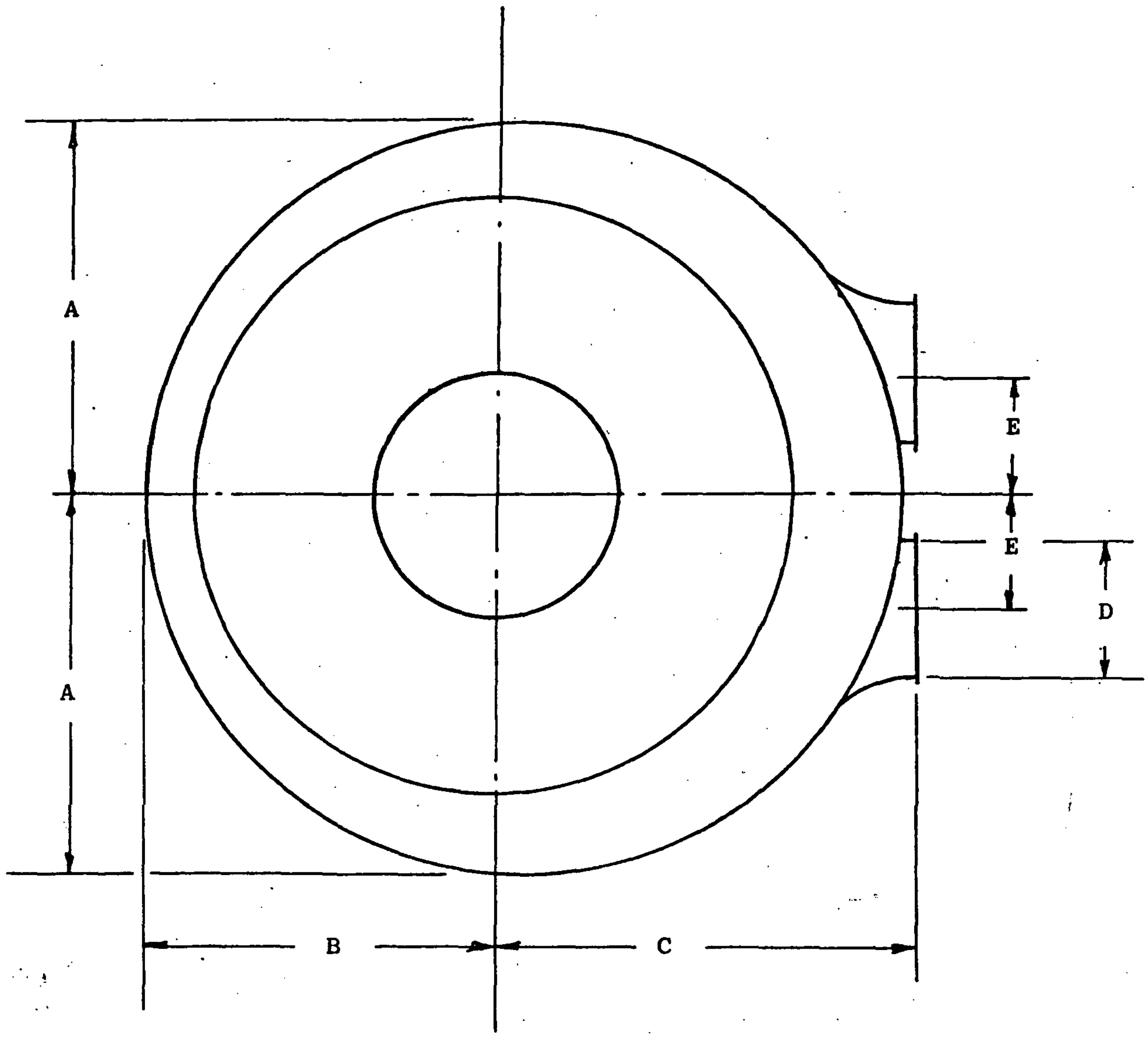

Figure 46-Two Stage Planform Dimensions

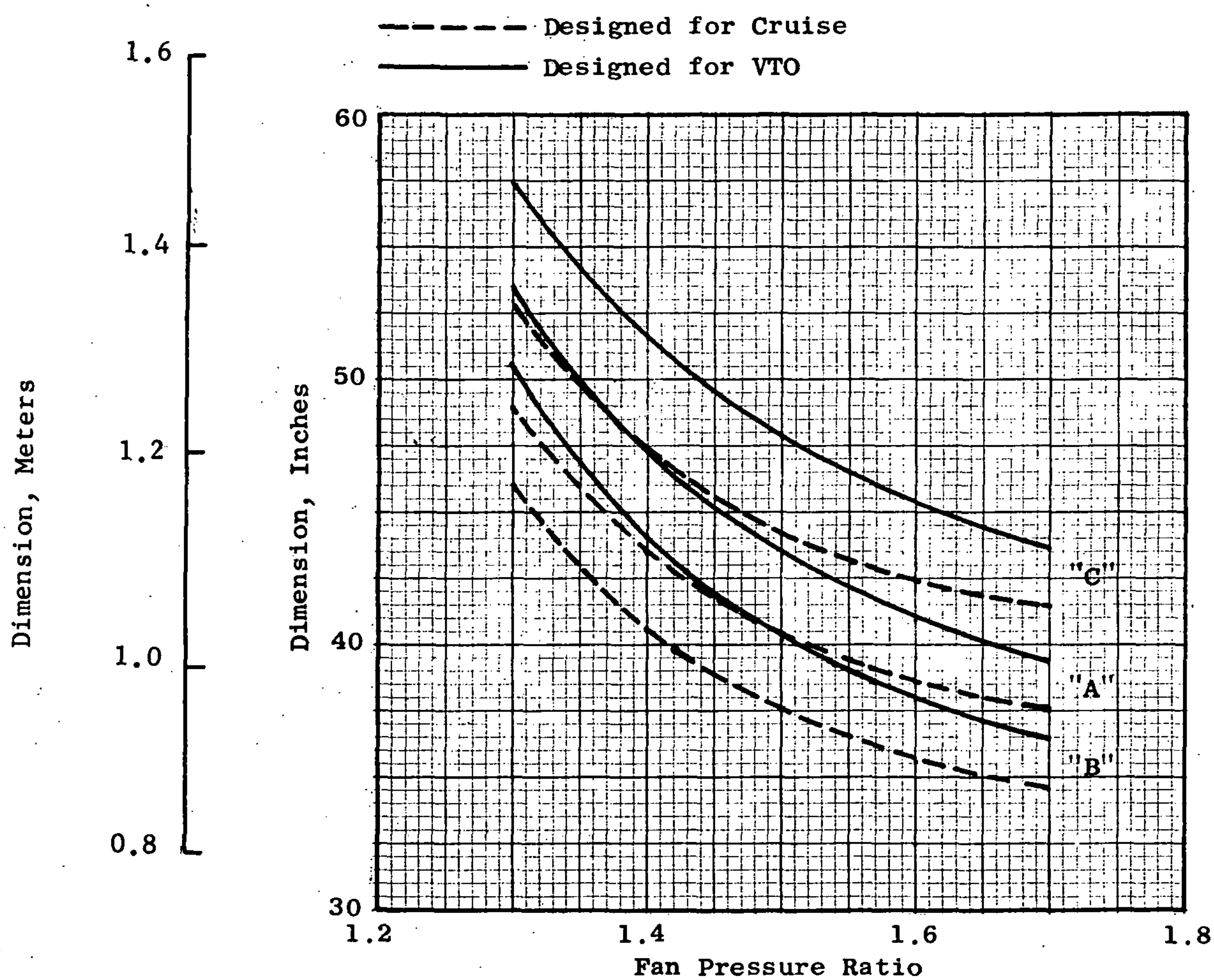

Figure 47 - Two Stage Fan Installation Dimensions "A", "B" and "C"

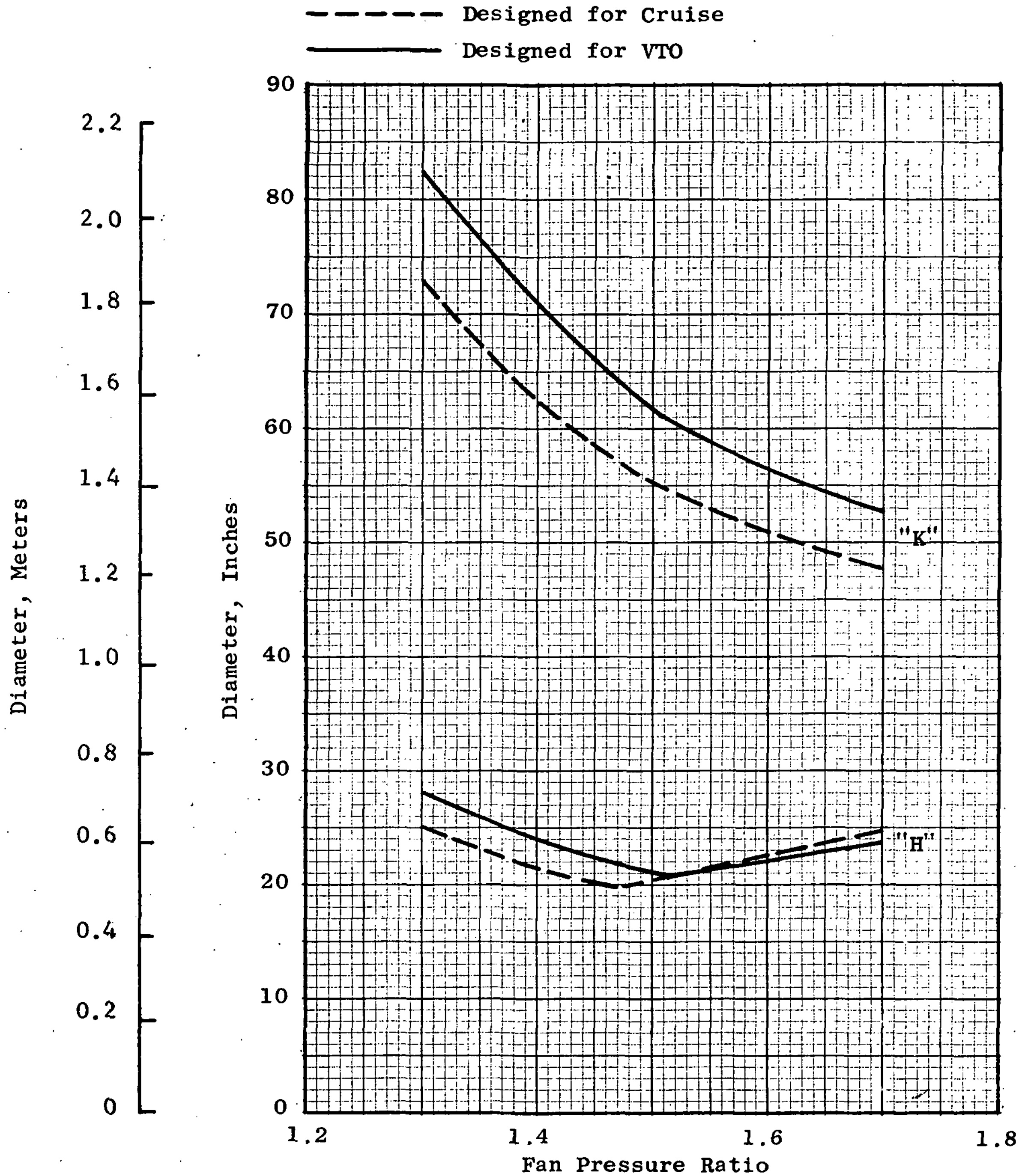

Figure 48 - Two Stage Fan Installation Dimensions "H" and "K"

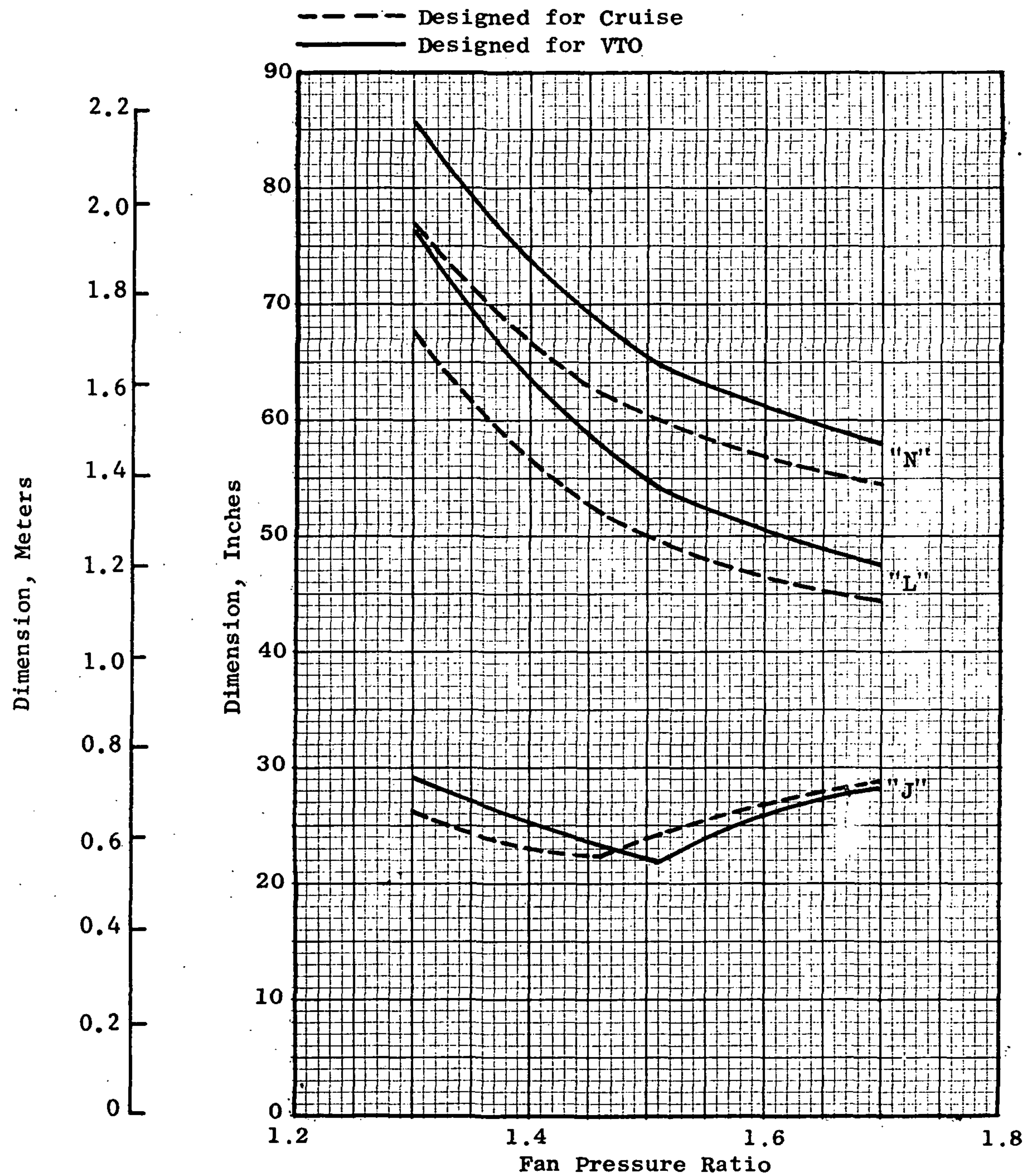

Figure 49 - Two Stage Fan Installation Dimensions "J", "L" and "N"

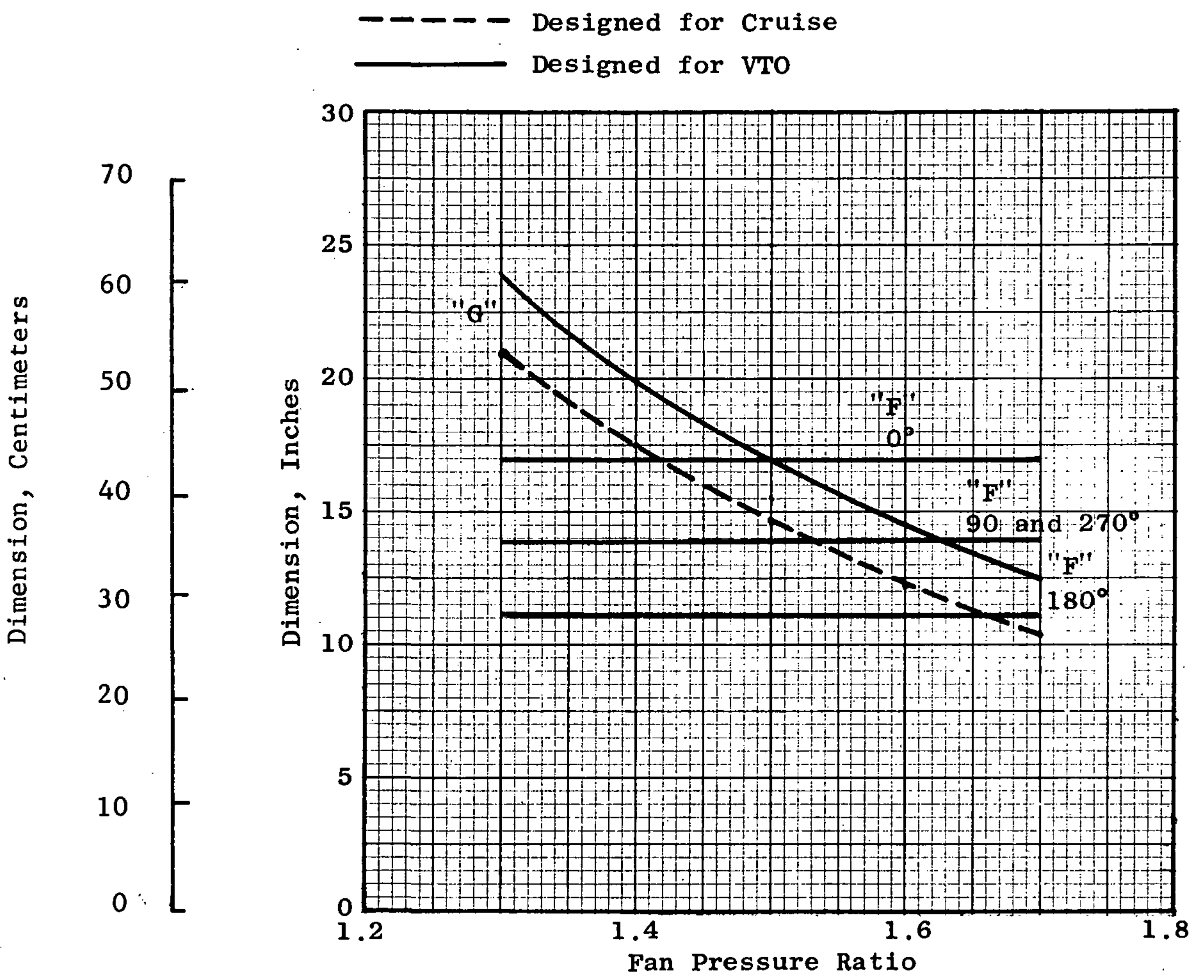

Figure 50 - Two Stage Installation Dimensions "F" and "G"

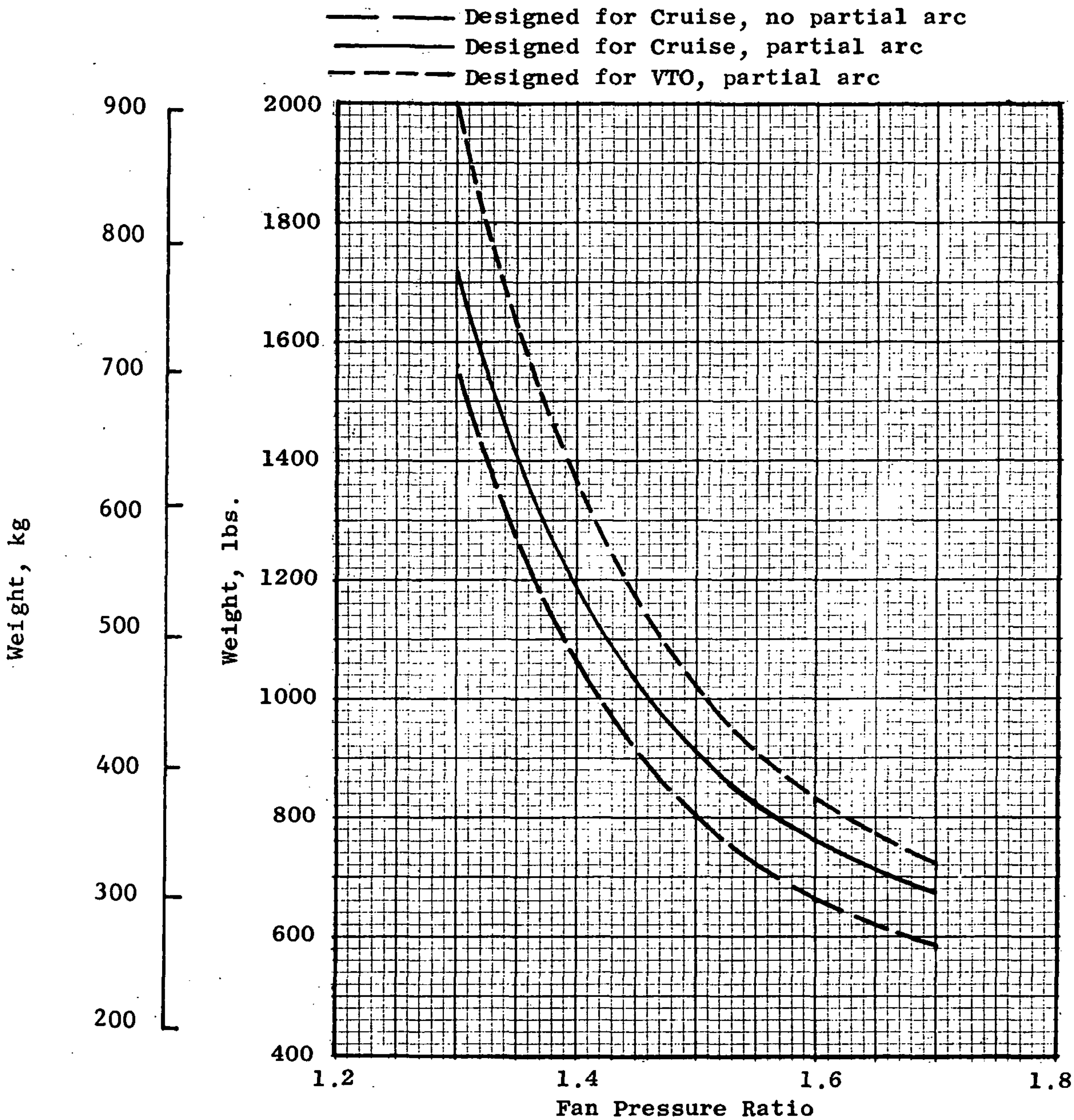

Figure 51 - Two Stage Fan Weights

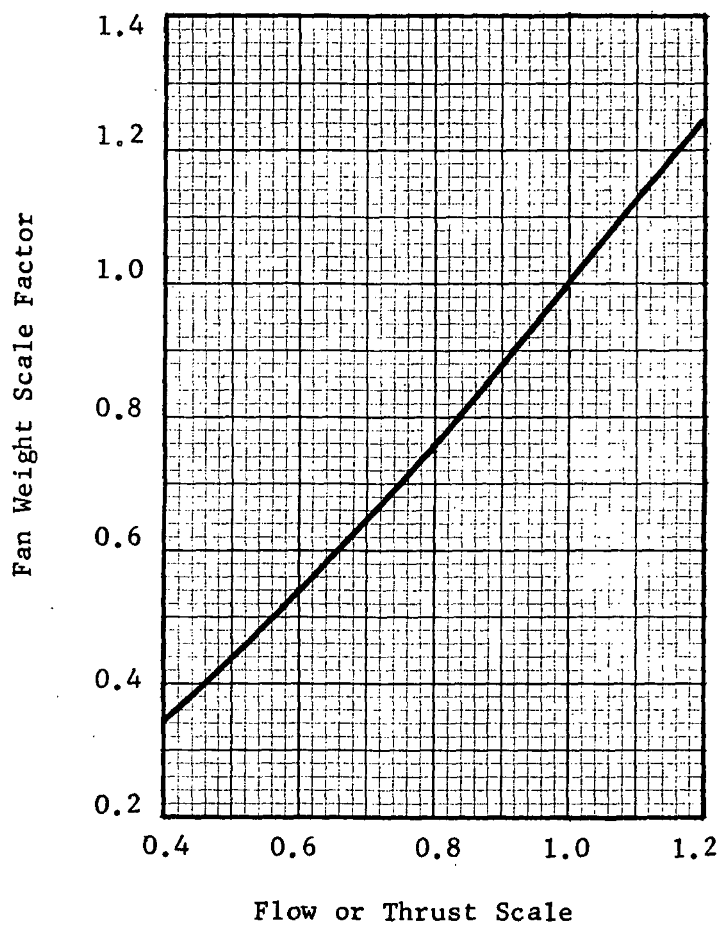

Figure 52 - Two Stage Fan Weight Scaling Factors

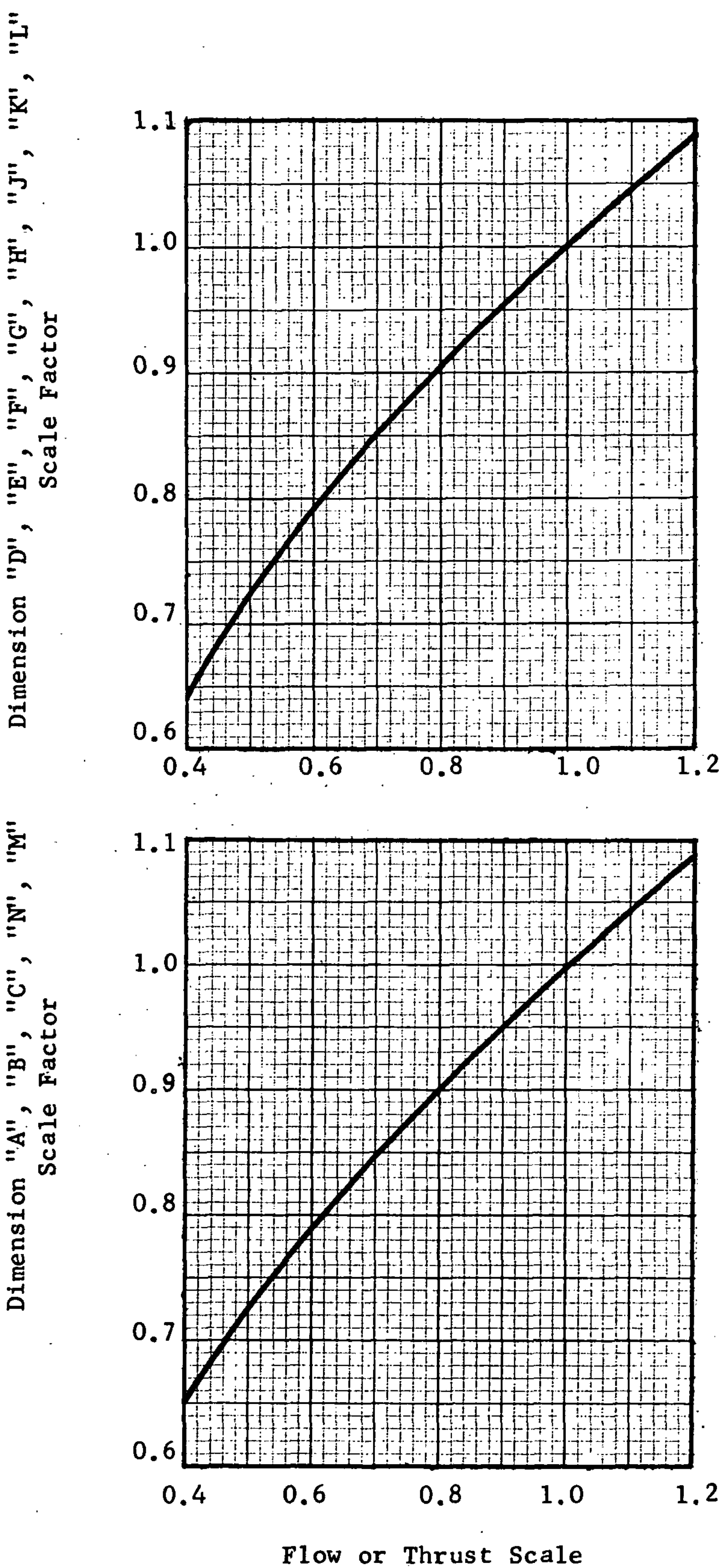

Figure 53 - Two Stage Dimension Scale Factors for Change in Fan Thrust Size

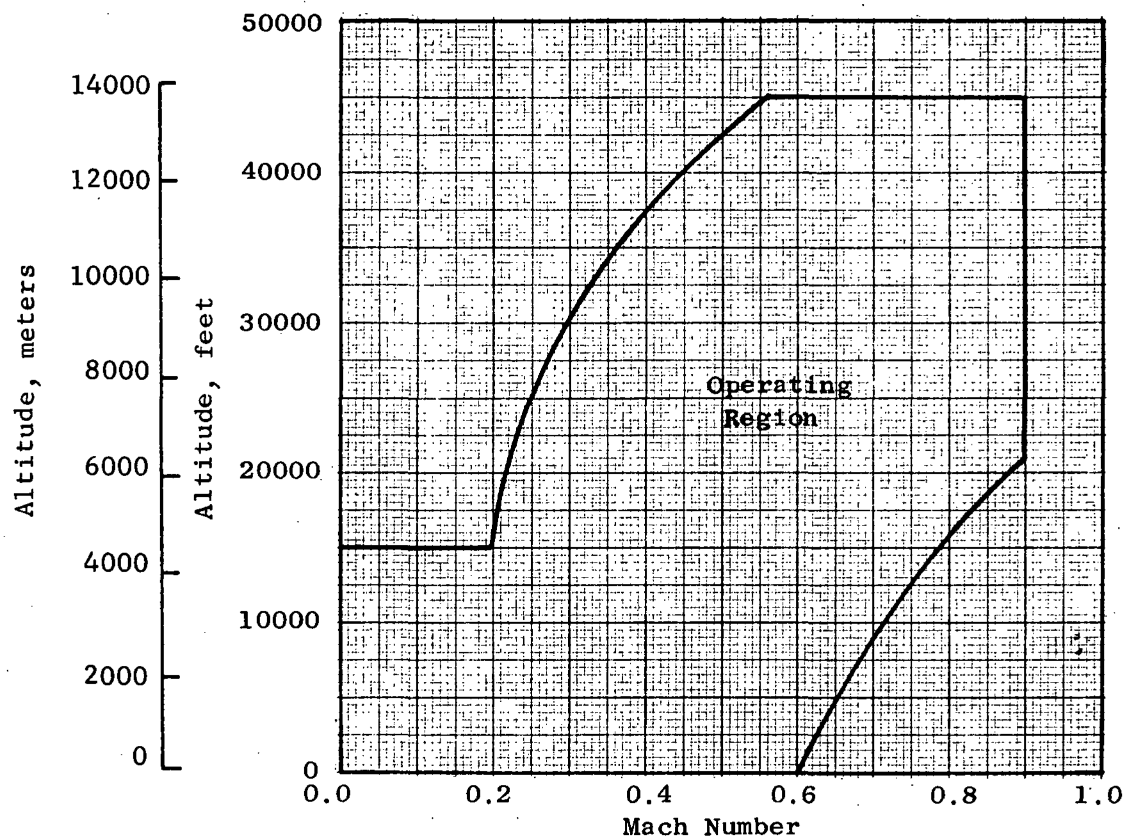

Figure 54 - Altitude - Speed Operating Envelope

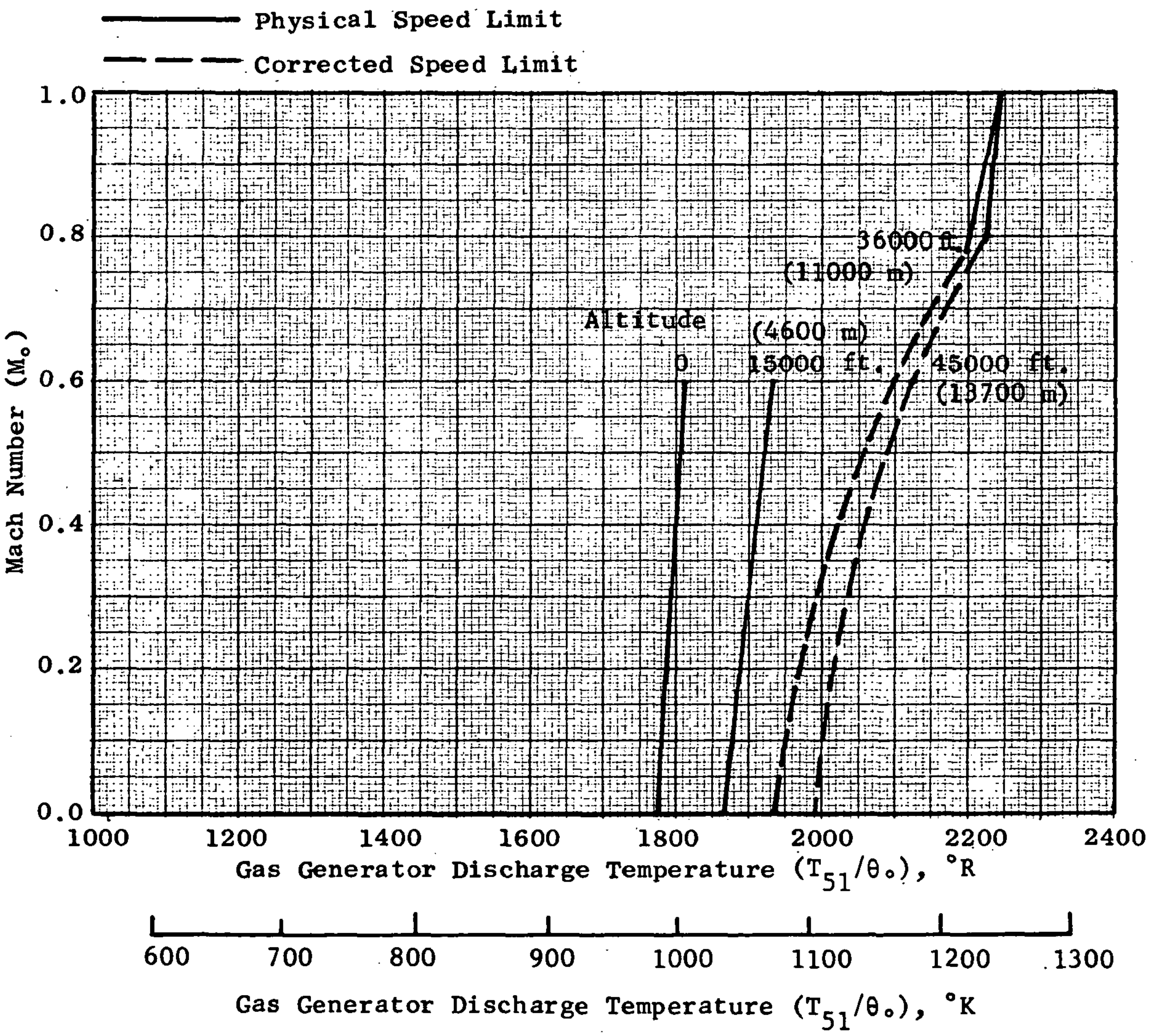

Figure 55 - Gas Generator Speed Operating Limits

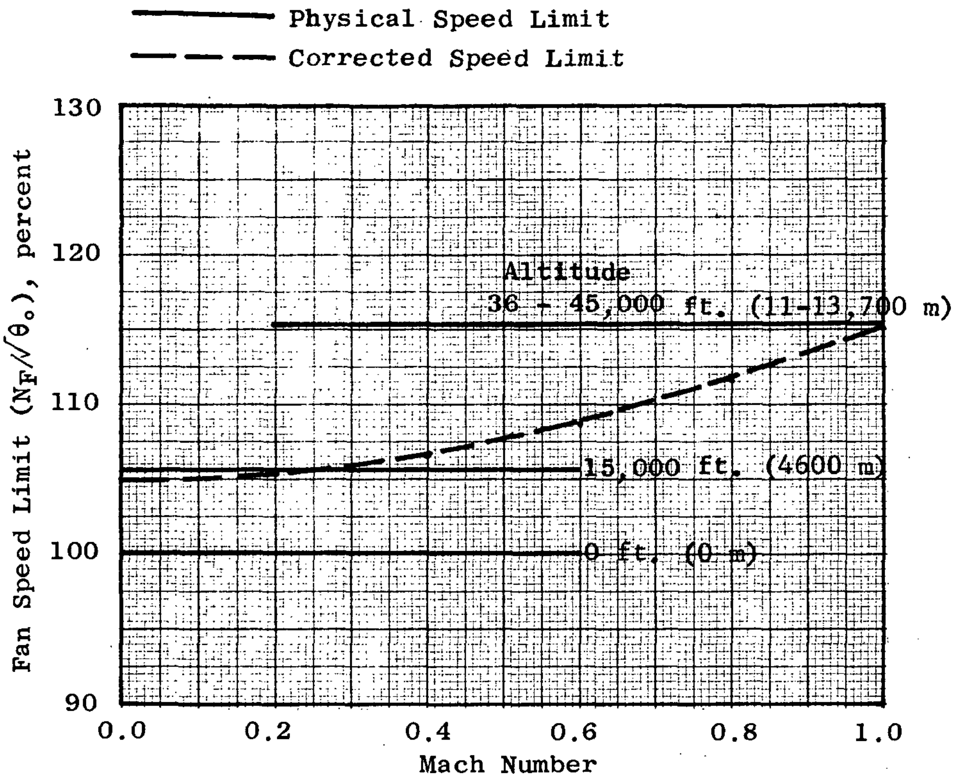

Figure 56 - Fan Speed Operating Limits

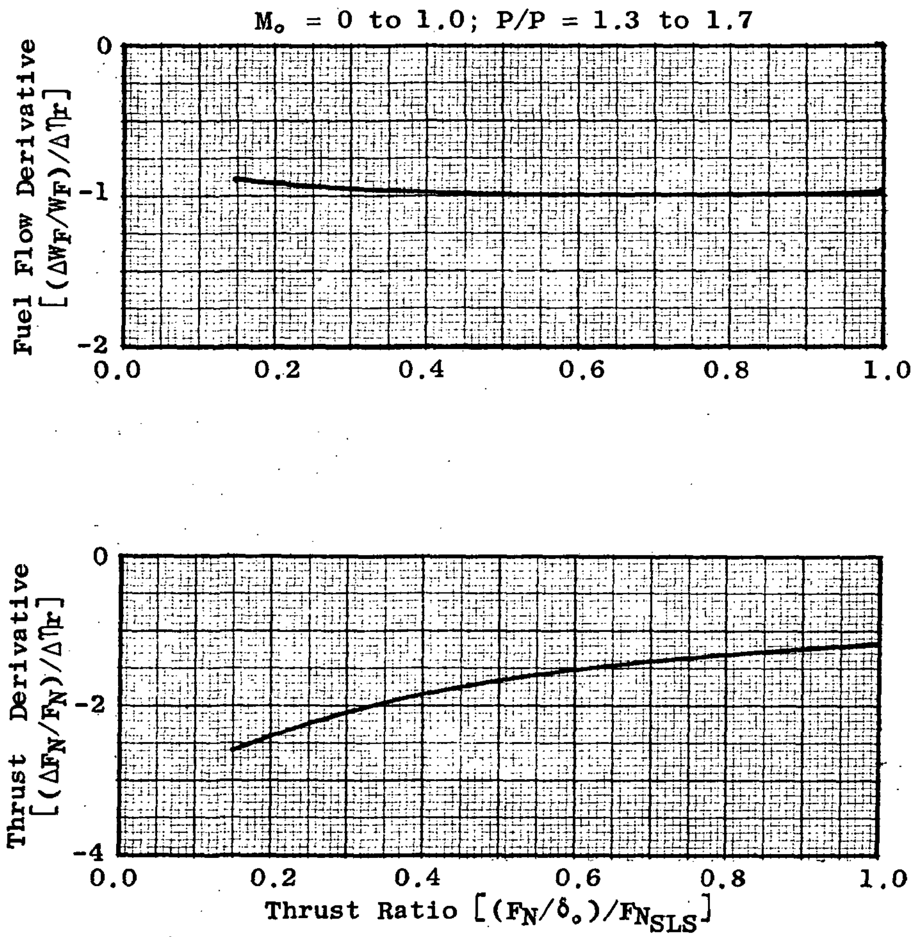

Figure 57 - Engine Inlet Recovery Derivative for Fans Designed for Cruise and VTO

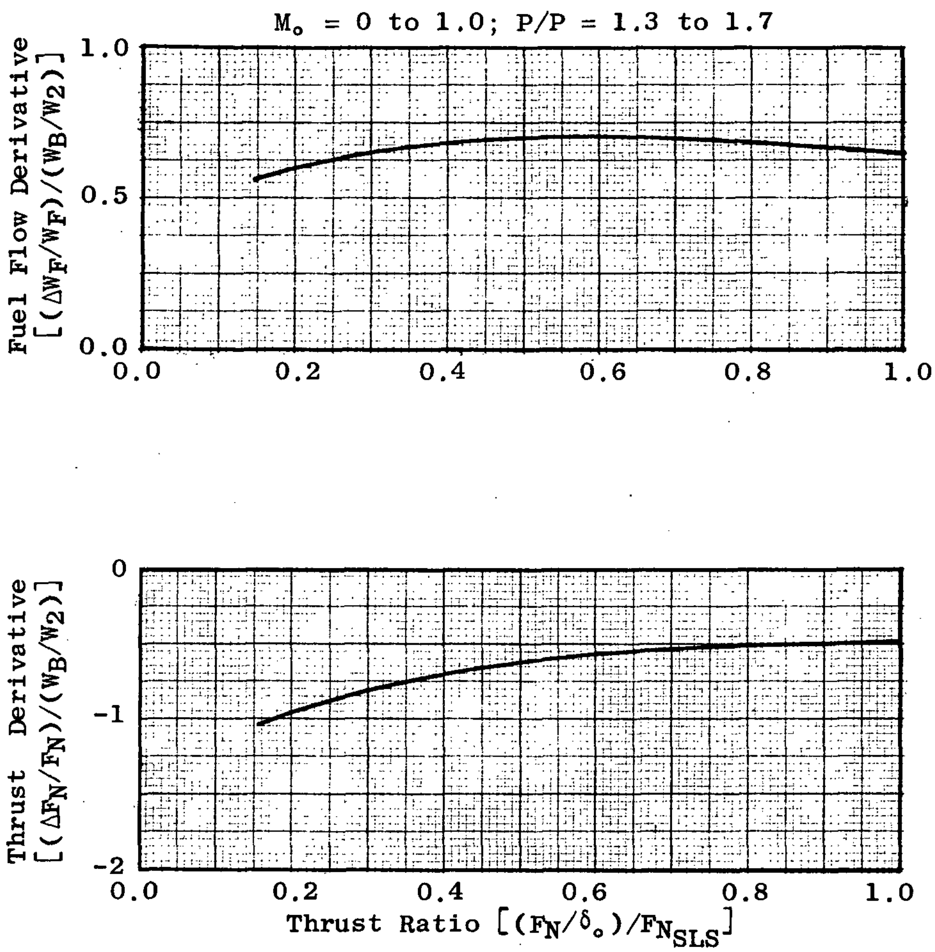

Figure 58 - Customer Bleed Derivative for Fans Designed for Cruise and VTO

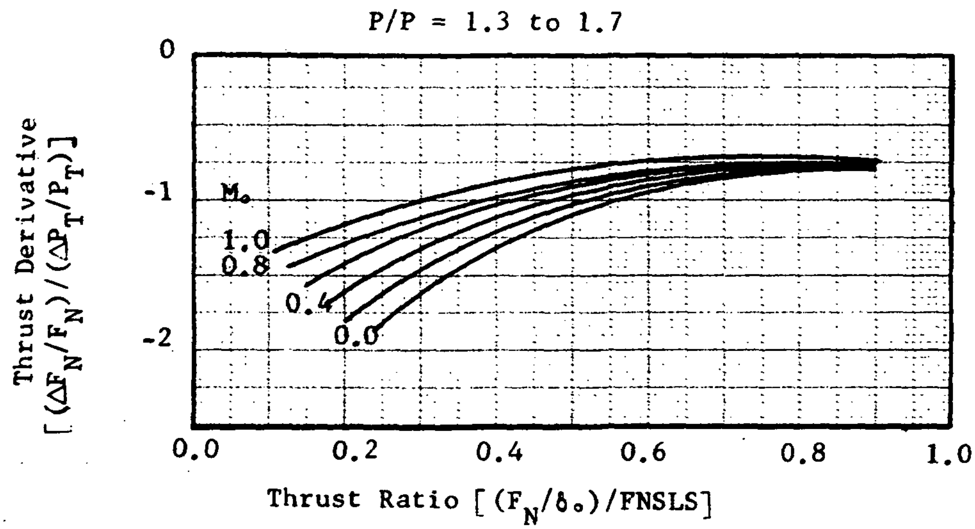

Figure 59 - Duct Pressure Loss Derivative for Fans Designed for Cruise and VTO

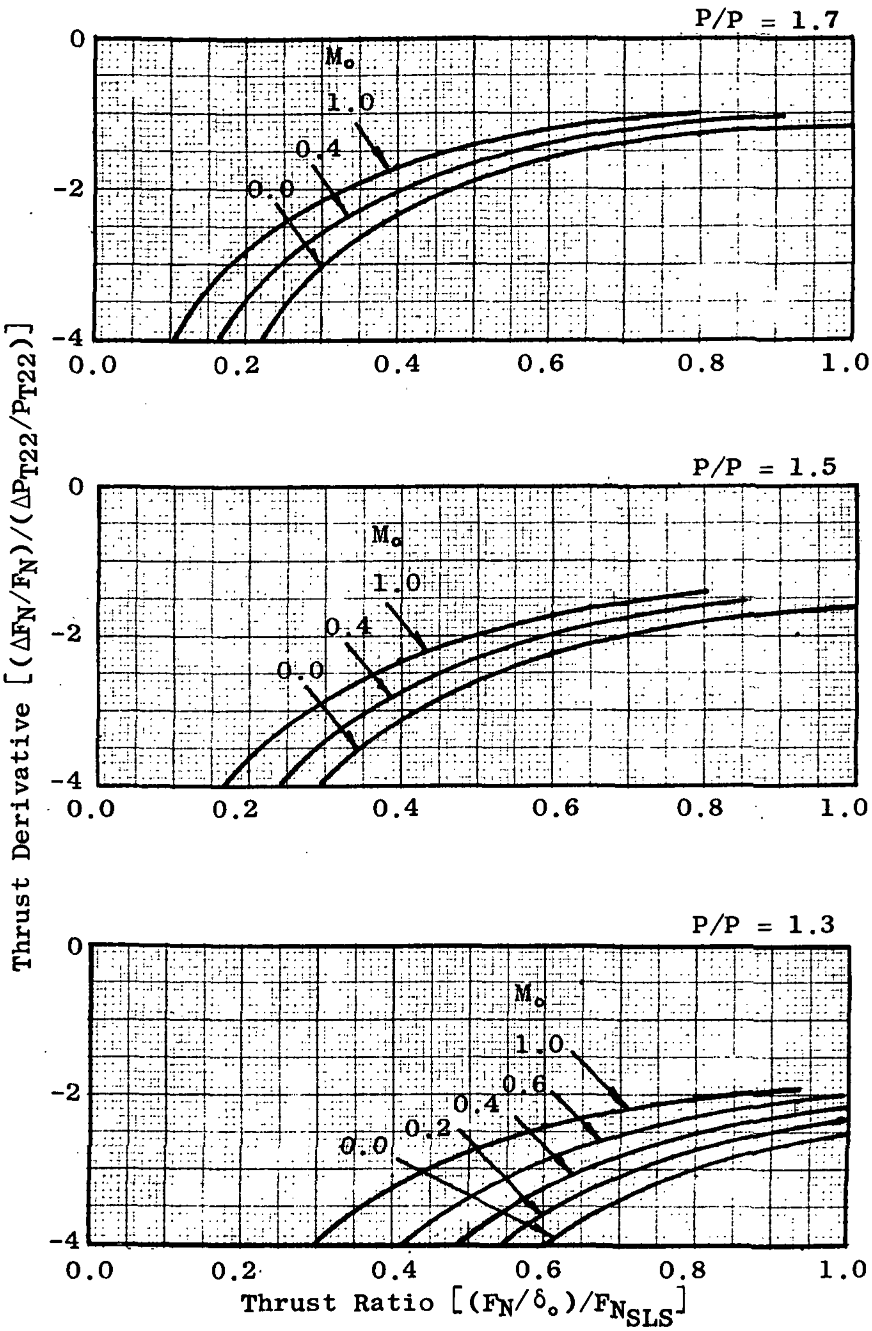

Figure 60 - Fan Inlet Loss Derivative for Fans Designed for VTO

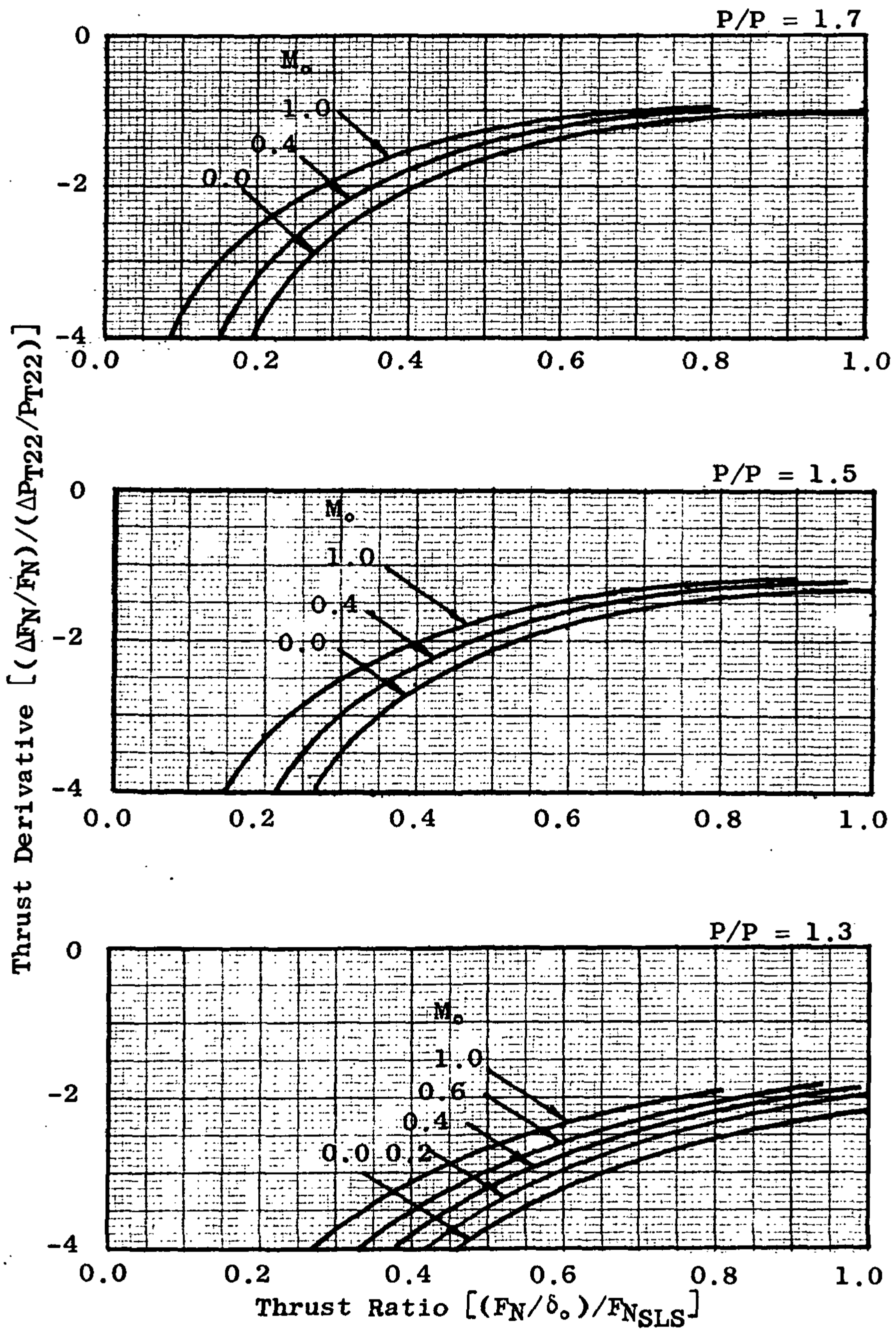

Figure 61 - Fan Inlet Loss Derivative for Fans Designed for Cruise

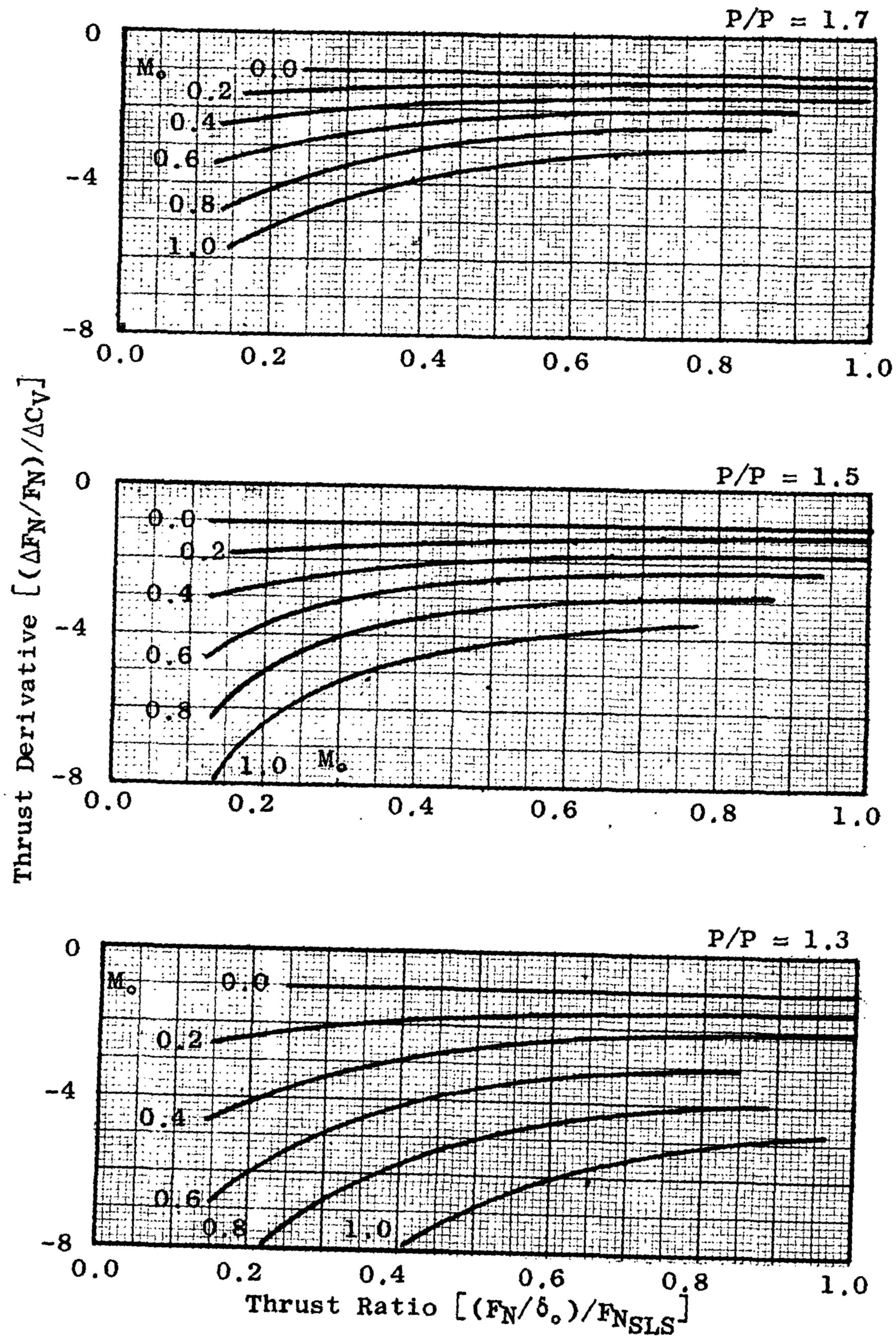

Figure 62 - Nozzle Velocity Coefficient Derivative for Fans Designed for VTO

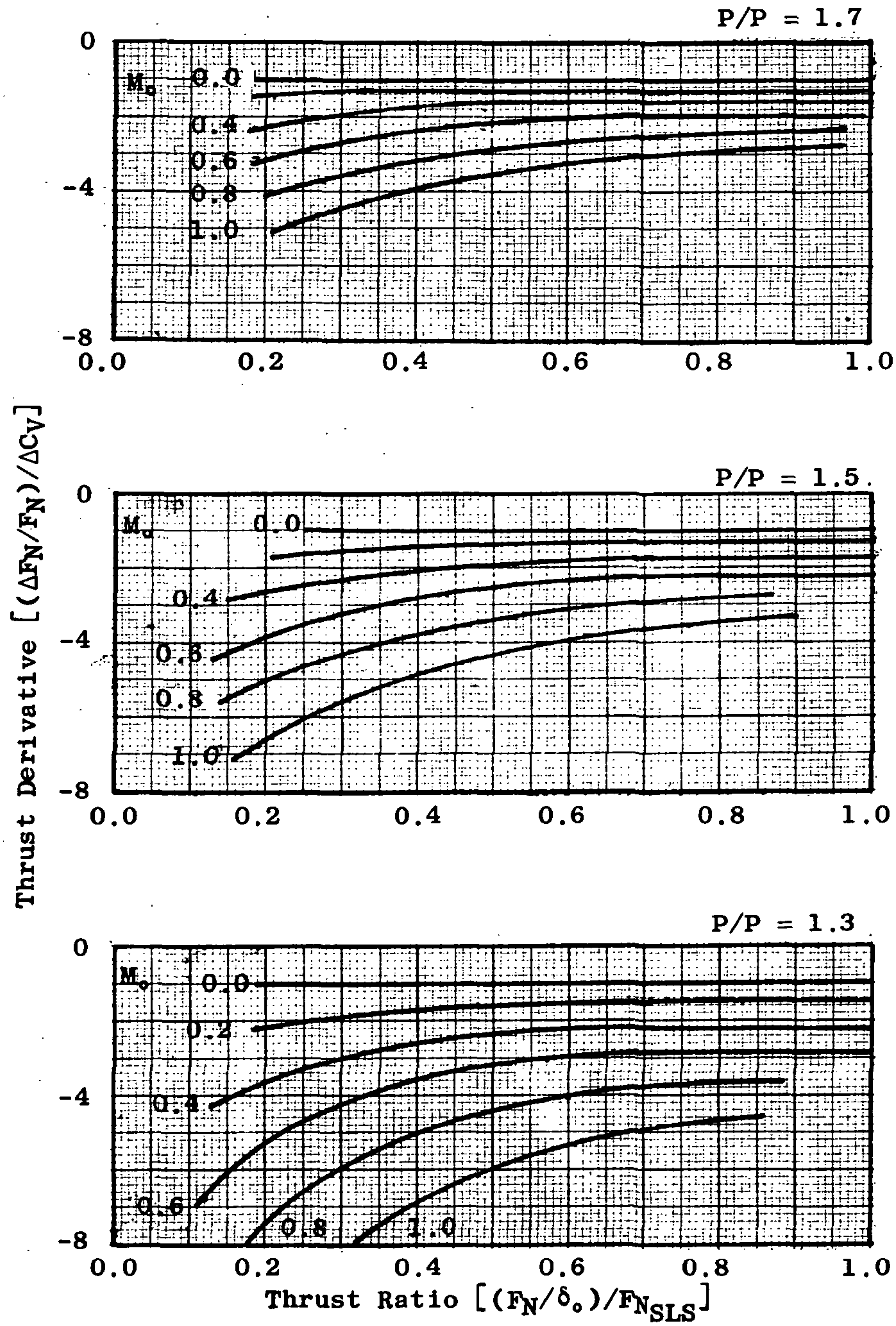

Figure 63 - Nozzle Velocity Coefficient Derivative for Fans Designed for Cruise

S = Nominal Rated (Standard Day)

1 = Nominal Rated (Hot Day)

2 = Nominal Maximum Control (Hot Day)

3 = Emergency Rated (Hot Day)

4 = Emergency Maximum Control (Hot Day)

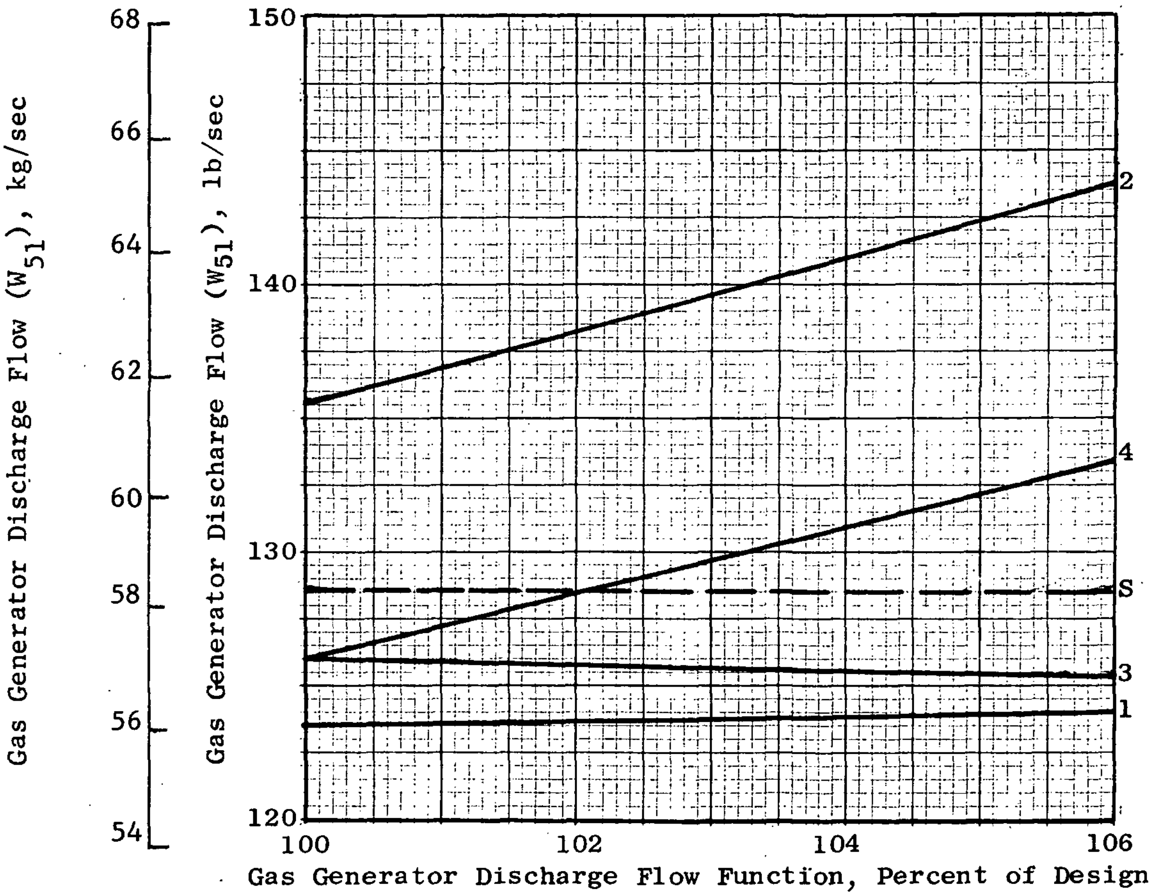

Figure 64 - Gas Generator Discharge Flow for Control Analysis

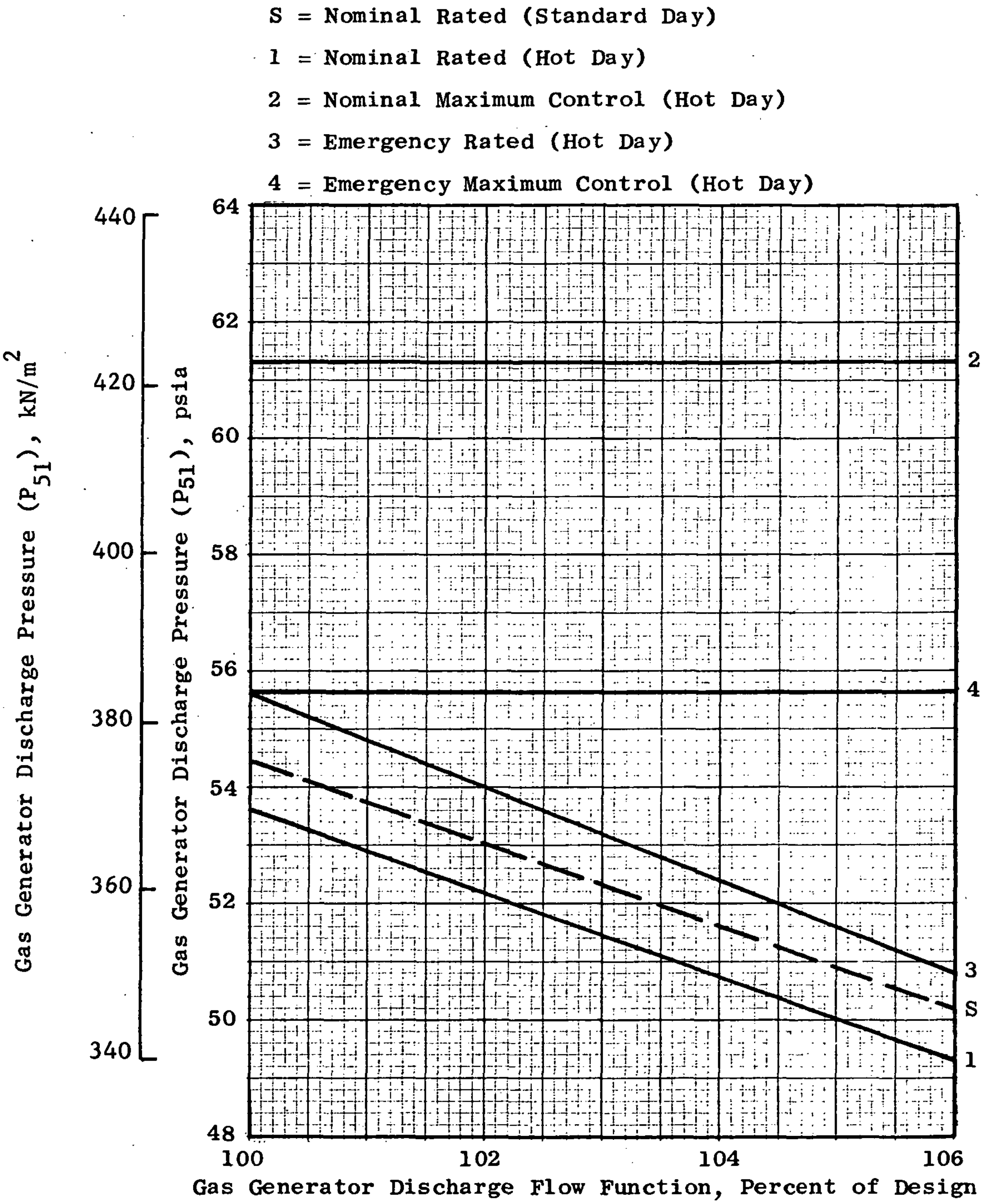

Figure 65 - Gas Generator Discharge Pressure for Control Analysis

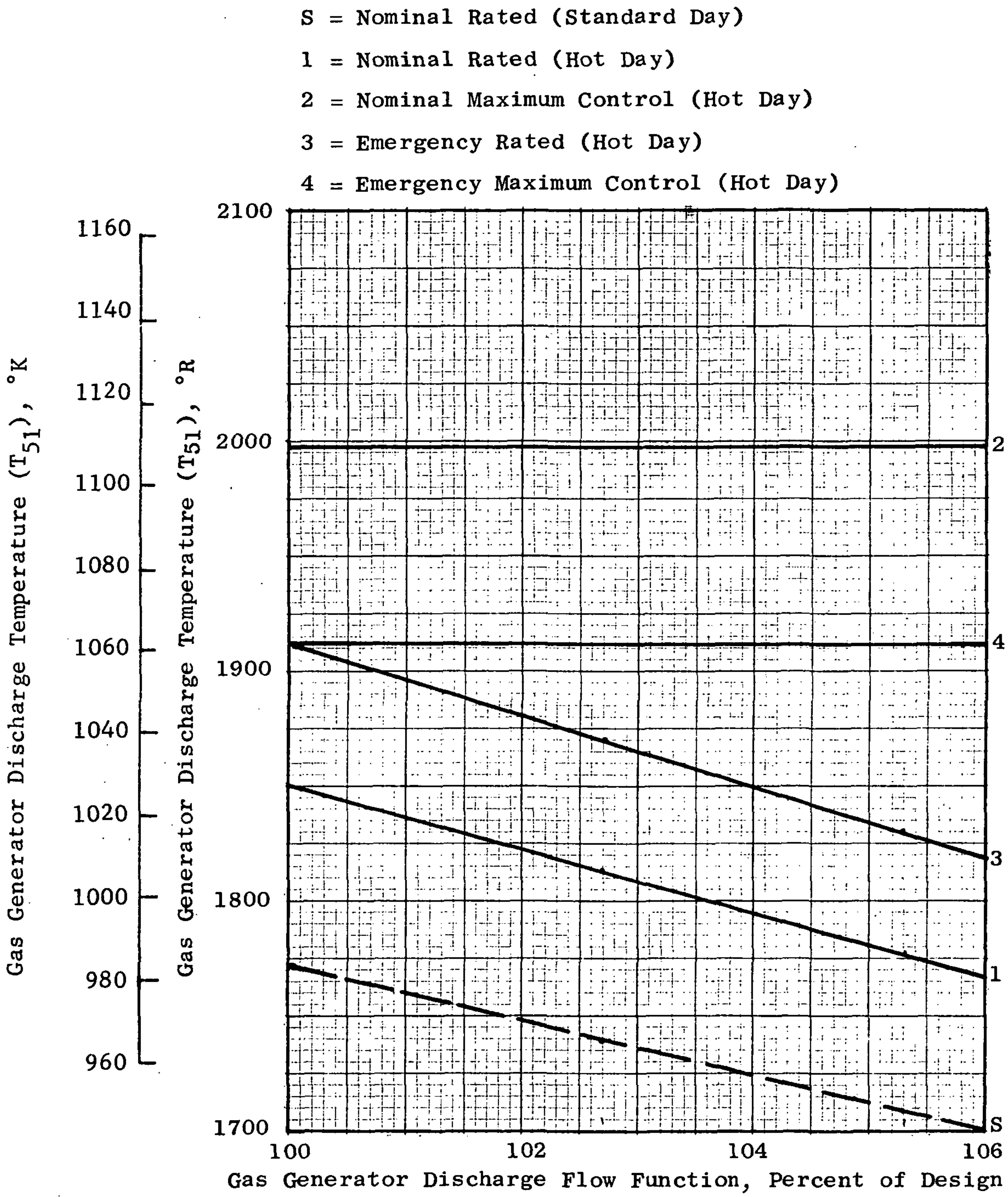

Figure 66 - Gas Generator Discharge Temperature for Control Analysis

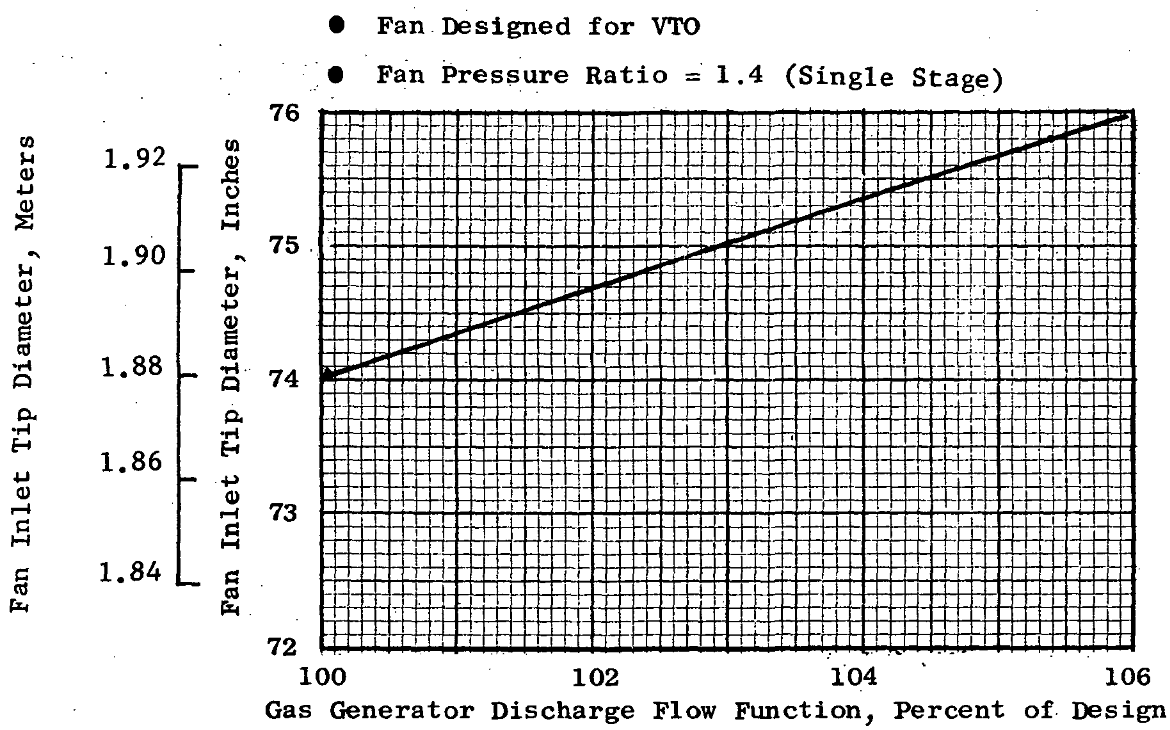

Figure 67 - Effects of Gas Generator Operating Point on Fan Sizing

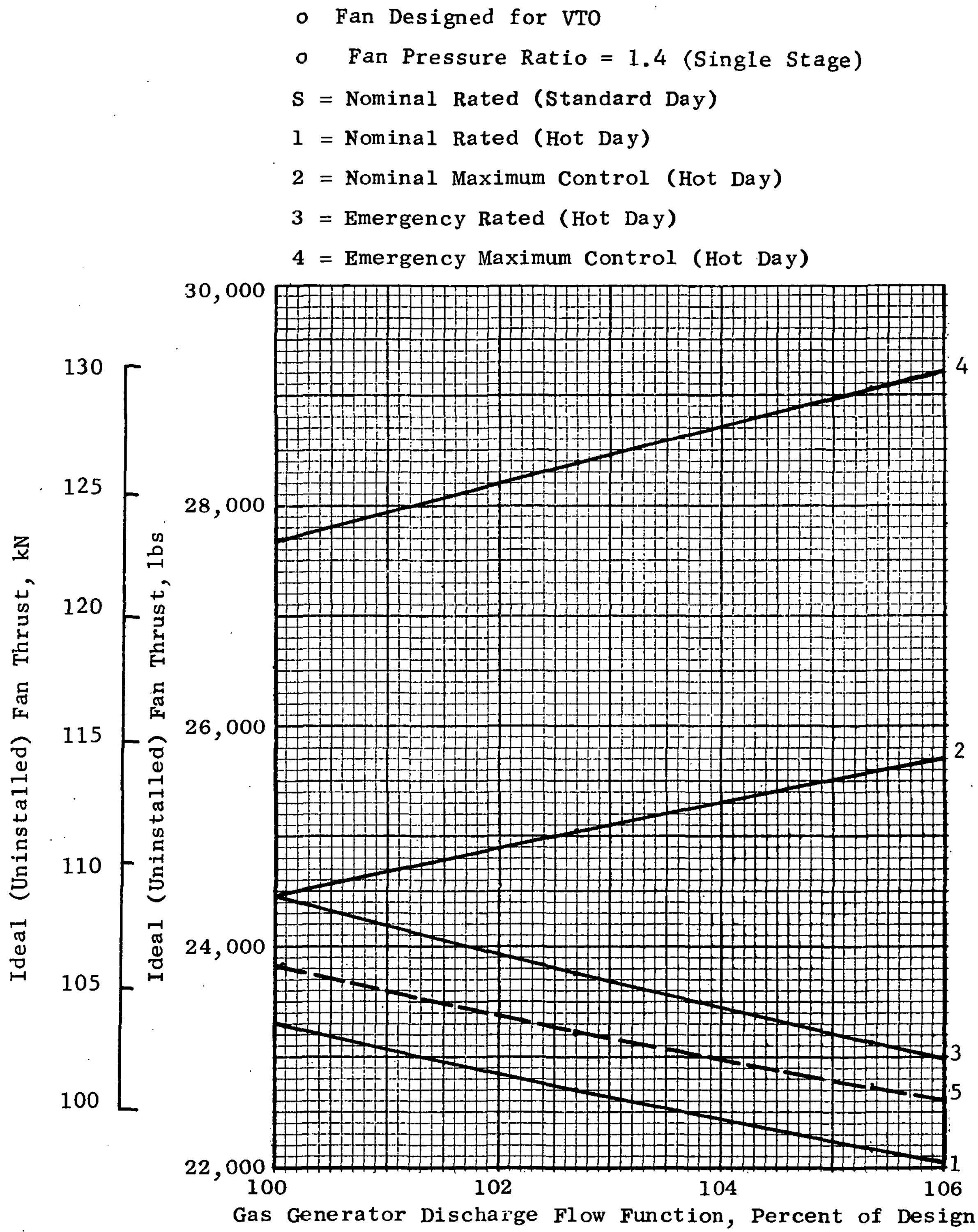

Figure 68 - Effects of Gas Generator Operating Point on Fan Lift and Control Margins

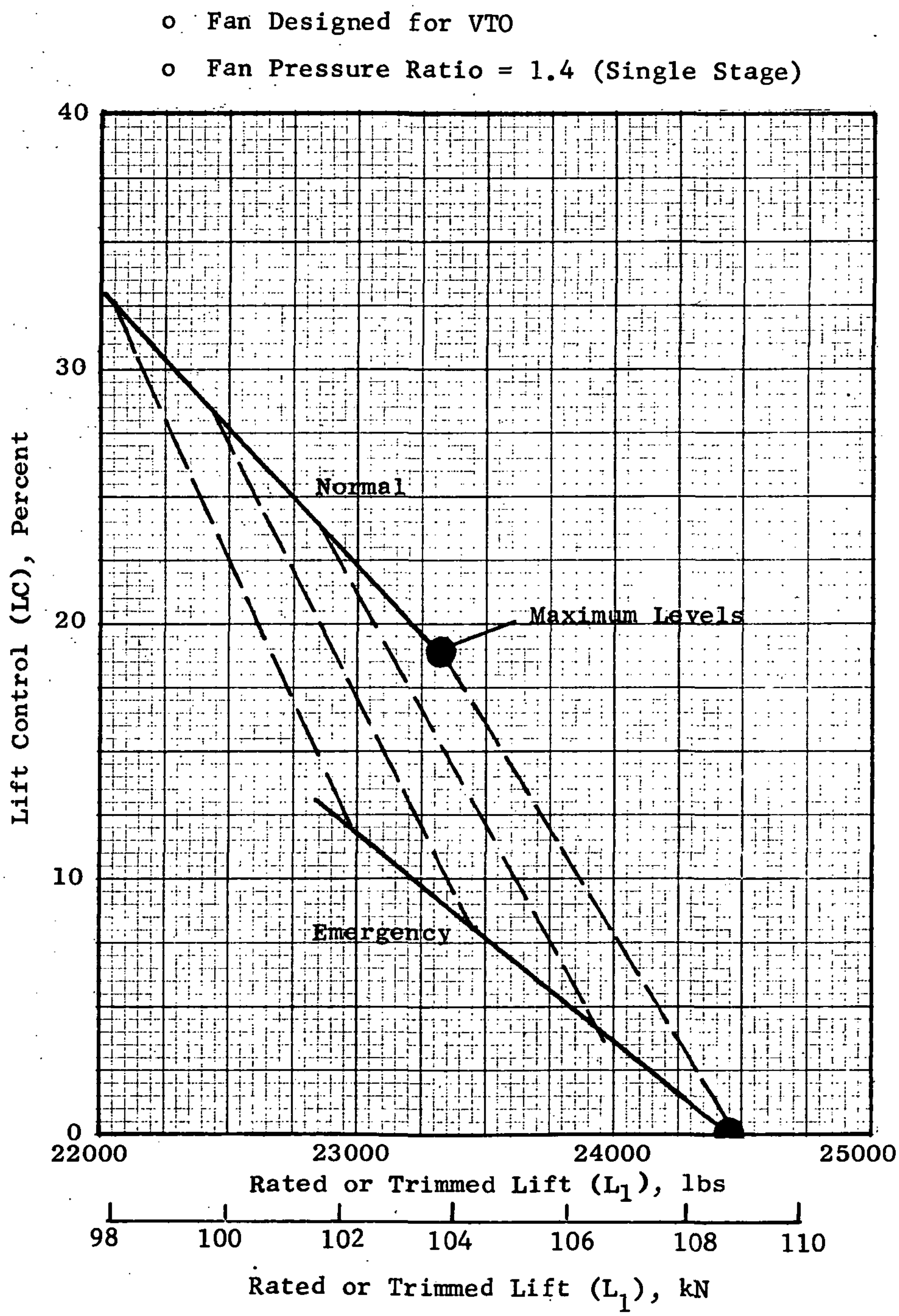

Figure 69 - Lift Control Capability for a Range of Rated Lift Levels

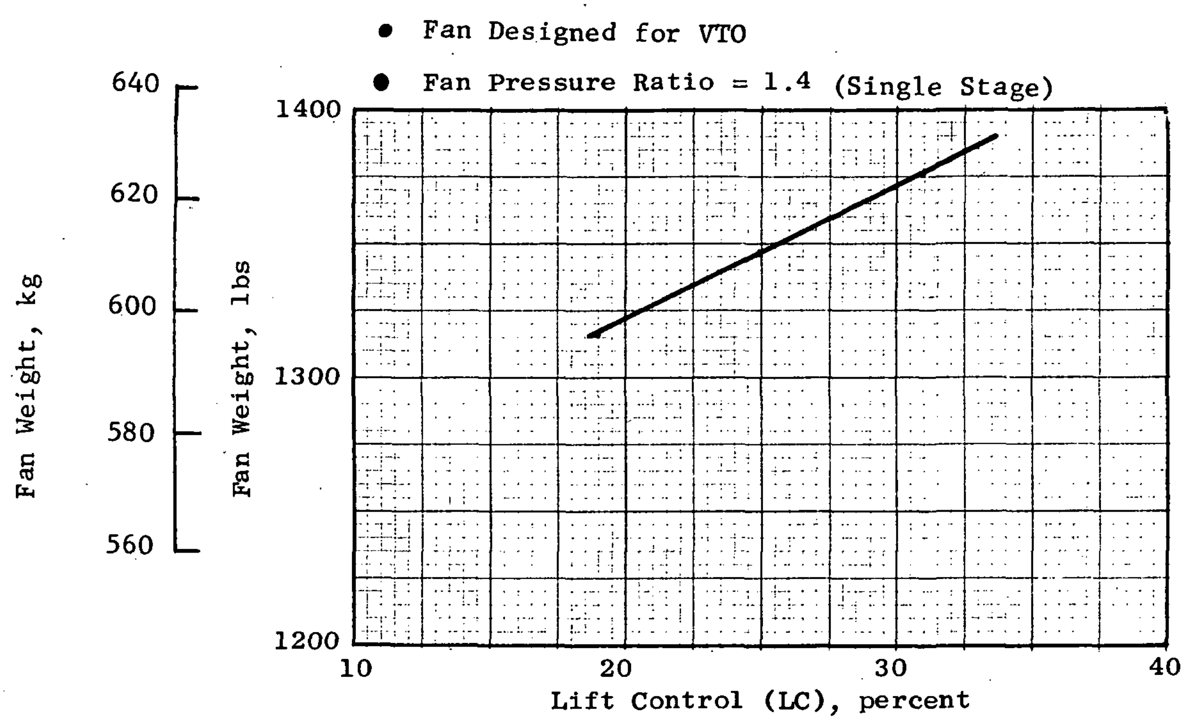

Figure 70 - Effects of Lift Control Margins on Fan Weight

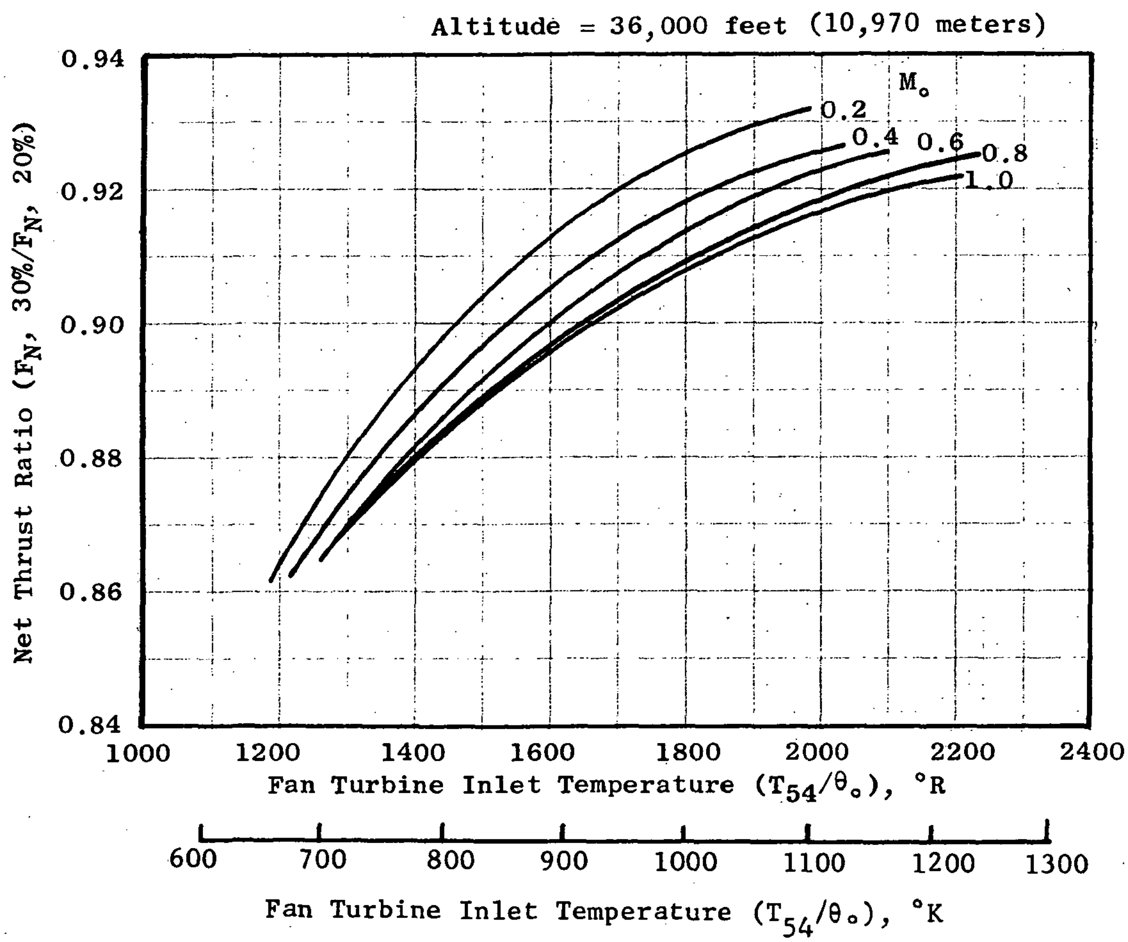

Figure 71 - Effects of Control Margin on Fan Net Thrust, P/P = 1.4

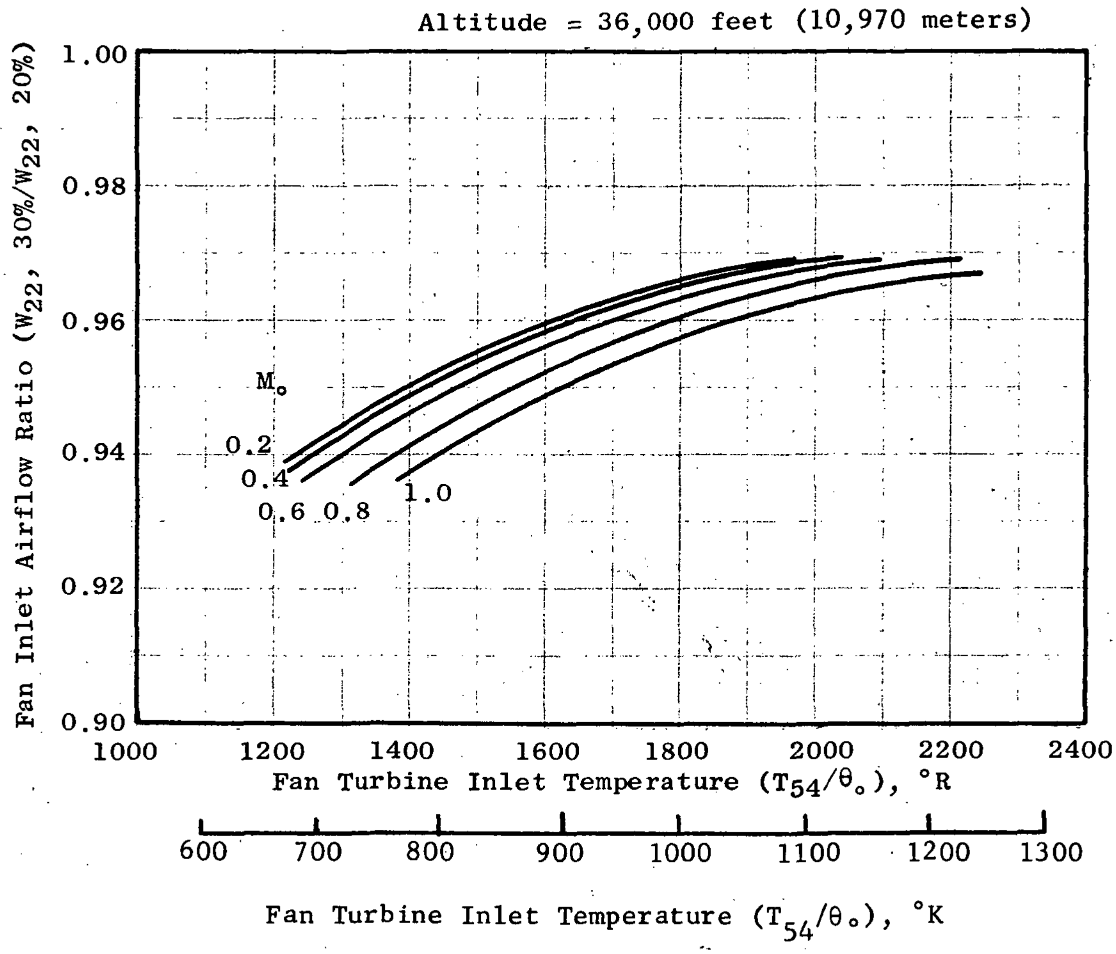

Figure 72 - Effects of Control Margin on Fan Inlet Airflow
P/P = 1.4

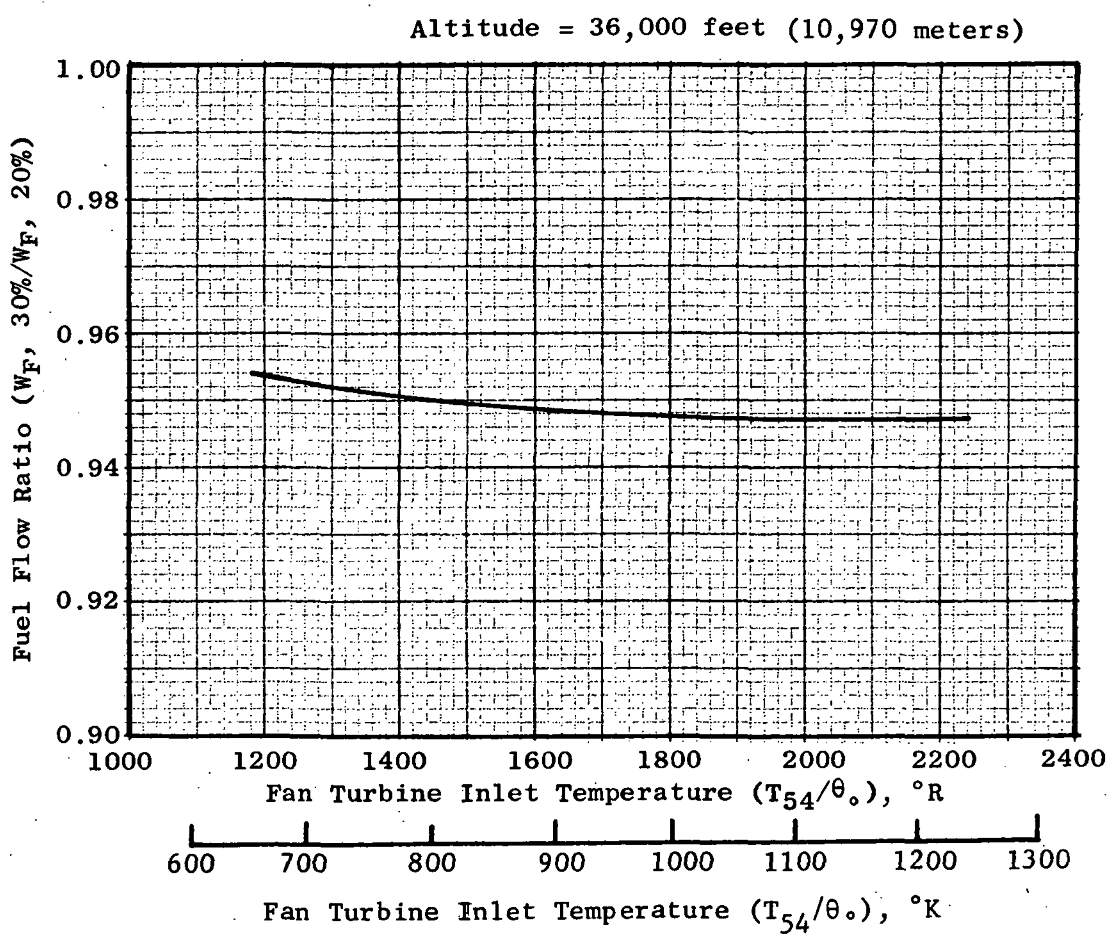

Figure 73 - Effects of Control Margin on Fuel Flow
P/P = 1.4

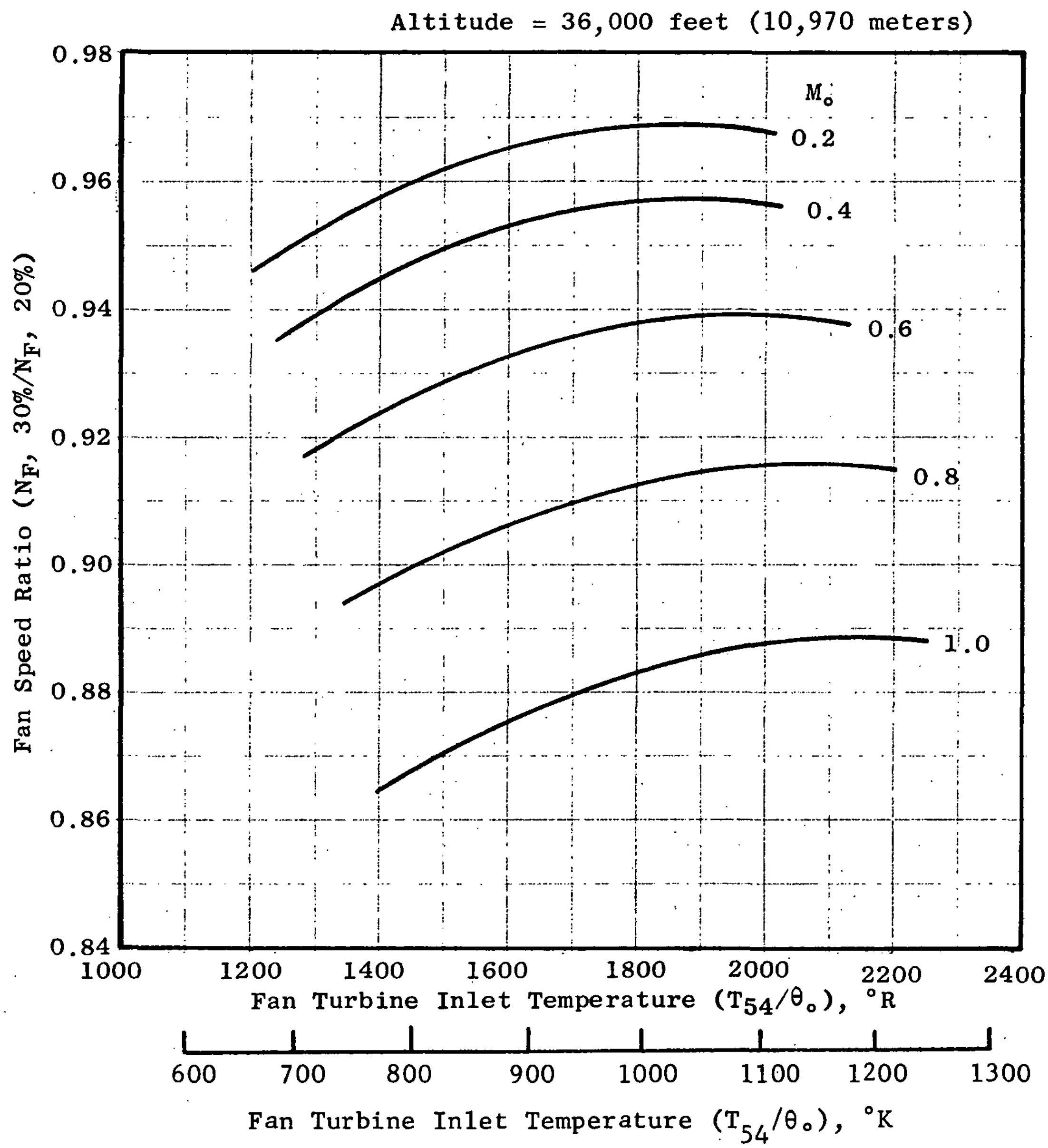

Figure 74 - Effects of Control Margin on Fan Speed
P/P = 1.4

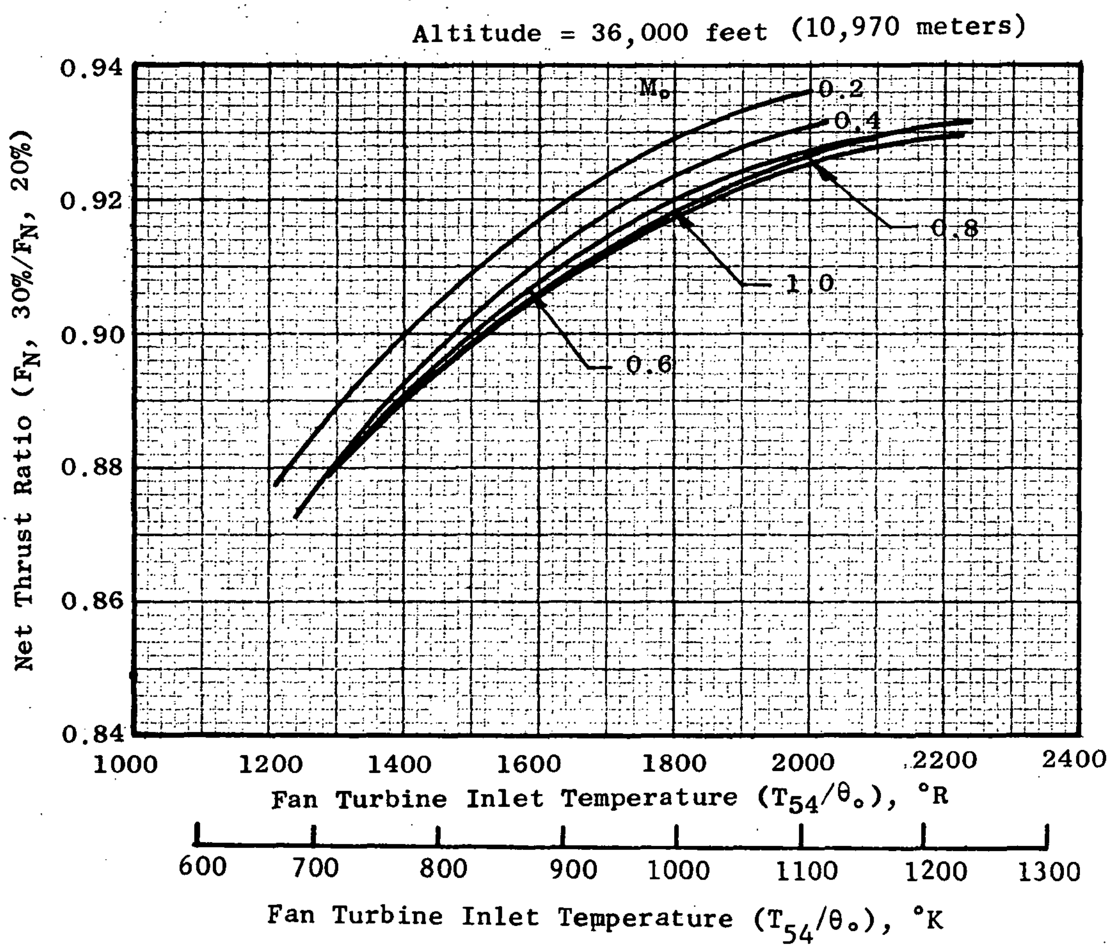

Figure 75 - Effects of Control Margin on Fan Net Thrust
P/P = 1.6

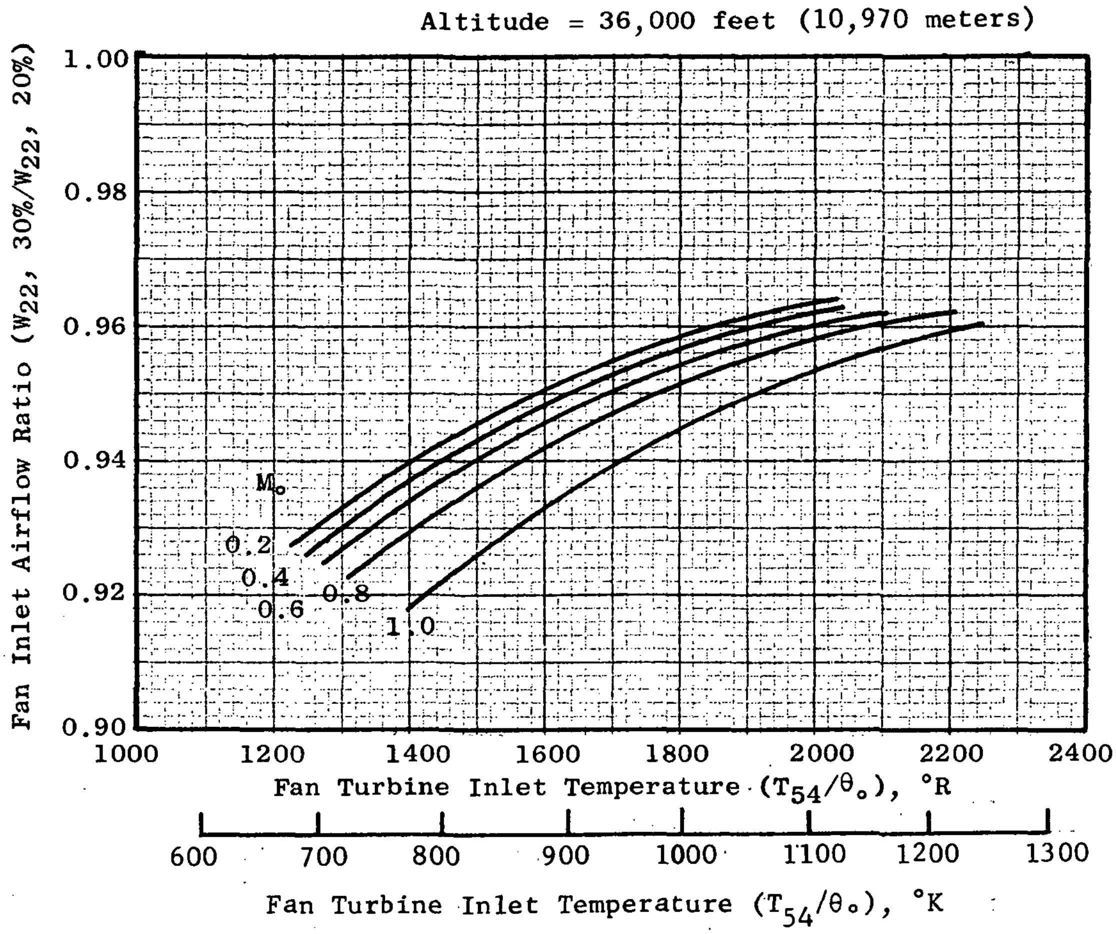

Figure 76 - Effects of Control Margin on Fan Inlet Airflow
P/P = 1.6

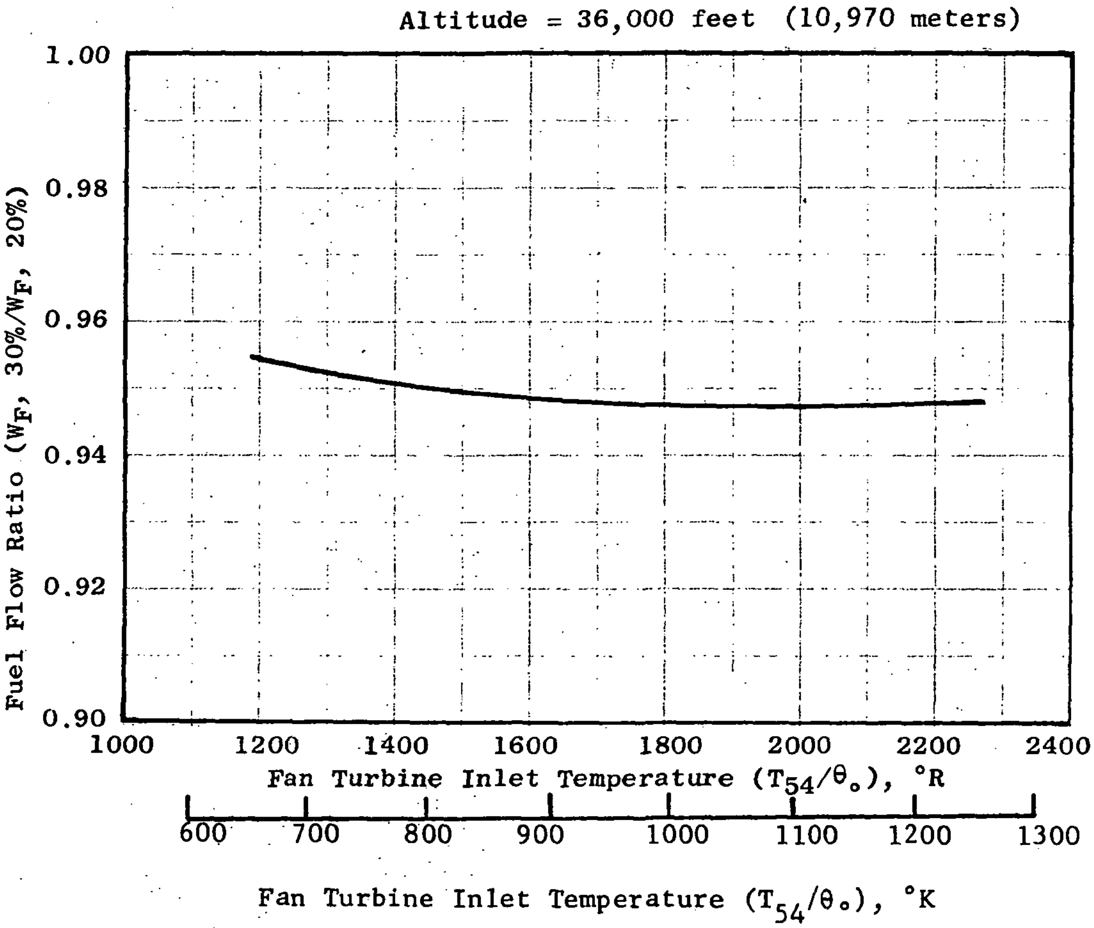

Figure 77 - Effects of Control Margin on Fuel Flow
P/P = 1.6

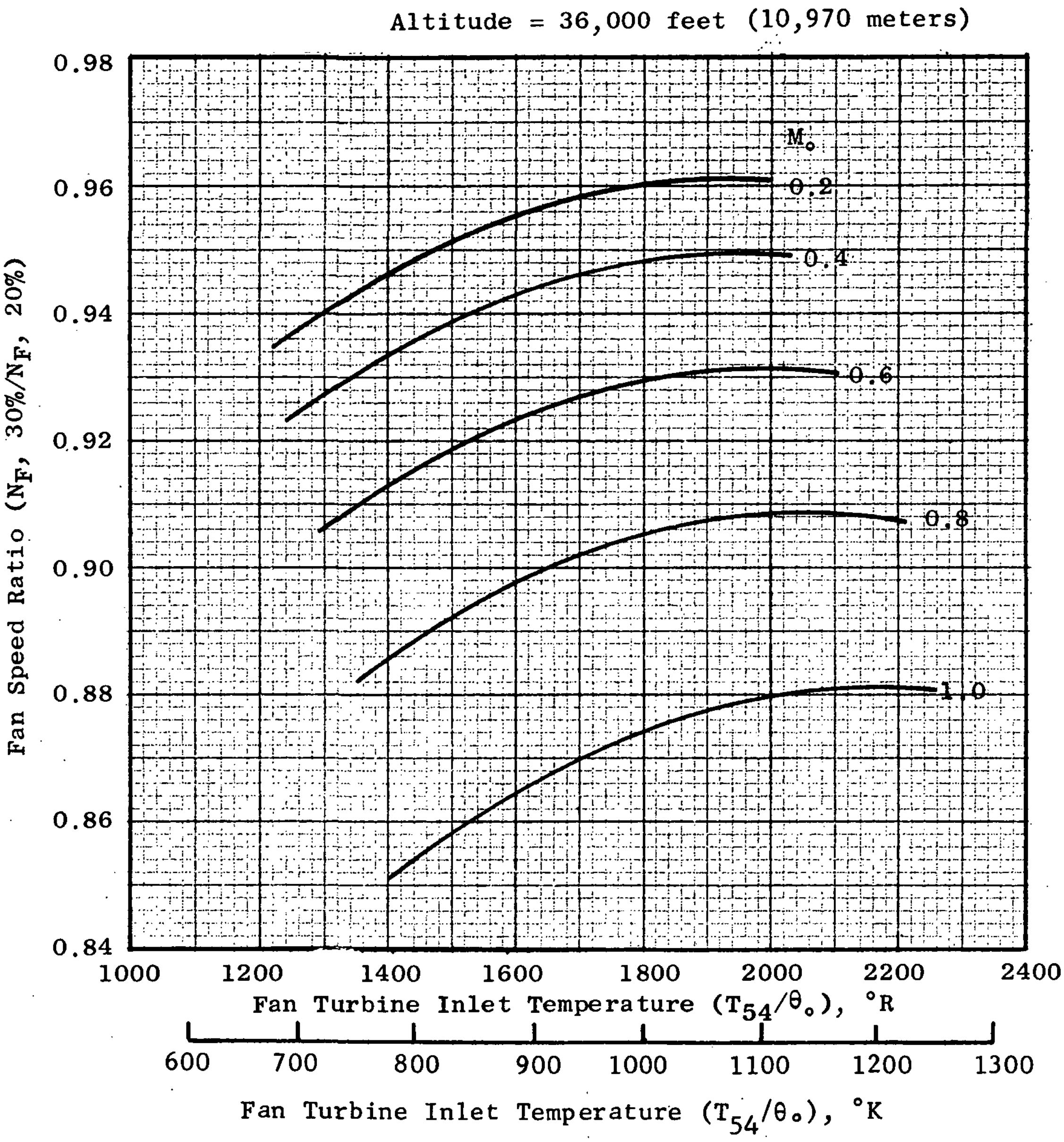

Figure 78 - Effects of Control Margin on Fan Speed
P/P = 1.6

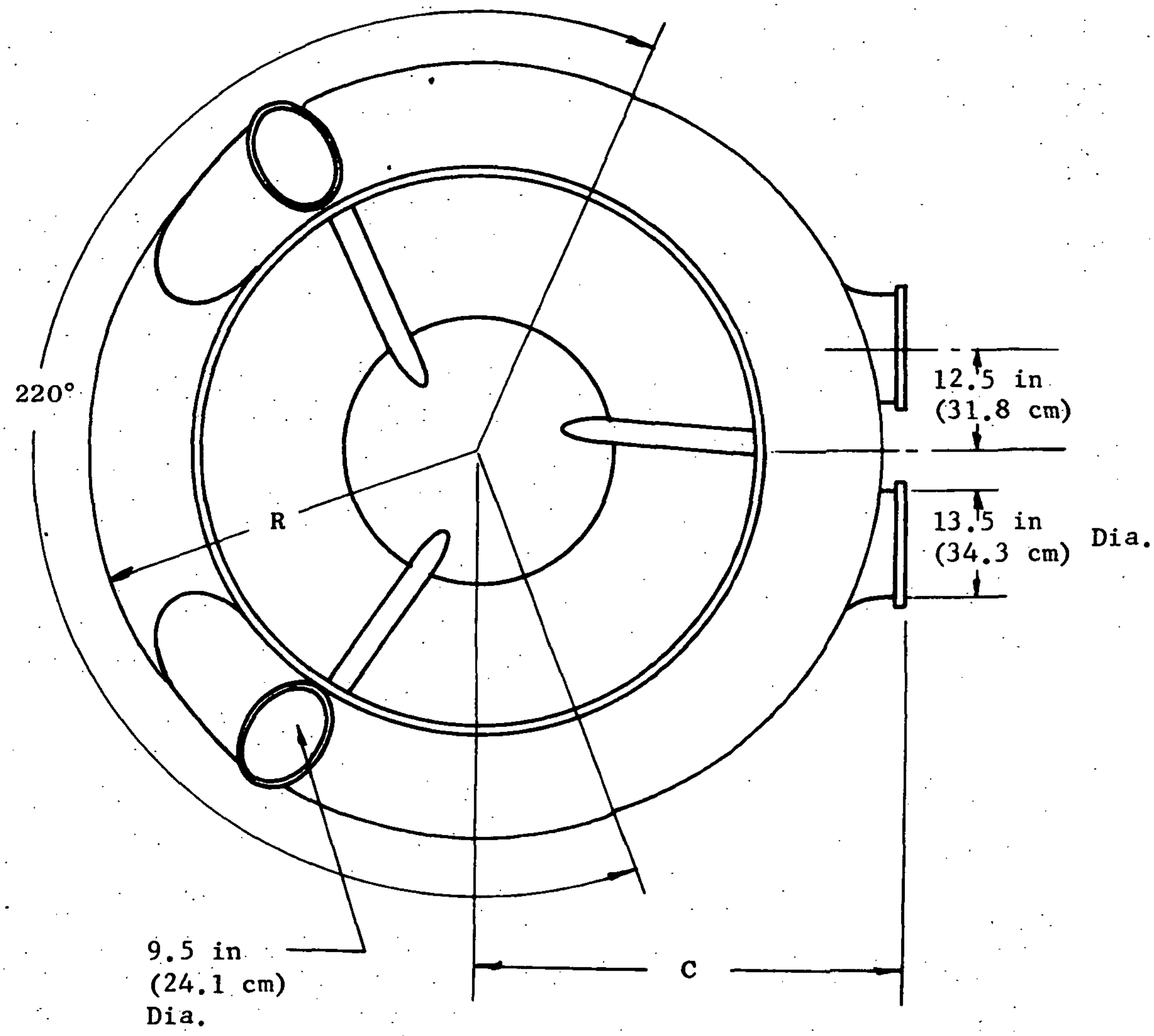

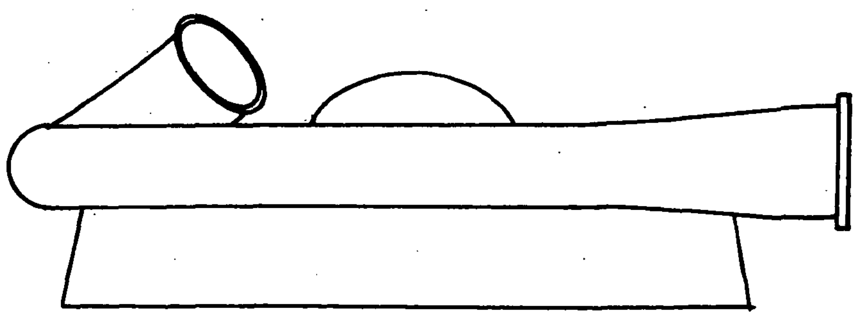

Figure 79 - Fan Planform Dimensions for Alternate Design with Auxiliary Inlets

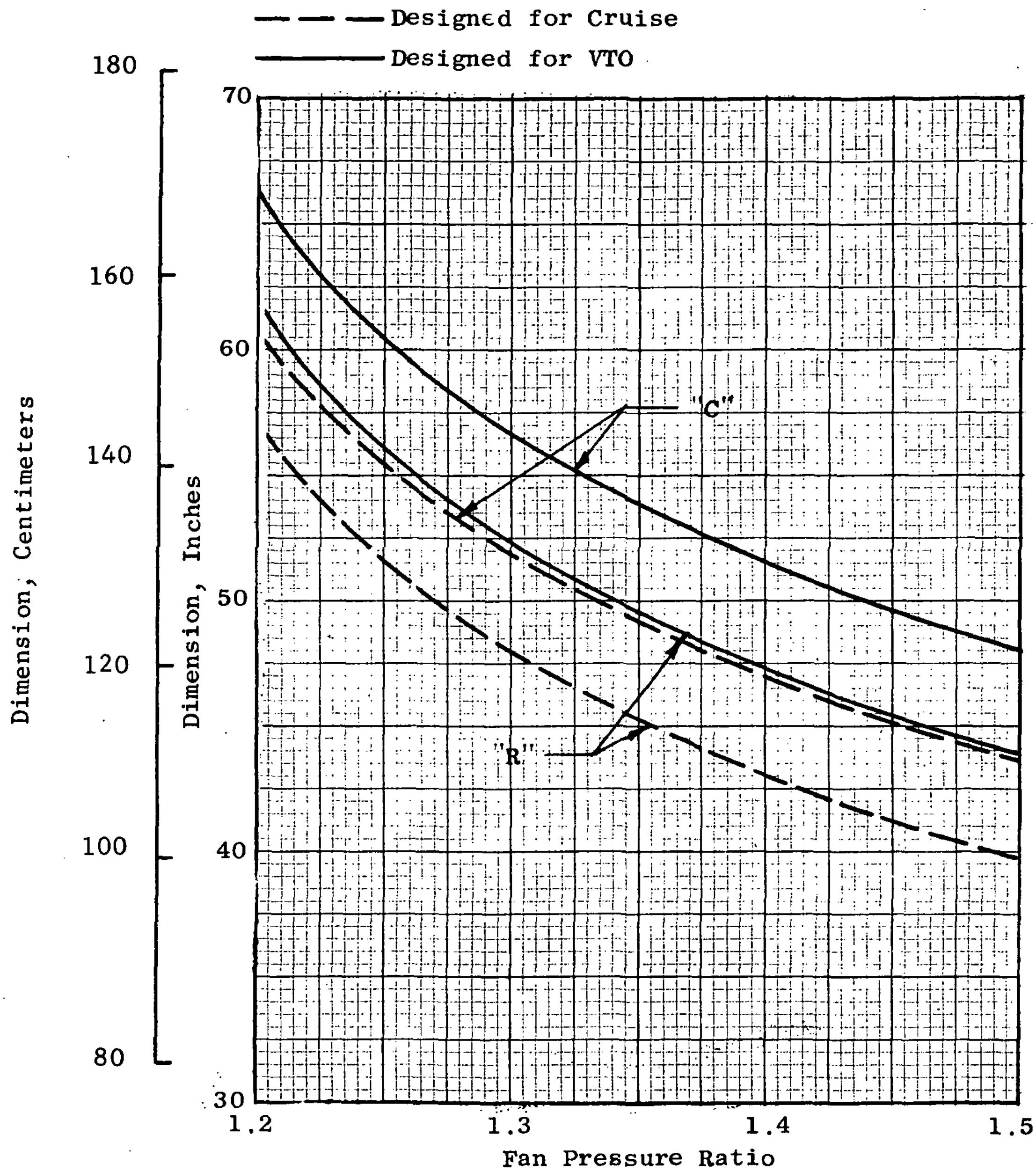

Figure 80 - Single Stage Fan Installation Dimension for Alternate Configuration with Auxiliary Inlets

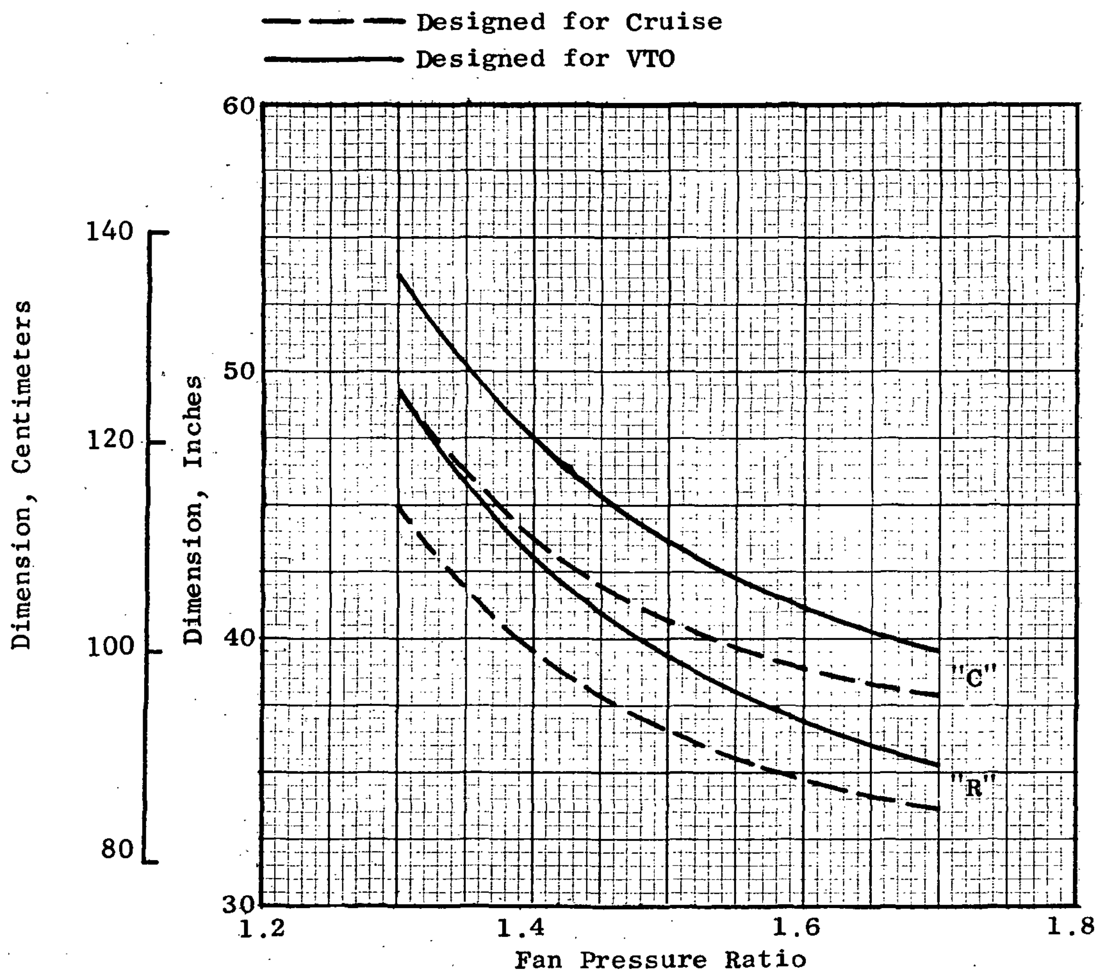

Figure 81 - Two Stage Fan Installation Dimensions for Alternate Configuration with Auxiliary Inlets

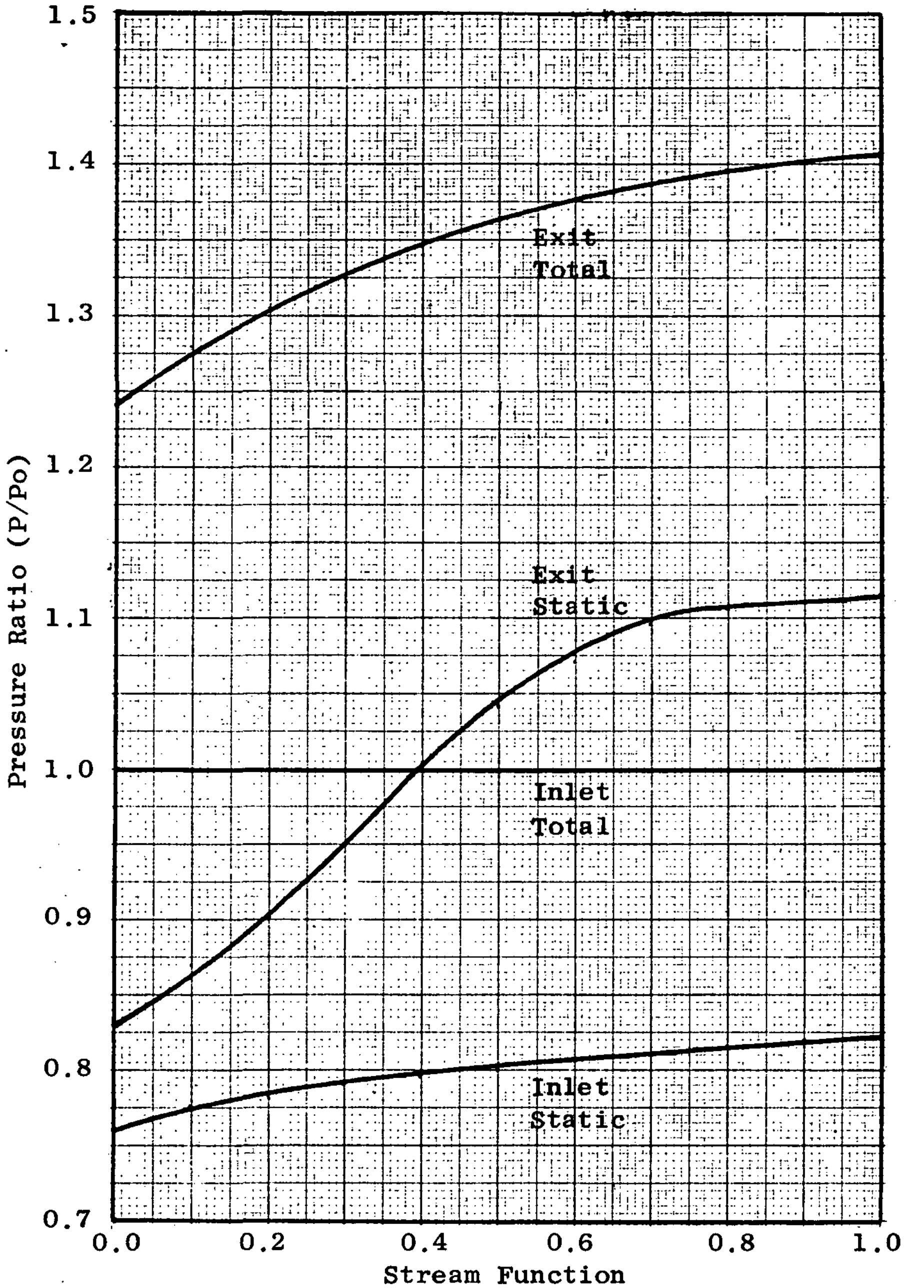

Figure 82 - Two Stage Fan Rotor I Pressure Distributions

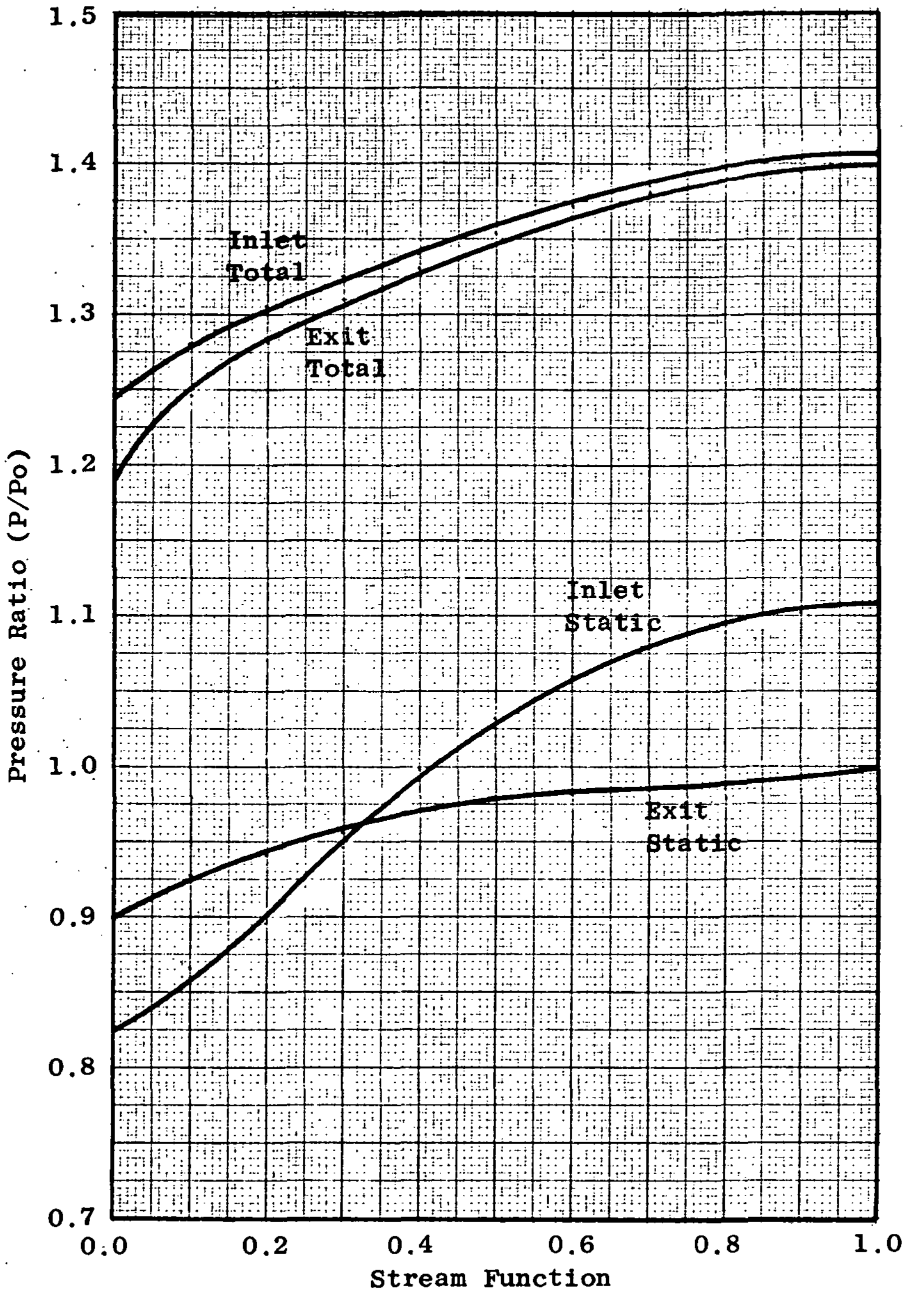

Figure 83 - Two Stage Fan Stator Pressure Distributions

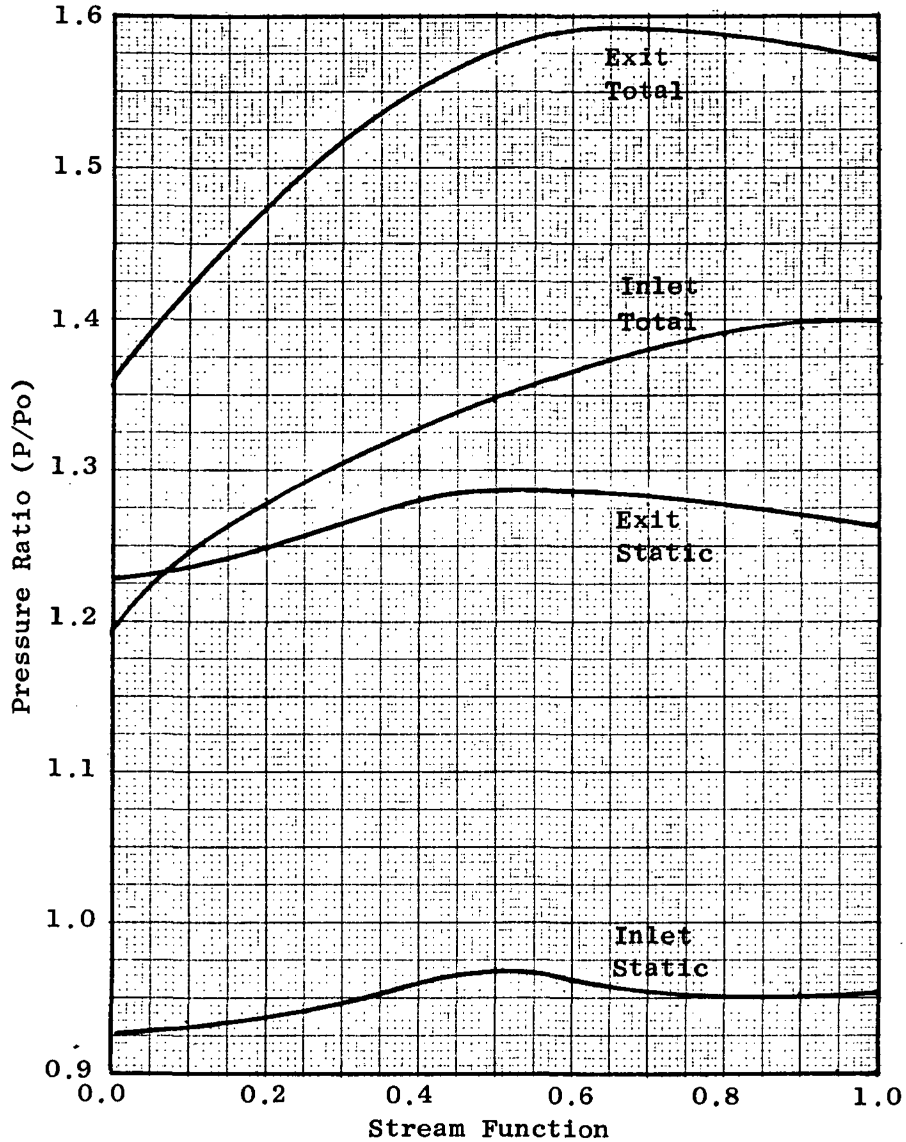

Figure 84 - Two Stage Fan Rotor II Pressure Distributions

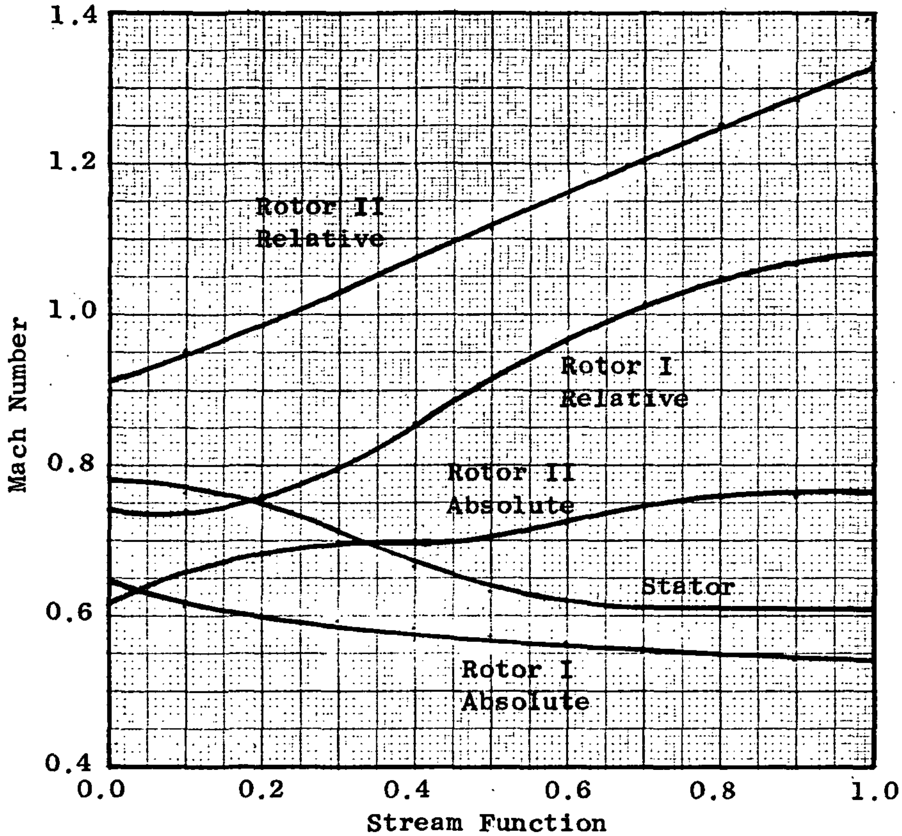

Figure 85 - Two Stage Fan Rotor and Stator Inlet Mach Number Distribution

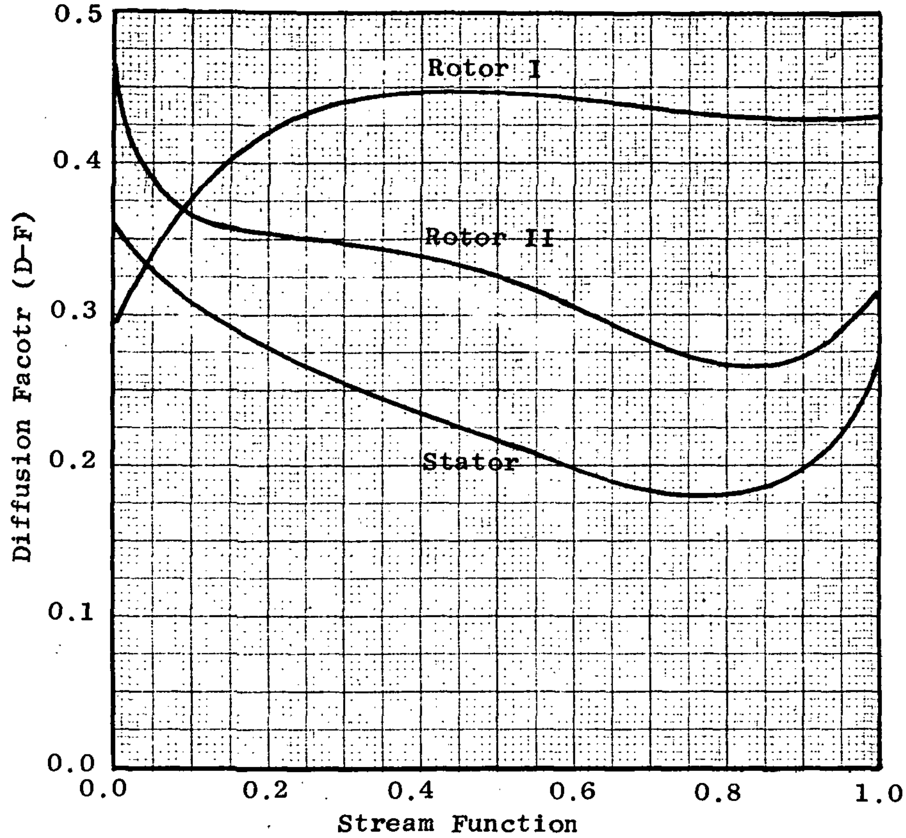

Figure 86 - Two Stage Fan Blading Diffusion Factors

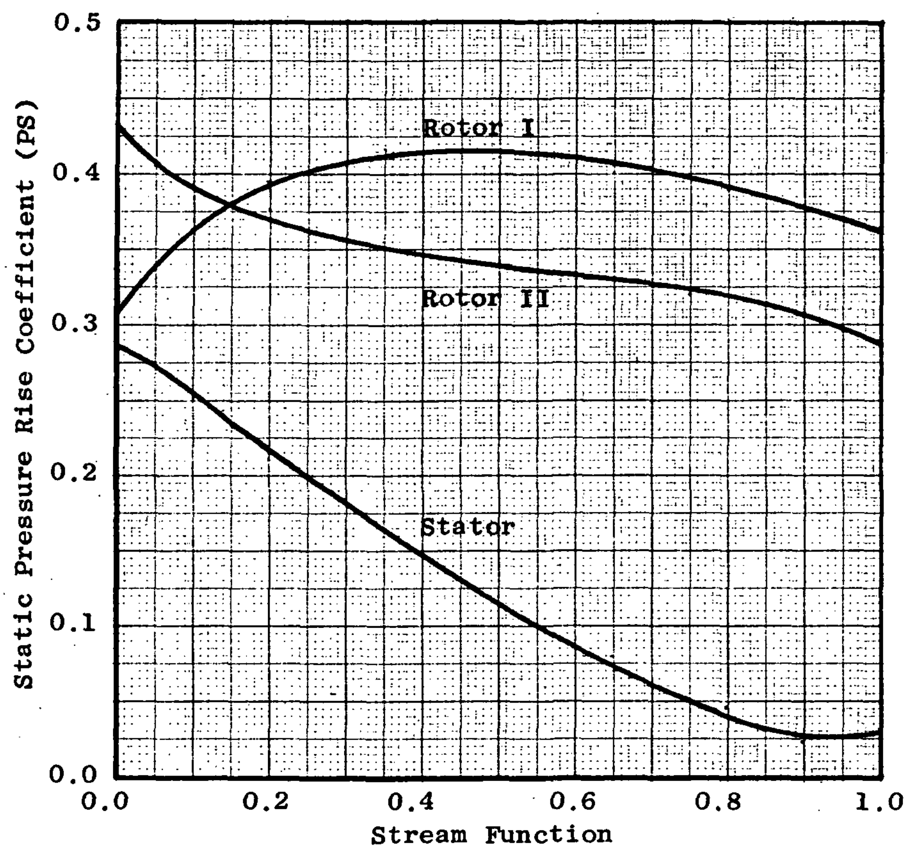

Figure 87 - Two Stage Fan Blading Static Pressure Rise Coefficients

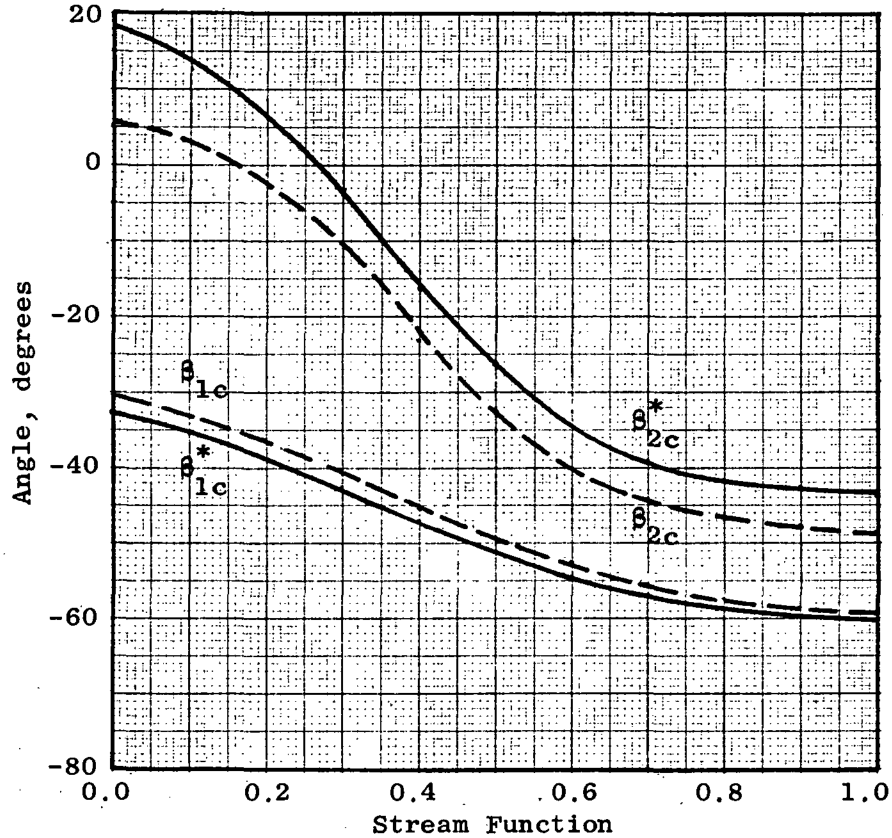

Figure 88 - Two Stage Fan Rotor I Air and Blade Angles

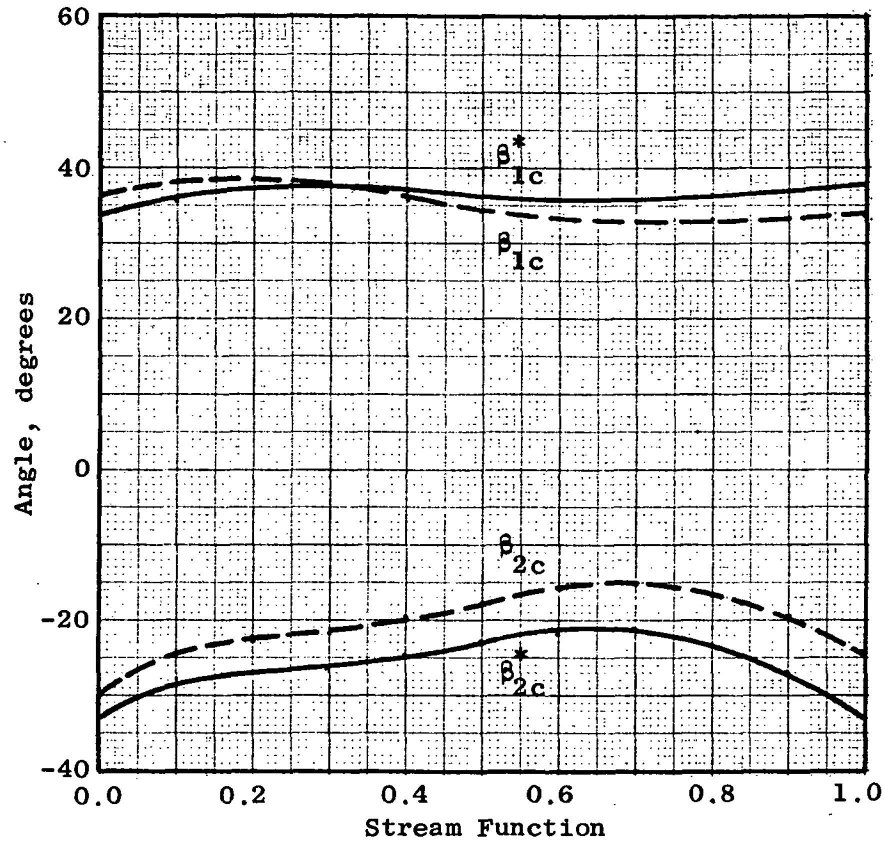

Figure 89 - Two Stage Fan Stator Air and Blade Angles

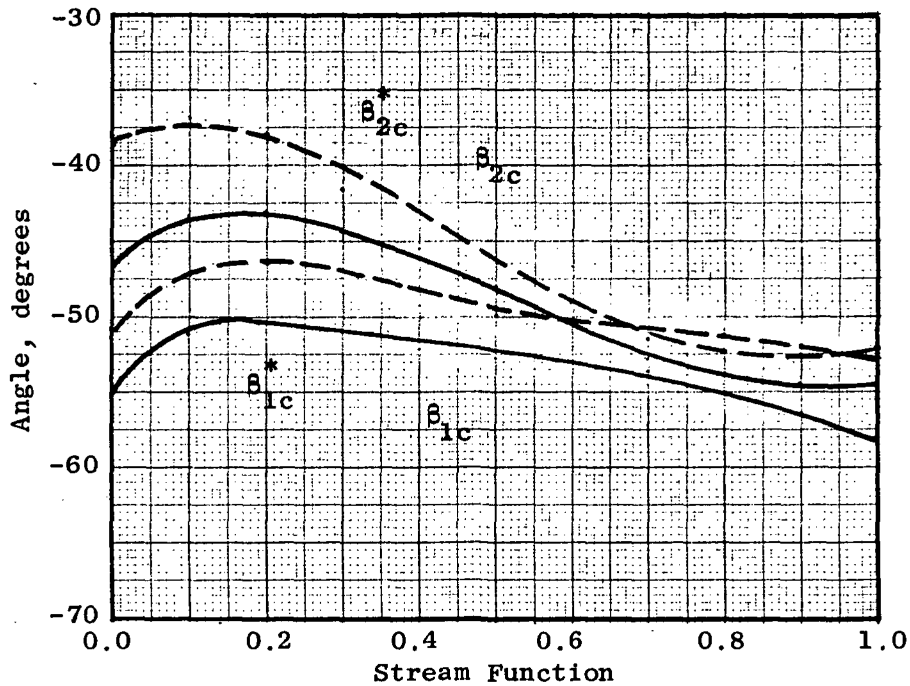

Figure 90 - Two Stage Fan Rotor II Air and Blade Angles

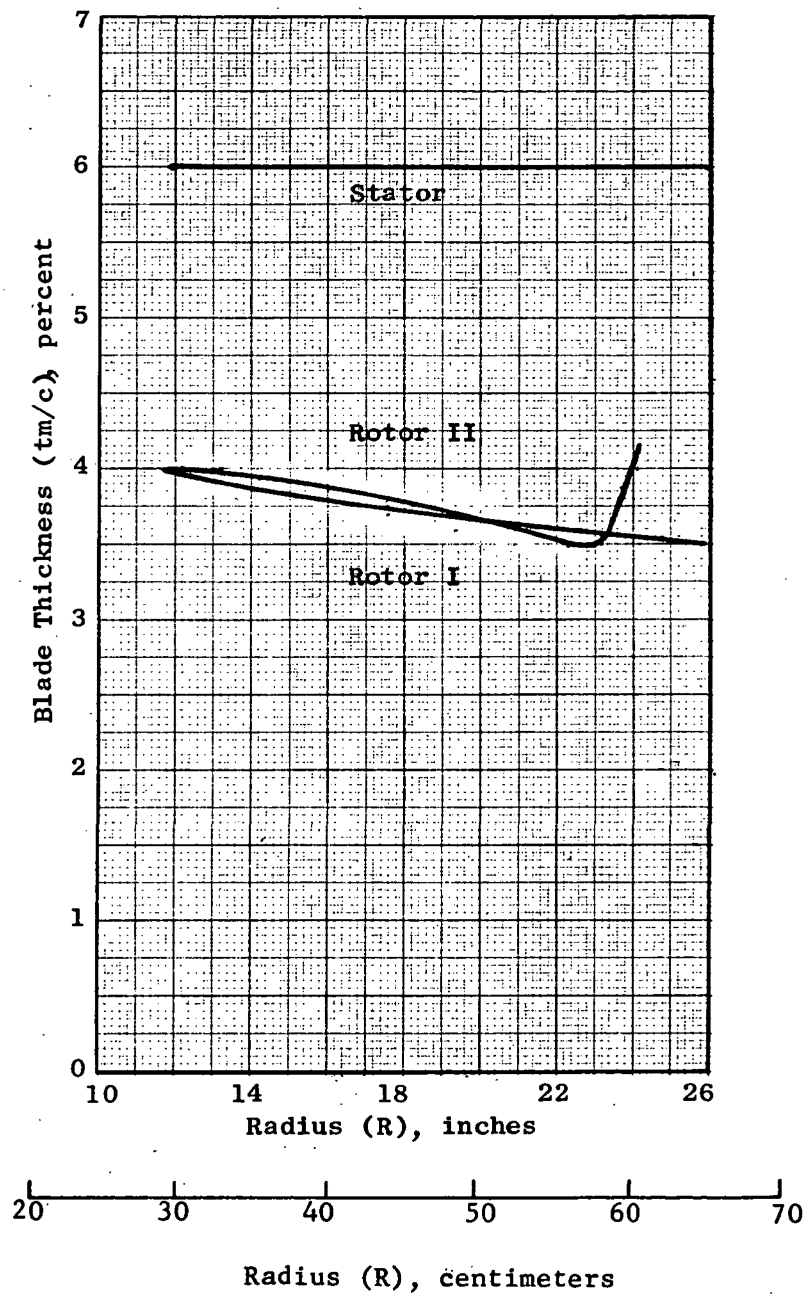

Figure 91 - Two Stage Blading Thickness Distributions

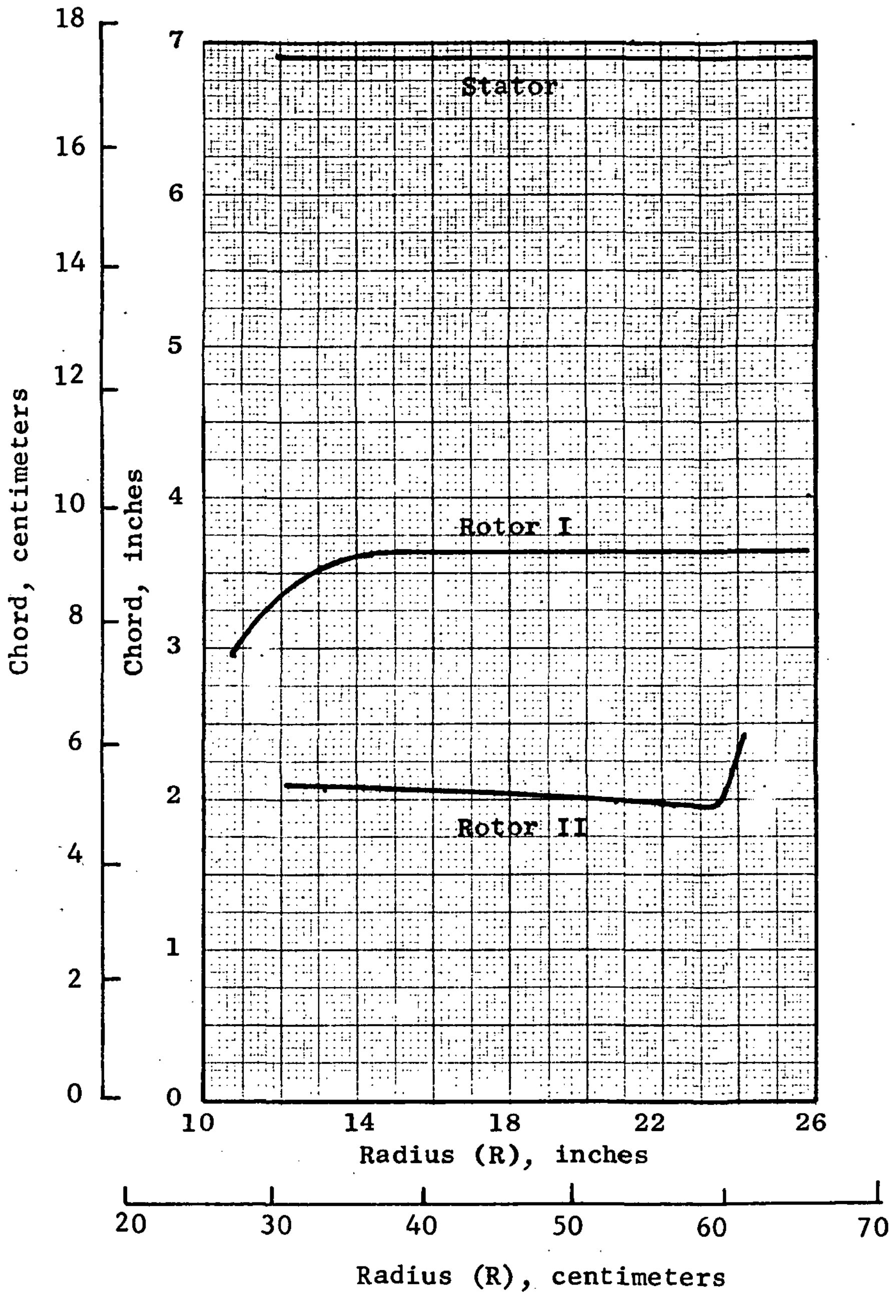

Figure 92 - Two Stage Fan Blading Chords

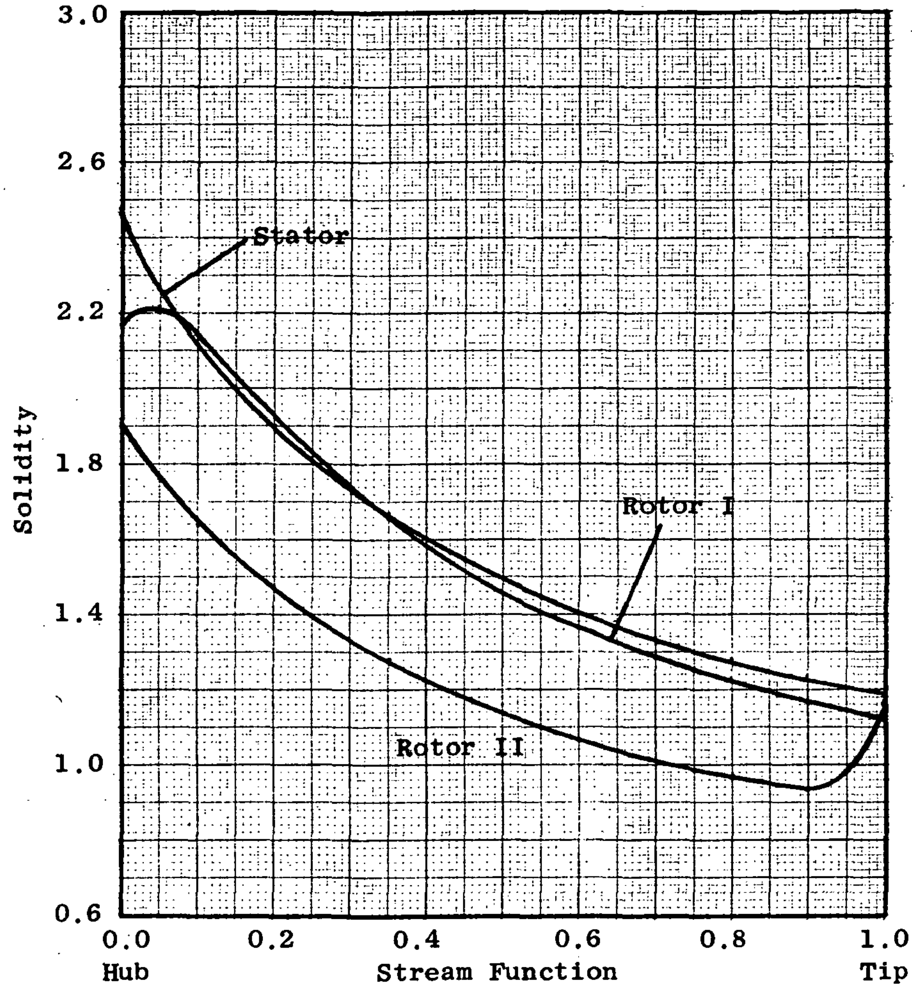

Figure 93 - Two Stage Fan Rotor and Stator Solidities

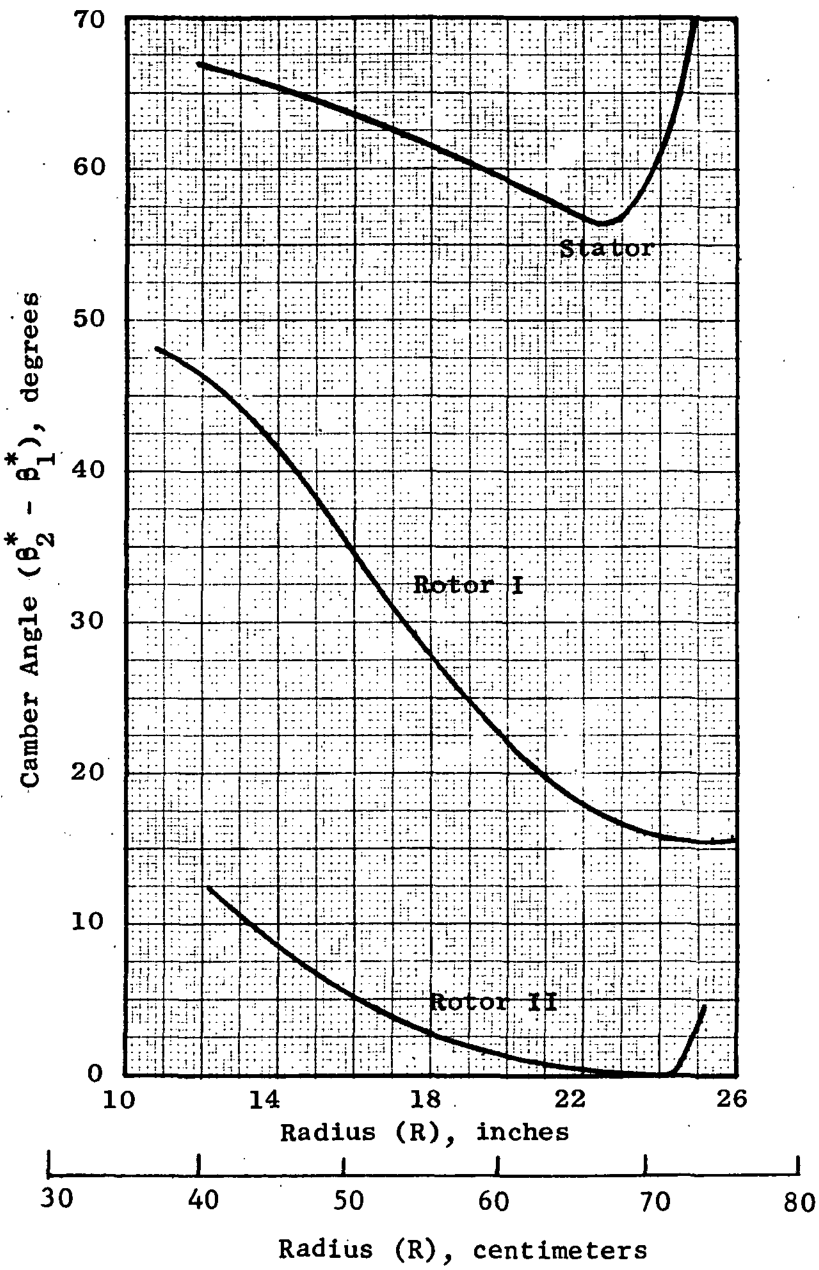

Figure 94 - Two Stage Fan Blading Camber Angle Distributions

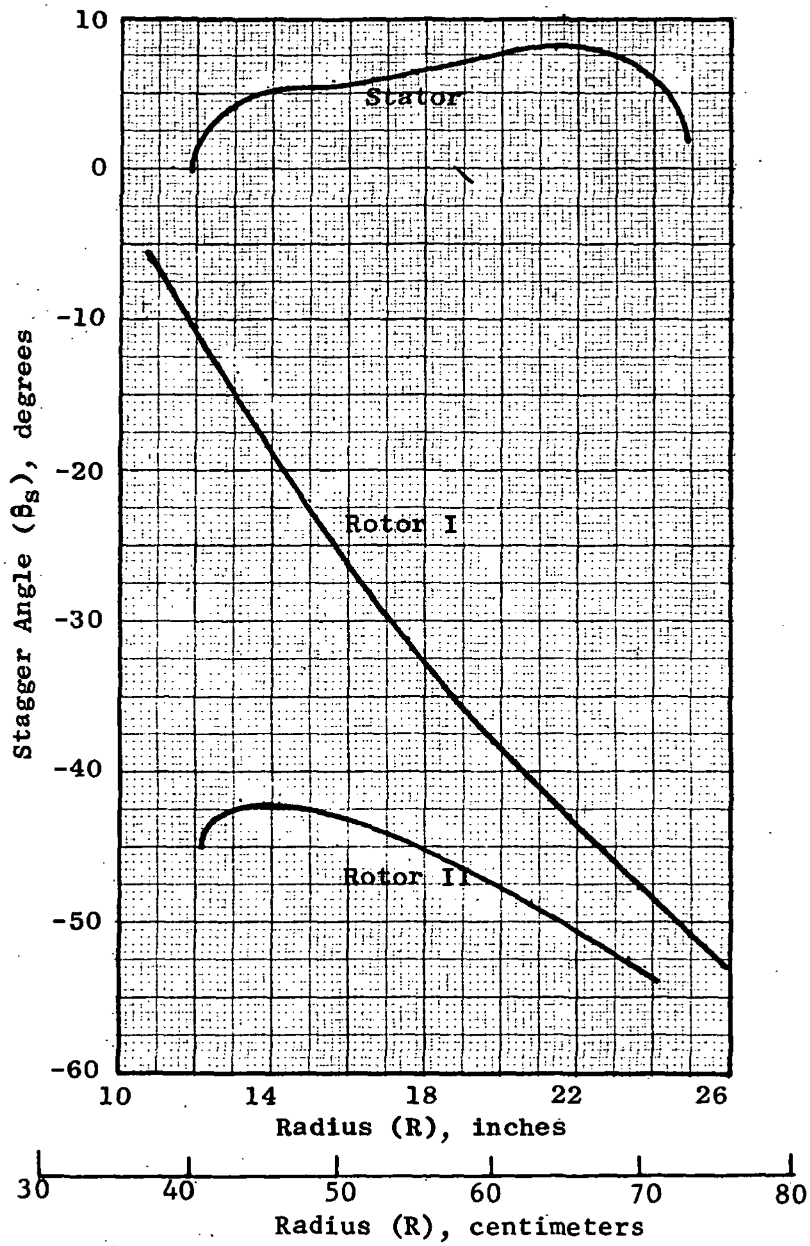

Figure 95 - Two Stage Fan Blading Stagger Angle Distributions

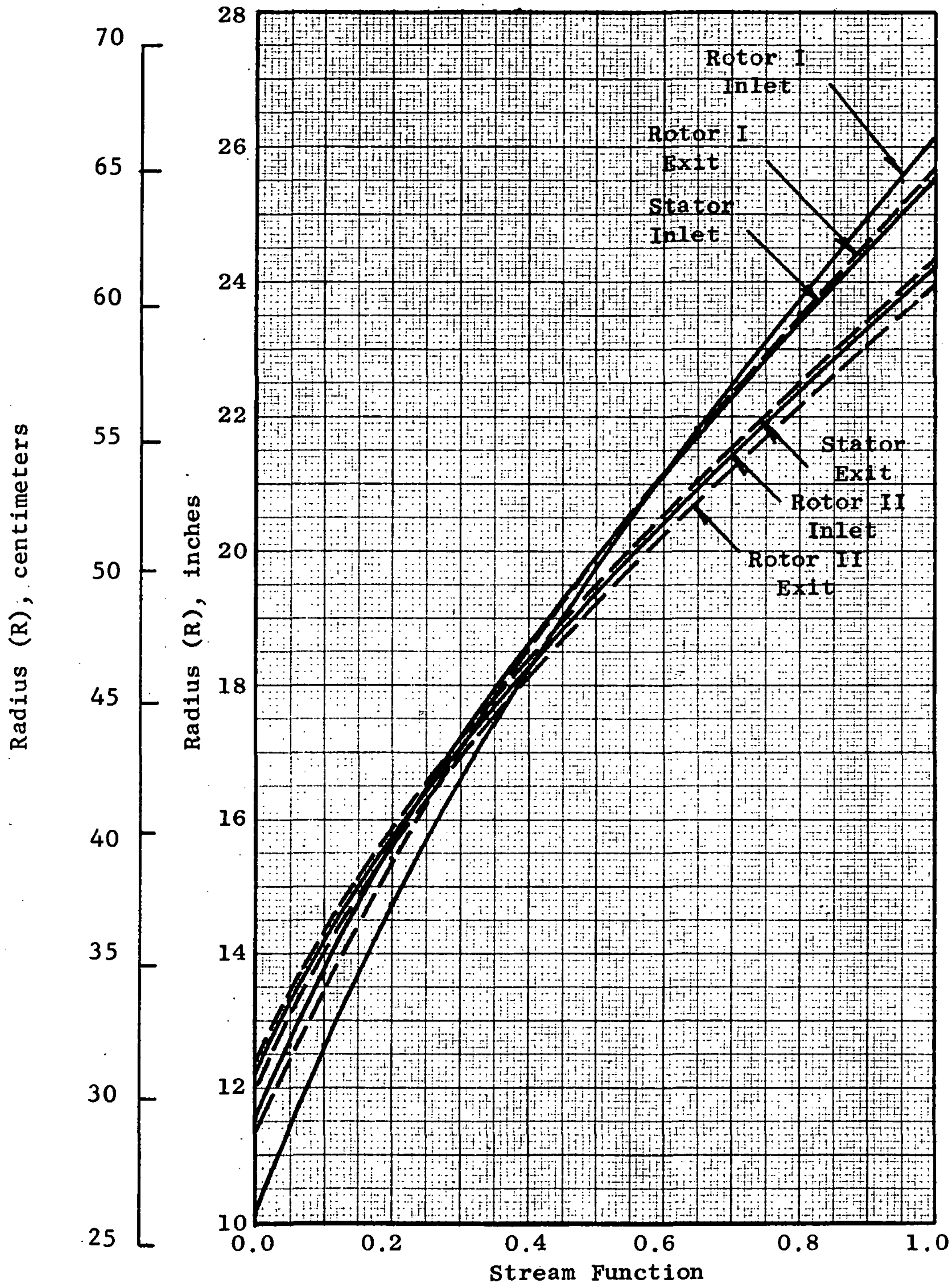

Figure 96 - Two Stage Fan Stream Function - Radius Relationship

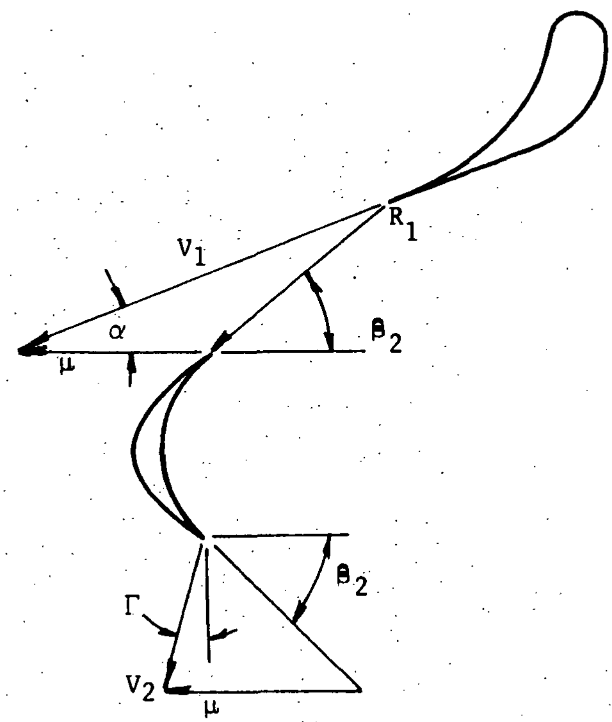

Velocities	ft/sec	m/sec	Angle	degrees	Mach Number	
V_1	2431	740.9	α	24.7	M_1	1.40
R_1	1414	431.0	β_1	45.7	MR_1	0.80
R_2	1296	395.0	β_2	53.4	MR_2	0.74
V_2	1114	339.5	Γ	22.8	M_2	0.58
μ	1223	372.7				

Figure 97 - Turbine Velocity Diagram, Single Stage Fan Design

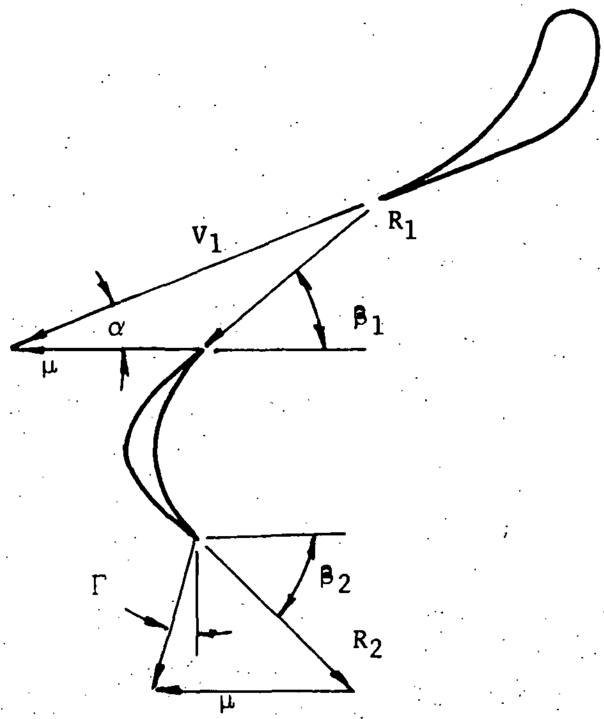

Velocities	ft/sec	m/sec	Angle degrees		Mach Number	
V_1	2277	694	α	25.5	M_1	1.27
R_1	1424	434	β_1	43.5	MR_1	0.79
R_2	1306	398	β_2	49.6	MR_2	0.71
V_2	1012	308	Γ	-10.0	M_2	0.55
μ						

Figure 98 - Turbine Velocity Diagram, Two Stage Fan Design

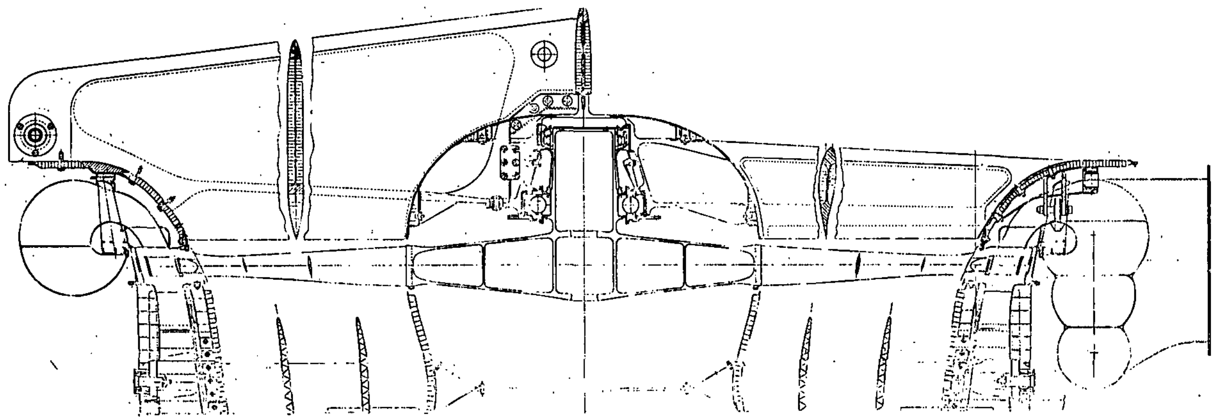

LF460 Lift Fan

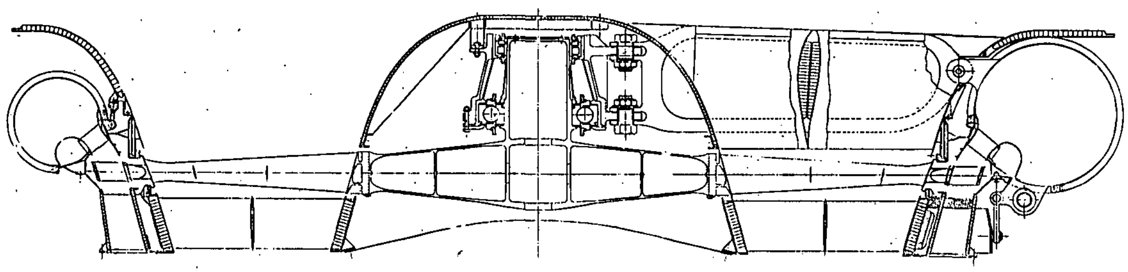

Military Lift Fan

Figure 99 - Comparison of LF460 and Military Lift Fans

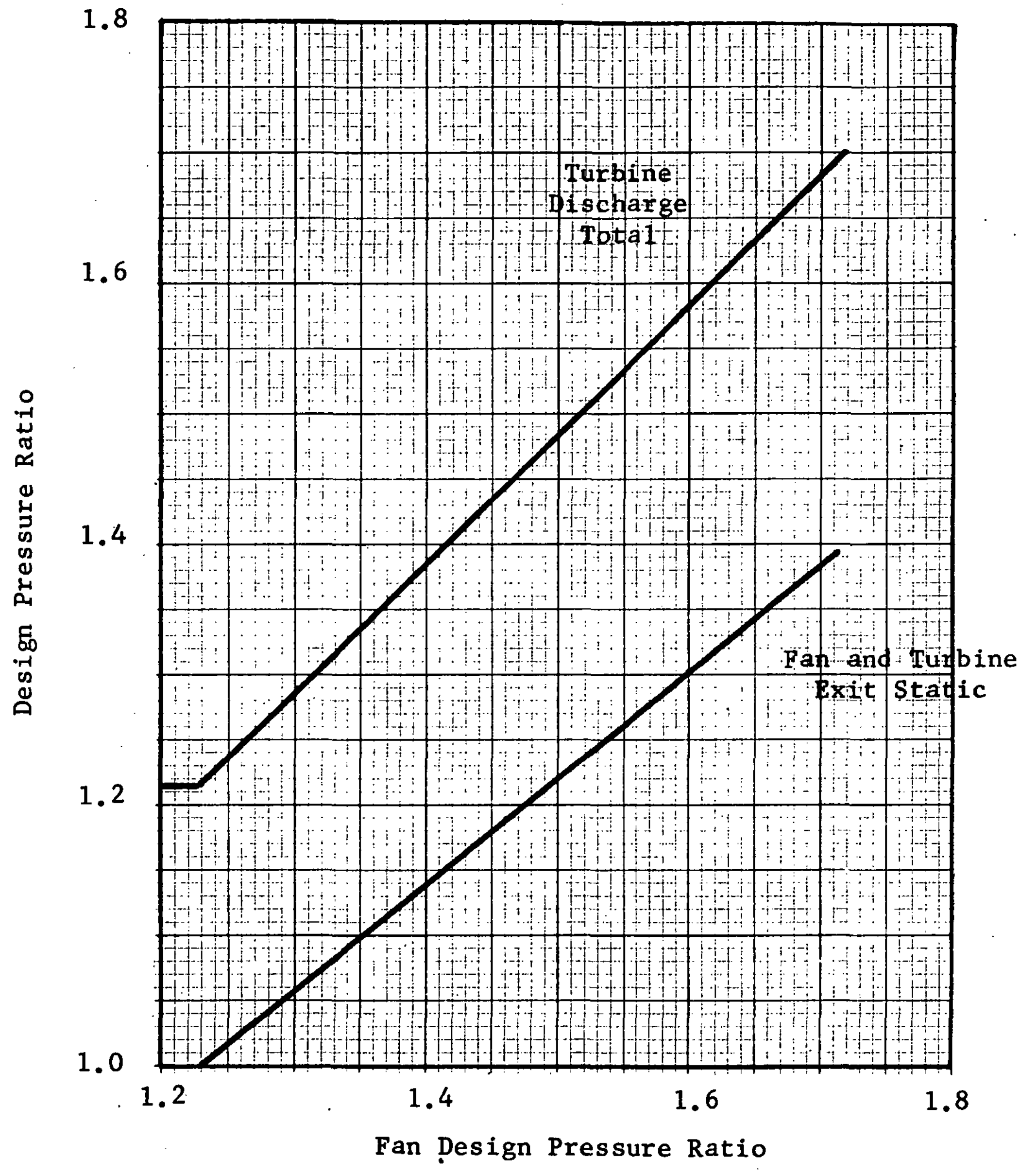

Figure 100 - Effects of Fan Pressure Ratio on Design Exit Pressures

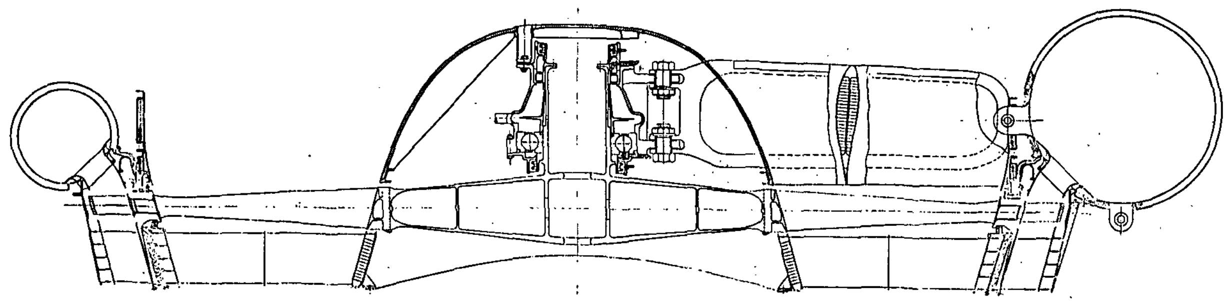

Figure 101 - Single Stage Fan Cross-Section

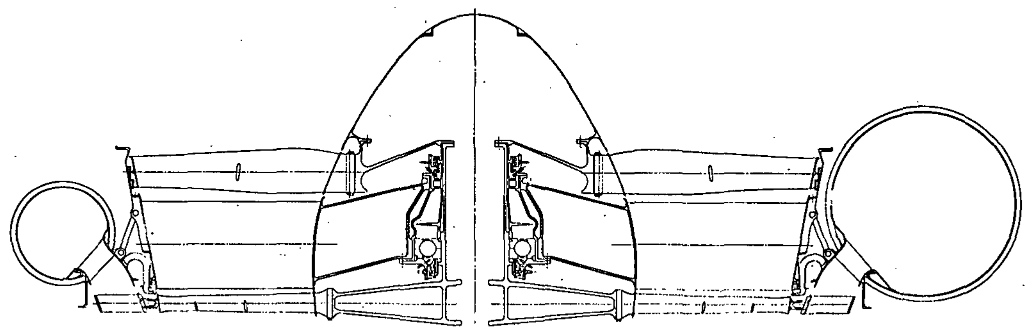

Figure 102 - Two Stage Fan Cross-Section

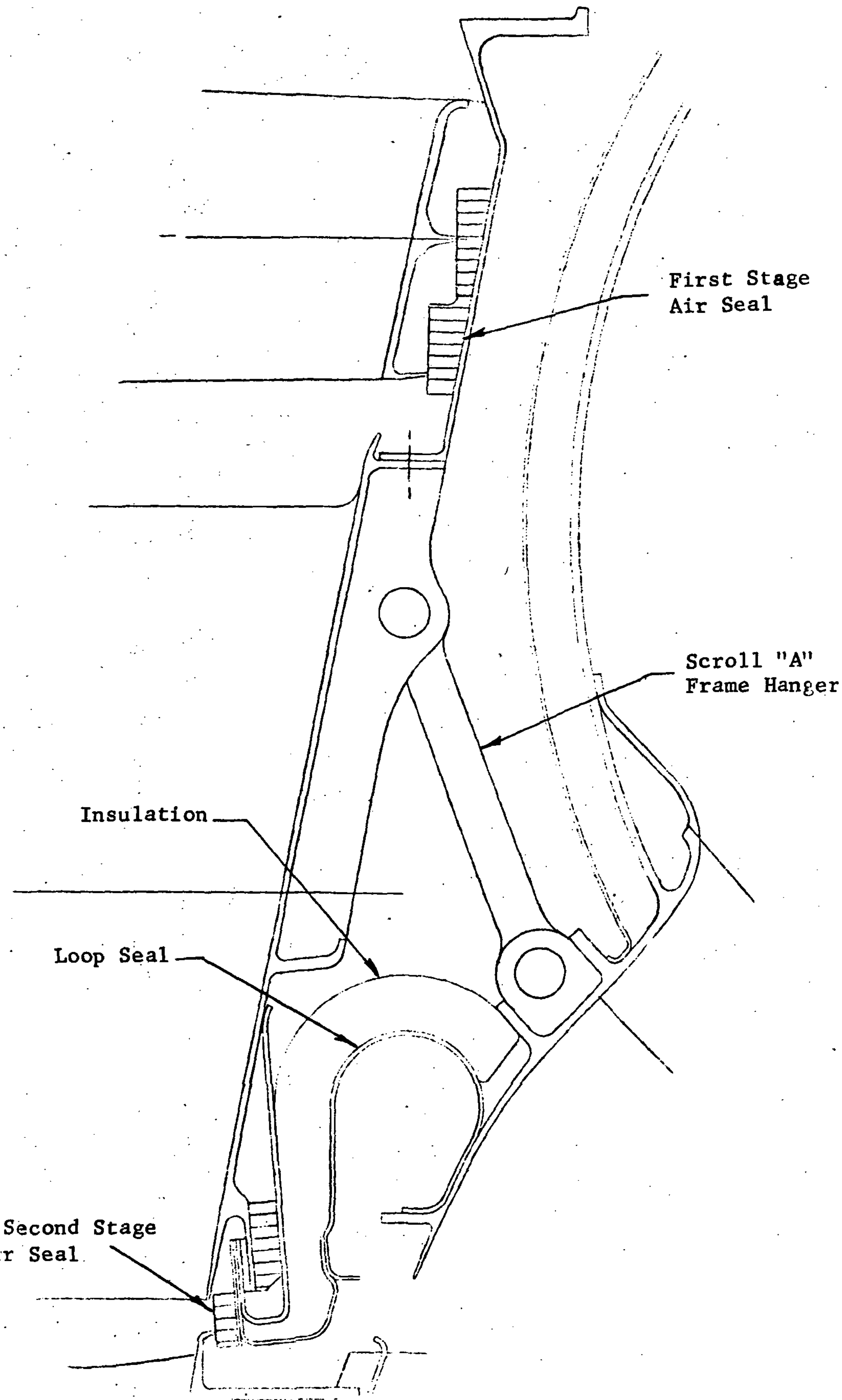

Figure 103 - Outer Flowpath Ring Structure

First Flex
(507 Hz)

Second Flex
(727 Hz)

First Torsion
(793 Hz)

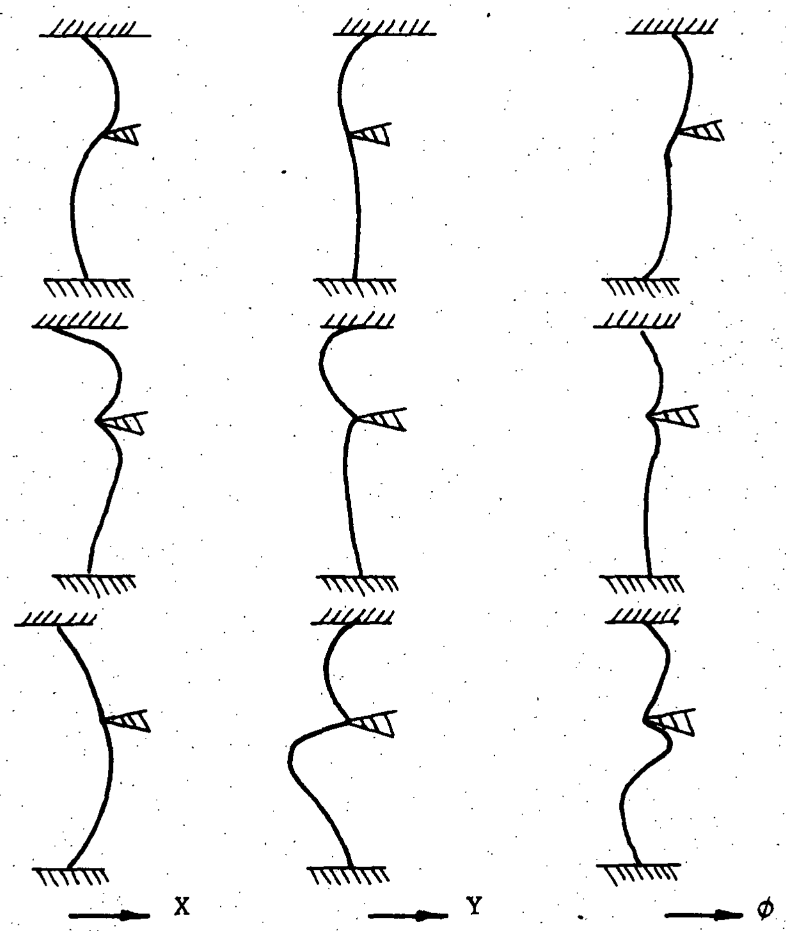

Relative Velocity = 1130 ft/sec (344 m/sec)
Chord = 3.64 in (9.25 cm)
V_R = 1.50

Figure 104 - Fundamental Frequencies and Nodal Patterns for First Stage Titanium Blades

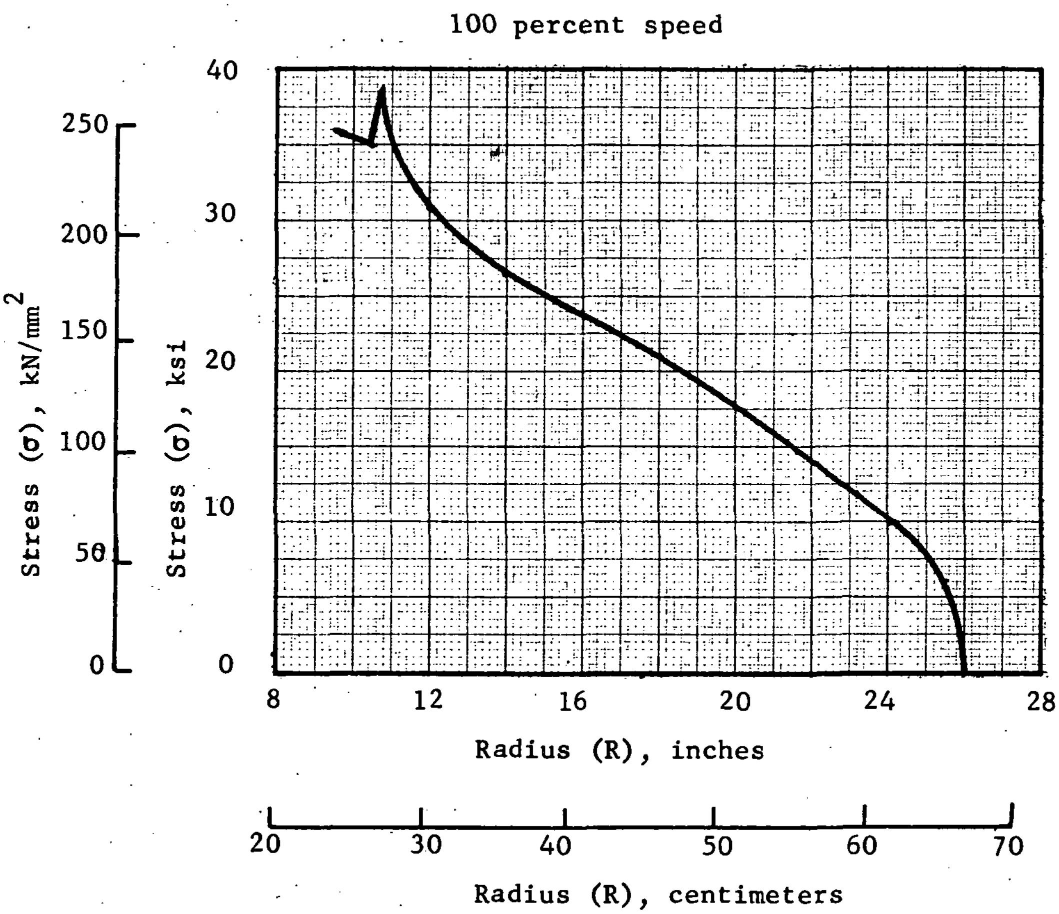

Figure 105 - Centrifugal Stress for Titanium Stage 1 Blade

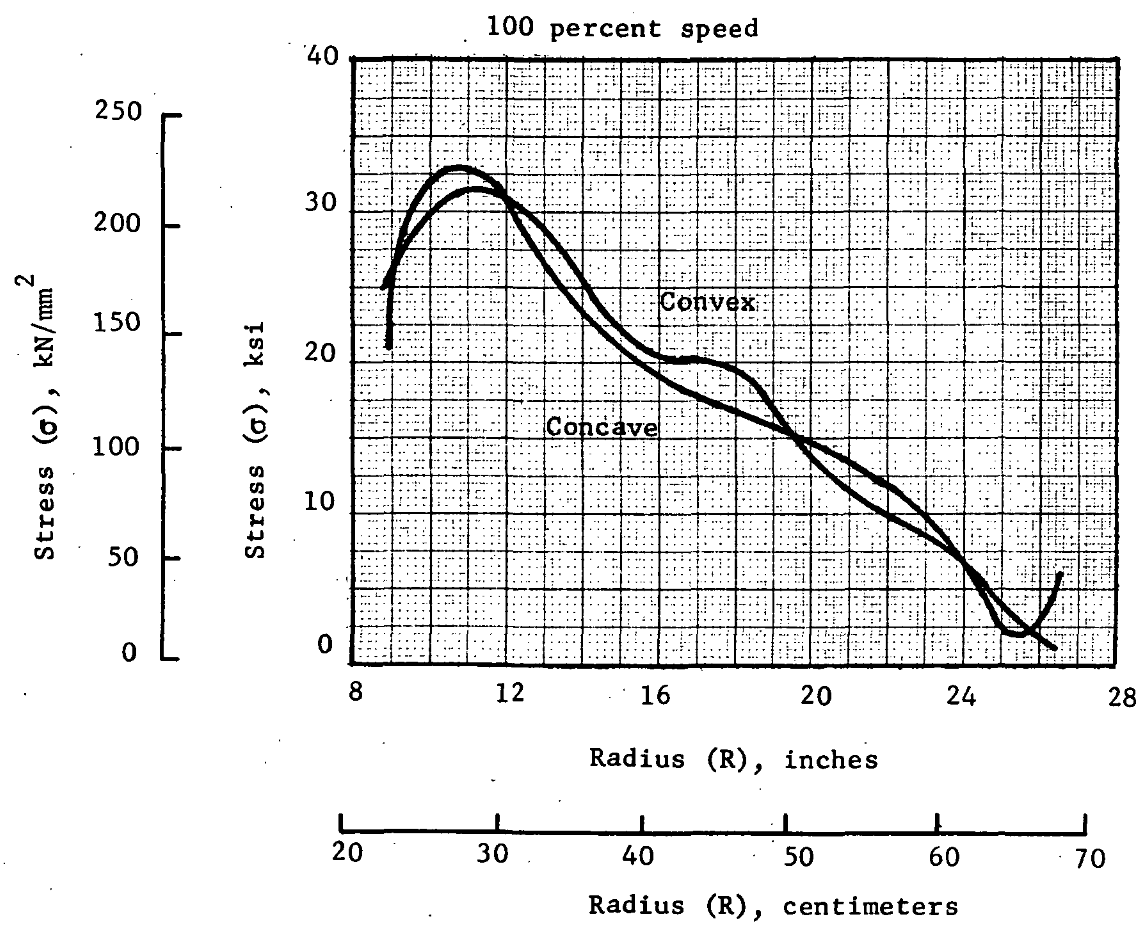

Figure 106 - Combined Stress for Titanium Stage 1 Blade

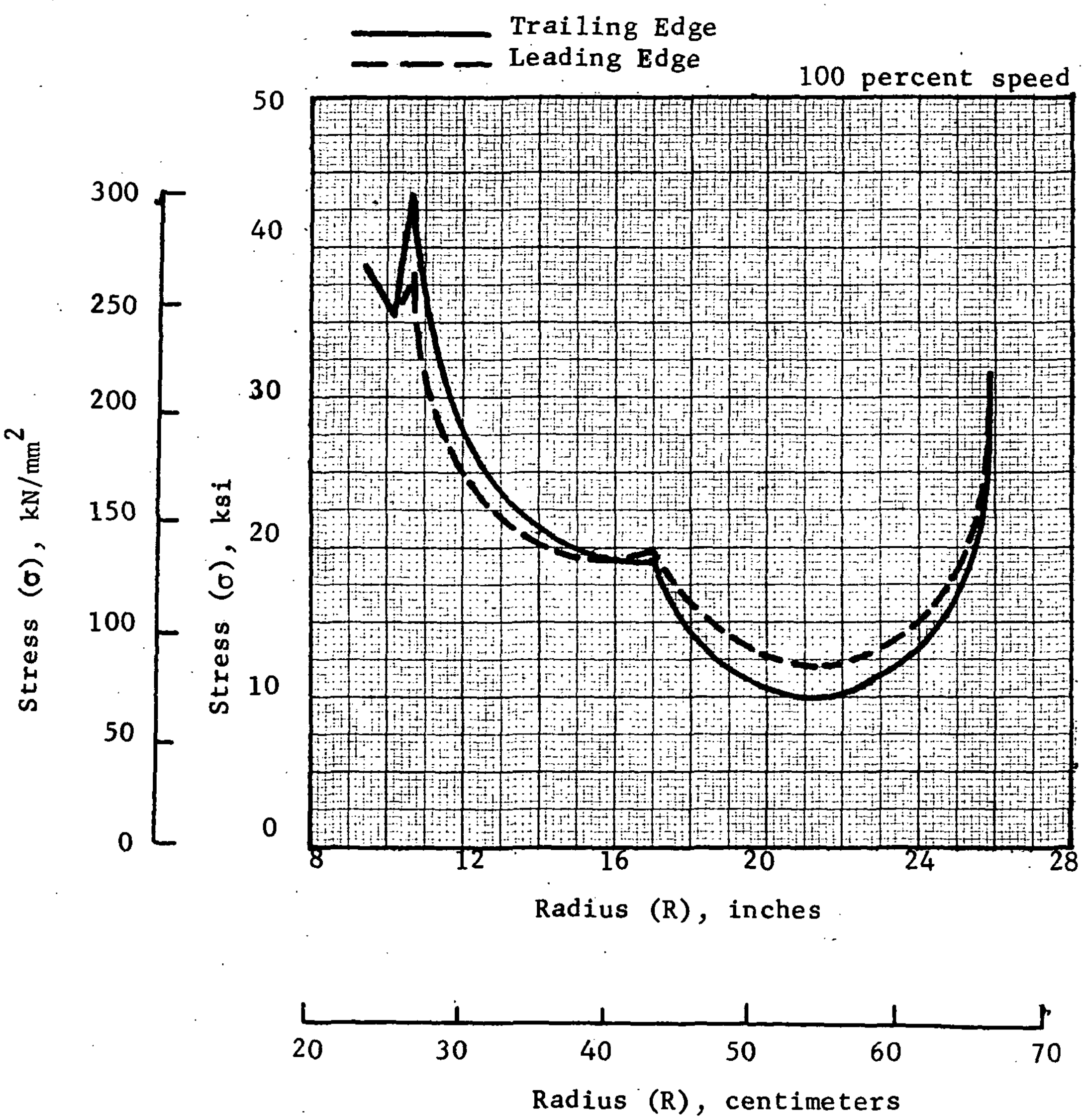

Figure 107 - Resultant Spanwise Stress for Titanium Stage 1 Blade

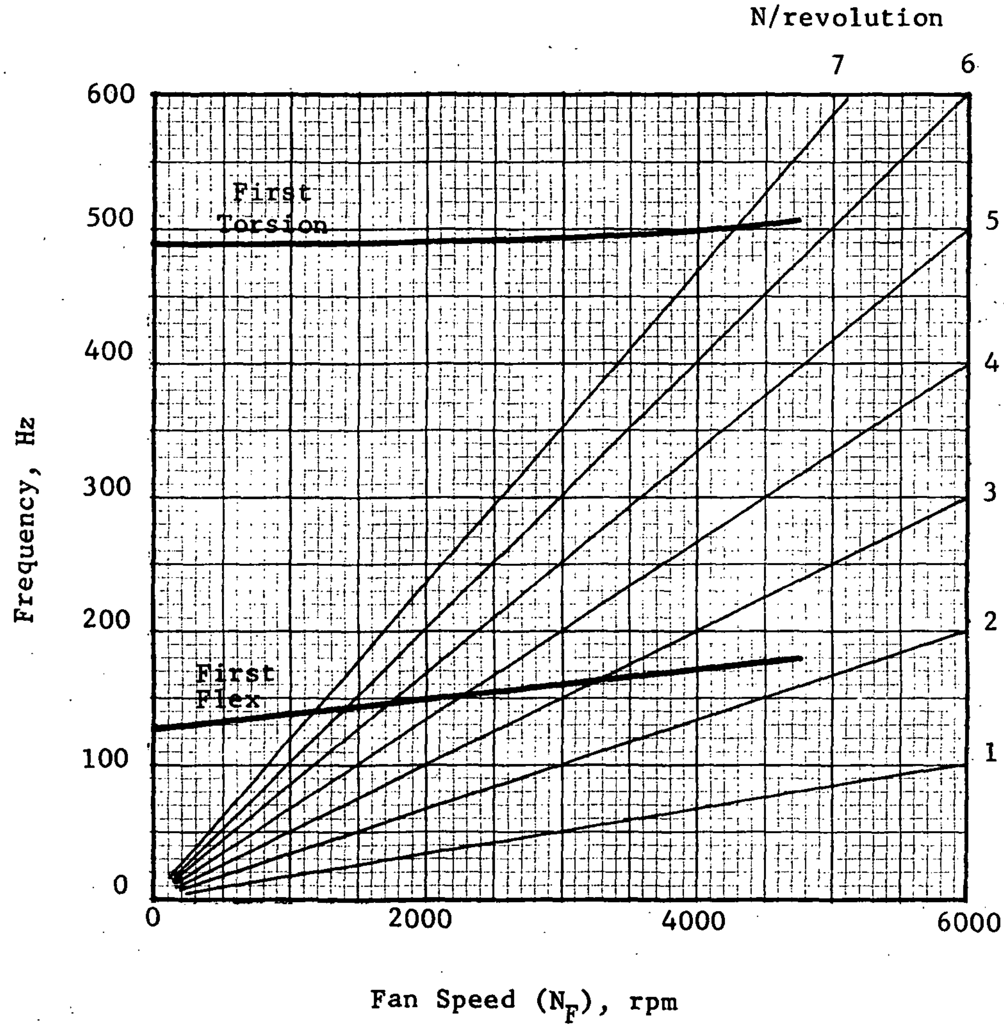

Figure 108 - Frequency Diagram for Composite Stage 1 Rotor

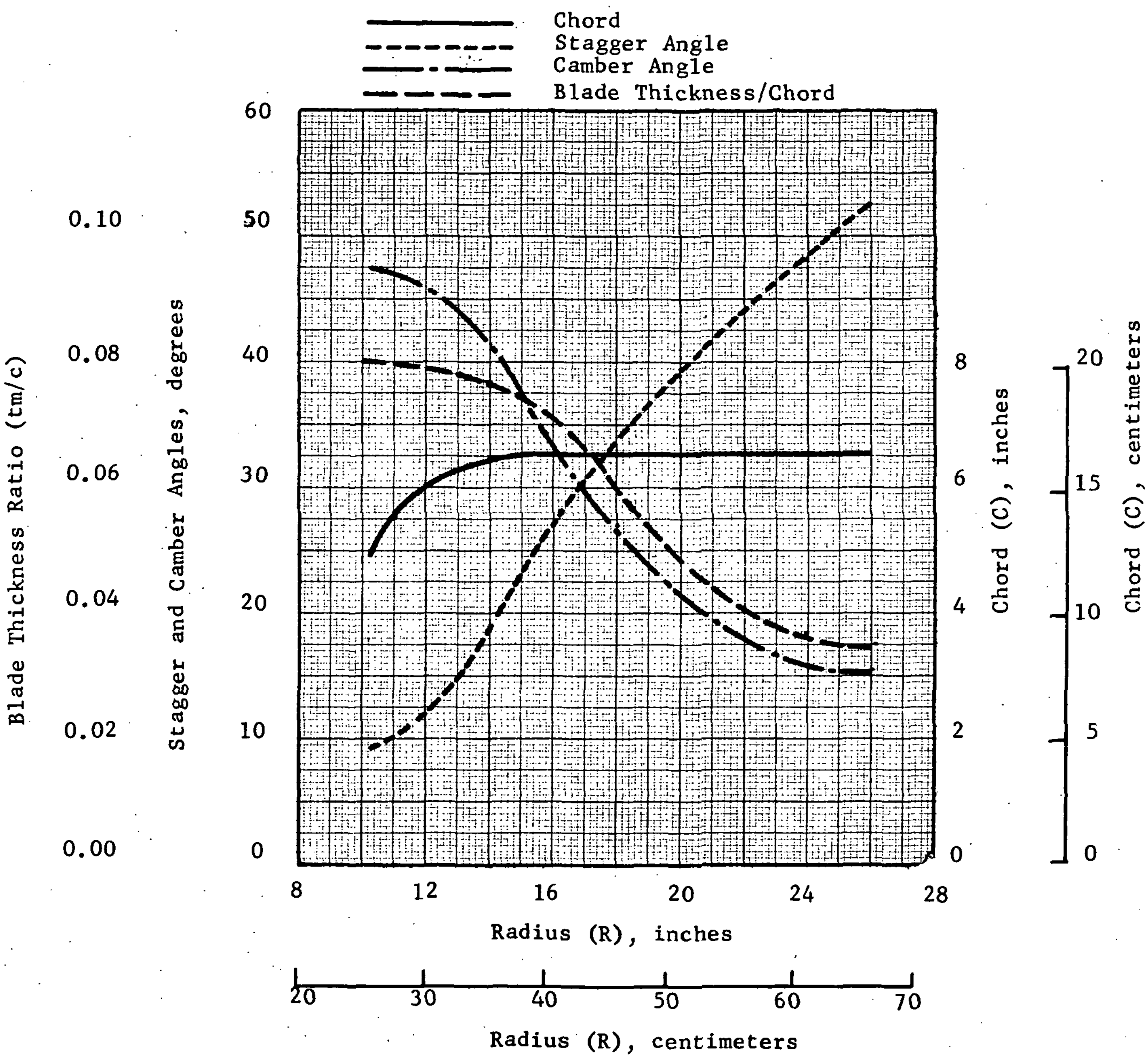

Figure 109 - Blade Geometry for Composite Stage 1 Rotor

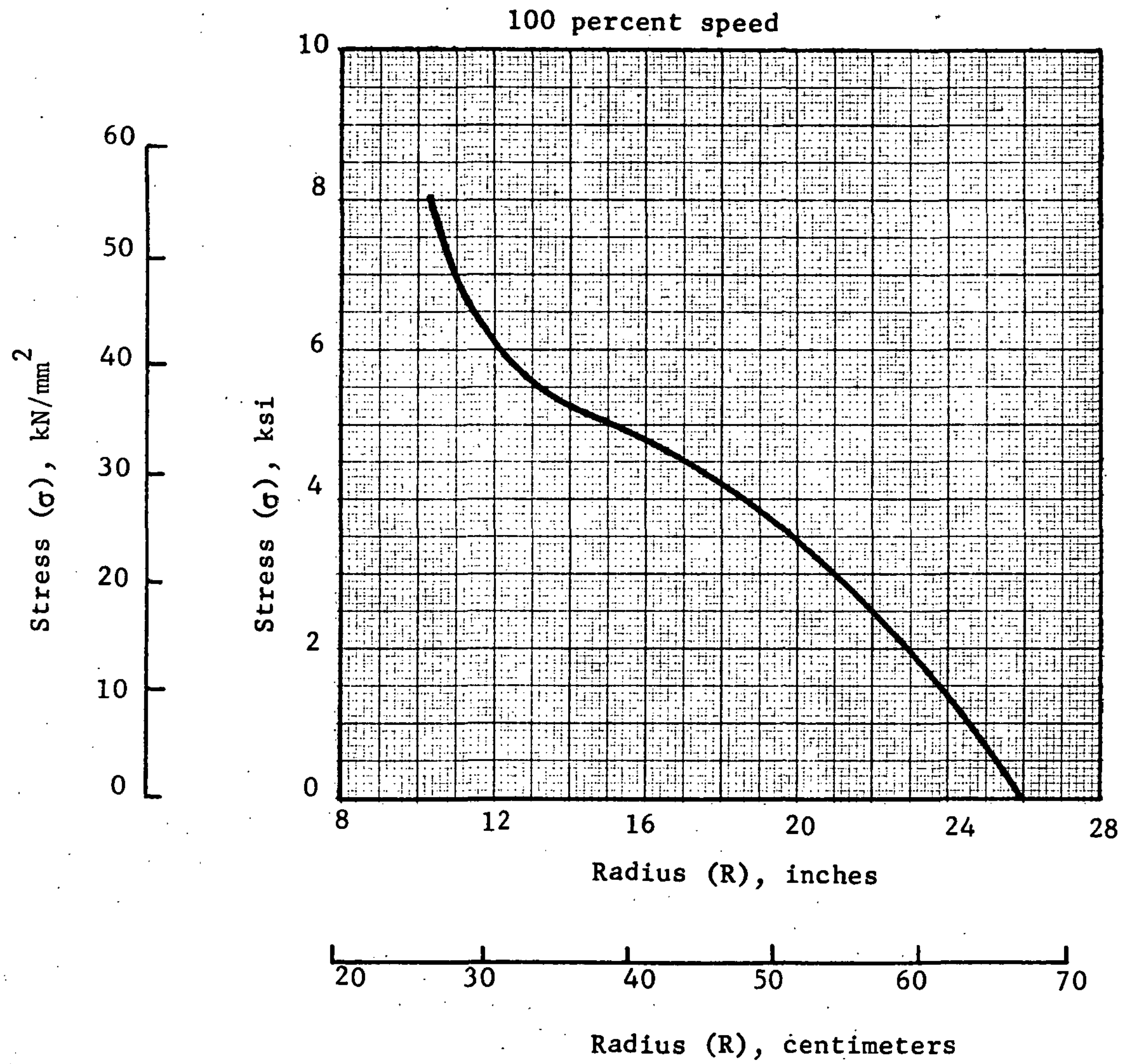

Figure 110 - Blade Average Steady State Stress, Stage 1 Composite Blade

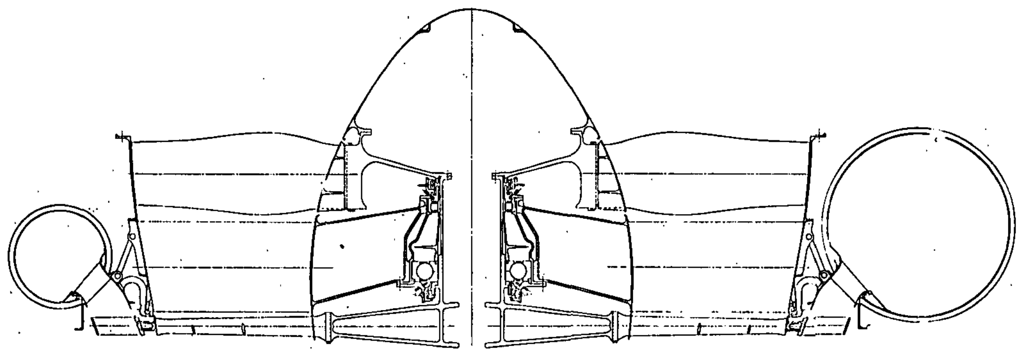

Figure 111 - Two Stage Fan With Composite Rotor

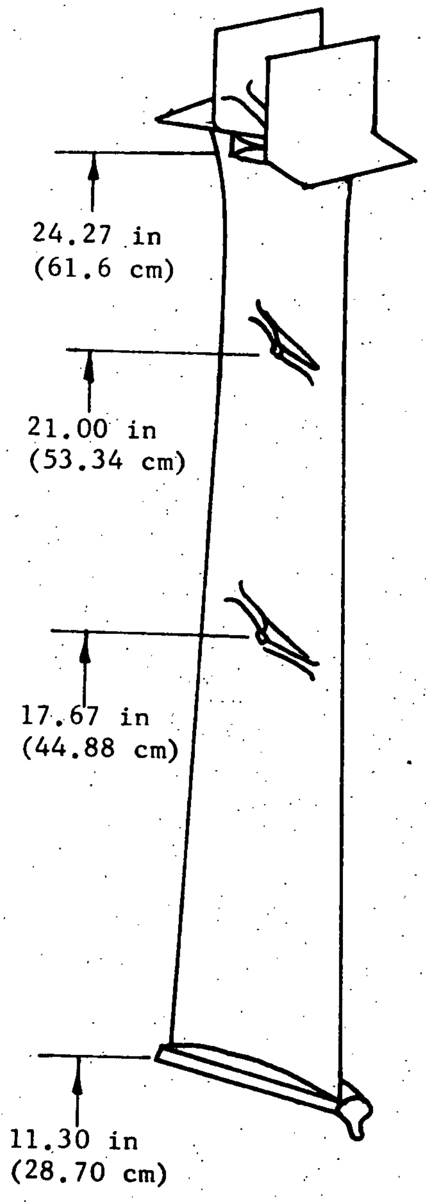

Figure 112 - Second Stage Fan Blade Geometry for Two Stage Fan

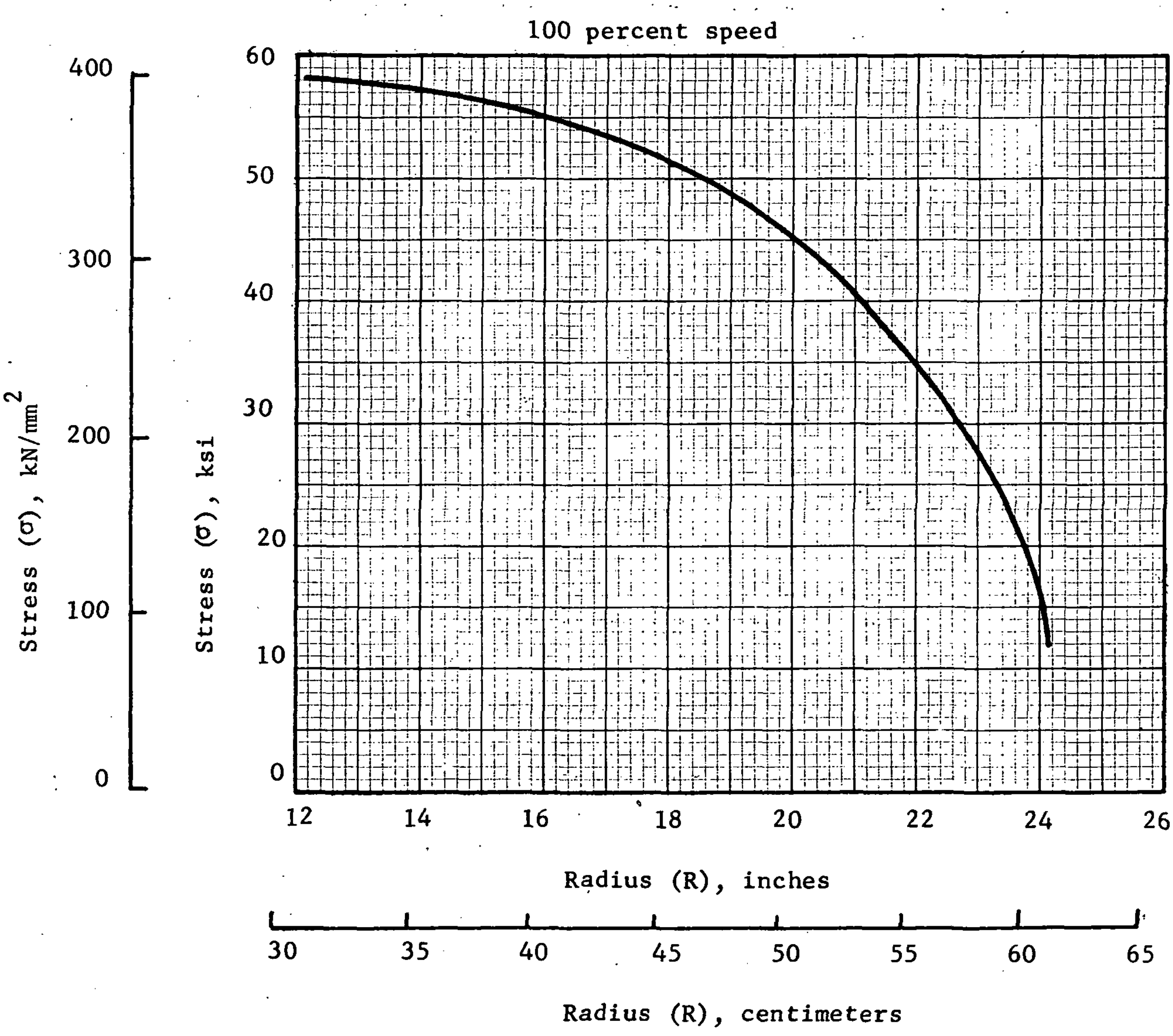

Figure 113 - Centrifugal Stress for Stage 2 Blade

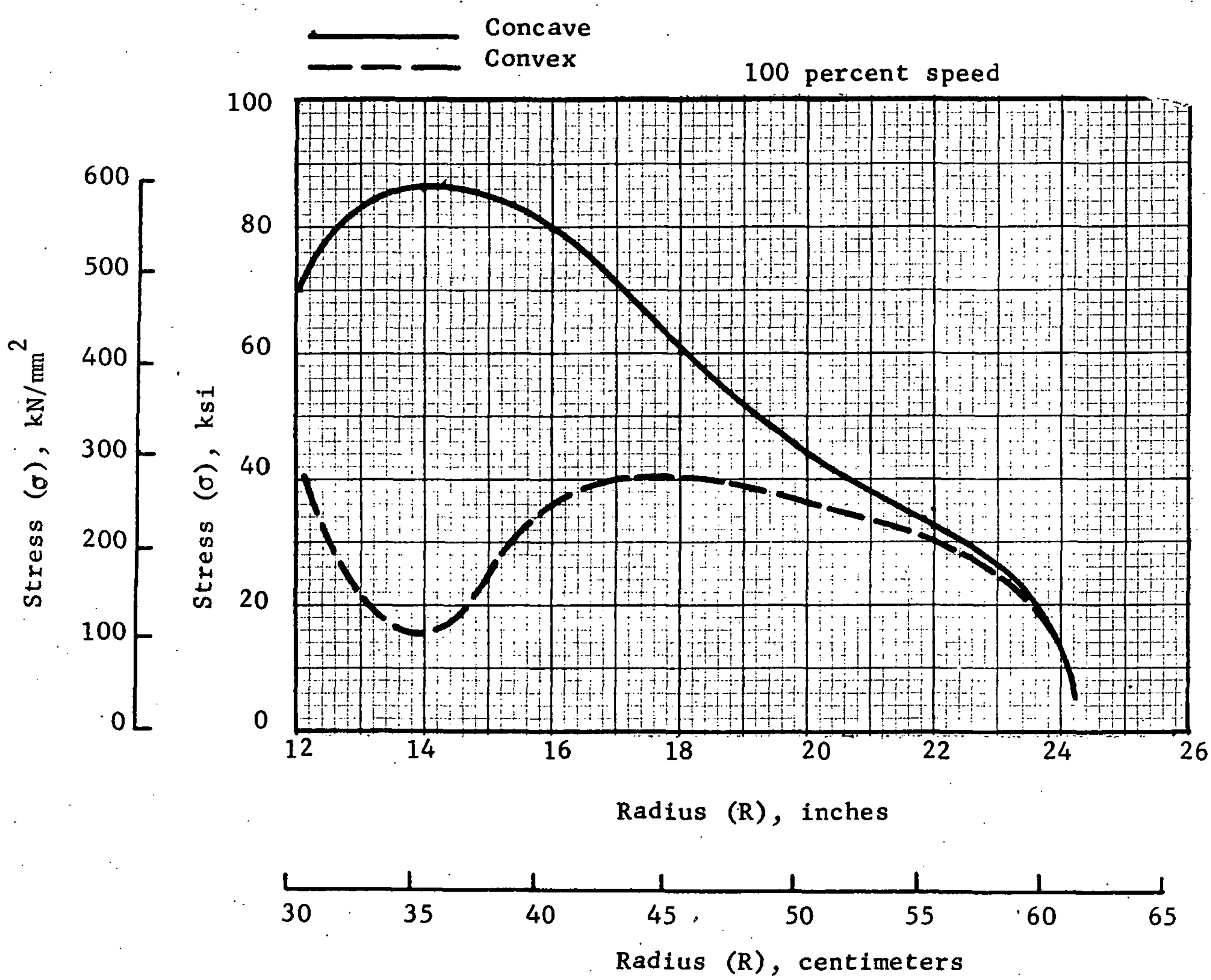

Figure 114 - Combined Stress for Stage 2 Blades

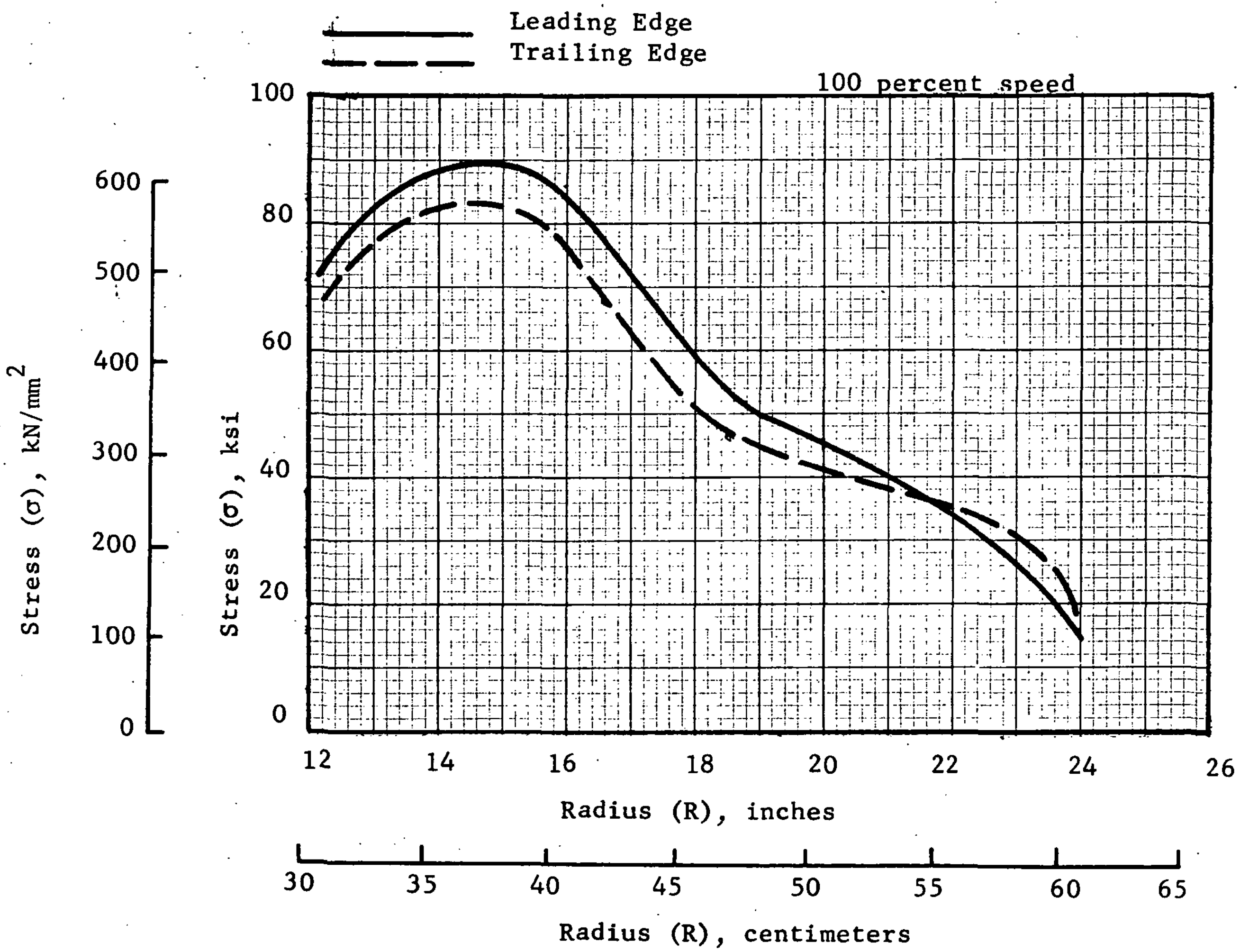

Figure 115 - Resultant Spanwise Stress for Rotor 2 Blade

First Flex
(1193 Hz)

First Torsion
(1726 Hz)

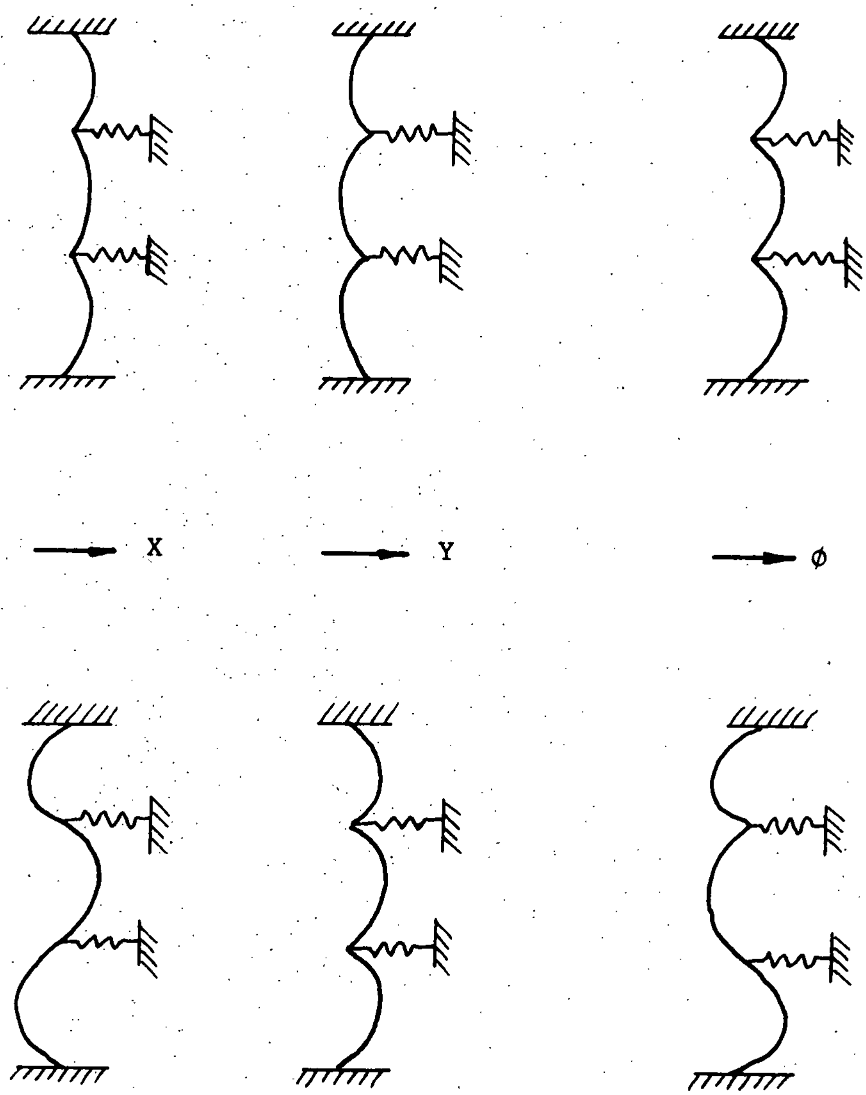

Relative Velocity = 1130 ft/sec (344 m/sec)
Chord = 2.45 in (6.25 cm)
V_R = 1.03

Figure 116 - Fundamental Frequency and Nodal Patterns for Second Stage Blades

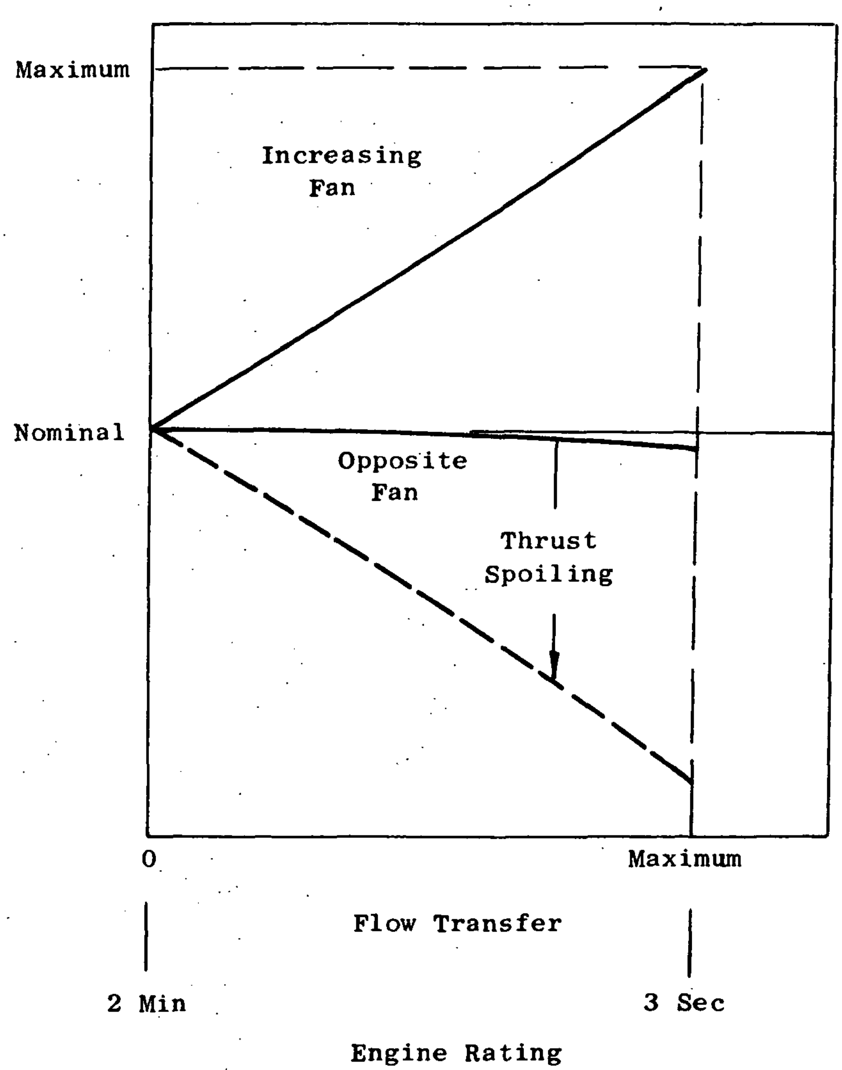

Figure 117 - Typical Fan Thrust Variations during Control Excursions

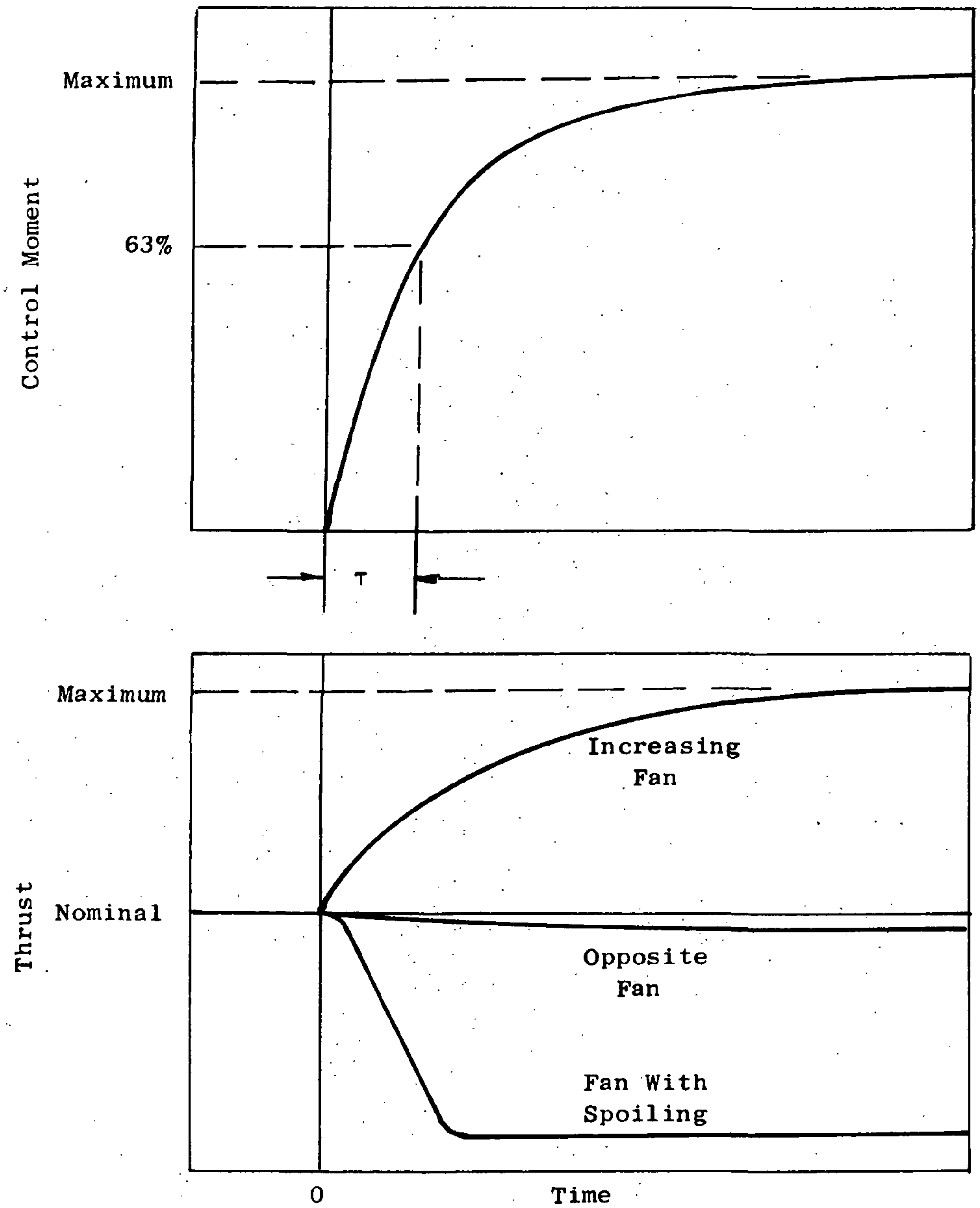

Figure 118 - Typical Fan Transient Response Characteristics

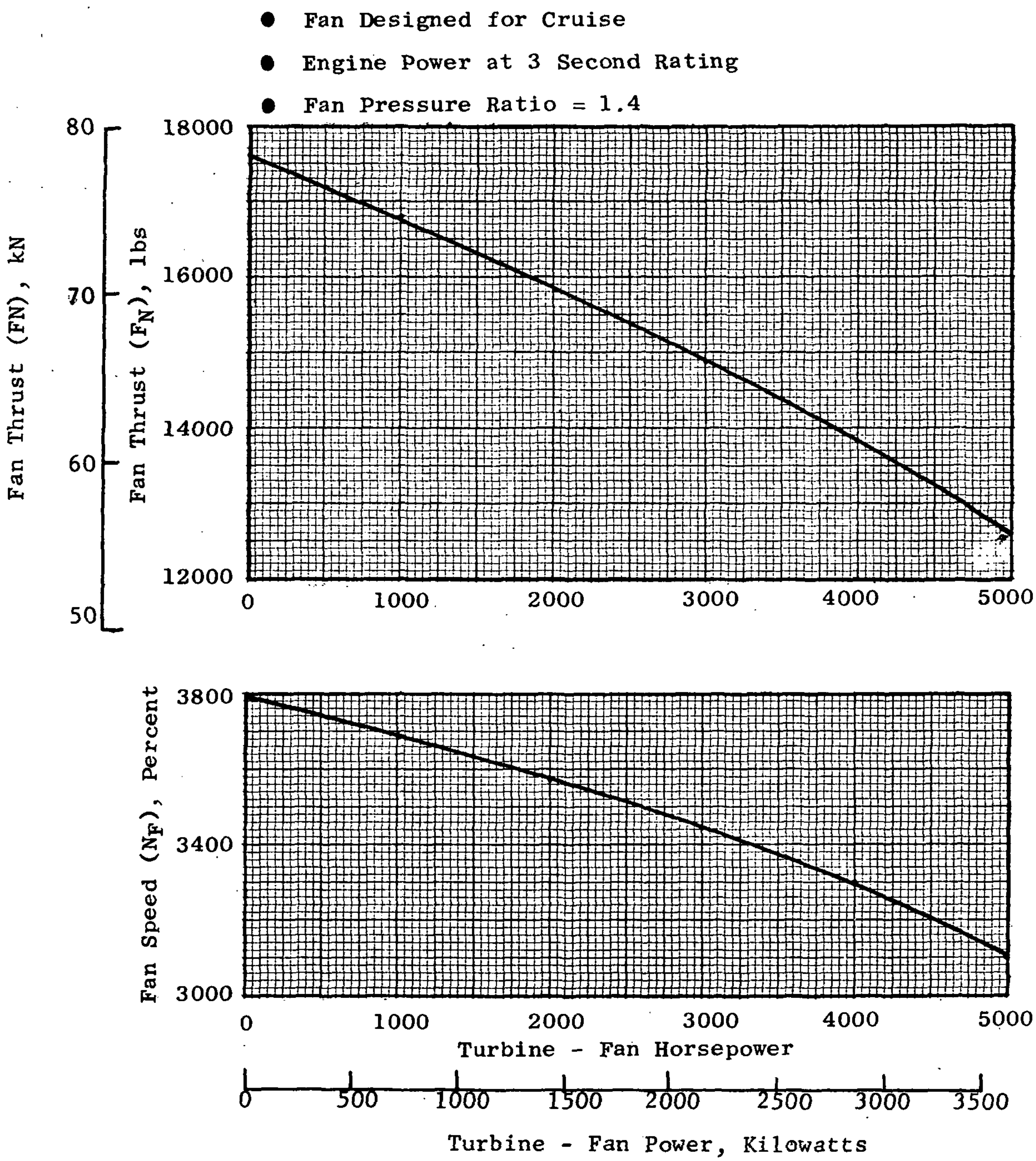

Figure 119 - Typical Fan Performance with Shaft Power Unbalance

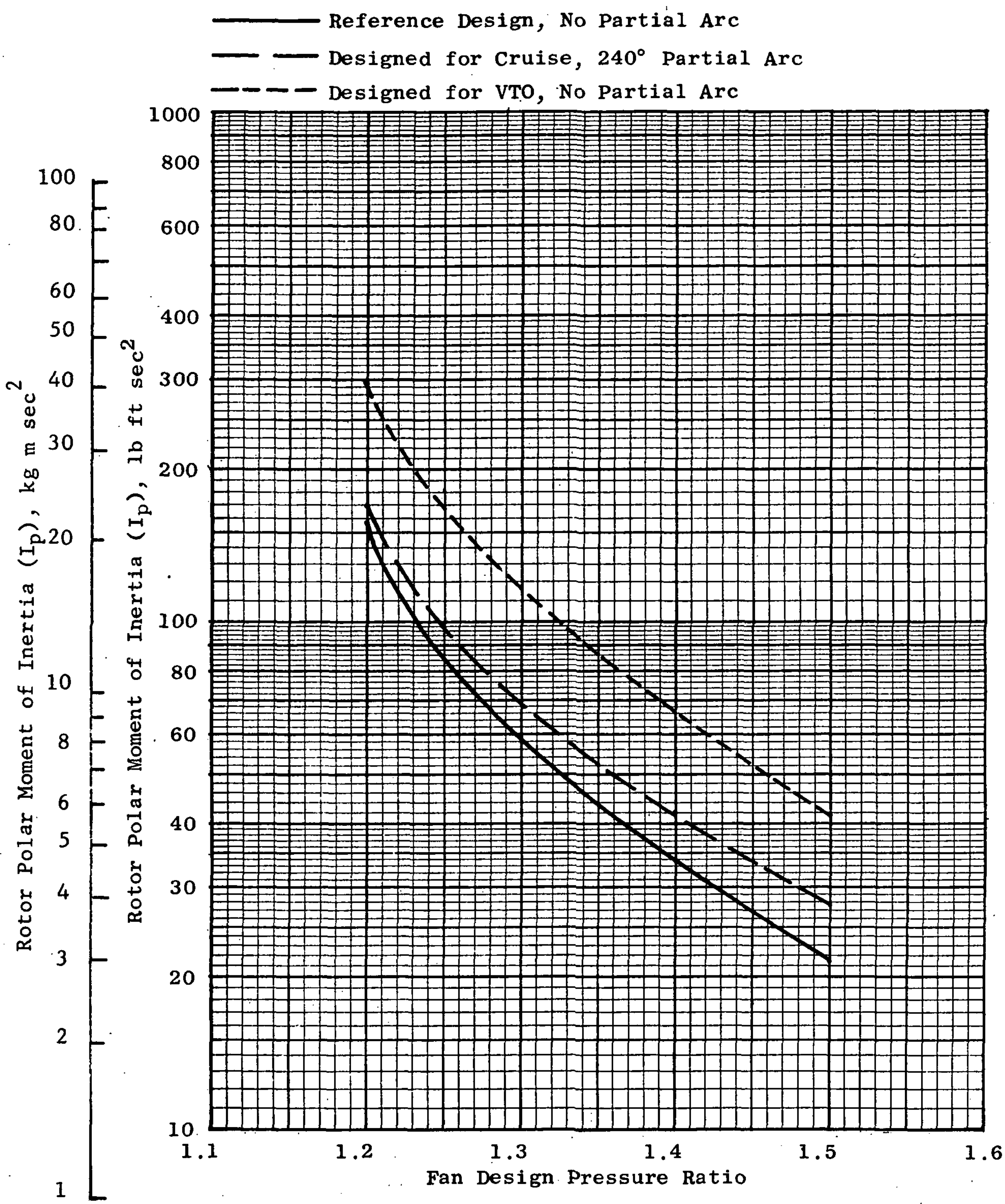

Figure 120 - Rotor Polar Moment of Inertia for Single Stage Fan Designs

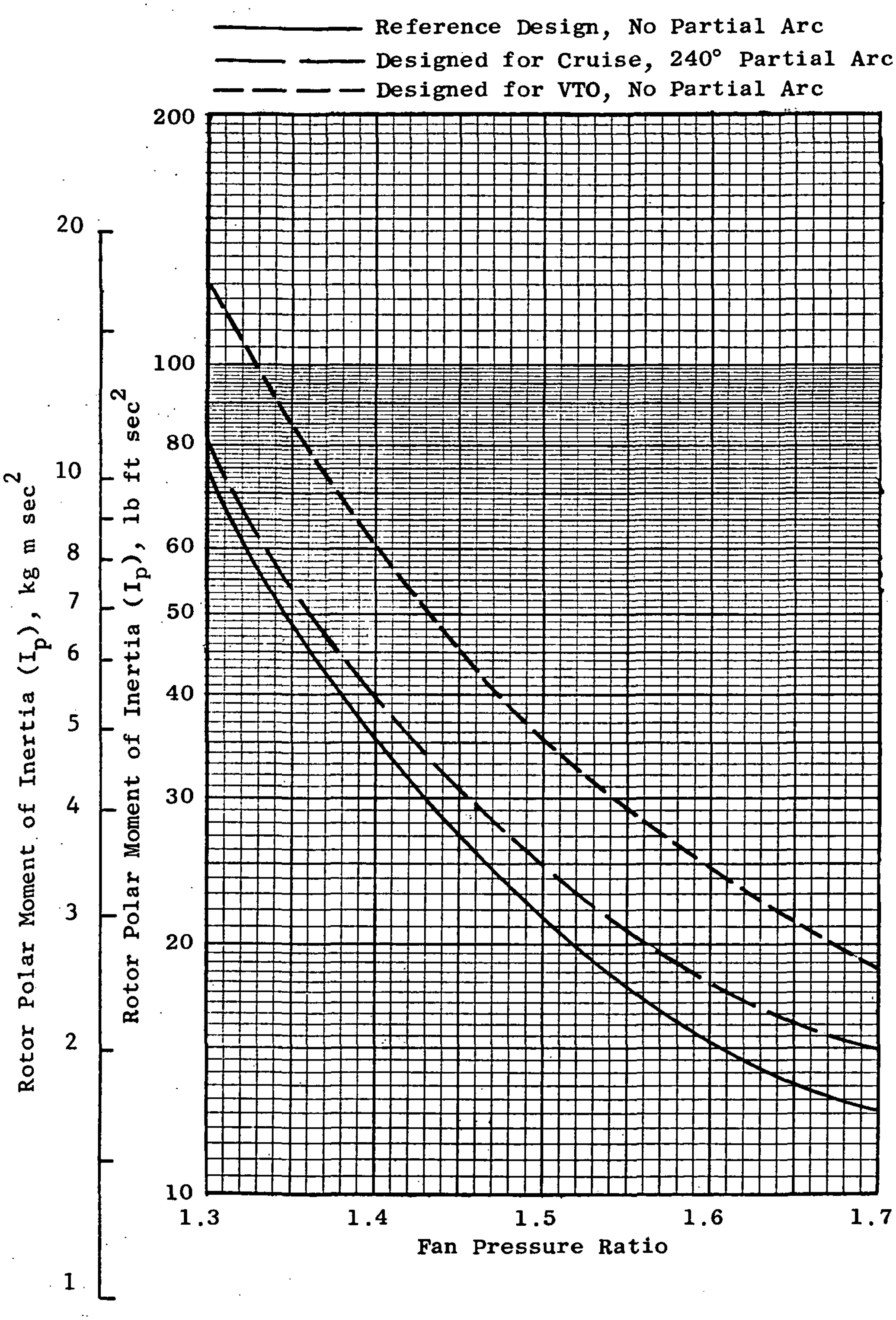

Figure 121 - Rotor Polar Moment of Inertia for Two Stage Fan Designs

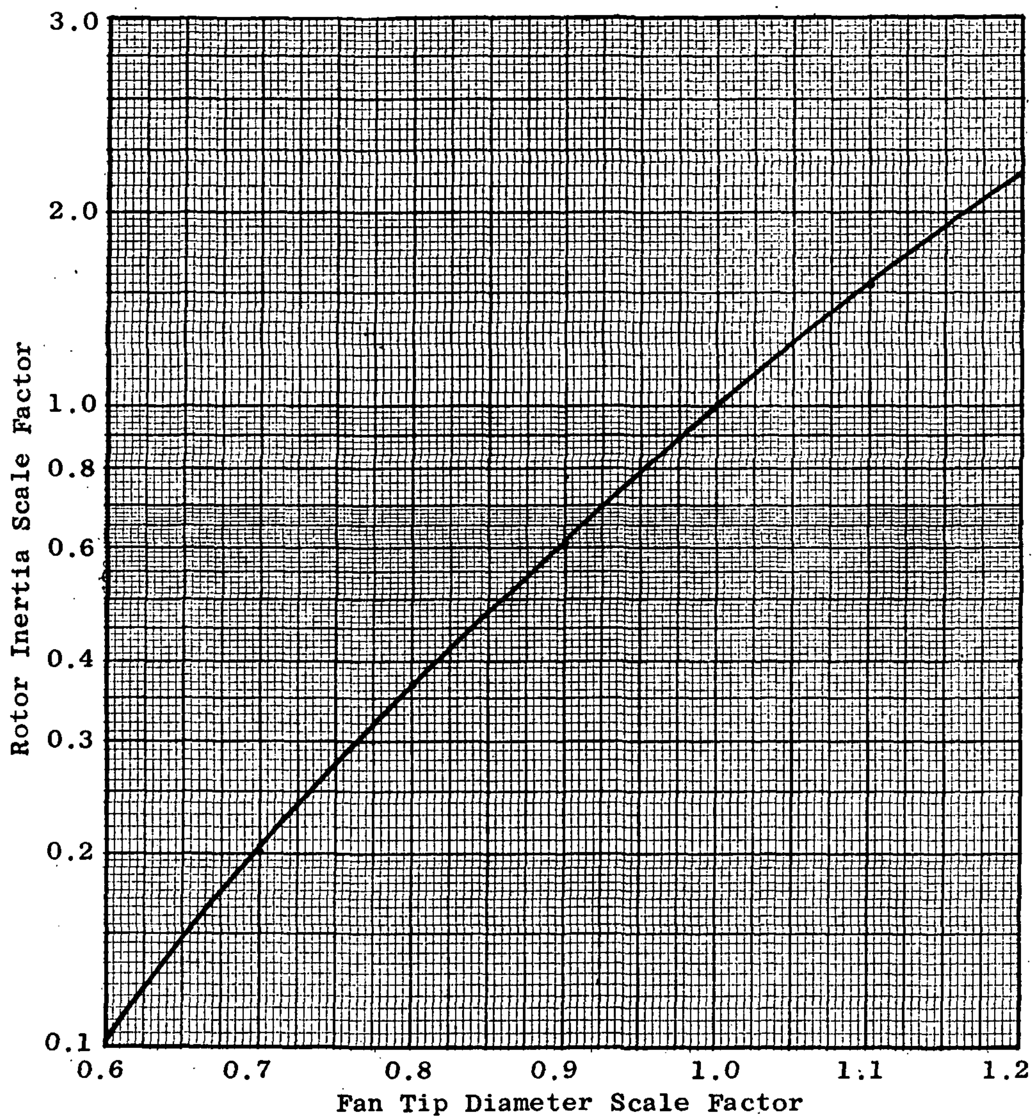

Figure 122 - Effects of Fan Size on Fan Rotor Inertias

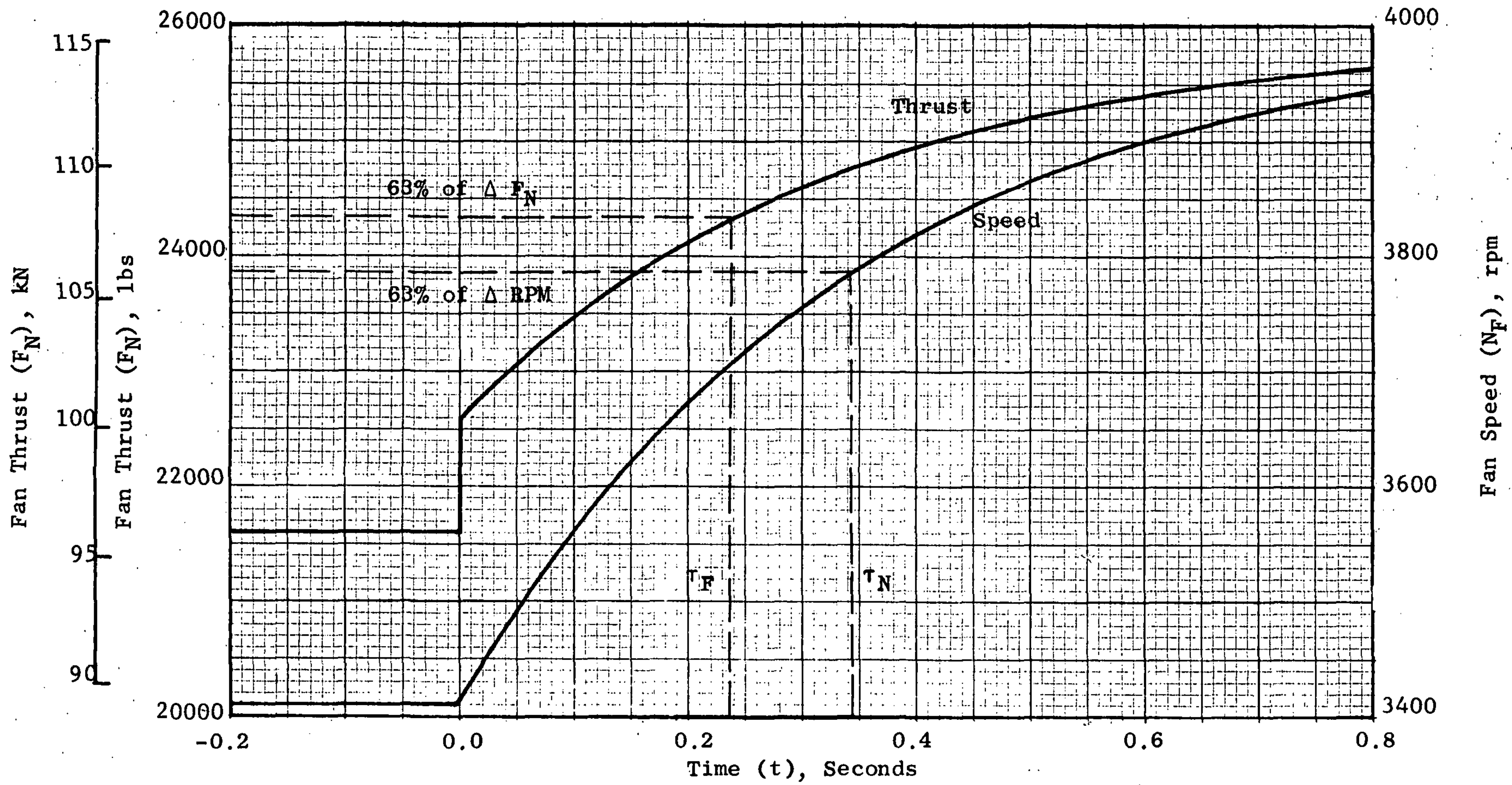

Figure 123 - Transient Response of Single Stage Fan Designed for VTO, Increasing Thrust, P/P = 1.4, DFT = 74.7 in

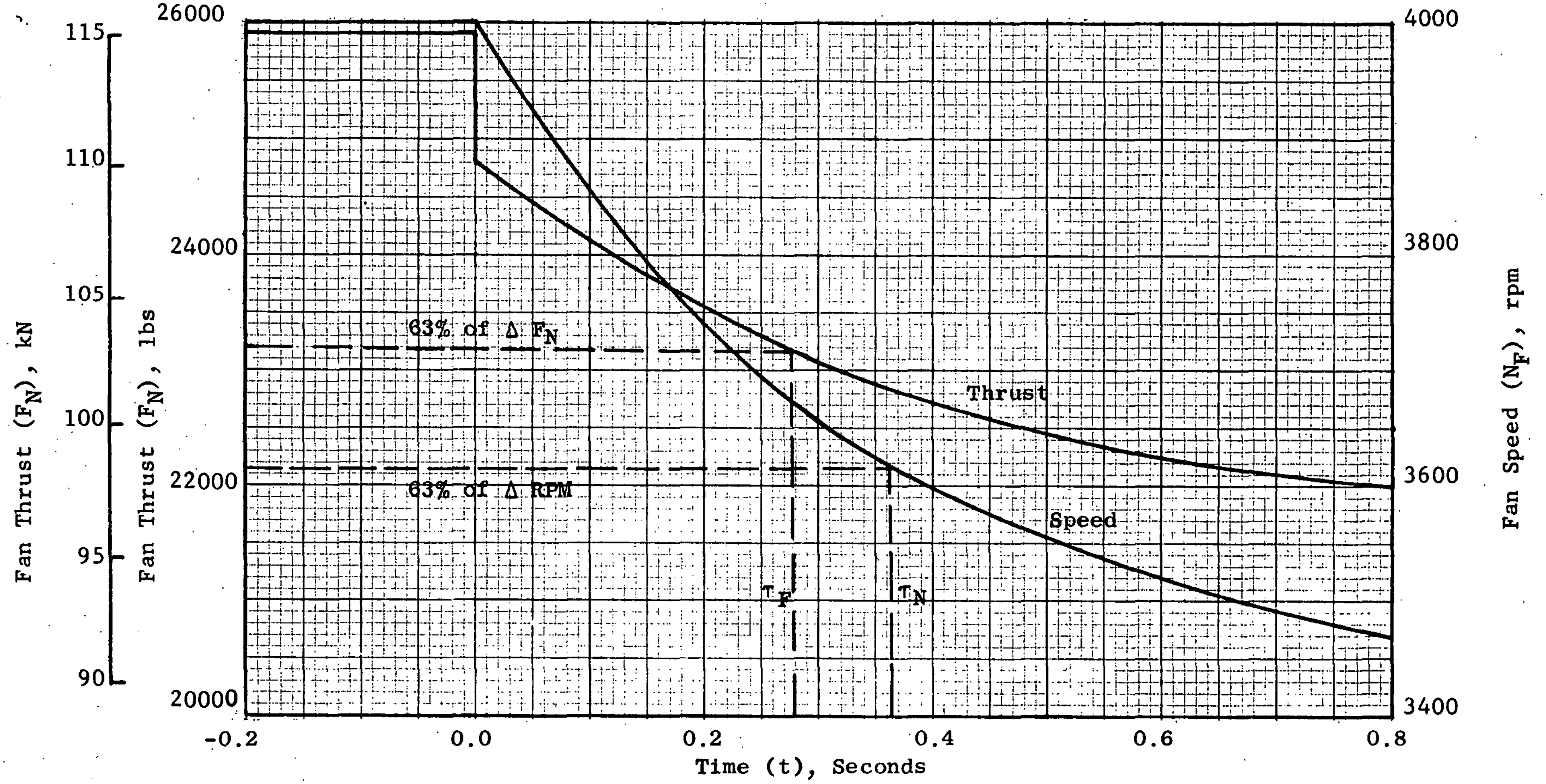

Figure 124 - Transient Response of Single Stage Fan Designed for VTO, Decreasing Thrust, P/P = 1.4, DFT = 74.7 in

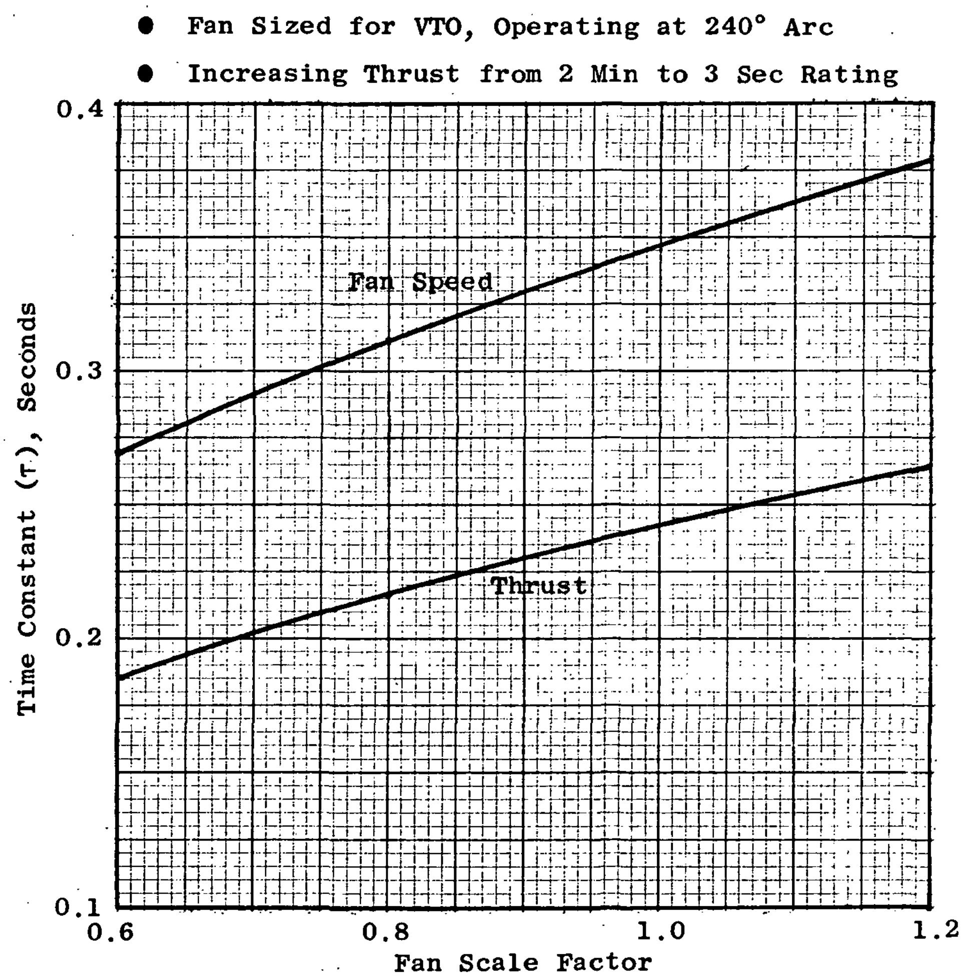

Figure 125 - Effects of Fan Scale Factor on Transient Response

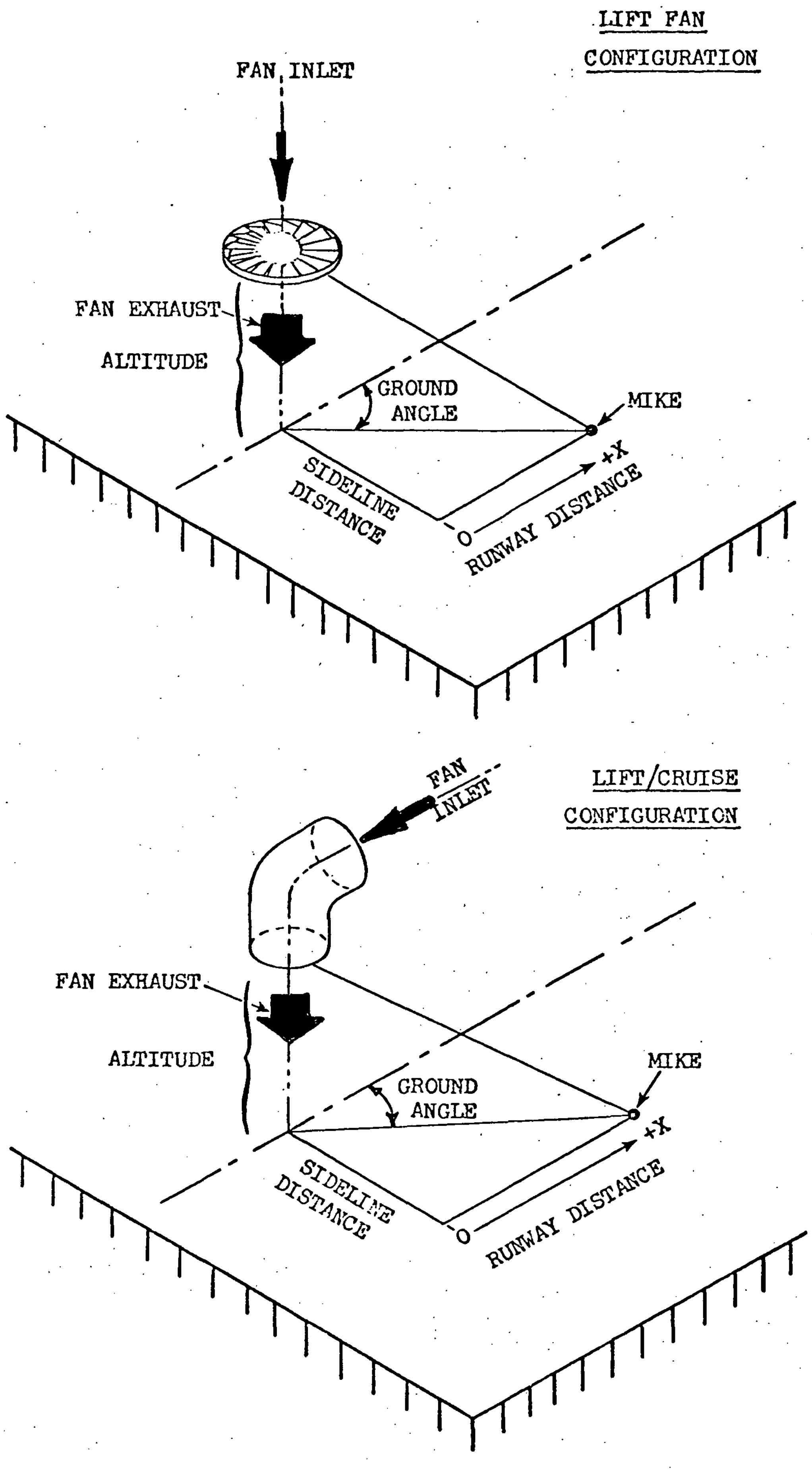

Figure 126 - Flyover Model Comparison of Lift and Lift/Cruise Configurations

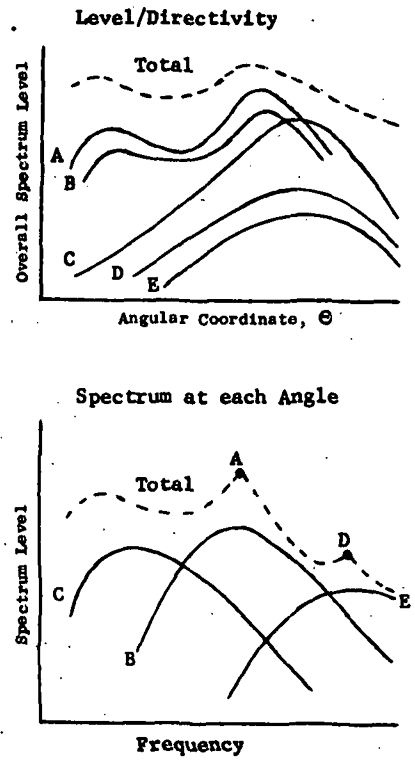

		LEVEL	DIRECTIVITY
A.	Fan Puretone	Analytical	Empirical CF6
B.	Fan Broadband	Empirical CF6, QEP	Empirical CF6 and QEP
C.	Jet Noise	GE/NASA for Fan. SAE Extrapolated Below 1000 Ft/Sec Velocity for Turbine	Empirical GE data
D.	Turbine Puretone	Analytical	Empirical Rolls Royce and GE
E.	Turbine Broadband	Empirical Rolls Royce and GE	Empirical Rolls Royce and GE data

		SPECTRUM
A.	Fan Puretone	One Cycle by Definition
B.	Fan Broadband	Empirical CF6 and QEP
C.	Jet Noise	SAE (Strouhal Number)
D.	Turbine Puretone	One Cycle by Definition
E.	Turbine Broadband	Empirical Rolls Royce and GE data

Figure 127 - Schematic of Noise Constituent Prediction and Summation

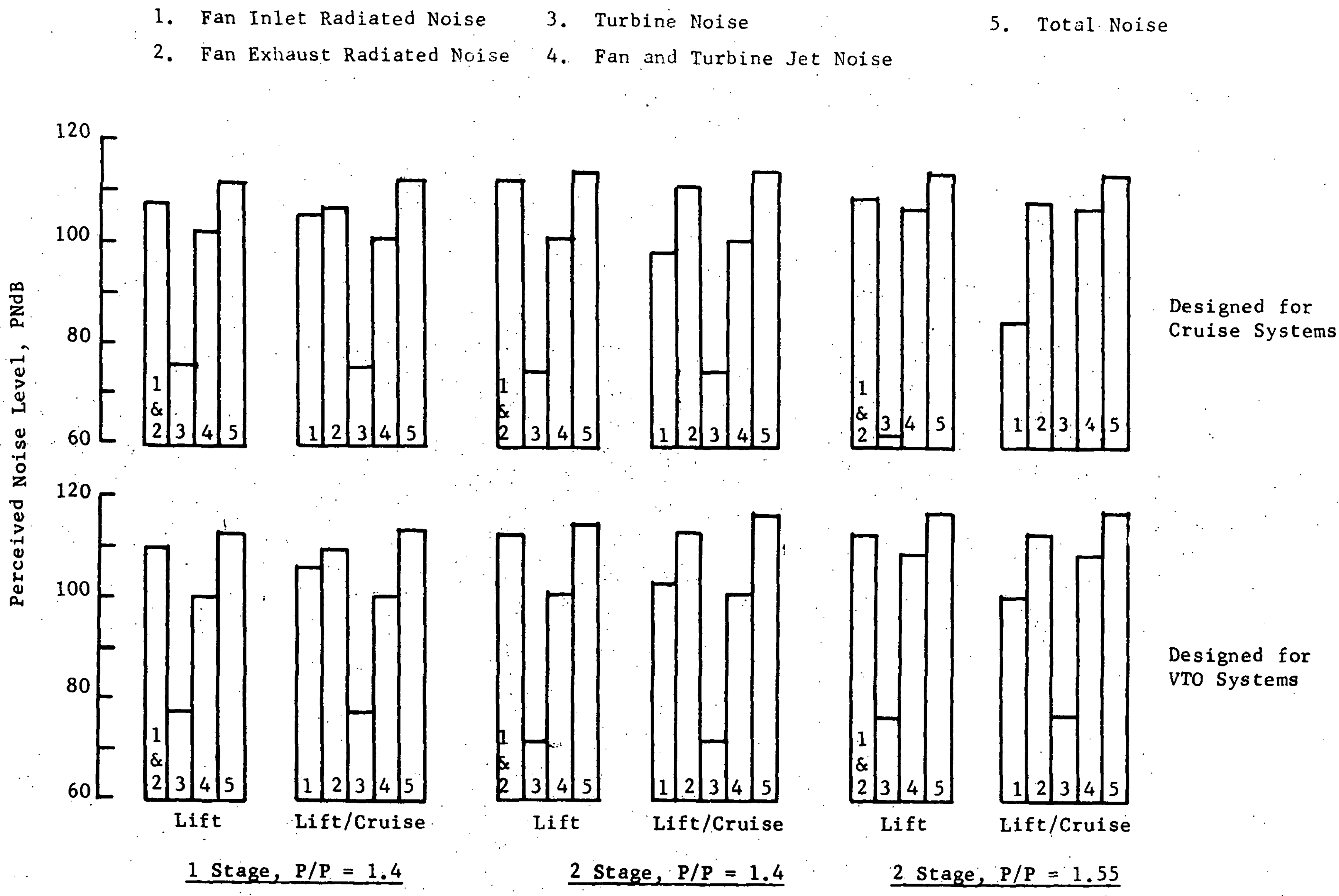

Figure 128 - Noise Constituents of Lift Fan Systems